

# **The role of miRNAs in resistance to HER2 targeted therapies**

A thesis submitted for the degree of PhD

by **Karen Howe, B.A**

September 2015

The work in this thesis was carried out under the supervision of

Dr. Norma O'Donovan

School of Biotechnology

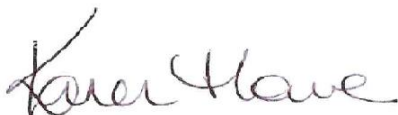
Dublin City University

&

Prof. John Crown

St. Vincent's University Hospital

I hereby certify that this material, which I now submit for assessment on the programme of study leading to the award of PhD is entirely my own work, that I have exercised reasonable care to ensure that the work is original, and does not to the best of my knowledge breach any law of copyright, and has not been taken from the work of others save and to the extent that such work has been cited and acknowledged within the text of my work.

Signed: 

(Candidate) ID No.: 10113681

Date: 02<sup>nd</sup> September 2015

# Table of Contents

Acknowledgements .....	8
Abbreviations .....	10
Communications arising from this work.....	13
Abstract .....	14
<b>Chapter One</b> .....	<b>15</b>
<b>Introduction</b> .....	<b>15</b>
1.1. Introduction.....	16
1.2. Diagnosis of breast cancer .....	18
1.3. Classification of breast cancer .....	18
1.4. Breast cancer treatment strategies.....	23
1.4.1. Conventional therapies.....	23
1.4.2. Targeted therapies .....	24
1.5. HER2 positive breast cancer .....	25
1.6. Current treatments for HER2 positive breast cancer .....	31
1.6.1 Trastuzumab- monoclonal antibody.....	32
1.6.1.1 Discovery and development of trastuzumab .....	32
1.6.1.2 Drug structure .....	34
1.6.1.3 Mechanism of Action.....	34
1.6.1.4 Mechanisms of Resistance .....	40
1.6.1.5 Biomarkers of trastuzumab resistance .....	42
1.6.2 Lapatinib- Tyrosine Kinase Inhibitor.....	42
1.6.2.1 Development and Discovery of Lapatinib.....	42
1.6.2.2 Drug Structure .....	43
1.6.2.3 Mechanism of Action.....	44
1.6.2.4 Lapatinib and trastuzumab .....	46
1.6.2.5 Mechanisms of Resistance .....	48
1.7. microRNAs .....	49
1.7.1 Introduction.....	49
1.7.2 miRNA biogenesis .....	50
1.7.3 miRNA function .....	51
1.7.4 Roles of miRNA .....	54

1.7.5	miRNAs and HER2 positive breast cancer.....	55
1.7.6	miRNAs and trastuzumab resistance .....	56
1.7.7	microRNAs and Lapatinib resistance .....	58
1.8.	Circulating miRNAs .....	59
1.9.	Cancer stem cells (CSCs).....	61
1.10.	Study Aims.....	63
	<b>Chapter Two.....</b>	<b>64</b>
	<b>Materials &amp; Methods .....</b>	<b>64</b>
2.1.	Cell lines, cell culture and reagents .....	65
2.2.	Proliferation assays .....	67
2.3.	microRNA extraction.....	67
2.4.	Agarose gels.....	68
2.5.	TLDA data analysis .....	68
2.6.	miRNA reverse transcriptase reaction (RT-PCR).....	70
2.7.	Gene expression reverse transcriptase reactions.....	71
2.8.	Real time quantitative reverse transcription polymerase chain reaction (qRT-PCR) .....	72
2.9.	MiRWalk- Target prediction & validation .....	74
2.10.	Lentiviral stable transduction.....	75
2.11.	Wound scratch migration assay .....	76
2.12.	Doubling time assays .....	76
2.13.	Preparation of cell lysates .....	77
2.14.	Western blotting.....	77
2.15.	miRNA extraction from conditioned media .....	80
2.16.	miRCURY RNA isolation kit- Biofluids.....	80
2.17.	ALDEFLOUR assay .....	81
2.18.	Establishment of primary mammosphere assays from cell lines.....	82
2.19.	Assessment of self-renewal – secondary mammosphere generation.....	84
2.20.	Preparation of cell culture blocks as block donors .....	85
2.21.	Sectioning and coring of cell culture donor blocks .....	86
2.22.	De-paraffinisation and H & E staining of sections .....	86
2.23.	HER2 Immunohistochemistry .....	87
2.24.	Formalin Fixed Paraffin Embedded (FFPE) - miRNA extraction.....	89

2.25.	RNA evaluation .....	90
2.26.	qRT-PCR analysis.....	91
2.27.	Patient population .....	91
2.28.	Statistical analysis .....	91
<b>Chapter Three .....</b>		<b>92</b>
<b>Characterisation of acquired trastuzumab and lapatinib resistant cell lines.....</b>		<b>92</b>
3.1.	Introduction.....	93
3.2.	Sensitivities of SKBR3-P and SKBR3-T cells to trastuzumab and lapatinib ...	93
3.3.	Doubling times.....	96
3.4.	Migratory properties of the acquired resistant cell lines.....	97
3.5.	Sensitivity of BT474-Tr acquired trastuzumab resistance cell line model .....	99
3.6.	HCC-1954-L acquired lapatinib resistance cell line model.....	100
3.7.	Microarray data analysis of the SKBR3-T and SKBR3-L cell lines .....	102
3.8.	ALDEFLUOR analysis of SKBR3-P & SKBR3-L cell lines.....	104
3.9.	Summary .....	107
<b>Chapter Four .....</b>		<b>109</b>
<b>miRNA expression in trastuzumab and lapatinib resistant cell lines .....</b>		<b>109</b>
4.1.	Introduction.....	110
4.2.	miRNA expression analysis (Taqman Low Density arrays).....	110
4.3.	RNA extraction .....	112
4.4.	qRT-PCR validation of miRNA targets in trastuzumab and lapatinib resistant cells .....	113
4.5.	Validation of miRNA targets in the BT474-Tr acquired trastuzumab resistance cell line model.....	116
4.6.	Validation of miRNA targets in the HCC-1954-L acquired lapatinib resistance cell line model.....	116
4.7.	Analysis of miRNA targets in a cell line panel of innate trastuzumab and lapatinib resistance .....	117
4.8.	Short-term trastuzumab treatment of SKBR3-P cell line .....	119
4.9.	Target prediction for microRNAs .....	121
4.10.	Summary .....	125
<b>Chapter Five .....</b>		<b>128</b>
<b>miR-9 and retinoic acid receptors in trastuzumab and lapatinib resistant cells...</b>		<b>128</b>
5.1	Introduction.....	129

5.2	Identification of potential miR-9 targets.....	129
5.3	All- <i>trans</i> retinoic acid (ATRA) treatment .....	130
5.2.1	SKBR3-P, SKBR3-T and SKBR3-L cell lines.....	130
5.2.2	Other cell line models –BT-474, HCC-1954 and EFM-192A.....	132
5.4	All- <i>trans</i> retinoic acid (ATRA) and trastuzumab combination treatment .....	134
5.4.1	SKBR3-P, SKBR3-T and SKBR3-L .....	134
5.4.2	Other cell line models –BT-474, HCC-1954 and EFM-192A.....	136
5.5	All- <i>trans</i> retinoic acid (ATRA) treatment - Lapatinib combinations .....	138
5.5.1	SKBR3, SKBR3-T and SKBR3-L cell lines .....	138
5.5.2	Other cell line models –BT-474, HCC-1954 and EFM-192A.....	140
5.6	RAR $\alpha$ expression analysis .....	143
5.6.1	RAR $\alpha$ mRNA expression .....	143
5.6.2	RAR $\alpha$ protein expression.....	144
5.7	RAR $\beta$ , RAR $\gamma$ and RxR $\alpha$ protein expression.....	145
5.8	24 hour ATRA treatment and the effect on the retinoic acid receptors .....	150
5.9	Summary .....	153
	<b>Chapter Six .....</b>	<b>155</b>
	<b>The role of miR-221 &amp; -222 in resistance, migration and ‘stemness’ .....</b>	<b>155</b>
6.1	Introduction.....	156
6.2	Characterisation of the stable transfected SKBR3-P cell line .....	156
6.2.1	Confirmation of transfection in the SKBR3-P cell line.....	156
6.2.2	Effect of miR-221 and -222 over-expression on morphology and doubling time .....	158
6.2.3	Effect of miR-221 and -222 on trastuzumab sensitivity .....	160
6.2.4	Effect of miR-221 and -222 on migration.....	161
6.3	Target Prediction for miR-221 and miR-222.....	165
6.4	miR-221 and -222 and their involvement in stemness.....	168
6.5	Summary .....	171
	<b>Chapter Seven .....</b>	<b>173</b>
	<b>miRNA expression in HER2 positive breast tumours .....</b>	<b>173</b>
7.1	Introduction.....	174
7.2	Assessment of FFPE miRNA extraction kits.....	174
7.2.1	Cell culture donor block preparation .....	174

7.2.2	Comparison of miRNA extraction methods .....	175
7.3	Primary tumour miRNA analysis in a FFPE HER2 positive breast cancer cohort .....	181
7.3.1	Patient characteristics.....	182
7.3.2.	HER2 immunohistochemistry and miRNA extraction .....	183
7.3.3.	qRT-PCR analysis.....	185
7.4	Conditioned media study .....	187
7.4.1	miRNA analysis from conditioned media.....	187
7.5	miRNA analysis from serum samples.....	191
7.6	Summary .....	194
	<b>Chapter Eight .....</b>	<b>196</b>
	<b>Discussion .....</b>	<b>196</b>
8.1.	Introduction.....	197
8.2.	Characterisation of acquired trastuzumab and lapatinib resistant cell lines ...	198
8.3.	microRNA expression analysis.....	202
8.3.1.	Cell line analysis .....	202
8.3.2.	Comparison of FFPE miRNA extraction kits .....	205
8.3.3.	miRNA analysis in the HER2 positive FFPE tumour samples .....	207
8.3.4.	miRNA analysis in conditioned media .....	209
8.3.5.	miRNA analysis in patient sera.....	210
8.4.	Evidence of miRNA value in resistance .....	211
8.5.	Target prediction for miRNAs .....	214
8.5.1	miR-9 and Retinoic acid receptor alpha.....	215
8.5.2	ATRA response, estrogen receptor status and RAR $\alpha$ amplification ...	219
8.5.3	miR-221 and -222 expression .....	221
8.5.4	miR-221 and -222 expression and ‘stemness’ .....	225
8.6.	Summary and conclusions .....	228
	<b>Chapter Nine .....</b>	<b>229</b>
	<b>Bibliography.....</b>	<b>227</b>

## Acknowledgments

Firstly, I wish to offer my utmost thanks to my supervisor, Dr. Norma O'Donovan. Without her support and guidance over the course of my PhD this body of work wouldn't exist. I have learned invaluable lessons not only in a professional capacity but in a personal one. To Prof. John Crown, I wish to thank you for the opportunity of this PhD, for the CCRT funding towards the end and for the insight in to clinical world of oncology.

Secondly, I wish to thank the members of Dr. O' Donovan laboratory. From post-docs to research assistants, their help, advice and numerous puns certainly made the years pass with a smile.

A huge thanks to my NICB family, you know who ye are. A special mention to a few special people;

- To Alex and Denis who taught me so much in the start and were always approachable for any advice or laughs.
- To Laura and Joanne, who passed on their tricks of the trades and reminded me to keep my head up in tough times.
- To Naomi, who became our stand in supervisor and dealt with all the craziness of the O'Donovan lab.
- To the coffee gang. Every morning was made easier to get to work with the knowledge there would be brekkie, tea and laughs.
- To Sandra and Erica, the two wisest and craziest postdocs that kept the mood light through the long nights and sad science times. To the numerous jaeger-bombs and kebabs along the way it was a pleasure to become long lasting friends with both of you.
- To Deirdre and Trish. I am so honoured to have met such fabulous friends. During the PhD, there were certainly tough times for us all and together I think we got through it. This degree is a test of endurance and sanity and without such great friends I do not think it would have been possible. Thank you for all the Geordie shore nights, the vintage soirees and epic amounts of laughter.

To my “outside PhD” mates, Karl, Robbie and Emma. Thank you for understanding that the PhD takes away from drinking times but also I sometimes needed to get away from it all and have fun.

This work would never have finished had it not been for Darren. I wish to thank him from the bottom of my heart for his wisdom as a scientist and for being my partner in crime. You helped me from start to finish. The last year of the PhD was extremely trying and difficult especially when we had an ocean between us but thank you for giving me advice and calming me down through the weepy skype calls. Thank you for always trying, maybe not always succeeding in cheering me up even when I couldn't see the light at the end of the tunnel. Thank you for sticking by me until the end.

On a very personal note, a thank you cannot cover the gratefulness and appreciation for my family over the last four years. To my dear parents, thank you for always supporting me in my choice to remain a student that little bit longer. For all the personal and monetary support throughout this journey and for being there when I just needed a hug. We have certainly had it hard throughout the last few years and there have been ups and downs but we managed to survive and come out the other end.

To my dearest and only sister, we are certainly cut from different cloths but I wouldn't change you for the world. Thank you for doing my minion work during the summers, for cooking for me when I was a hangry bear and for letting my nest on your floor in the final few weeks of this PhD. I can only hope I can give you the same support, perhaps not floor space, in your PhD.

To my second Mammy, Jella, who has been my one of my biggest supporters throughout my life. Without your love and guidance along with my parents I wouldn't be the person I am today.

## Abbreviations

5FU	fluorouracil
5-HT	5-hydroxytryptamine
ADCC	antibody dependent cell cytotoxicity
Ago	argonaute family protein
AI	aromatase inhibitor
AIF	apoptosis inducing factor
AKT	protein kinase B
ALDH1	aldehyde dehydrogenase 1
AMPK	5' AMP-activated protein kinase
ATG5	autophagy related protein 5
ATG8	autophagy related protein 8
ATRA	All- <i>trans</i> retinoic acid
BAAA	BODIPY-aminoacetaldehyde
BCA	bicinchoninic acid
BID	BH3 interacting-domain death agonist
BIM	Bcl-2 interacting mediator of cell death
BRCA1	breast cancer 1, early onset
BRCA2	breast cancer 2, early onset
BTC	$\beta$ -cellulin
CCDB	Cell culture donor blocks
CD49f	integrin subunit $\alpha$ 6
CDK	cyclin dependent kinase
CDKN1A/p21 <sup>Cip1</sup>	Cyclin-dependent kinase inhibitor 1A
CDKN1B /p27 <sup>kip1</sup>	Cyclin-dependent kinase inhibitor 1B
CDKs	cyclin dependent kinases
CHO	Chinese hamster ovary
CISH	chromogenic <i>in situ</i> hybridisation
CmiRNA	Circulating miRNAs
CML	chronic myelogenous leukemia
CNS	central nervous system
COX2	cyclooxygenase-2
CT	computerised tomography
DAG	diacylglycerol
DCM	dilated cardiomyopathy
DDFS	distant disease free survival
DEAB	Diethylaminobenzaldehyde
DFS	disease free survival
ECD	Extracellular domain
EGF	epidermal growth factor (EGF)
EMT	epithelial-to-mesenchymal transition
EpCAM	epithelial cell adhesion molecule
ER $\alpha$	estrogen receptor $\alpha$

EREG	Epiregulin
ERK 1/2	extracellular signal-related kinase 1/2
ESA	epithelial surface antigen
FAK	focal adhesion kinase
FBS	Fetal bovine serum
FDA	Us Food & Drug Administration
FISH	fluorescent <i>in situ</i> hybridisation
GADPH	glyceraldehyde-3-phosphoate dehydrogenase
G-CSF	granulocyte-colony stimulating factor
GFP	green fluorescent protein
GRB2	growth factor receptor bound protein 2
GRB7	Growth factor receptor bound protein 7
HB-EGF	heparin-binding EGF-like growth factor
HER2	human epidermal growth factor 2
HGF	hepatocyte growth factor
HR	Hormone receptor
HSP90	heat shock protein 90
IAP	inhibitor of apoptosis
IBC	inflammatory breast cancer
IGF	insulin-like growth factor
IGF-1R	insulin-like growth factor 1 receptor
IGFBP2	insulin-like growth factor binding protein 2
IL-8	interleukin-8
IP3	inositol triphosphate
MAPK	mitogen activated protein kinase
MBC	metastatic breast cancer
MCL-1	myeloid cell leukemia 1
MEK	MAPK kinase
MFE	mammosphere formation efficiency
miRNP	miRNA-containing ribonucleo-protein particle
MREs	miRNA-Recognition Elements
mTOR	mammalian target of rapamycin
mTORC1	mammalian target of rapamycin complex 1
MUC4	membrane associated glycoprotein
NK cells	natural killer cells
NmU	neuromedin
NPC	nasopharyngeal carcinoma
NPM1	nucleophosmin 1
NRG	neuregulin
NSCLC	non-small cell lung cancer
ORR	overall response rate
OS	overall survival
p4E-BP1	phosphorylated 4E binding protein
PARP	Poly (ADP-ribose) polymerase
PBS	Phosphate buffered saline

PCD4	protein programmed cell death 4
pCR	pathological complete response
pCSCs	putative cancer stem cells
PFGE	platelet-derived growth factor receptor
PFS	progression free survival
PI3K	phosphatidylinositol-3 kinase
PKC	protein kinase C
PLC $\gamma$	phosphodiesterase phospholipase C $\gamma$
PPM1H	protein phosphatase, Mg <sup>2+</sup> /Mn <sup>2+</sup> dependent, 1H
PR	progesterone receptor
PTEN	phosphatase and tensin homolog deleted on chromosome 10
qRT-PCR	quantitative real time polymerase chain reaction
RAR $\alpha$ , $\beta$ , $\gamma$	Retinoic acid receptor alpha, beta, gamma
Rb	Retinoblastoma
RISC	RNA induced silencing complex
RNApol II	RNA polymerase II
RTK	Receptor tyrosine kinase
RxR $\alpha$ , $\beta$ , $\gamma$	Retinoid X Receptor alpha, beta, gamma
SDS	sequence detection systems
snoRNAs	small nucleolar non-coding RNA
SOCS1	suppressor of cytokine signalling
SOS	son of sevens
T-DM1	ado-trastuzumab emtansine
TGF1	transforming growth factor 1
TGF $\alpha$	transforming growth factor alpha
TKI	tyrosine kinase inhibitor
TLDA	Taqman Low Density Array
TNBC	Triple negative breast cancer
TRAF4	TNF-receptor associated factor 4
TRAIL	tumour necrosis factor-related apoptosis-inducing ligand
TSC1/2	tuberous sclerosis complex 1/2
TSP-1	thrombospondin
UTR	untranslated region
VEGF	vascular endothelial growth factor
XIAP	X-linked inhibitor of apoptosis

## Communications arising from this work

### Book Chapter

- Neil A. O'Brien, Alexandra Canonici, **Karen Howe**, Martina SJ McDermott, Denis M. Collins, Brigid C. Browne, John Crown and Norma O'Donovan. **HER2 targeted therapies**. eBook series Frontiers in Anticancer Drug Discovery.

### Published Abstracts

- **Poster** - *Altered expression of miRNAs in acquired trastuzumab resistance*. AACR 2014, San Diego, CA 4<sup>th</sup> – 9<sup>th</sup> April 2014.
- **Poster** - *miR-221 and -222 in acquired and innate trastuzumab resistant cell lines*. IACR 2014, Galway, Ireland. Feb 2014.
- **Oral Presentation**- *miR-221 and -222; Do they play a role in trastuzumab resistance?* School of Biotechnology Research Day, DCU. 7<sup>th</sup> Feb 2014
- **Oral Presentation** – *microRNAs in trastuzumab and lapatinib resistant breast cancer cells*. 1<sup>st</sup> Dublin microRNA Day, May 2013
- **Poster**- *microRNA- 224, - 375 and -9 in trastuzumab and lapatinib acquired resistant HER2 positive breast cancer cells*. 24th EORTC-NCI-AACR Symposium on 'Molecular Targets and Cancer Therapeutics', Dublin 6-9 Nov 2012
- **Poster** - *microRNA expression analysis in trastuzumab and lapatinib resistant HER2 positive breast cancer cells*. Biotechnology in Action 2012, 4-6 September 2012. The Helix, Dublin City University.
- **Poster Discussion** - *microRNA-9 and -224 in trastuzumab resistant HER2 positive breast cancer cells*. ESMO Congress, Vienna, Austria 28<sup>th</sup> Sep – 2<sup>nd</sup> October 2012
- **Poster** - *microRNA expression analysis in trastuzumab resistant HER2 positive breast cancer cells*. 2012 IACR annual meeting, Belfast, Ireland, 1-2 March 2012

### Awards

- EACR Travel Fellowship May 2014
- Roche Researcher of the Year Feb 2014
- NCI Molecular Prevention Course (Health Research Board (HRB)) Aug 2013

## **Abstract**

### **The role of miRNAs in resistance to HER2 targeted therapies**

**Karen Howe**

Trastuzumab, a monoclonal antibody, and lapatinib, a tyrosine kinase inhibitor are approved treatments for HER2 positive breast cancer; however, patients that initially respond frequently develop resistance. The aims of this study were to investigate microRNA expression in acquired and/or innate trastuzumab and lapatinib resistant cell lines, and in a cohort of HER2 positive breast cancer patients.

Four miRNAs were identified as altered in the acquired trastuzumab resistant cell lines; miR-221, -222, -224 and -9. miR-221 and -224 are also involved in innate trastuzumab resistance. miR-221, -224, -30e-3p, -550, -92a and -9 are altered in acquired lapatinib resistant cells lines and miR-221 is associated with innate lapatinib resistance. These microRNAs are potential predictive biomarkers of innate and/or acquired resistance to HER2 targeted therapies.

*All-trans* retinoic acid (ATRA) treatment alone or in combination with trastuzumab or lapatinib may overcome resistance in some HER2 positive breast tumours. Co-amplification of retinoic acid receptor alpha (RAR $\alpha$ ) with HER2 may be a potential biomarker to predict benefit from combined ATRA and HER2 targeted therapies.

Over-expression of miR-221 and -222 in the SKBR3-P cell line does not confer resistance to trastuzumab. However, they increase the migratory potential of the SKBR3-P cell line. We identified miR-221, -222 and -9 expression is higher and miR-224 is lower in patients who did not achieve a durable complete response (non-DCR) compared to the DCR cohort. This miRNA profile may be predictive for acquired trastuzumab resistance.

This is the first report of the involvement of miR-222, -224 and miR-9 in innate and acquired trastuzumab and/or lapatinib resistance in HER2 positive breast cancer. These miRNAs represent potential biomarkers of resistance and ATRA treatment may be a potential therapeutic strategy to overcome resistance, in some cases.

# **Chapter One**

## **Introduction**

## 1.1. Introduction

Cancer is the abnormal growth of cells caused by multiple changes in gene expression leading to a dysregulated balance of cell proliferation and cell death ultimately evolving into a population of cells that can invade and metastasise to distant sites causing significant morbidity and, if untreated, death of the patient [1]. Breast cancer is cancer of the breast tissue and generally affects the ducts and lobules and can spread to distant sites via the lymph system (**Figure 1-1**) [2].

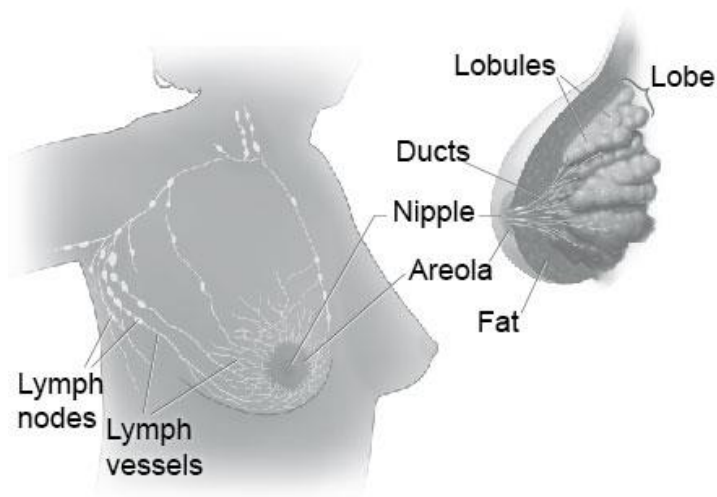


**Figure 1-1:** Overview of the anatomy of the breast [2].

Cancer is the second leading cause of death in Ireland. Breast cancer is the most prevalent form of invasive cancer, (excluding non-melanoma skin cancer) (2010-2012) as shown in **Figure 1-2**. The average incidence rate of female breast cancer is 122.7 women per 100,000 cases of breast cancer [3]. However, regular screening campaigns have increased the total number of reported cases since 2000. This and advances in treatment have led to improved prognosis and improved survival rates (>80% net survival).

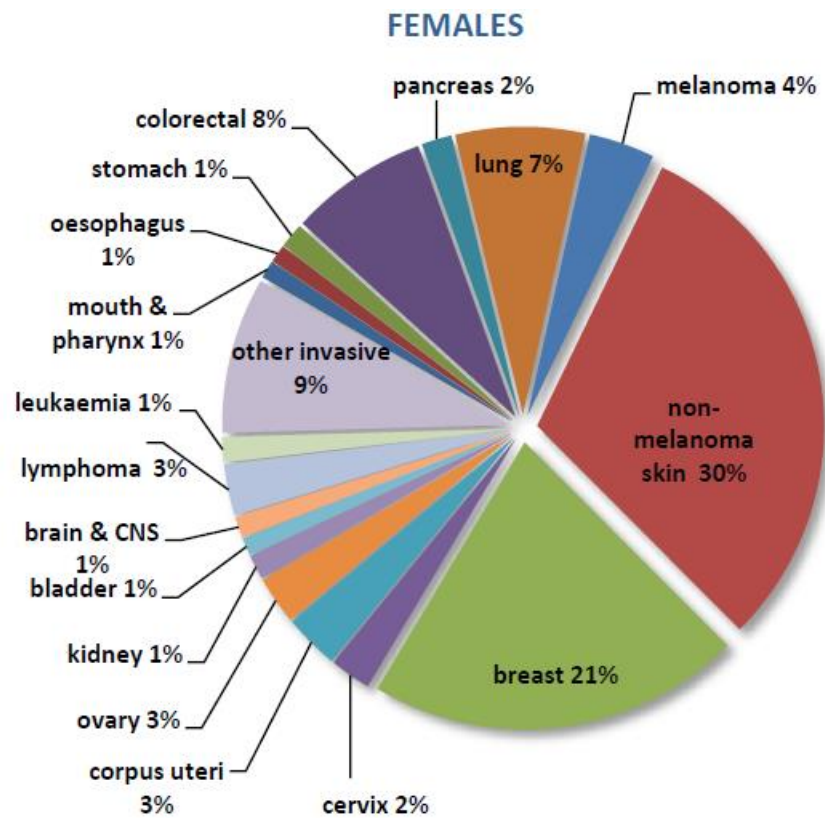


**Figure 1-2:** Relative frequency of the main invasive cancers diagnosed during 2010-2012 in females, in Ireland [3].

The causes of most cancers are unknown but there are some clues as to who may be at a higher risk of developing breast cancer. According to the Mayo Clinic risk factors include; age, being female, previous personal or family history of breast cancer, obesity, women who have never been pregnant or women who have undergone postmenopausal hormone therapies and UV radiation to name but a few. Family history and genomic changes are the strongest determinants of risk [4]. History of breast cancer in a person's family and mutations in genes known to be involved in cancer e.g. p53 and in breast cancer susceptibility genes breast cancer 1 and 2, early onset gene (BRCA1 and BRCA2) are often linked with the development of breast cancer [5].

## 1.2. Diagnosis of breast cancer

Initial identification of breast cancer can vary in each case with symptoms ranging from detection of lump(s), changes in the skin, nipple and size and shape of breast, unusual swelling and any pain in the general area [6]. Once recognised, further testing is carried out including a physical examination, imaging tests including x-rays and Computerized tomography (CT) scans, blood tests, biopsies, immunohistochemistry and surgical reports if the tumour has been excised [6]. Classification of cancer histology, stage, grade, estrogen receptor  $\alpha$  (ER) and human epidermal growth factor 2 (HER2) receptor status and whether cancerous cells have spread to the lymphatic system are extremely important determinants for prognosis and response to treatment plans [7].

## 1.3. Classification of breast cancer

Originally, cancer was typed according to the location that the cancerous cells occurred in e.g. breast, pancreatic, lung cancer. In the pre- molecular era, breast cancer was classified according to the histological/cellular type of tumour e.g. ductal, lobular, nipple or Paget's and whether it was *in situ*, invasive or inflammatory [8]. In the last decade with the introduction of high throughput micro arrays, breast cancer typing has taken a dramatic change. Perou *et al.* initiated the post molecular era by systematic investigation into a new classification system for breast cancer [9]. They examined gene expression patterns in tumour samples and found that specific genes expression patterns were associated with certain types of cancers. Perou *et al.* termed these the "intrinsic subtypes" as they are a representation of the intrinsic properties of these cancers [9]. Four subtypes with individual molecular features were distinguished to classify breast cancer (**Table 1-1**) [10].

Basal-like breast cancers are distinguished by their lack of ER, progesterone receptor (PR) and HER2 and are therefore termed triple negative tumours [11, 12]. However, not all basal-like breast cancers follow this “triple negative” behaviour as approx 25% do not concur with this classification [13]. These particular types of cancers contain high expression levels of cytokeratins 5 and 17, laminins, fatty acid binding protein 7 and growth factor receptors including epidermal growth factor (EGF), c-kit, hepatocyte growth factor (HGF) and insulin-like growth factor (IGF) [10, 11]. These tumours also contain high frequency of mutated p53 (tumour suppressor gene) and generally are associated with poor prognosis and weakened sensitivity to systemic therapy [14]. In 2007, it was found that retinoblastoma (Rb) protein was mutated in basal-like breast cancers [15] and that this along with the p53 mutation was the cause for the high rate of proliferation seen within this cancer subtype [13]. Another mutation that is commonly linked to basal-like cancer phenotype is the BRCA1 gene mutation [11, 16]. BRCA1 is a tumour suppressor gene that is involved in DNA repair, cell cycle and chromosome stability [17]. Women who have a deleterious mutation in the BRCA1 gene and develop breast cancer will most likely be diagnosed with the basal-like breast cancer subtype [13]. Overall, basal-like cancers are associated with shorter overall survival time and relapse-free survival [10].

**Table 1-1:** Microarray based classification of breast cancer subtypes including characteristic genes, immunohistochemistry (IHC) markers and clinical features. Abbreviations: ER- estrogen receptor, PR- progesterone receptor, HER2- human epidermal growth factor receptor 2, GRB7- growth factor receptor bound protein 7. Information adapted from [10, 18].

<b>Sub-type</b>	<b>IHC Markers</b>	<b>Clinical features</b>
<b>Basal-like</b>	ER-/PR-/HER2- and genes characteristic of basal epithelial cells and epithelial cytokeratins 5/6	High grade, strong association with BRCA1 mutation carriers, high risk of recurrence, responsive to chemotherapy and no known targeted treatment
<b>Luminal Subtype A</b>	ER+ and or PR+/ HER- and GATA binding protein 3, X-box binding protein 1, Trefoil factor, FOXA-1 and LIV-1 and luminal cytokeratins 8/18 and Ki-67 (Low)	Low grade, most common form of breast cancer, low risk of recurrence, responsive to endocrine therapy and some are less responsive to chemotherapy
<b>Luminal Subtype B</b>	ER+ and/or PR+/ HER2+, luminal cytokeratins 8/18 and Ki-67 (High)	Varies in grade and response to chemotherapy, responsive to endocrine therapy. If HER2+ is responsive to anti-HER2 strategies
<b>Normal-Like</b>	Similar genes as found in basal epithelial cells and adipose tissue	Samples are generally contaminated with normal breast tissue
<b>ERBB2+/HER2+</b>	ER-/PR-/HER2+ and high expression of genes on the 17q2FF4 amplicon incl; HER2, GRB7	High grade, involved in axillary lymph nodes at presentation, high risk of recurrence, responsive to chemotherapy, targeted therapies include trastuzumab (monoclonal antibody) & tyrosine kinase inhibitor lapatinib

Luminal breast cancers are generally cancers that originate from the luminal epithelial cells within the mammary gland [19] and were originally characterised by their high expression of the ER [9]. This subtype is classified as hormone receptor positive due to the expression of ER and PR [13]. In 2001, Sorlie *et al.* discovered that this luminal ER positive group could be divided into three subgroups- luminal A, B and C [10]. Luminal A cancers were distinguished by their high expression levels of the ER gene, low expression of HER2 and proliferation- associated gene Ki-67 and transcription factors (**Table 1-1**) [10]. Cancers of this subtype are generally associated with good prognosis and longest overall survival times [10] and are sensitive to therapy [11].

Luminal B and C cancers are often grouped together as they are both distinguished by intermediate levels of ER in comparison to the luminal A cancers [10]. In contrast to luminal A subtype, luminal B subtypes have lower expression of ER, higher expression of HER2, higher expression of Ki-67 and contain p53 mutations [13]. Due to this, luminal B breast cancers are generally of a higher grade and are insensitive to treatments [11].

Normal-like breast cancers are hard to distinguish as they share common factors with normal breast tissue as their name suggests. Classification of this group came after hierarchical clustering determined that it included genes that are expressed by adipose tissue and genes associated with basal epithelial cells (**Figure 1-3**) [10]. This normal-like breast subtype also clustered with the luminal A subtype due to their moderate expression of luminal epithelial genes [13]. Normal-like breast cancers are associated with moderate relapse free and overall survival rates [9].

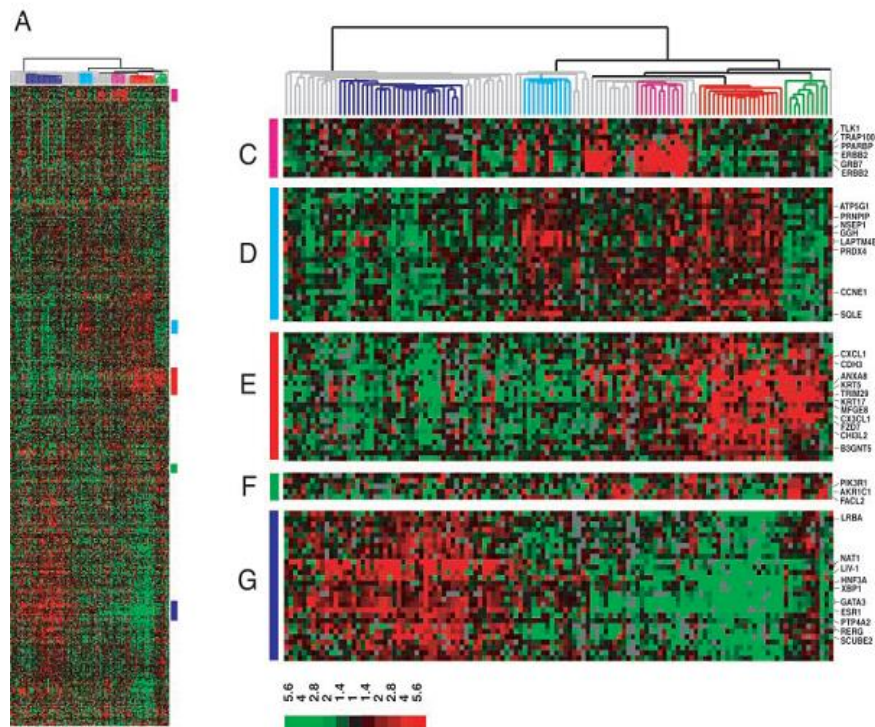


**Figure 1-3:** Statistical analysis and hierarchical clustering of 115 tumour tissues and 7 non-malignant tissues determined using the intrinsic gene set as per Perou *et al.* [9]. (A) Shows the entire cluster. C-G represents gene clusters grouping similar genes together. Gene clusters representing the ERBB2/HER2 oncogene and related genes (C), luminal subtype B (D), basal subtype (E), normal breast like subtype (F) and the ER positive luminal subtype A (G). Figure taken from [13].

HER2 positive breast cancers are distinguished by their over-expression of several genes on the HER2 amplicon at 17q22.24 including; HER2, GRB7, TGF $\beta$ 1-induced anti-apoptotic factor 1 and TNF-receptor associated factor 4 (TRAF4) [20] and their lack of expression of ER [18]. HER2 tumours have also been correlated with shorter survival times, high levels of recurrence, poor prognosis and have more involved lymph nodes [18]. This subtype will be dealt with in more details in section 1.4.

#### **1.4. Breast cancer treatment strategies**

Breast cancer treatment options include conventional therapies such as surgery, radiotherapy, chemotherapy, hormone therapy and targeted therapy. Determining the breast cancer subtype is crucial as different therapies are available for each subtype and they are often linked to prognosis, aggressive behaviour of tumour, survival and drug resistance.

##### ***1.4.1. Conventional therapies***

Surgery is the first step in treatment for most patients with early stage breast cancer, where the type of cancer and location of the tumour are deciding factors in the type of surgery carried out. Breast conserving therapy (lumpectomy) is used in the treatment of primary breast cancer that is small in size. A total mastectomy is carried out when the tumour has spread into other areas or is advanced, and in some of these cases chemotherapy may be given to shrink the size of the tumour prior to surgery. Lymph nodes are removed as a means of determining the extent of the cancer and if cancer is present in these nodes it confirms the cancer has metastasised and that further adjuvant treatment (hormonal or chemotherapy) is needed. Removal of the lymph nodes is not a curative measure but it is used to inform treatment decisions [21].

Radiation therapy is often part of a patient's treatment plan when diagnosed with primary breast cancer. It is normally the next step in treatment after surgery to ensure there are no remaining cancer cells around the excised tumour [21]. The principle of radiation therapy is using x-rays, gamma rays and charged particles to damage DNA directly or by the creation of charged particles (free radicals) within cells and therefore damaging the DNA [22].

Chemotherapy can be given to early stage breast cancer patients post-surgery to minimise the risk of recurrence (adjuvant treatment), however, it can also be given to patients with metastatic breast cancer to either shrink the tumour or to improve the patient's prolonged survival and quality of life. In early stage breast cancer, chemotherapy is normally given in combinations to patients, as this reduces the risk of resistance e.g.; [21].

#### **1.4.2. Targeted therapies**

Hormone therapy is used for breast cancers that are positive for the ER and PR. Tamoxifen is a non-steroidal anti-estrogen that also acts upon the ER to inhibit proliferation of breast cancer cells [21]. Aromatase inhibitors are used to block the production of estrogen and therefore prevent proliferation of breast cancer cells. There are irreversible and reversible inhibitors that either bind irreversibly or reversibly to aromatase. Antibody based therapies are a new generation of 'targeted therapies' that are specific to a molecular target that plays a vital role in tumour growth. Trastuzumab and pertuzumab are monoclonal antibodies and are examples of antibodies approved for the treatment of HER2 positive early stage and metastatic breast cancer by the U.S. Food and Drug Administration (FDA) in 1998 [23] and 2012 [24], respectively. As initial response rates with trastuzumab were low [25], small molecule inhibitors tyrosine kinase inhibitors (TKIs) were developed. Lapatinib is a first generation TKI, which targets both HER1 (EGFR) and HER2 and is approved for the treatment of metastatic HER2 positive breast cancer [26]. Second generation TKIs include neratinib (HKI-272) which targets HER1 and HER2 [27] and afatinib (BIBW-2992) [28] which targets all HER family members [29] and they are currently in clinical trials. More recently, ado-trastuzumab emtansine (T-DM1) (Kadcyla<sup>TM</sup>, Genentech) is an antibody-drug conjugate which is FDA approved for the treatment of HER2 positive breast cancer. It is

composed of the HER2 monoclonal antibody trastuzumab linked, via 4-(3-mercapto-2,5-dioxo-1-pyrrolidinylmethyl)-cyclohexanecarboxylic acid (MCC), to the cytotoxic chemotherapy drug emtansine. In 2013, the FDA approved T-DM1 for the treatment of HER2-positive, metastatic breast cancer [30].

### **1.5. HER2 positive breast cancer**

In 1981, HER2, originally designated *neu* was discovered in rat neuroblastomas that had undergone chemical induction and were found to have oncogenic properties [31]. *neu*/HER2 was described as 50% homologous to an epidermal growth factor receptor (EGFR) that was at the time unknown and contained 80% similarity to tyrosine kinases [32]. Schechter *et al.* discovered that *neu*/HER2 belongs to a family of EGF-like receptors that contain tyrosine kinase domains [33]. In 1987, Slamon *et al.* discovered that this gene is over-expressed and amplified in invasive breast cancer [34] and that this alteration of HER2 appears in approx 25-30% of breast and ovarian cancer [35]. Further studies confirmed that *neu*/HER2 is a prognostic factor as it was related to shortened disease free and overall survival among patients with amplified HER2 [34]. It is also a predictive factor in determining response to conventional cancer therapies [36]. In 2000, the HER2/ERBB2 positive subgroup was confirmed as a subtype of breast cancer in the microarray study carried out by Perou *et al.* [9]. This group is identified by high expression of the HER2 proto-oncogene that is located on the 17q22.24 amplicon along with other genes that are present at this region including GRB7 [10]. HER2 is over expressed or amplified in approximately 25% of breast cancer cancers [34] and is also identified by its low or non-expression of ER and PR. Diagnosis of this subtype of breast cancer in patients requires testing that measures the amplification of genes by fluorescent *in situ* hybridisation (FISH) or chromogenic *in situ* hybridisation (CISH)

[37]. HER2 over-expression induces increased proliferation, apoptosis suppression and increased formation of solid structures [38] and also increases the invasive potential of cells [39, 40]. Due to these factors, tumours of this subtype have a poor prognosis and are related to a shorter survival rate [18]. However, these subtypes are quite responsive to chemotherapy and trastuzumab (Herceptin™) [18].

In order to understand the HER2 positive subtype of breast cancer, the structure, mechanism of action and signalling pathways of the HER family needs to be explored. In 1984, this proto-oncogene was classified further by Schechter *et al.* [33] as being a 185-kilodalton glycoprotein that is associated with tyrosine kinase activity. HER2 is a member of the EGFR family [41]. This family is comprised of HER1 (EGFR/ErbB1), HER2 (ErbB2/neu), HER3 (ErbB3) and HER4 (ErbB4). This family are class I receptor tyrosine kinases (RTKs) [33]. These types of RTKs have specific structural features including an extracellular binding, transmembrane and an intracellular domain (**Figure 1-4**) [42].

## EGF Receptor

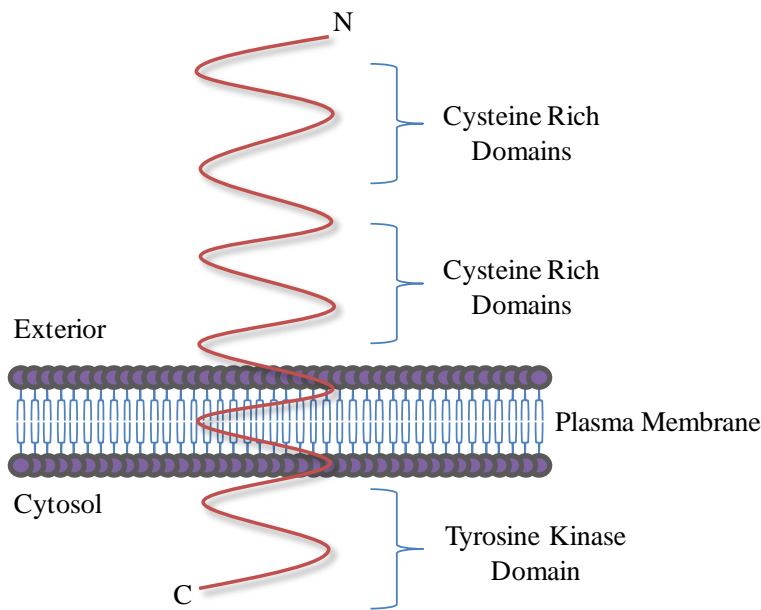


**Figure 1-4:** Structure of Class I Receptor Tyrosine Kinases showing the extracellular cysteine rich region and the intracellular tyrosine kinase region.

RTK domains have very specified roles. The extracellular domain is a region that contains two cysteine rich domains where ligands bind to induce a response [43]. ligands include transforming growth factor alpha ( $TGF\alpha$ ), EGF and amphiregulin (AR) for HER1 only. HER2 does not directly interact with ligands. Ligands for HER3 include neuregulin 1 and 2 (NRG1 and NRG2) Ligands for HER4 are NRG3 and NRG4. HER1 and HER4 share ligands including  $\beta$ -cellulin (BTC), heparin-binding EGF-like growth factor (HB-EGF) and epiregulin (EREG) (**Figure 1-5**).

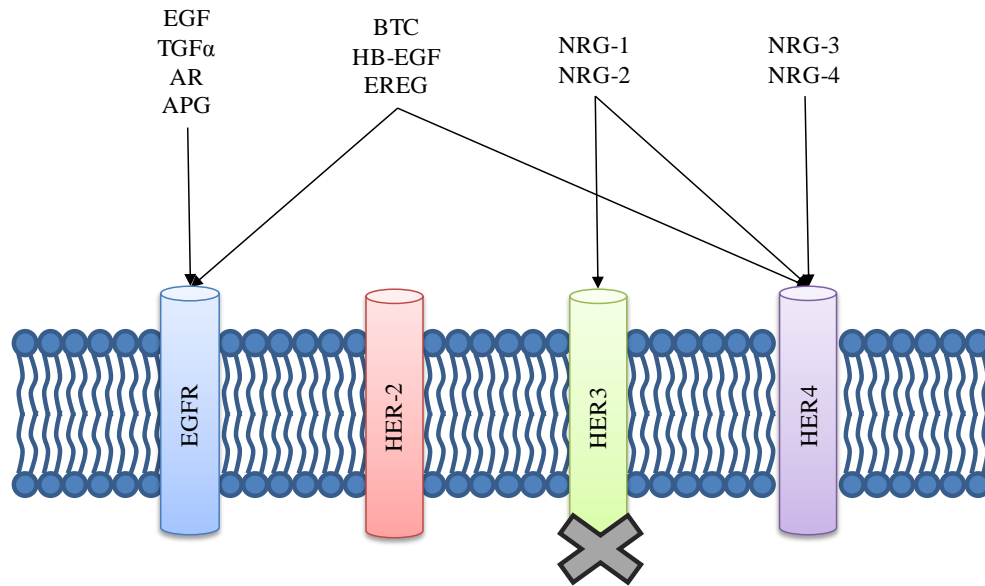


**Figure 1-5:** Ligands that bind to specific HER family members. Adapted from [44].

The intracellular domain contains the tyrosine kinase region and a carboxyl tail region where the phosphorylation sites reside [42]. This family of receptors are monomeric and upon ligand binding undergo dimerisation with other family members and can form either homo- or hetero-dimers depending on the dimerisation partner [37]. Once in dimer formation, the tyrosine residues in the intracellular domains cross-phosphorylate, activating the kinase domain leading to phosphorylation of substrates including signalling intermediates in the phosphatidylinositol-3 kinase/AKT (PI3K/AKT), Ras/mitogen activated protein kinase (Ras/MAPK) and phosphodiesterase phospholipase C $\gamma$ /protein kinase C (PLC $\gamma$ /PKC) pathways (**Figure 1-6**). HER2 has no known ligand and is activated only upon dimerisation with another HER2 receptor or other family members that have been activated by their specific ligands [37]. HER2 is the favoured dimerisation partner within this family and it also holds the strongest kinase activity and a lower ligand dissociation creating a strong prolonged signal [45].

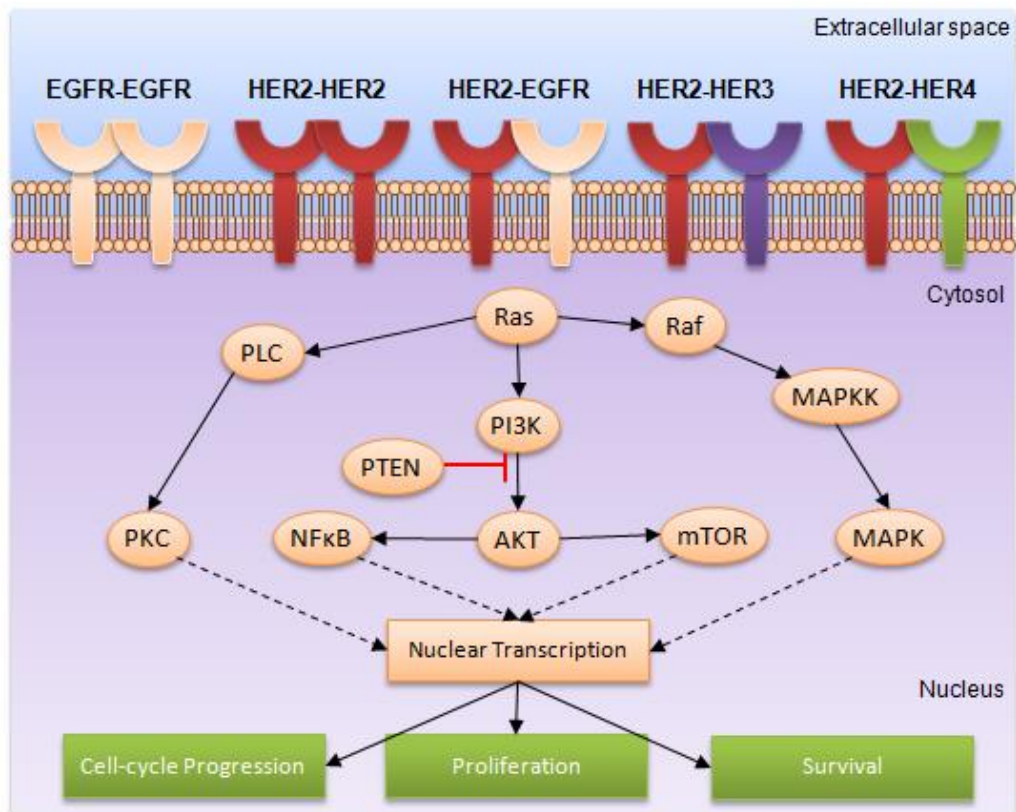


**Figure 1-6:** Overview of the HER-induced pathways. Ligand binding induces dimerisation between HER family members and induces tyrosine kinase properties of its intracellular domain resulting in activation of many downstream signalling cascades including; PI3K/AKT, Ras/MAPK and PLC/PKC pathway inducing cell proliferation, migration and survival. Adapted from [46].

These signalling pathways are the key to cell proliferation and survival as shown in (Figure 1-6). The PI3K/AKT pathway plays a role in cell growth and survival [37]. Briefly, PI3K is a protein which contains SH2 and SH3 domains which are activated upon binding to the RTK domains of HER receptors [47]. Once *neu*/HER2 is activated via dimerisation with HER3 in turn PI3K is activated [48]. This pathway involves the production of lipids (PIP2 and PIP3) which in turn activate protein kinase B (AKT), which is an inhibitor of the pro-apoptotic protein BAD which is involved in the promotion of apoptosis [37]. Inhibition of this protein therefore promotes cell survival. Regulation of this pathway is crucial in the balance of pro- and anti-apoptotic proteins

and determining cell survival and proliferation or cell death [49]. Phosphatase and tensin homolog deleted on chromosome 10 (PTEN) is a known tumour suppressor protein and is a key regulator of this pathway [50]. PTEN dephosphorylates the lipids that initially activate AKT and therefore drive apoptosis. AKT can also activate the mammalian target of rapamycin (mTOR) pathway via phosphorylation of tuberous sclerosis complex 1/2 (TSC1/2), a pathway which is involved in cell growth and proliferation [49]. This pathway regulates mRNA translation, ribosome biogenesis and nutrient metabolism and is crucial in cellular growth [49].

The Ras/MAPK pathway is frequently mutated in cancers. Briefly, activation of RTKs induces the recruitment of proteins that can further activate downstream signalling cascades. One such recruit is the growth factor receptor bound protein 2 (GRB2) which in turn recruits son of sevens (SOS) which regulates the Ras protein and downstream kinases including MAPK, MAPK kinase (MEK) and extracellular signal-related kinase 1/2 (ERK 1/2) [49]. Ras belongs to a family of small GTPases which when bound to SOS (guanine nucleotide exchange factor) undergoes dissociation to generate a Ras-GTP complex which activates a serine-threonine kinase, Raf-1 which phosphorylates MEK (threonine-tyrosine kinase), which in turn activates MAP kinase [51, 52]. This signalling cascade controls cell differentiation, cell proliferation and cell death [53], therefore disruption of this pathway can interrupt cellular control leading to cellular dysfunction.

Another pathway that is important in the HER kinase signalling cascade is the PLC $\gamma$ /PKC pathway. RTKs bind PLC $\gamma$  via Src 2 homology domains (SH2 domains) [54]. SH2 domains are involved in many important signalling pathways and protein-

protein interactions and function as adaptors for these reactions [55]. Phosphorylation of PLC $\gamma$  upon binding with the active HER2 dimer via these SH2 domains induces hydrolysis of PIP2 producing the second messengers inositol triphosphate (IP3) and diacylglycerol (DAG) [56]. These second messengers induce increased intracellular calcium concentration, which together with DAG activates PKC [56]. PKC initiates the MAPK pathway and therefore the expression of cyclin D, an important factor governing cell cycle progression from the G1 to S phase [57]. Cyclin D phosphorylates the tumour suppressor protein Rb [56] and is a key regulator of the cell cycle progression from G1 to S stage via phosphorylation of cyclin dependent kinases (CDKs), thus mediating cell proliferation [58].

#### **1.6. Current treatments for HER2 positive breast cancer**

Due to the nature of HER2 and its over-expression in breast cancer, its prognostic characteristics and its pathogenic and aggressive qualities, it has become a prime target for targeted therapies. There are important factors that have been taken into account when developing a HER2 targeted therapy including; the levels of HER2 in human cancer cells is much higher in relation to normal cells which suggests that the level of toxicity associated with anti-cancer drugs may be limited, levels of the receptor correlate with the pathogenesis, prognosis and disease free survival rate of HER2 breast cancer. HER2, due to its amplification/over-expression, is present in a high percentage of tumour cells and is found in the primary tumour site and metastatic sites indicating that targeted therapy would target most cancerous cells and all disease sites [59-61]. Monoclonal antibodies and TKIs are the two main types of anti-HER2 treatments that have been developed and are generally used in combination with chemotherapy (**Figure 1-7**)

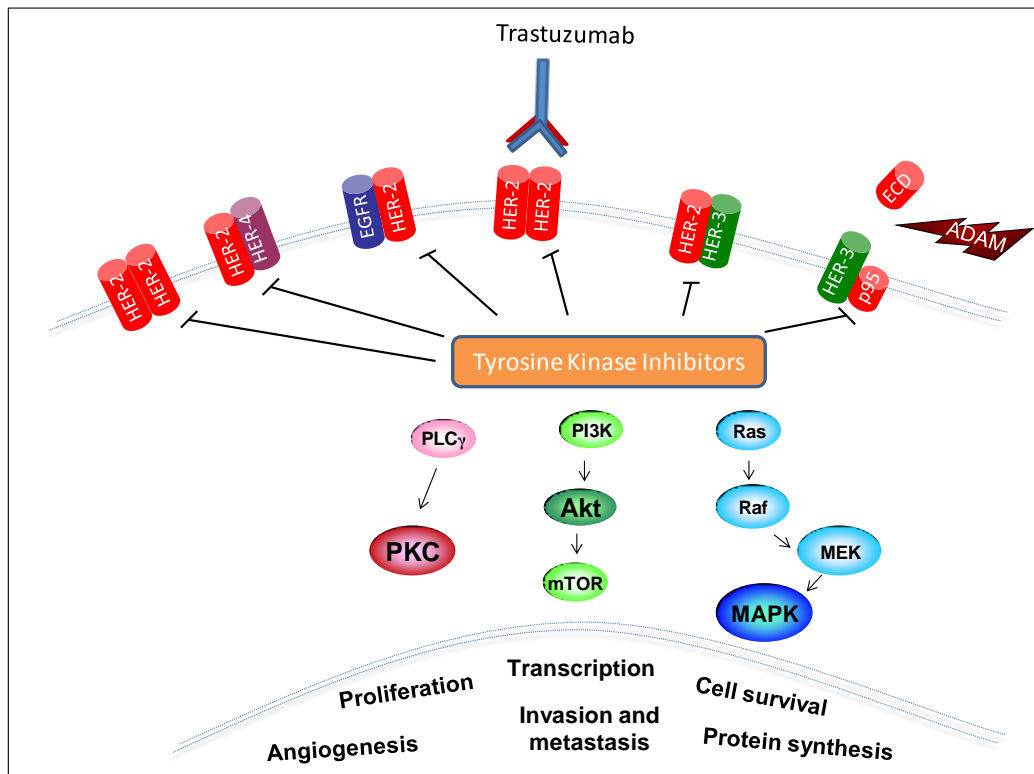


**Figure 1-7:** Inhibition of HER-2 signalling: Trastuzumab binds the extracellular domain of HER-2 dimers and reduces HER-2 signalling. The tyrosine kinase inhibitors (TKIs) include; lapatinib which reversibly inhibits the tyrosine kinase domain of HER-2 and EGFR; whereas neratinib, afatinib and dacomitinib are irreversible pan-Her inhibitors [62].

## 1.6.1 Trastuzumab- monoclonal antibody

### 1.6.1.1 Discovery and development of trastuzumab

The discovery and development of trastuzumab spans 2 decades and it is the most successful monoclonal antibody discovery for the treatment of breast cancer. It originally stemmed from two pivotal discoveries in the 1980s; the identification of 185 kDa phosphoprotein called *neu* [63] and the discovery that *neu*, or HER2 as it is now referred to, was up-regulated in 20-30% of human primary breast cancers [34]. Researchers saw this change as an attractive target for the development of possible new treatments. Several groups including researchers at Genentech developed murine

monoclonal antibodies directed against the extracellular domain (ECD) of HER2, p185<sup>HER2</sup> [64, 65]. Ultimately, Genentech Inc discovered a potent murine monoclonal antibody, muMAb 4D5 which significantly inhibited cell growth of HER2 over-expressing cell lines but had little effect on HER2 normal cell lines [66]. Tumour cell sensitivity to tumour necrosis factor was enhanced upon treatment with the 4D5 antibody [64, 67]. Further demonstration of this new antibody's efficacy came from its activity against human breast cancer xenografts [68]. Due to these potent anti-tumour effects, the 4D5 murine monoclonal antibody was chosen for further clinical development.

However, due to its murine origin the antibody was humanised to overcome the limiting factor of an anti-globulin response during therapy [69]. Utilising gene conversion and site-directed mutagenesis, Carter *et al.*, subcloned the hypervariable region of the muMAb 4D5 into plasmids encoding the IgG1 constant region and a human  $\kappa$  light chain to generate eight chimeric antibodies [70]. One variant, humAb4d5-8 bound three times more tightly to the ECD of p185<sup>HER2</sup> than the muMAb 4D5 and had anti-proliferative effects on the HER2 over-expressing cell line, SKBR3 [70]. Interestingly, humAb4D5-8 also mediated an antibody dependent cell cytotoxicity (ADCC) response against SKBR3 cells in the presence of human effector cells whereas the murine variant does not [70]. This vector was then transduced into Chinese hamster ovary (CHO) cells that are used in large scale production and was further purified [71]. Overall, this humanised monoclonal antibody, called trastuzumab (Herceptin<sup>TM</sup>), is 95% human and 5% murine and is specific for HER2 [71]. In 1998, this monoclonal antibody received approval for use in the treatment of metastatic breast cancer, alone or in combination with chemotherapy [72]. In 2006, trastuzumab was approved for treatment of early

breast cancer (postoperative or adjuvant setting) in combination with chemotherapy [73].

### ***1.6.1.2 Drug structure***

Trastuzumab is an immunoglobulin G (IgG1) monoclonal antibody composed of 1,328 amino acids and has a molecular weight of approximately 148 kDa [74]. It consists of two antigen specific sites derived from the murine 4D5, the human variable region and an IgG<sub>1</sub> conserved Fc portion (**Figure 1-8**) [70, 75].

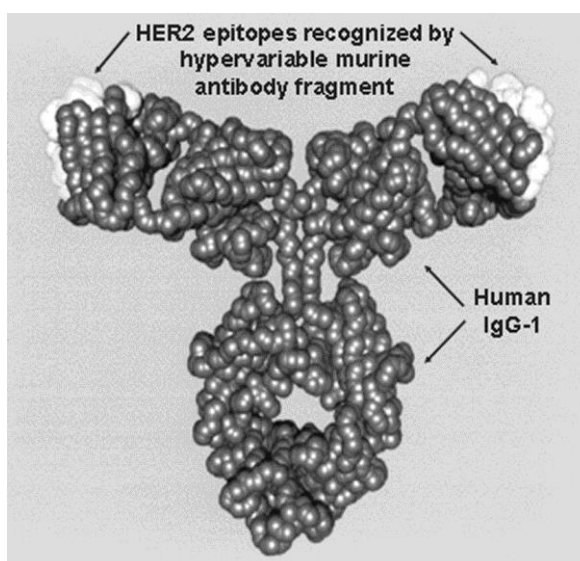


**Figure 1-8:** Overall structure of Trastuzumab monoclonal antibody. It is composed of a human IgG1 antibody (95%) which has two antigen specific epitopes for HER2. Reproduced from Ross *et al.* [76].

### ***1.6.1.3 Mechanism of Action***

Several mechanisms of action have been proposed for trastuzumab. The prevailing hypothesis is that the innate and adaptive immune system and a host of numerous other processes are involved (**Table 1-2**). Firstly, it has been suggested that trastuzumab accelerates the endocytic degradation of the HER2 receptor [77]. In 2000, Klapper *et al.* showed that upon trastuzumab binding, a ubiquitin ligase, c-Cbl, is recruited to its docking site and HER2 is ubiquitinated which ultimately leads to its degradation [78].

However, this degradation process is yet to be explored further. Upon over-expression, HER2 undergoes proteolytic cleavage which results in the extracellular domain (ECD) HER2 (110kDa) and a membrane bound truncated form, p95 in breast cancer cell lines and tissue extracts [79]. In 2001, Molina *et al.* proposed a new mechanism of action for trastuzumab, they detected p95 in over 50% of human breast cancer samples [80]. They demonstrated that trastuzumab treatment blocked shedding of the ECD of HER2 from breast cancer cell lines, and therefore inhibited production of p95. Further clinical studies have shown a correlation with the decrease in ECD HER2 in patient serum during trastuzumab treatment and tumour response and progression free survival [81, 82]. Overall, these studies indicate that trastuzumab may act by inhibition of HER2 cleavage.

Another mechanism that has been proposed is that trastuzumab acts by disrupting the ligand independent interaction between HER2/HER3 and the PI3K/AKT pathway. HER2 over-expression in HER2 amplified cells leads to ligand-independent activation of HER2/HER3 complexes and HER3 phosphorylation (**Figure 1-9**) [83]. This in turn activates the downstream PI3K/AKT pathway. Junttila *et al.* found trastuzumab inhibits this ligand-independent HER2/HER3 dimerisation and in turn down-regulates the PI3K pathway [83].

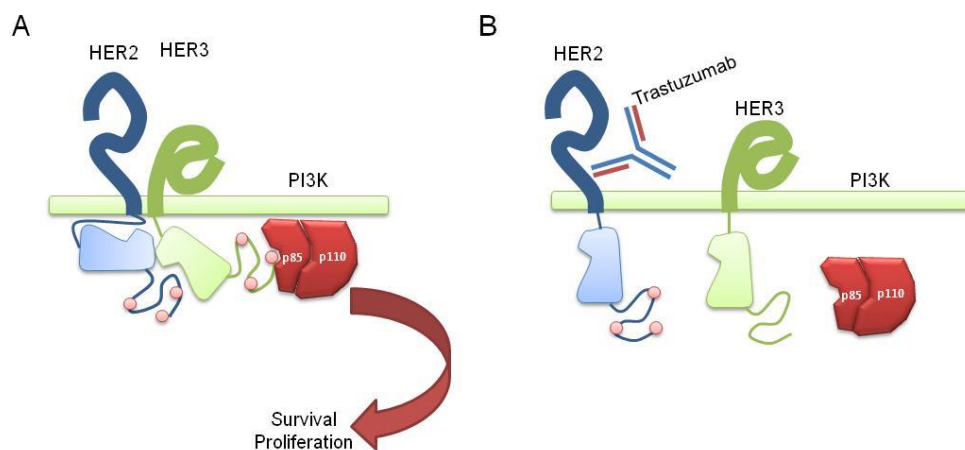


**Figure 1-9:** Ligand independent HER2/HER3 dimerisation upon HER2 over-expression and subsequent HER3 phosphorylation. (A) pHER3 activates the PI3K pathway which promotes cell survival and proliferation. (B) Trastuzumab disrupts the HER2/HER3 dimerisation which leads to HER3 dephosphorylation and inhibition of the PI3K pathway and cell proliferation. Adapted from [83].

Trastuzumab also reduces signalling via the MAPK pathways [84, 85]. Delord *et al.* demonstrated trastuzumab had an inhibitory effect on cell proliferation through the MAPK and AKT pathway in ovarian cancer [84]. Another method of PI3K pathway blockade was proposed by Nagata *et al.* which involves Src and PTEN [85]. They demonstrated that trastuzumab disrupts HER2/Src interactions leading to Src inactivation which in turn reduces PTEN phosphorylation, increases PTEN phosphatase activity and AKT dephosphorylation resulting in inhibition of cell growth [85]. Interestingly, downstream components of the PI3K pathway, p27 and Cdk2 have been shown to be involved in the molecular mechanisms of trastuzumab. Increased association with p27 and Cdk2 complexes results in the inactivation of Cdk2 which ultimately inhibits cell proliferation [86, 87].

Trastuzumab treatment is also associated with an immune response. ADCC mediated via natural killer (NK) cells has been shown to correlate with trastuzumab response

[88]. NK cells are activated upon binding of their Fc gamma receptors to the Fc domain of trastuzumab (**Figure 1-10**) [89]. Clynes *et al.* developed Fc receptor knockout mice and discovered that the cytotoxicity and anti-tumour ability was impaired indicating that the Fc/Fc $\gamma$  receptor interaction is important for the trastuzumab mediated ADCC [89]. Correspondingly, patients who responded to trastuzumab treatment had significantly higher levels of NK cells and ADCC [90]. They also identified a correlation between progression free survival and NK cells [90].

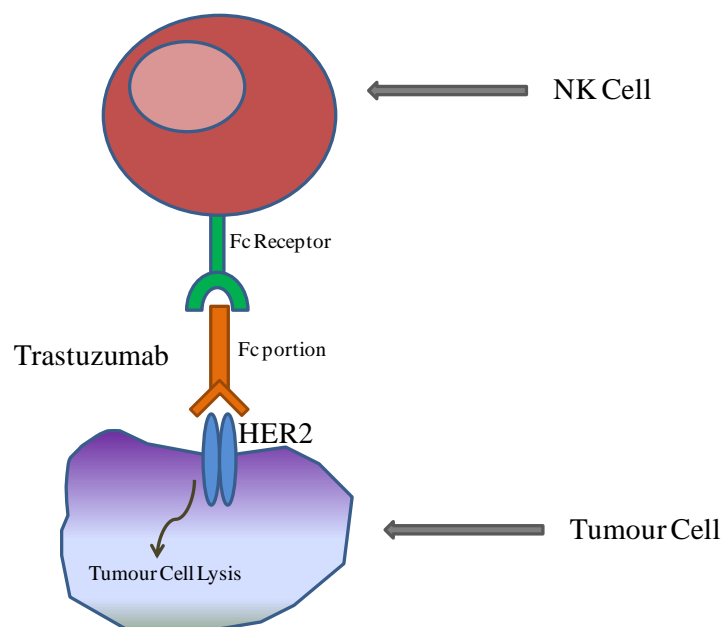


**Figure 1-10:** Activation of ADCC upon trastuzumab binding. NK cells which express the Fc gamma receptors in turn bind to the Fc domain of trastuzumab which leads to tumour cell lysis or apoptosis.

Trastuzumab has been shown to enhance apoptosis induction. Combination treatment of HER2 over-expressing cell line (BT474 and SKBR3) with trastuzumab and tumour necrosis factor-related apoptosis-inducing ligand (TRAIL) resulted in apoptosis [91]. Down-regulation of the HER2 receptor was shown to induce this TRAIL enhancement and inhibition of AKT activation [91]. In 2005, TRAIL and its association with

trastuzumab treatment were further investigated [92]. Similarly, they found an increased response to TRAIL in the SKBR3 cell line; however, they found trastuzumab decreased the BT474 cell line sensitivity to TRAIL. Down-regulation of the TRAIL receptor 1 and 2 was associated with inhibition of the HER2/PI3K/AKT pathway in BT474 cells but not SKBR3 cells. Apoptotic events including; caspase-8 activation, BH3 interacting-domain death agonist (BID) processing and Poly (ADP-ribose) polymerase (PARP) cleavage were inhibited in the HER2/PI3K/AKT-suppressed BT474 cells, and the authors surmised that HER2/PI3K/AKT pathway may play a cell-type specific pro-apoptotic role enhancing cells sensitivity to TRAIL [92]. Trastuzumab also enhances response to chemotherapy, most likely via enhanced induction of apoptosis [93].

Finally, HER2 positive breast cancer has been shown to correlate with increased angiogenesis [94]. Inhibition of angiogenesis may be another mechanism of trastuzumab action *in vivo*. Izumi *et al.* showed that trastuzumab suppressed angiogenesis via reduction in pro-angiogenic factors e.g.: vascular endothelial growth factor (VEGF) and promotion of anti-angiogenic factors e.g.: thrombospondin-1 only *in vivo* [95]. HER2 over-expressing cell lines were found to have an increase in VEGF expression at the mRNA and protein levels [96]. Klos *et al.*, discovered that inhibition of angiogenesis was greater in xenografts treated with a combination of trastuzumab and paclitaxel than the antibody alone [97]. Another important finding from their study was that AKT/PI3K and mTOR signalling pathways were involved in regulation of trastuzumab controlled VEGF activity [97]. Treatment with trastuzumab or silencing of HER2 resulted in a decrease in VEGF levels and interleukin-8 (IL-8) expression (pro-angiogenic factors) and an increase in thrombospondin (TSP-1) expression (anti-angiogenic factor) [98]. In BT474 xenografts in immunosuppressed mice, growth was

inhibited, microvascular density was decreased and the results corroborated with the *in vitro* study [98].

**Table 1-2:** Overall summary of proposed mechanisms of action of trastuzumab. Adapted from [99].

<b>Proposed mechanism of action</b>	<b>Details</b>
<b>Effects on HER2 levels</b>	Induction of HER2 receptor internalisation and degradation via endocytosis [64, 91, 100] Blocks cleavage of HER2 ECD suppressing formation of p95HER2 [80]
<b>Effects on dimerisation</b>	Disruption of ligand-independent HER2/HER3 interactions [83]
<b>Effects on downstream signalling</b>	Inhibition of PI3K and MAPK pathways [83, 84]
<b>Effects on cell cycle regulators</b>	Induction of p27, p21 [86] Cdk2 inhibition [87]
<b>Immune effects</b>	Stimulation of ADCC [90]
<b>Effects on apoptotic regulators</b>	Enhancing TRAIL-induced apoptosis [91]
<b>Effects on angiogenesis</b>	Reduction in VEGF levels and angiogenesis [95]

#### ***1.6.1.4 Mechanisms of Resistance***

Despite the success of trastuzumab in the clinic, *de novo* or acquired resistance is a problem, particularly for patients with metastatic disease. In a recent study of metastatic breast cancer patients treated with trastuzumab-containing regimens, it was reported that 9% of this cohort had a durable complete response [101]. Unfortunately many HER2 positive metastatic breast cancer patients have primary resistance [25], and patients who initially show a significant response frequently develop secondary resistance within a period of 1-2 years [60, 102]. Several resistance mechanisms have been proposed as outlined briefly in **Table 1-3**.

**Table 1-3:** Brief details of several proposed mechanisms of trastuzumab resistance.

<b>Mechanisms of Resistance</b>	<b>Details</b>
<b>PTEN loss &amp; PI3K/AKT activity</b>	<ul style="list-style-type: none"> <li>• Trastuzumab treatment resulted in PTEN membrane localisation and increased phosphatase activity, mediated by a reduction in PTEN tyrosine phosphorylation via Src inhibition [85].</li> <li>• Loss of PTEN and thus activation of the PI3K/AKT pathway correlated with trastuzumab resistance in a panel of HER2 positive breast cancer cell lines [103].</li> </ul>
<b>Alternative signalling pathways</b>	<ul style="list-style-type: none"> <li>• IGF-1R levels were increased in trastuzumab resistant cell line models (SKBR3-T) [104].</li> <li>• Inhibition of Met increases trastuzumab sensitivity [105].</li> <li>• Over-expression of HER3 and HER2 leads to HER2/HER3 heterodimers which activate the PI3K/AKT pathway [83]</li> </ul>
<b>Serum HER2 &amp; ECD shedding</b>	<ul style="list-style-type: none"> <li>• Retrospective studies have found an association with p95 HER2 expression and poor patient outcome and an aggressive phenotype [106, 107].</li> </ul>
<b>Over-expression of MUC4</b>	<ul style="list-style-type: none"> <li>• MUC4, a membrane bound glycoprotein binds and sterically hinders HER2 from binding to trastuzumab and knock-down of MUC4 leads to increased binding of trastuzumab [108].</li> </ul>
<b>Molecular chaperones</b>	<ul style="list-style-type: none"> <li>• Heat shock protein 90 (HSP90) is known to regulate the stability of HER2 which decreases receptor turnover and thereby strengthening HER2 signalling effects [109]</li> </ul>

### ***1.6.1.5 Biomarkers of trastuzumab resistance***

There is a critical incentive to elucidate biomarkers of trastuzumab resistance and identify patients prior to treatment that are unlikely to respond. As mentioned previously there are several mechanisms of both innate and acquired resistance hypothesised however, none have been successfully validated clinically. Multivariate analysis of core biopsies from the GeparQuattro trial, identified aldehyde dehydrogenase 1 (ALDH1) and phosphorylated 4E binding protein (p4E-BP1) as significantly up-regulated in patients who relapsed, suggesting that the mTOR pathway (p4E-BP1) and stem cells features (ALDH1) may play a role in trastuzumab resistance [110]. Markers of sensitivity are also being explored; phosphorylated HER2 and co-amplification of c-Myc and HER2 have been postulated as markers of trastuzumab/lapatinib sensitivity [111]. PTEN, c-Myc and p95 HER2 are predictive biomarkers that are currently being investigated in the ALTTO and NeoALTTO trials [112]. More recently, neuromedin (NmU) was identified as an extracellular biomarker of HER2 targeted therapy resistance. Over-expression of NmU was associated with both acquire and innate resistance to lapatinib, trastuzumab, neratinib and afatinib [113]. Ectopic over-expression of NmU in sensitive cell lines conferred resistance to all HER2 targeted therapies. However, the only validated predictive marker of response to anti-HER2 therapies is the over-expression and/or amplification of HER2.

## **1.6.2 Lapatinib- Tyrosine Kinase Inhibitor**

### ***1.6.2.1 Development and Discovery of Lapatinib***

Small molecules which target growth factors such as HER1 and HER2 were investigated as potential therapies in the late 1980's. Novel chemistry, kinase biochemical screening platforms and cell line testing identified potential molecules that selectively and potently target HER1 and HER2 [114]. *In vivo* xenograft models

combined with the previous *in vitro* research led to the identification of GW2016 (GW572016) which was later named lapatinib [114].

Lapatinib (Tykerb) is a reversible dual small molecule TKI which selectively inhibits both HER1 and HER2 [115]. Lapatinib can be administered orally, has a half life of 24-48 hours and there is evidence that lapatinib can cross the blood brain barrier [116]. In 2007, lapatinib was FDA approved for the treatment of metastatic HER2 positive breast cancer in combination with capecitabine in patients who have previously received prior treatment with anthracyclines, taxanes and trastuzumab [26, 115]. Patients with HER2 positive metastatic breast cancer who have previously been treated with trastuzumab may develop brain metastases due to the aggressive nature of this cancer type [116]. TKIs are small in size and are therefore able to cross the blood brain barrier [117] and in a preclinical murine model, lapatinib was found to inhibit formation of large metastases however, did not completely prevent further metastasis [118].

#### 1.6.2.2 Drug Structure

Lapatinib is present as the monohydrate of the ditosylate salt (**Figure 1-11**) [119]. It has a molecular weight of 581.1 g/mol and formula  $C_{29}H_{26}ClFN_4O_4S$ . It is a member of the 4-anilinoquinazoline class of kinase inhibitors.

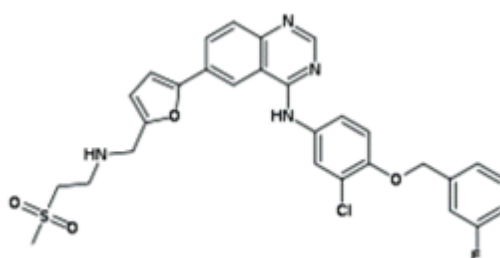


**Figure 1-11:** Chemical structure of lapatinib [120].

### ***1.6.2.3 Mechanism of Action***

The proposed mechanisms of action for lapatinib include inhibition of HER2 signalling, induction of cell cycle arrest and apoptosis, and induction of stress related responses (autophagy). The reversible binding to the ATP-binding site of both HER1 and HER2 and blocking their activation [121] leads to growth arrest and induces apoptosis in HER1 and HER2-dependent tumour cell lines [122]. However, lapatinib sensitivity is independent of HER1 status in HER2 over-expressing cell lines suggesting [123]. In tumour samples, lapatinib response also correlates with HER2 expression not HER1 expression [124, 125]. Inhibition of both MAPK-ERK1/2 and AKT by reducing the phosphorylation of HER1 and HER2 in HER2 positive breast cancer cell lines and human tumour xenografts [122]. Functional genomic studies carried out by Hegde *et al.* comparing lapatinib responsive cell lines (BT474 and SKBR3) to non-responsive cell lines (MDA-MB-468 and T47D) found differential expression of members of the AKT pathway. AKT1, MAK9, HSPCA, IRAK and CCND1 were down-regulated in lapatinib responsive and FOXO3A, which is negatively regulated by AKT, was up-regulated in lapatinib responsive cells. The ER and PR receptors were stimulated upon treatment with lapatinib and genes involved in cell cycle control, glycolysis and fatty acid metabolism were altered [126].

Lapatinib induces apoptosis by inhibition of AKT in HER2 positive breast cancer cells and human tumour xenografts [122], and inhibition of survivin [127]. Survivin is an inhibitor of apoptosis (IAP) which can protect breast cancer cells from apoptosis and down-regulation has been observed in HER2 breast cancer patients treated with lapatinib [127, 128]. Induction of cell cycle arrest occurred in HER2 positive breast cancer cells (G1 accumulation) upon treatment of HER2 positive cells with lapatinib

[123]. Lapatinib has also been associated with an increase apoptosis protein Bcl-2 interacting mediator of cell death (BIM) through inhibition of the MAPK signalling pathway [129]. The anti-apoptotic protein, myeloid cell leukemia 1 (MCL-1) has been show to be increased in response to lapatinib treatment [130].

Autophagy has been reported as a potential mechanism of lapatinib action in chronic myelogenous leukemia (CML) K562 cells [131] and HER2 breast cancer cells [132]. In BT474 and AU565 HER2 over-expressing cells increased levels of cleaved caspase-3 and PARP, and autophagy were detected in response to lapatinib treatment [132]. They also observed induction of apoptosis, upon pre-treatment with a specific autophagy inhibitor, 3-methyladenine (3-MA). This suggests that lapatinib treatment induces autophagy to initiate cell death.

Another potential mechanism of action is the through inhibition of the HER2/AKT/mTOR pathway. Lapatinib sensitivity is associated with decreased AKT and p70S6K phosphorylation [133]. Inhibition of mTOR by rapamycin caused an increase in lapatinib sensitivity and reduced phospho-AKT levels in lapatinib insensitive cells. Combination treatment with rapamycin and lapatinib synergistically inhibited cell proliferation and reduced tumour growth *in vivo*, in innately trastuzumab resistant breast cancer cells. This suggests that trastuzumab resistance and poor response to lapatinib treatment may be overcome by simultaneous mTOR inhibition.

Lapatinib treatment has been reported to increase the phosphorylation of 5' AMP-activated protein kinase (AMPK), which is involved in the mammalian target of rapamycin complex 1 (mTORC1) complex. AMPK activation regulates tumour growth

through mTOR inhibition which led to decreased protein synthesis [134]. Lapatinib treatment has not been previously associated with cardiotoxicity and a lapatinib analogue, GW2974, protects cardiomyocytes from apoptosis through the activation of AMPK [135]. AMPK switches cells from an anabolic to catabolic state of metabolism suggesting lapatinib induced activation of AMPK is necessary to induce apoptosis in tumour cells while protecting cardiac cells.

#### ***1.6.2.4 Lapatinib and trastuzumab***

Preclinical data determined that lapatinib and trastuzumab combination treatment was synergistic in HER2 over-expressing cell lines [136]. Interestingly, lapatinib also retained activity on acquired trastuzumab resistant cell lines which suggests that lapatinib alone or in combination with trastuzumab may overcome trastuzumab resistance. This was investigated by Blackwell *et al.* in a randomised phase III clinical trial where the combination significantly improved progression free survival and overall survival compared to lapatinib alone despite relapse on a previous trastuzumab based therapy [137, 138]. Further preclinical studies suggest that dual target of HER1/HER2 with lapatinib and trastuzumab in combination with chemotherapy improves response compared to either agent alone [139]. However, more recently, results were presented at the American Society of Clinical Oncology (ASCO 2014) from the ALTTO trial showed that lapatinib in combination with trastuzumab was no more effective than trastuzumab treatment alone [140].

In the neoadjuvant setting, two pivotal trials have investigated the efficacy of lapatinib in combination trastuzumab. The NeoALTTO trial hypothesised that administering two anti-HER2 therapies would be greater than one [141]. This phase III study investigated lapatinib plus paclitaxel versus trastuzumab plus paclitaxel versus combined lapatinib

and trastuzumab plus paclitaxel when administered as neoadjuvant therapy in HER2 positive breast cancer patients. Patients received the HER2 target therapies alone for 6 weeks and then in combination with paclitaxel for a further 12 weeks. Following surgery, patients received adjuvant chemotherapy with fluorouracil (5FU), epirubicin and cyclophosphamide (FEC) followed by 1 year of the same targeted therapy in the neoadjuvant stage. pCR was significantly higher in the lapatinib and trastuzumab arm (51.3 %) compared to trastuzumab (29.5 %) or lapatinib alone (24.7 %). Another randomised phase III clinical trial, GeparQuinto investigated the efficacy and safety of lapatinib versus trastuzumab when added to an anthracycline-taxane-based neoadjuvant chemotherapy regimen [142]. Patients received four cycles of epirubicin plus cyclophosphamide (ECL) plus neoadjuvant treatment of trastuzumab (ECH-TH) or lapatinib (ECL-TL) before surgery. The pCR rate for the ECH-TH arm was 30.3 % and 22.7 % in the ECL-TL. Substantial toxicities were seen in the ECL-TL arm and 33.1 % of patients withdrew from this arm due to adverse events. Trastuzumab showed a better clinical outcome in the neoadjuvant setting than lapatinib alone; however, long term follow up is ongoing.

The CHER-LOB neoadjuvant trial reported an 80 % increase in pCR rate in the chemotherapy plus trastuzumab and lapatinib arm compared with chemotherapy or trastuzumab or lapatinib alone [143]. The NSABP-B41 trial found similar pCR rates between the lapatinib and chemotherapy arm (52.5 %) and the trastuzumab and chemotherapy arm (53.2 %) however, dual blockade seems more favourable (62.0 %) than either agent alone but the difference was not statistically significant [144].

### 1.6.2.5 Mechanisms of Resistance

Lapatinib has been shown to overcome trastuzumab resistance in HER2 over-expressing cell lines that are trastuzumab resistant [123]. However, resistance to lapatinib is also an emerging problem [145]. Several mechanisms of resistance have been proposed as outlined briefly in **Table 1-4**.

**Table 1-4:** Brief details of several proposed mechanisms of lapatinib resistance.

<b>Mechanisms of Resistance</b>	<b>Details</b>
<b>Over-expression of AXL</b>	<ul style="list-style-type: none"> <li>Increased AXL expression was identified by western blotting, mass spectrometry and qRT-PCR in a lapatinib resistant cell line model [145]</li> </ul>
<b>Induction of autophagy</b>	<ul style="list-style-type: none"> <li>In lapatinib resistant cell lines, there was increased levels of the autophagosome and that treatment of these cells with an autophagy inhibitor re-sensitised the cells to lapatinib [146]</li> </ul>
<b>Over-expression of MCL-1</b>	<ul style="list-style-type: none"> <li>A BCL-2/BCL-X(L)/MCL-1 inhibitor (obatoclax-GX15-070) restored lapatinib sensitivity in the HT116-parental and HT116-lapatinib resistant colon cancer cells [147].</li> </ul>
<b>Re-activation of the Estrogen Receptor</b>	<ul style="list-style-type: none"> <li>Gene expression analysis of lapatinib resistant cell lines compared to parental cells correlated ER signalling with the development of resistance to lapatinib [148].</li> </ul>
<b>Over-expression of XIAP</b>	<ul style="list-style-type: none"> <li>Overexpression of XIAP and resistance to apoptosis was found in lapatinib resistant inflammatory breast cancer cells: SUM-190 (HER2 over-expressing) and SUM-149 (HER1 activated) [149].</li> </ul>
<b>Up-regulation of Src kinase activity</b>	<ul style="list-style-type: none"> <li>Increased phosphorylation of Src family kinases was found in six lapatinib resistant cell lines and inhibition of Src blocked PI3K-AKT signalling and lapatinib sensitivity was restored [150]</li> </ul>

Any of these potential resistance mechanisms may also serve as potential predictive biomarkers to lapatinib resistance.

## **1.7. microRNAs**

### ***1.7.1 Introduction***

In 1993, during the study of the gene *lin-14* in *C.elegans* development, the first microRNA (miRNA), *Lin-4*, was discovered by Victor Ambros. They found that *lin-14* abundance was under regulation of a short RNA product encoded by the *lin-4* gene, which regulates timing in larval development in worms [151]. miRNAs are a family of 21–25-nucleotides-long RNAs expressed in a wide variety of organisms ranging from plants to worms and humans [152]. miRNAs account for greater than 3% of all human genes [153]. They regulate gene expression sequence specific recognition of their target mRNAs. miRNAs play vital roles in apoptosis, control of growth in development, cell proliferation and stem cell properties [154-157]. In 2005, it was discovered that there are great changes in miRNA expression in cancers and in the development of tumours [158, 159]. By 2013, over 2000 miRNAs were found to be encoded by the human genome and the searchable miRNA database, miRBase version.21 has 5,441 mature miRNA sequences [3]. However, validation of miRNAs and their potential mRNA target interactions by experimental approaches has been limited [160]. miRNA genes are non-randomly distributed in the human genome and some are found within clusters sharing the same promoter [161]. Interestingly, miRNA genes are frequently located near tumour susceptibility loci in mouse cancer models [162] and deleted or amplified genomic regions [21].

### 1.7.2 *miRNA biogenesis*

There are two broad categories of miRNA promoters: intergenic and intragenic [22, 163]. Intergenic miRNAs are located between genes and their transcription is independent of coding genes as they are transcribed by RNA polymerase II (RNAPol II) [117]. This suggests the miRNAs form independent transcriptional units [118]. Intragenic miRNAs are located within exons or introns of protein coding genes [116] and are transcribed by RNAPol II as part of their hosts transcription. miRNAs were found among repetitive elements that are transcribed by RNAPol III and processed the same way [164]. The biogenesis of a mature miRNA occurs in a stepwise fashion (**Figure 1-12**) where, firstly, the miRNA gene undergoes transcription by RNAPol II to produce a pri-miRNA [165]. These pri-miRNAs are 5'-7-methylguanosine capped, spliced and 3'-polyadenylated [124]. Pre-miRNAs have a coding capacity for one or more mature miRNAs and are then processed by Drosha family of enzymes (double stranded RNA specific ribonuclease), DGCR8 or Pasha (ds-RNA binding protein that dimerises with Drosha) in the nucleus and produce 70-100 nucleotide hairpin miRNAs called pre-miRNAs [152]. This pre-miRNA is transported to the cytoplasm in a Ran-GTP dependent manner via Exportin-5 (nuclear export factor) [166, 167]. These pre-miRNAs are cleaved by Dicer and TRBP (human immunodeficiency virus (HIV) transactivating response RNA (TAR) binding protein) into an approximately 20 nucleotide miRNA duplex [168]. One of these strands functions as mature miRNA and is guided into an effector complex called the miRNA-containing ribonucleo-protein particle (miRNP), which is similar to the RNA induced silencing complex (RISC) [152, 169], via the argonaute family protein (Ago) to form the mRISC complex [170]. This complex is guided to its target mRNA via complementary base pairing between the miRNA and its target mRNA 3' untranslated region (UTR) and thus negatively

regulates mRNA [152]. The other strand in the duplex undergoes degradation [171]. Once sequence complementarity has been established between the miRNA and the target mRNA, the miRNA:RISC complex mediates gene repression by translational repression, mRNA target cleavage and mRNA deadenylation.

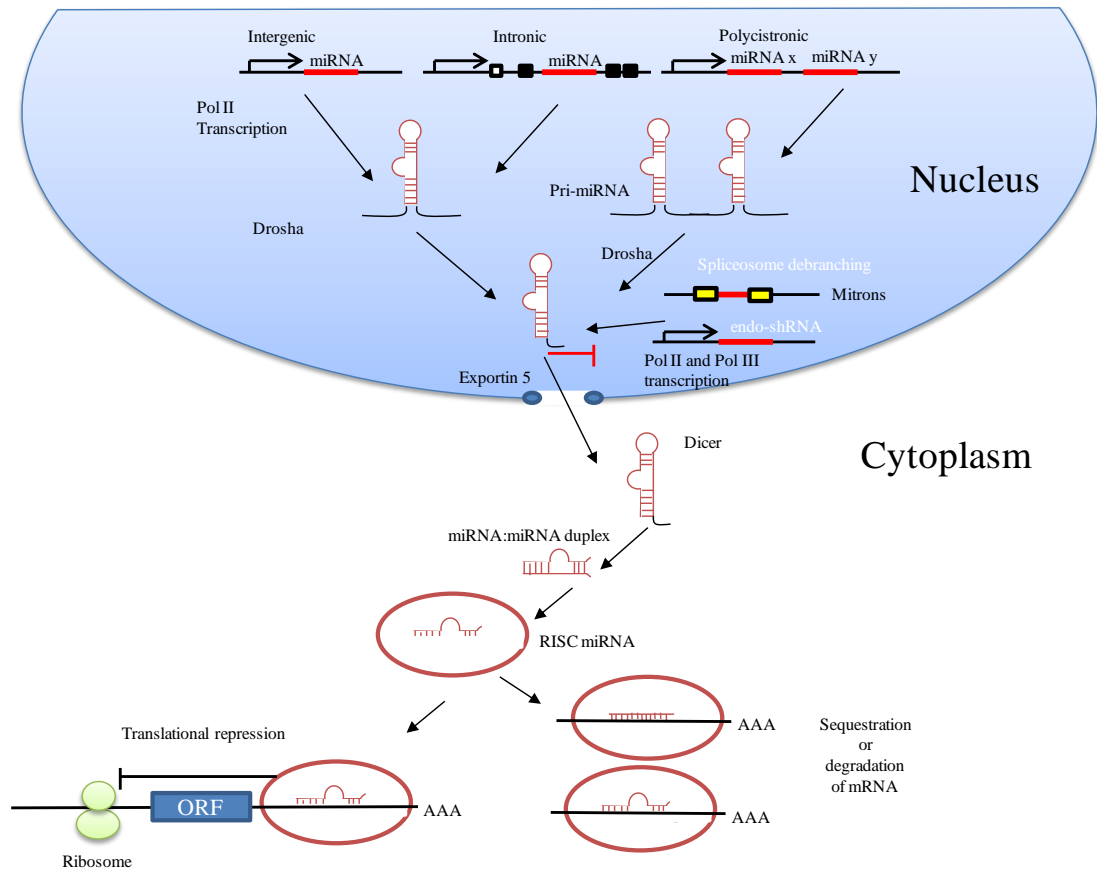


**Figure 1-12:** Overview of miRNA biogenesis. Adapted from [126] .

### 1.7.3 miRNA function

Primarily, miRNA function in gene expression repression carried out by mRNA cleavage, mRNA degradation and translational repression [172]. However, it has been reported that miRNAs may exert their effects directly and/or indirectly on the gene in response to external conditions [127]. The outcome is also dependent on the strength of the miRNA:mRNA interaction and the repressive effect of the miRNA [127, 173]. The mode of post-transcriptional control is determined by the sequence complementarity

between miRNA and its target mRNA based on Watson-Crick pairing of miRNA 5'proximal seed region (nucleotide 2-8) to the 3'UTR match site in the target mRNA [174]. It has also been reported that miRNAs can target the 5'UTR and/or coding region of their target mRNAs [175, 176]. Multiple miRNA-Recognition Elements (MREs) of a single miRNAs are present within the 3' UTR of several mRNA transcripts and several MREs belonging to different miRNAs can be found within the same UTR resulting in synergistic miRNAs [177]. As previously mentioned, miRNAs exert their function as gene regulators. In 2010, gene regulation was reportedly carried out by mRNA cleavage, mRNA degradation and translational repression [172]. The RISC complex contains Ago protein members (1-4), however, Ago-2 has been implicated as the main driving force in miRNA:mRNA cleavage [178, 179]. The mode of post transcriptional control is determined by the sequence complementarity between miRNA and its target mRNA. mRNA target cleavage occurs when complete near-perfect base-pairing occurs between miRNA and its target mRNA and is carried out by the attached Ago2 protein only [171, 180]. Partial sequence complementarity between miRNA and its target mRNA results in mRNA degradation and translational inhibition by Ago2 and Ago4 [172, 180]. miRNA target specificity may be changed due to alterations in the seed sequence depending on the Drosha/Dicer-dependent addition or deletion of 1-2 nucleotides in the 5' and 3' ends of miRNAs [181]. Translation occurs through a number of steps including initiation, elongation and termination [180]. miRNAs are reported to repress translation during initiation or post initiation [182]. However, recent years, nine potential mechanisms have been reported for miRNA function. Morozova *et al.* detailed a model of the potential mechanisms of miRNA function based on literature analysis [183]. Nine potential mechanisms of action have been detailed (M 1-M 9)

(**Table 1-6**) including cap inhibition, elongation inhibition, ribosome drop-off and mRNA decay. The proposed model of these mechanisms is shown in **Figure 1-13**.

**Table 1-5:** Proposed mechanism of action of miRNA function as detailed by Morozova *et al.* [183].

Mechanism No	Proposed Mechanism
<b>M 1</b>	Cap Inhibition (Inhibition of translation initiation via cap-40S association)
<b>M 2</b>	60S Joining Inhibition (Inhibition of translation initiation via 40S-AUG-60S association)
<b>M 3</b>	Inhibition of elongation
<b>M 4</b>	Ribosome drop-off (premature termination)
<b>M 5</b>	Cotranslational protein degradation
<b>M 6</b>	Sequestration in P-bodies
<b>M 7</b>	mRNA decay (degradation, destabilization)
<b>M 8</b>	mRNA cleavage
<b>M 9</b>	Transcriptional Inhibition (miRNA-mediated chromatin reorganization following by gene silencing)

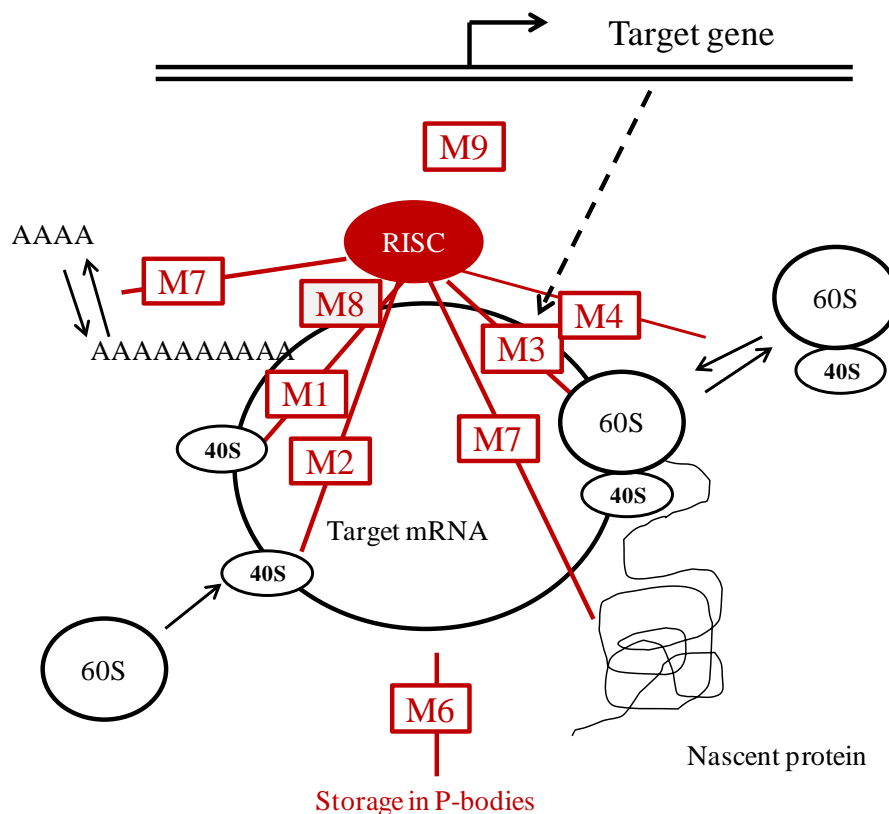


**Figure 1-13:** Overview of proposed mechanisms of miRNA action (Black). Mechanisms of gene expression from DNA to protein (Red). The mechanisms (M) are numbered as in Table 1-6. Adapted from [183].

#### 1.7.4 Roles of miRNA

miRNA have many physiological functions such as developmental timing, cell proliferation and differentiation, apoptosis, disease and anti-viral defence [171]. Due to the regulatory nature of miRNAs, it is extremely likely that they play a role in cancer. Studies carried out on the mir-17-92 cluster showed that miRNAs can modulate tumour formation and that this cluster is a potential oncogene [158]. It has been reported that miRNA expression is dysregulated in many human cancers and in breast cancer [184]. In 2005, it was reported that certain miRNAs were differentially expressed in breast cancer tissue in comparison to normal breast tissue [184]. Some were found to be down-regulated: miR-10b, miR-125b and miR-145 and others up-regulated: miR-21 and miR-

155 [184]. Recently, miR-21 has been identified as an oncomiR along with other miRNAs in glioblastoma multiforme (GBM) [185]. miRNAs have been found to be predictive of the receptor status in breast cancer [186]. miRNAs have reported roles in metastasis and tumour invasion [187], [188, 189]. Some miRNAs function as metastasis suppressors [188]. In 2005 it was reported that miRNA expression profiles may classify cancer types [190]. More recently, Ganepola *et al.* discovered a panel of three miRNAs that could be used as diagnostic markers for early pancreatic cancer [191]. A miRNA panel was identified from patient plasma samples as a predictive biomarker panel for early diagnosis of gastric cancer [192]. These small molecules may also provide useful in the detection and profiling of cancers. In September 2010, the American Association for Cancer Research (AACR) released a press release for a miRNA-based screening tool that can be used to detect early stage colorectal cancer [193].

#### ***1.7.5 miRNAs and HER2 positive breast cancer***

miRNA expression correlates with the receptor status of breast cancer [186]. ER, HER2 and PR status were analysed and miRNAs were identified which are capable of distinguishing tumours with different hormone receptors status [186]. miR-183 has been implicated in HER2 positive breast cancer as it is significantly increased in HER2 positive tumours in comparison to HER2 negative tumours [194]. Synthetic miRNAs targeting over-expressed protein have been shown to reduce HER2 levels in ovarian cancer cells [195], suggesting a potential role for miRNA targeting therapies for breast cancer.

Many miRNAs that potentially regulate the HER2 proto-oncogene have been identified. In 2006, a bioinformatical search revealed that miR-125a and miR-125b target

sequences are within the 3'UTR of HER2 and HER3 [196]. In experiments using the HER2 over-expressing cell line, SKBR3, transfection with miR-125a and miR-125b retroviral constructs resulted in the suppression of the HER2 and HER3 at the mRNA and protein level [196]. Suppression of AKT/PI3K and ERK1/2 activation occurred in these transfected cells. Another interesting finding was that in these transfected cells there was a reduction in migration and invasion [196]. Target elements for miR-584d-3p and miR-559 were also identified in the 3'UTR of HER2 [197]. Determination of the miRNA-mRNA interactions showed that both of these miRNA interact specifically with the 3'UTR of HER2 mRNA [197]. Transfection of both miRNAs together caused repression of HER2 mRNA whereas either mRNA alone did not [197].

In the SKBR3 and BT474 HER2 positive breast cancer cell lines, microarray analysis showed that miR-194 was up-regulated in both cell lines after treatment with trastuzumab [198]. MiR-194 over-expression inhibited cell migration/invasion *in vitro* and inhibited cell growth *in vivo* and knockdown of miR-194 increased cell migration. A link between miR-194 and talin 2 (cytoskeleton protein) was determined and over-expression of miR-194 down-regulated levels of talin2 indicating it is a direct target of miR-194. miR-337 and -305f were identified as over-expressed whereas miR-139 and -129 were identified as under-expressed in HER2 positive breast and gastric cancer patients samples [199]. miR-4728 is encoded within the intron of the HER2 gene and found to regulate expression of ER alpha [200].

#### ***1.7.6 miRNAs and trastuzumab resistance***

In 2010, a link between the PTEN tumour suppressor, miR-21 and trastuzumab resistance was reported [201]. Over-expression of miR-21 in HER2 over-expressing cell lines was shown to correlate with reduced levels of PTEN expression which led to

trastuzumab resistance [201, 202]. High levels of miR-21 expression is also associated with aggressive disease [201]. Another study found that miR-21 was up-regulated by HER2 signalling and this promoted cell invasion [203]. This miRNA is up-regulated via the Ras/MAPK pathway upon HER2/*neu* stimulation and the metastasis suppressor protein programmed cell death 4 (PCD4) is down-regulated by miR-21 in HER2 over-expressing breast cancer cells [203]. More recently, miR-21 expression was evaluated in HER2 positive and negative tumours, however miR-21 up-regulation did not predict resistance to trastuzumab [204]. In 2011, Jung *et al.*, investigated plasma levels of miRNA in breast cancer patients and revealed altered expression of miR-210. This was confirmed in trastuzumab resistant cells compared to trastuzumab sensitive cells. miR-210 circulating levels were significantly higher in patients who had residual disease than those who achieved pCR, before surgery than after surgery and in patients whose cancer had metastasised to the lymph nodes [205]. These results suggest that plasma levels of miR-210 maybe used to predict response to trastuzumab therapies [205]. Over-expression of miR-375 restored sensitivity to trastuzumab resistant SKBR3 cells *in vitro* and IGF1R was determined as a direct target [206]. miR-221 was identified as a promoter of trastuzumab resistance and was involved in inhibition of apoptosis and promotion of metastasis in HER2 positive breast cancers. PTEN was identified as a direct target of miR-221 and potential targeting of miR-221 along with trastuzumab may improve overall patient benefit [207]. In trastuzumab resistant SKBR3 cells, miR-220c was identified as the most significantly down-regulated miRNA [208]. Zinc finger protein 217 (ZNF217) was identified as a target and through restoration of miR-220c expression and silencing of ZNF217 trastuzumab sensitivity was restored and invasion was suppressed in the SKBR3 trastuzumab resistant cell lines.

### ***1.7.7 microRNAs and Lapatinib resistance***

To date only three studies have investigated miRNA expression in lapatinib resistance. Firstly, down-regulation of miR-205 was identified in breast cancer tumours compared to normal breast tissue by Iorio *et al.* [209]. Target validation for miR-205 identified HER3 as a direct target and it has inhibitory action on the activation of AKT in SKBR3 and MCF-7 cells [209]. Transfection of miR-205 in the SKBR3 cells caused a decrease in levels of AKT and inhibited cell growth. Transfection of miR-205 increased the sensitivity of SKBR3 cells to gefitinib and lapatinib and decreased the HER3-mediated resistance suggesting it could be a potential onco-suppressor and biomarker of TKI response. In triple negative breast cancer cells, lapatinib treatment was examined due to the high percentage (80%) of TNBC cases expressing HER1 [210]. Unfortunately lapatinib treatment in combination with paclitaxel led to worse clinical outcome for patients with TNBC and HER2 negative disease [211]. A potential explanation suggested for this worsened outcome is miR-7 expression and its ability to enhance migration and invasion of MDA-MB-231 triple negative cell lines through the induction of HER1 and COX-2 expression [212]. More recently in 2014, a study investigating TKI resistance and miRNAs identified miR-630 as an altered miRNA in innate and acquired lapatinib resistant cell lines compared to their parent cell lines [213]. Introduction of miR-630 in the resistant cells enhanced growth inhibition by TKIs (lapatinib, neratinib and afatinib). Alternatively, inhibition miR-630 expression reduced sensitivity to TKI treatment. miR-630 was also associated with a more aggressive phenotype suggesting that miR-630 may be a potential diagnostic and predictive marker for HER2-targeted drug response.

## 1.8. Circulating miRNAs

Circulating miRNAs (CmiRNA) have become a recent topic of investigation due to their stability and ability to survive freeze-thaw cycles, extended storage and extreme variations in heat and pH [214, 215]. CmiRNAs have been identified as predictive markers of invasion and metastasis of cancers and could be extremely useful non-invasive biomarkers [216]. Dysregulation of some of the key players in miRNA biogenesis pathway have been found in cancer progression. DiGeorge syndrome critical region gene 8 (DGCR8) and the RISC components argonaute-1 (Ago1), argonaute-2 (Ago2), as well as double-stranded RNA-binding proteins PACT, TARBP1, and TARBP2 levels are elevated in skin cancer [217]. In ovarian cancer, silencing DGCR8 resulted in inhibition of proliferation and migration of ovarian cancer cells [218]. Mature miRNAs have been identified in a range of biological fluids including saliva [219], urine [220], blood, amniotic fluid, breast milk, cerebrospinal fluid and pleural fluid [221]. The mechanism by which miRNAs are released or secreted is still unclear. One suggested mechanism is miRNAs are secreted through a ceramide-dependent secretory pathway which induces secretion of exosomes [222]. Other possible mechanisms of release include passive leakage from cells due to injury [223, 224], active secretion via exosomes [222] and apoptotic bodies [225] or active secretion and transport with high density lipoproteins [226], or Ago2 [227] and nucleophosmin 1 [228] (**Figure 1-14**).

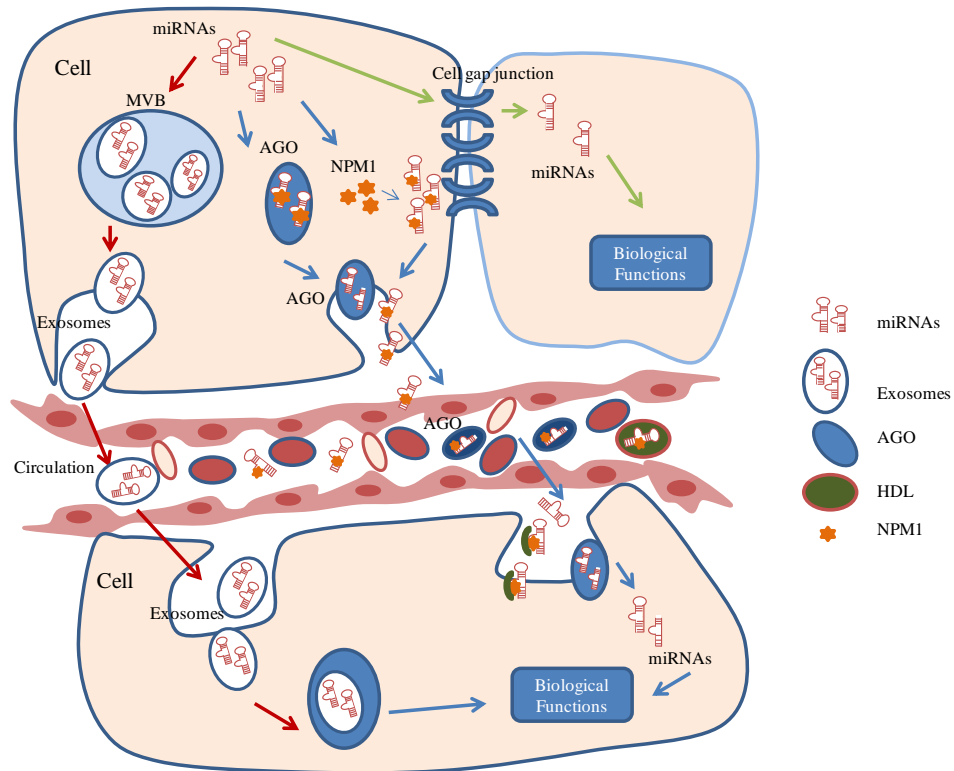


**Figure 1-14:** Overview of potential mechanisms of CmiRNA release and uptake. Three potential mechanisms are detailed. (1) Exosomal release indicated by red arrows, (2) High-density lipoproteins or RNA binding proteins indicated by blue arrows and (3) direct transfer through leaky cells indicated by green arrow. Abbreviations: MVBs, multi-vesicular bodies; NPM1, nucleophosmin 1; AGO2, Argonaute-2; HDL, high-density lipoprotein. Adapted from [229].

Utilising CmiRNAs as biomarkers can distinguish cancer patients from healthy populations. CmiRNAs have been identified within serum samples of lung [230], prostate [231], colorectal [232], gastric [192], liver [233], hematologic [234] and breast [235] cancer patients. In early stage breast cancers, oncomiRs (miR-155, miR-19a, miR-181b, miR-24, relative to let-7a) were determined to predict the onset of breast cancer [236]. As these miRNAs can be measured non-invasively, are stable within biological specimens and can indicate a cancerous phenotype, they represent ideal biomarkers for translational research. However, there are still issues with sample collection, RNA

isolation and quantification. For example, plasma processing and platelet contamination can lead to high variation in CmiRNA expression profiles [237]. These factors need to be optimised and standardised for successful circulating biomarker studies.

### ***1.8.1. Circulating HER2 positive breast cancer miRNAs***

CmiRNA expression profiles from HER2 positive patients plasma samples undergoing neoadjuvant trastuzumab based chemotherapy were investigated by Jung *et al.* [205]. They also investigated the trastuzumab sensitive (BT-474) and trastuzumab resistant variants (BTR65) HER2 positive breast cancer cell line and determined that circulating miR-210 levels correlated with trastuzumab sensitivity and tumour presence. Serum from patients enrolled in the Geparquinto trial was examined for CmiRNAs which could possible predict response to trastuzumab or lapatinib [238]. Elevated levels of miR-21, -210 and -373 were identified in patients before and after treatment compared to normal healthy volunteers. They also identified that miR-21 and -373 levels increased further after chemotherapy treatment and miR-21 is a prognostic biomarker of overall survival.

miRNAs have proven to be valuable as indicators of prognosis, predictors of response and are involved in resistance to chemotherapy and targeted therapies. Thus they hold potential as targets for the treatment of HER2 positive breast cancer patients and merit further investigation.

## **1.9. Cancer stem cells (CSCs)**

According to the National Institute of Health (NIH), a stem cell is an unspecialised cell that has the ability to form multiple cell types which contain special characteristics

[239]. These characteristics include; the ability to self renew through division, being unspecialised and the ability to specialise into tissue or organ specific cells. Cancer stem cells (also known as tumour initiating cells TICs) share properties of normal stem cells in that they have three defining features. The ability to form tumours in immune-compromised mice, to self renew and to differentiate [240]. Cancer stem cells were initially identified by Al-Hajj *et al.* using specific cell surface marker expression, CD44<sup>+</sup>/ CD24<sup>-low</sup>/Lin<sup>-</sup> [241]. They identified that cells from breast cancer patients with this pattern of cell surface markers had enhanced tumour initiating abilities in NOD/SCID mice and could also self renew (be serially passaged) and differentiate (reproduce the tumour). Other markers have been used to isolate cancer stem cells including aldehyde dehydrogenase (ALDH) activity [242] and used in combination with CD44<sup>+</sup>/ CD24<sup>-low</sup> surface markers can isolate enriched cancer stem cell populations. CSCs have been linked to increased cancer aggression and metastatic potential of tumours especially in secondary sites [243]. Interestingly, resistance has also been proposed to play a part in CSCs and their involvement in recurrence. CSCs have been identified as more resistant to lapatinib based neoadjuvant chemotherapy than the primary bulk breast tumour [244]. Previously, it has been show that targeting the CSCS through the inhibition of cellular transformation by the diabetic drug Metaformin can overcome Herceptin resistance in xenografts models [245]. Therefore a therapy in which the bulk tumour and the CSCs (TICs) are both targeted could improve overall survival by combating resistance.

### **1.10. Study Aims**

The aims of this study were as follows:

1. To identify novel miRNAs which are altered in acquired and innate trastuzumab and lapatinib resistant cell lines.
  - a. investigate the functional relevance of miRNAs altered in trastuzumab and lapatinib resistant cell lines
  - b. identify miRNA gene targets that may serve as potential biomarkers and/or targets in trastuzumab and lapatinib resistant cells.
2. To examine altered miRNA in tumour specimens from HER2 positive breast cancer patients who achieved a durable complete response following trastuzumab-based therapy.
3. To examine circulating miRNA expression in serum samples from HER-2 positive breast cancer patients who received neoadjuvant chemotherapy and trastuzumab with/without lapatinib.

## **Chapter Two**

### **Materials & Methods**

## 2.1. Cell lines, cell culture and reagents

The cell lines SKBR3, BT474, HCC1419, HCC-1569, HCC-1954, MDA-MB-361, MDA-MB-453, UACC-732 and EFM-192A were obtained from the American Type Culture Collection (ATCC). JIMT-1 cells were purchased from the German Collection of Microorganisms and Cell Cultures (DSMZ). All cell lines were cultured in RPMI 1640 medium (Sigma Aldrich, R8758) supplemented with 10 % fetal calf serum (FCS) (PAA Laboratories). The acquired trastuzumab and lapatinib resistant cell lines (**Table 2-1**) were created by continuous culture cells for a minimum of 6 months in RPMI supplemented trastuzumab or lapatinib as described in **Figure 2-1** [123, 246, 247], with aged matched media controls (parental). The trastuzumab and lapatinib response details of all cell lines used in this study are detailed in **Table 2-2**. Trastuzumab (Herceptin™) was obtained from St. Vincent's University Hospital and lapatinib (Tykerb®) was obtained from GlaxoSmithKline. All cell lines were routinely tested for the presence of mycoplasma using the indirect staining method [248]. In addition, mitochondrial DNA from all cell lines, including newly developed lapatinib-resistant cell lines, was sequenced in 2010 to confirm their identity (in collaboration with Dr. Neil O'Brien and Dr. Charles Ginther in UCLA).

**Table 2-1:** Summary of cell line models of trastuzumab and lapatinib acquired resistance used in this study.

Model of Resistance	Cell Line
Trastuzumab	SKBR3-T
	BT-474-Tr
Lapatinib	SKBR3-L
	HCC1954-L

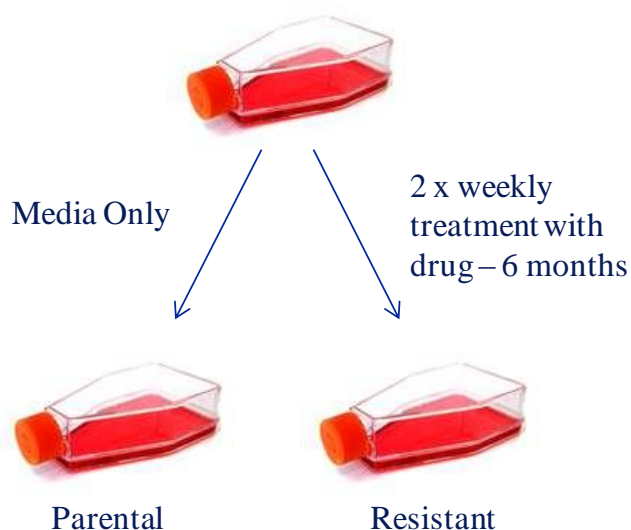


**Figure 2-1:** Overview of creation of cell line models of resistance. Resistant cell lines were created by continuous culture of cells for a minimum of 6 months in RPMI supplemented trastuzumab or lapatinib. Aged matched parental controls were also included.

**Table 2-2:** Trastuzumab and lapatinib response details of all cell lines used in this study. R: resistant and S: sensitive to drug inhibition. Information is adapted from [103].

Cell Line	Trastuzumab Response	Lapatinib Response
BT-474	S	S
BT-474-Tr	R	S
EFM-192A	S	S
SKBR3	S	S
SKBR3-T	R	S
SKBR3-L	R	R
MDA-MB-361	S	S
UACC-732	R	R
HCC-1419	R	S
JIMT-1	R	R
HCC-1954	R	S
HCC-1954-L	R	R
HCC-1569	R	R
MDA-MB-453	R	R

## **2.2. Proliferation assays**

Cells were seeded at density of  $3 \times 10^4$  (SKBR3, SKBR3-T, BT474, HCC1419, HCC1569, HCC-1954, MDA-MB-361, MDA-MB-453, UACC-732 and JIMT-1), and  $5 \times 10^4$  (BT474, BT474-Tr and EFM-192A) in 96 well flat bottomed plates and incubated overnight at 37 °C with 5% CO<sub>2</sub>. Cells were treated with appropriate media controls, 10/100 µg/mL trastuzumab (SKBR3/BT474), serial dilutions of lapatinib ranging from 0.2 – 10 µM or all-*trans*-retinoic acid (ATRA) ranging from 0.05 - 0.2 µM (Sigma, R2625). Proliferation was measured after 5 days using the acid phosphatase method. Briefly, media was removed and each well rinsed with phosphate buffered saline (PBS); 100 µL of acid phosphatase substrate (10 mM p-nitrophenol phosphate (Sigma, 34045) in 0.1 M sodium acetate pH 5.5, 0.1% triton-100 (Sigma, X100) was added to each well and incubated at 37°C for 1-2 hours after which 50 µL of 1 M NaOH (Sigma, S5881) was added to each well and the absorbance was read at 405 nm with 620 nm as a reference on a Biotek microplate reader. Proliferation was calculated relative to untreated controls. Each assay was carried out in triplicate.

## **2.3. microRNA extraction**

microRNA (miRNA) was extracted using the mirVana™ miRNA Isolation Kit (Ambion, AM1560). Briefly, cells were grown to 70-80% confluency, trypsinised (trypsin-EDTA (Gibco)) and centrifuged at 160 x g for 3 mins. Cell pellets were washed with PBS, centrifuged as before and placed on ice. Cells were lysed in 300-600 µL of lysis buffer and 1/10 volume miRNA homogenate additive was added, vortexed and incubated on ice for 10 mins. A volume of acid:phenol chloroform equal to the amount of lysis buffer was then added, vortexed for 30-60 secs and centrifuged at top speed

(17,530 x g) for 5 mins at room temperature. The top aqueous layer was then removed (volume noted) and 1.25 volumes of room temperature ethanol (100%) was added. The mixture was added to a filter cartridge, centrifuged for 15 sec at 12,400 x g and the flow through was discarded. Wash solution 1 was added (700 µL) and centrifuged as before followed by wash solution 2/3 (500 µL) twice and centrifuged as before with flow through discarded each time. The filter cartridge was centrifuged for 1 min to remove residual ethanol and placed in a fresh collection tube. Pre-heated (95°C) nuclease free water (100 µL) was applied to the filter cartridge and incubated for 1 min at room temperature. The filter cartridge was centrifuged at 12,400 x g for 20-30 sec to elute miRNAs. miRNA extracts were stored at -80°C. Each extraction was carried out in triplicate. The RNA concentration (ng/µL) was determined using the Nanodrop ND 1000 (Thermo Scientific).

#### **2.4. Agarose gels**

A 0.8% agarose (Sigma Aldrich, A9539) gel was prepared in 50 mL 1X TAE buffer (Tris-Acetate-EDTA) with 2 µL ethidium bromide (Sigma Aldrich, E1510) added. Molecular weight markers (P1473, Sigma) and RNA (1 µg) were loaded into the appropriate wells (10 µL of sample: 10 µL of 1X loading buffer (30% glycerol, 0.1 M EDTA, 0.25% bromophenol blue). The gel was electrophoresed at 90 V for 20 min. RNA was visualised on the Epi Chemi II Darkroom (Ultra-Violet Products, UVP) using the software Labwork 1 (Bioimaging Systems).

#### **2.5. TLDA data analysis**

Previously, Taqman Low Density Arrays (TLDA) were carried out by Salima Soualhi. The overall workflow is outlined in **Figure 2.2**. The experimental design was to identify

potential microRNAs involved in trastuzumab and lapatinib resistance by screening the SKBR3-T and SKBR3-L cell lines and calibrating these results to their parental cell line, SKBR3-P.

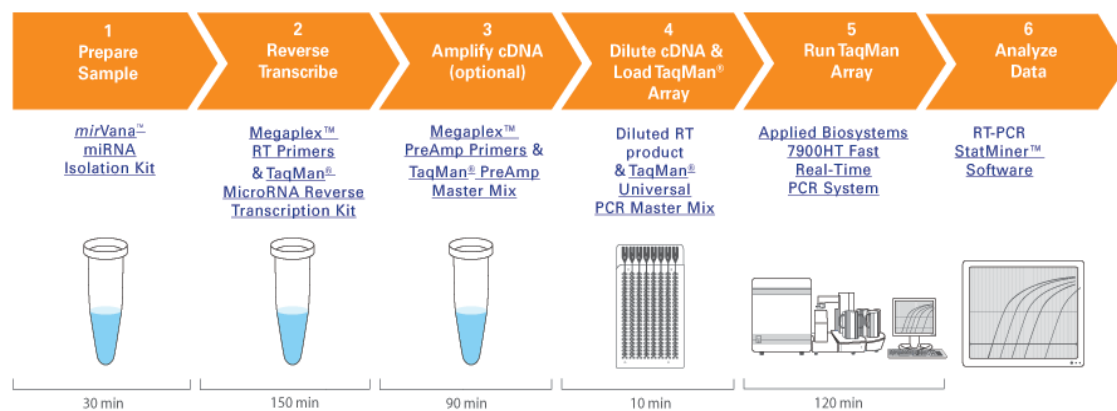


**Figure 2-2:** Array workflow for Taqman Low Density Arrays (TLDA). Isolated microRNA is reverse transcribed with megaplex RT-primers, diluted RT product is then mixed with universal PCR master mix and loaded onto pre-configured 384-well micro fluidic cards which include endogenous controls. The data is then analysed to identify microRNAs of interest. Image taken from [www.lifetechnologies.com](http://www.lifetechnologies.com)

The sequence detection systems (SDS) files from the SDS 2.2.2 software (Applied Biosystems) were analysed as follows: the two resistant cell lines, SKBR3- H and SKBR3-L were compared to the SKBR3 cell line which was set as a calibrator using a manual threshold of 2.0. Expression values were calculated using the comparative threshold cycle (Ct) method. RNU48 was selected as the endogenous control. The threshold cycle Ct indicates the cycle number by which the amount of amplified target reaches a fixed threshold. The Ct data for each specific miRNA and RNU48 were used to create delta Ct ( $\Delta Ct$ ) values.  $\Delta\Delta Ct$  values were calculated by subtracting the calibrator (SQ) from the  $\Delta Ct$  value of each target (e.g. resistant minus control). Relative quantification (RQ) values were calculated using the equation:

$$RQ = 2^{\Delta\Delta Ct} = 2^{\Delta Ct_{control} - \Delta Ct_{test}} = 2^{(Ct.X-Ct.R)_{control} - (Ct.X-Ct.R)_{test}} \quad [249]$$

Where, CtX is the cycle threshold of the gene of interest and Ct.R is the cycle threshold of the endogenous reference gene.

## 2.6. miRNA reverse transcriptase reaction (RT-PCR)

Stock solutions of RNA (2 ng/ $\mu$ L) were prepared by diluting miRNA with RNase free water (Ambion, 9932). An RT master mix solution was prepared as per **Table 2-3**. Briefly, for each reaction 5  $\mu$ L of miRNA sample (10 ng), 7  $\mu$ L of master mix and 3  $\mu$ L of miRNA assay (5X) (**Table 2-4**) were combined in PCR tubes, mixed gently, briefly centrifuged and incubated on ice for 5 min. Samples were then loaded into the thermo-cycler (G-STORM), reaction volume was set to 15  $\mu$ L and the RT reaction performed as per **Table 2-5**. The samples were then stored at -20°C until required. Controls were included in the RT reaction; non-target control (NTC) which was prepared without the RNA template, and a minus reverse transcriptase control (RT-) which was prepared without the reverse transcriptase enzyme. Each sample was tested in triplicate.

**Table 2-3.** Components and make up of RT reaction master mix

<b>Component</b>	<b>Master mix volume per one reaction*</b>
100 mM dNTPs (with dTTP)	0.15
10X Reverse Transcription Buffer	1.50
RNase Inhibitor (20 U/ $\mu$ L)	0.19
Nuclease free water	4.16
MultiScribe™ Reverse Transcriptase (50 U/ $\mu$ L)	1.00
Master Mix Total Volume	7.00
TaqMan® miRNA assay (5X)	3.00
RNA (10 ng)	5.00
<b>Total</b>	<b>15.00</b>

\* Each 15  $\mu$ L RT reaction consists of 7  $\mu$ L master mix, 3  $\mu$ L of 5X RT primer (miRNA assay) and 5  $\mu$ L RNA sample.

**Table 2-4:** TaqMan® miRNA assays for RT (5X) and qRT-PCR (20X). Assay ID refers to the ordering code for each specific miRNA (Applied Biosystems).

Assay Name	Assay ID	Assay Name	Assay ID
<b>miR-100</b>	000437	miR-30a-5p	000417
<b>miR-135a</b>	000470	miR-30e-3p	000422
<b>miR-148a</b>	000471	miR-30d	000420
<b>miR-192</b>	000491	miR-31	002279
<b>miR-194</b>	000493	miR-375	000564
<b>miR-203</b>	000507	miR-9	000583
<b>miR-205</b>	000509	miR-92	000430
<b>miR-21</b>	002438	miR-550	002410
<b>miR-221</b>	000524	miR-let7a	000377
<b>miR-222</b>	002276	miR-let7c	000379
<b>miR-224</b>	002099	RNU48	001006
<b>miR-30a-3p</b>	000416		

**Table 2-5.** G-Storm thermal cycler program for RT-PCR reaction

Temperature (°C)	Time (min)
16	30
42	30
85	5
4	∞

## 2.7. Gene expression reverse transcriptase reactions

Stock solutions of RNA (1 µg /10 µl) were prepared by diluting RNA extracts with RNase free water (Ambion, 9932). Using a high capacity cDNA Reverse Transcription Kit (Applied Biosystems, 4368814), a 2X master mix solution was prepared as per

**Table 2-6.** For each reaction 10 µl of RNA sample and 10 µL of master mix were combined in PCR tubes, briefly centrifuged and loaded into the thermo-cycler (G-

STORM) and the reverse transcription run as per **Table 2-7**. The samples were then stored at 4 °C until required. Controls were included: non-target control (NTC) which was prepared without the RNA template, and a minus reverse transcriptase control (-RTC) which was prepared without the reverse transcriptase enzyme.

**Table 2-6:** Components of master mix for RT reactions.

<b>Component</b>	<b>Volume / Reaction (µl)</b>
10X RT buffer	2.0
25X dNTP Mix (100 mM)	0.8
MultiScribe™ Reverse transcriptase	1.0
RNase-free water	4.2
10X RT random primers	2.0
<b>Total per reaction</b>	<b>10.0</b>

**Table 2-7:** Thermo-cycler steps, indicating the temperature and duration, for RT reactions.

<b>Step</b>	<b>Temperature (°C)</b>	<b>Time (min)</b>
1	25	10
2	37	120
3	85	5
4	4	Hold

## **2.8. Real time quantitative reverse transcription polymerase chain reaction (qRT-PCR)**

qRT-PCR was performed using individual TaqMan® miRNA assays (20X) as per or TaqMan® Gene Expression Assays (20X) as per **Table 2-8**. TaqMan® miRNA and gene expression experiments were carried out in 20 µL reactions as detailed in **Table 2-**

9 and added to the appropriate wells in a 96-well PCR reaction plate (Applied Biosystems, 4346906). cDNA was then added to the appropriate wells (1  $\mu$ L). The PCR plate was sealed using optical adhesive film, mixed gently and placed on ice for 5 min. The qRT-PCR reaction was performed on the ABI7900HT standard system using SDS automated controller software (version 2.2) (Applied Biosystems) with the thermal cycling conditions detailed in **Table 2-10**.

**Table 2-8:** TaqMan® Gene Expression Assay (20X) details. Assay ID refers to the ordering code for each specific miRNA (Applied Biosystems).

Assay Name	Gene ID	Assay ID
p27 <sup>Kip1</sup>	CDKN1B	Hs00153277_m1
RAR $\alpha$	RARA	Hs00940446_m1
GAPDH	GAPDH	HS02758991_g1

**Table 2-9:** Components of qRT-PCR reaction.

Component	Volume ( $\mu$ L)/ 20 $\mu$ L reaction
TaqMan® Universal PCR Master Mix*	10.0
TaqMan® MiRNA assay (20X)	1.0
Nuclease Free Water	8.0
cDNA from RT reaction	1.0
<b>Total Volume</b>	<b>20.0</b>

\* No AmpErase UNG (2X)

**Table 2-10:** ABI 7500 Fast real-time PCR system thermal cycler program for qRT-PCR

Step	Step Type	Time	Temperature (°C)
Initial Step	HOLD	10 min	95
PCR (40 cycles)	Cycle	15 sec 1 min	95 60

### 2.9. MiRWalk- Target prediction & validation

miRWalk is a comprehensive database that provides information on both predicted and validated miRNAs associated with particular genes, pathways and diseases. (<http://www.umm.uni-heidelberg.de/apps/zmf/miRWalk/index.html>). The database consists of two modules; predicted and validated target modules as shown in **Figure 2-3**. The predicted targets module holds information on miRNA-target interactions on the complete sequence of all known genes of humans, mouse and rat. miRWalk obtains results from eight established miRNA target prediction programs; miRanda, DIANA MT, miRDB, PICTAR 4 & 5, RNA22, Target Scan and miRWalk, where each of these programs contain different algorithms. miRWalk compiles a table of all predicted targets using all the above programs and also provides predicted binding sites on genes associated with biological pathways (449) and OMIM (online mendelian inheritance in man) disorders (2356). The validated targets module provides information on miRNA-target interactions that have been experimentally validated with associations to genes, pathways, diseases, organs, cell lines and OMIM disorders. It also yields information on proteins involved in miRNA processing [250].

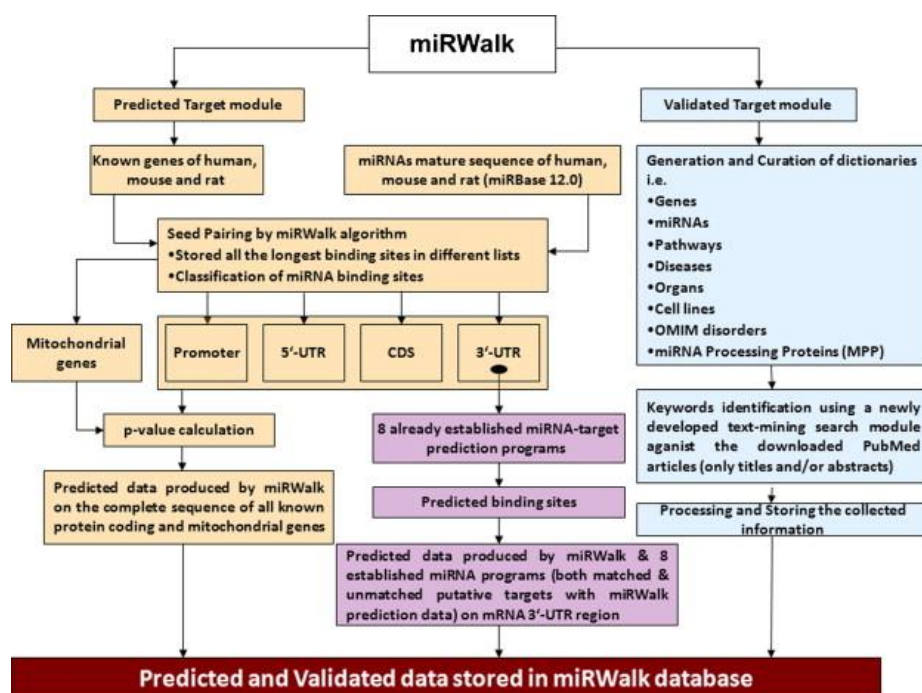


**Figure 2- 3:** Overview of the miRwalk database for prediction and validation of targets [251].

## 2.10. Lentiviral stable transduction

The lentiviral stable transduction for miR-221 and -222 was performed by Dr. Laoighse Mulrane in University College Dublin (UCD) [252]. The lentiviral vector system used in this study was obtained from the Trono laboratory, University of Geneva, Switzerland. It consists of the shRNA lentivector, pLVTHm system and the accessory viral packaging (psPAX2) and envelope (pMD2.G) constructs. Viral particles were produced in HEK 293T cells by transfection using Genejuice transfection reagent (Millipore, Billerica, MA, USA). Viral production and infection of target cells was carried out in a P2 containment facility and infected cells were passaged twice following selection before being returned to the main tissue culture facilities. Stable ectopic expression of miR-221/222 was carried out using the pEZXR03 vectors (Genecopoeia, Rockville, MD, USA) containing expression cassettes for each miRNA.

A control for ectopic expression of miR-221/222, was also included with a pEZX-MR03 vector expressing a scrambled miRNA sequence. Selection was carried out in media containing 2 µg/mL puromycin (Sigma-Aldrich, St Louis, MO, USA) over a period of 2-5 days. Ectopic expression was validated by fluorescent microscopy using the Leica DFC 500 microscope (GFP-positivity) and quantitative real time polymerase chain reaction (qRT-PCR). Further information is available from the laboratory's website (<http://tronolab.epfl.ch/>).

### **2.11. Wound scratch migration assay**

The wound scratch migration assay was conducted in triplicate under serum-reduced (2% FBS) conditions to reduce proliferation as described previously [253]. Cells were seeded at a density of  $1.0 \times 10^5$  in a 12 well tissue culture plate. Once the cells reached 100% confluency, they were incubated in PBS for 15 min, after which, a scratch was made using a P200 tip. Cells were rinsed once with PBS and RPMI-1640 medium supplemented with 1% FCS was then added to the cells. Images were captured at T0, T24 and T48 using the Nikon Eclipse TS100 microscope with attached Olympus DP70 digital microscope camera. The quantification was conducted using Tscratch software [254]. All open areas at T0 were set to 100% and all open areas at later time points were calculated relative to the T0 value.

### **2.12. Doubling time assays**

Cells were seeded at density of  $1 \times 10^4$  in 96 well flat bottomed plates and media controls or media containing trastuzumab (1 µg/mL) was added on Day 0 to appropriate wells and incubated in a CO<sub>2</sub> incubator at 37 °C overnight. We chose this trastuzumab concentration as previous dose analysis (not presented) on our stable transduced cell lines showed treatment with 1 µg/mL yielded similar results to treatment at 10 µg/mL.

Proliferation was measured at Day 1 (24 hrs after plating), Day 3, Day 5 and Day 7 using the acid phosphatase method as per 2.2. Doubling time was calculated as:  $\ln_2(96)/\ln_2(\text{Abs}^{\text{Day7}}/\text{Abs}^{\text{Day3}})$ . Each assay was carried out in triplicate.

### **2.13. Preparation of cell lysates**

Cells were grown in petri dishes (100 mm) until 70-80% confluent. Trastuzumab (10  $\mu\text{g}/\mu\text{L}$ ), lapatinib (250 nM) or media controls were set up for 24 h and 48 h. Whole cell lysates were prepared as follows: cells were washed thrice with cold phosphate buffered saline solution (PBS) and 250-500  $\mu\text{L}/\text{dish}$  RIPA buffer ((Sigma, R0278) 5 mM Tris-HCl pH 7.4, 1% NP-40, 0.1% SDS, 150 mM NaCl, 1% Triton x-100) containing 1x Protease Inhibitor cocktail (Calbiochem, 539131), 2 mM PMSF (Sigma, P7626), and 1 mM sodium orthovanadate (Sigma, 6508), was added and cells were incubated on ice for 20 minutes. Cells were scraped into lysis buffer. The lysis buffer was collected, passed through a 21G needle and centrifuged at 16,100 x g for 10 minutes at 4 °C. The pellets were discarded and the supernatants collected and stored at -80°C. Protein quantification was performed using the bicinchoninic acid (BCA) quantitation kit (Pierce, 23227).

### **2.14. Western blotting**

Protein (20-50  $\mu\text{g}$ ) was electrophoretically resolved on NuPAGE® Novex® 4-12% Bis-Tris gels (BioSciences, NP0329) under denaturing conditions. The resolved proteins were then transferred to nitrocellulose membranes (Invitrogen, IB3010-01) using the iBlot transfer system (Invitrogen, IB1001). Protein transfer was visually confirmed using Ponceau S staining (Sigma, P7170). Membranes were blocked for 1hr using 1x NET buffer (0.5 M NaCl, 0.05 M EDTA, 0.1 M Tris pH 7.8) at room temperature and

incubated overnight at 4 °C with primary antibodies in 1x NET. Stock 10X NET buffer is prepared using the components listed in **Table 2-11**. The 1X NET buffer is prepared by the addition of water (17.5 L) to a 20 mL container with the addition of 10X NET (2 L). Dissolved gelatine (50g in 0.5 L of H<sub>2</sub>O) is added to the 10X NET/H<sub>2</sub>O solution. The blotting conditions for each primary antibody are detailed in **Table 2-12**. Membranes were washed with 1x NET 3 times for 10 mins each, both prior to and following incubation with secondary antibodies. Proteins were visualised using horseradish peroxidase-conjugated anti-mouse, anti-goat or anti-rabbit antibodies (Sigma) and Luminol reagent (Santa Cruz Biotechnology, SC2048) or Clarity Western ECL substrate (BioRad, 170-5060). Protein bands were semiquantified by densitometry, and protein levels were calculated relative to  $\alpha$ -tubulin levels by Image J.

**Table 2-11.** Protocol for the preparation of 10X NET Buffer.

<b>Stock Conc</b>	<b>Compound</b>	<b>Volume (mls.)</b>	<b>Final Conc</b>
<b>5M</b>	NaCl	600	1.5M
<b>0.5M</b>	EDTA	200	0.05M
<b>1M</b>	Tris pH 7.8	1000	0.5M
<b>100%</b>	Triton X-100	10	0.5%
<b>100%</b>	H <sub>2</sub> O	190	
<b>Total Volume</b>		2000	

**Table 2-12:** Details of Primary and Secondary antibodies used in this study, including blotting conditions and source.

<b>Antibody</b>	<b>dilution</b>	<b>Blotting conditions</b>	<b>Secondary</b>	<b>+ ve control</b>	<b>Company</b>	<b>Cat no.</b>
<b><math>\alpha</math>-tubulin</b>	1:1000	1X NET	Mouse		Sigma	T6199
<b>anti-RAR<math>\alpha</math></b>	1:200	1X NET	Mouse	MCF7	Abcam	#9272
<b>anti-RAR<math>\beta</math></b>	1:500	1X NET	Rabbit	MCF7	Abcam	ab53161
<b>anti-RAR<math>\gamma</math></b>	1:500	1X NET	Mouse	MCF7	Abcam	ab41938
<b>anti-RXR<math>\alpha</math></b>	1:200	1x NET	Rabbit	MCF7	Santa Cruz	sc-553
<b>anti-p27Kip1</b>	1:400	1X NET	Mouse	HEK-293	Santa Cruz	sc-53871
<b>anti-rabbit secondary</b>	1:2000	1X NET	Rabbit		Sigma	A6154
<b>anti-mouse secondary</b>	1:1000	1X NET	Mouse		Sigma	A6782

### **2.15. miRNA extraction from conditioned media**

miRNA was isolated from conditioned media as previously described [255]. Briefly, cells at 70-80% confluency were incubated in appropriate media (RPMI + 10% FCS) in a T75cm<sup>2</sup> for 24 hr at 37°C and 5% CO<sub>2</sub>. The supernatant was then harvested for 4 min at 160 x g at 4°C. The samples were stored at -20°C. miRNA extraction was carried out on 1 mL of the collected conditioned media, TRIzol (15596-026, Life Technologies) was added (700 µL), the sample was vortexed and incubated at room temperature for 5 min. Acid: phenol chloroform (140 µL) was added and vortexed vigorously for 15 sec. Sample was then centrifuged at 17,530 x g for 15 min at 4°C. The upper aqueous phase was transferred to a new tube and the miRvana extraction protocol was followed from the ethanol separation step as detailed in 2.3. RNA concentration (ng/µL) was assessed using the NanoDrop ND1000.

### **2.16. miRCURY RNA isolation kit- Biofluids**

miRNA was extracted from patient serum samples using the miRCURY biofluids kit (Exiqon, 300112). Briefly, 250 µL of serum samples were centrifuged at 3000 x g for 5 min to pellet any debris or insoluble components. Supernatant (200 µL) was transferred to a new tube and lysis solution BF (60 µL) was added, vortexed for 5 sec and incubated at room temperature for 3 min. Protein precipitation solution BF (20 µL) was added, vortexed for 5 sec and incubated at room temperature for 1 min. Sample was then centrifuged at 11,000 x g for 3 min. The clear supernatant was transferred to a new collection tube (2 mL) and isopropanol (270 µL) was added. Solution was vortexed for 5 sec, transferred to a miRNA mini spin column BF in a collection tube and incubated at room temperature for 5 sec. Sample was then centrifuged at 11,000 x g for 30 sec, flow through discarded and column placed back in collection tube. Wash solution 1 BF (100

μL) was added, centrifuged at 11,000 x g for 30 sec and flow through discarded. Wash solution 2 BF (700 μL) was added, centrifuged at 11,000 x g for 30 sec and flow through discarded. A final wash with wash solution 2 BF (250 μL) was added and centrifuged at 11,000 x g for 2 min to dry the membrane completely. The miRNA mini spin column BF was added to a new collection tube (1.5 mL), RNase free H<sub>2</sub>O was added directly to centre of membrane and incubated at room temperature for 1 min. Sample was then centrifuged 11,000 x g for 1 min. Purified RNA was stored at -80 °C for downstream experiments.

### **2.17. ALDEFLUOR assay**

The ALDEFLUOR assay was carried out in collaboration with Dr. Michael Gallaghers ‘Cancer Stemness Group’ in Trinity College Dublin. Briefly, cell pellets were prepared from 70-80% confluent cells in a T75cm<sup>2</sup> flask, trypsinised and washed in PBS and centrifuged briefly to pellet the cells. These cells were then analysed by ALDEFLUOR (ALDH) assay in TCD. This assay, which is detailed in **Figure 2-4**, identifies putative cancer stem cells (pCSCs) based on their ability to metabolise a synthetic aldehydehydrogenase 1 substrate, BODIPY-aminoacetaldehyde (BAAA), to produce a brightly fluorescing substance (BODIPY-aminoacetate). This reaction can be inhibited by an aldehydehydrogenase inhibitor called Diethylaminobenzaldehyde (DEAB). By adding BAAA to a sample of cells one can discriminate pCSCs and non-pCSCs based on fluorescent intensity. When DEAB is added to the reaction it prevents the production of the fluorescent by-product thus acting as a negative control. By subtracting the negative control data from the uninhibited sample data, pCSCs and non-pCSCs sub-populations can be discriminated and quantified.

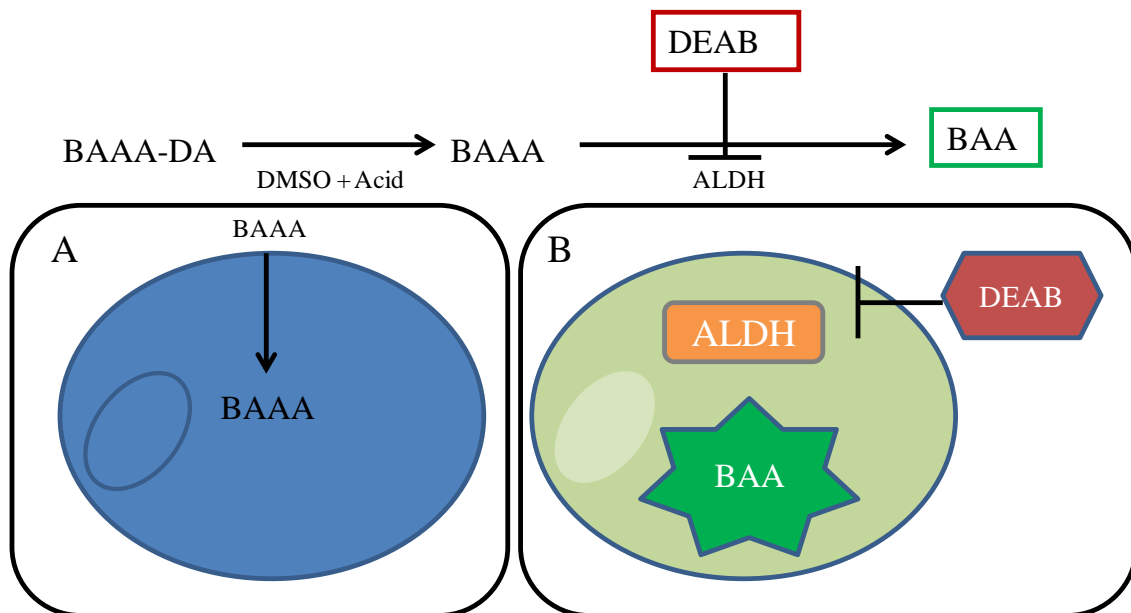


**Figure 2-4:** ALDEFUOR assay which is depicted in (A) ALDH-negative cells and (B) ALDH-positive cells. Bodipy-aminoacetaldehyde diethyl acetal (BAAA-DA) is converted to the ALDH substrate Bodipy-aminoacetaldehyde (BAAA) in the presence of dimethylsulfoxide (DMSO) and hydrochloric acid, which diffuses freely across the plasma membrane of intact viable cells. Intracellular ALDH converts BAAA into the fluorescent product BAA (BODIPY-aminoacetate). In the presence of ALDH, cellular fluorescence can be detected with the green fluorescence channel of a standard flow cytometer and compared with treatment using the ALDH inhibitor diethylamino-benzaldehyde (DEAB) as a negative control. Adapted from [256].

## 2.18. Establishment of primary mammosphere assays from cell lines

The primary mammosphere protocol was previously described [257] and is shown in the illustration in **Figure 2-5**. Cells were grown to 70-80% confluency. Cells were trypsinised and resuspended in RPMI media supplemented with 10% FCS, centrifuged at 100 x g for 3 min and the media supernatant was removed. Cells were resuspended in 10 mL PBS, syringed using a 25 gauge needle to form a single cell suspension and a cell count was performed. Mammosphere media (2 mL) (detailed in **Table 2-13**) was added to corresponding wells on a 6-well polyhema coated plate with/without

trastuzumab (10  $\mu\text{g/mL}$ ) or lapatinib (50 nM). Cells were seeded at an optimised seeding density as per **Table 2-14**. Plates were incubated in a CO<sub>2</sub> incubator at 37°C for 5 days without moving/disturbing the plates and without replenishing the media. After 5 days, the numbers of mammospheres greater than 50  $\mu\text{m}$  were counted using the Nikon TS100 microscope (40X magnification) fitted with a graticule as shown in **Figure 2-6**. Primary mammosphere formation is expressed as percentage mammosphere formation efficiency (MFE), that is: (number of mammospheres formed/original number of cells seeded)\*100.

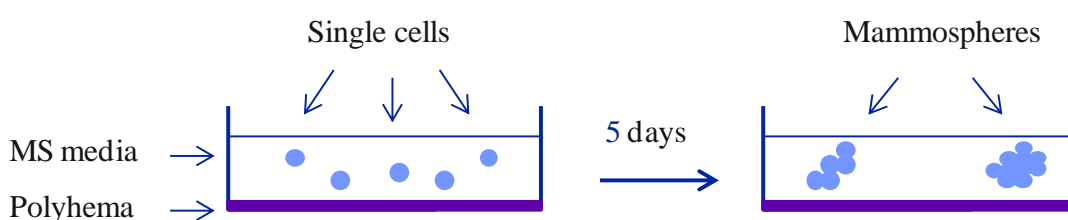


**Figure 2-5:** Overview of the primary mammosphere protocol. Single cells suspension is plated out into polyhema coated 6-well plates in mammosphere media (MS media). The resulting mammospheres are counted after 5 day incubation in 5% CO<sub>2</sub> at 37°C.

**Table 2-13.** Constituents of Mammosphere Media.

Constituents	Company & Catalogue Number
<b>DMEM/F12</b>	Gibco, 21041
<b>B27 supplement (no vitamin A)</b>	Invitrogen, 12587
<b>Recombinant epidermal growth factor (20ng/<math>\mu\text{L}</math>)</b>	Sigma Aldrich, E-9644

**Table 2-14:** Optimised seeding densities for mammospheres for each cell line.

Cell Line	Density
SKBR3-Parental	300 cells/well
SKBR3-T	500 cells/well
SKBR3-L	500 cells/well
SKBR3-P-Scramble	500 cells/well
SKBR3-P-221	500 cells/well
SKBR3-P-222	500 cells/well
SKBR3-P-221-222	500 cells/well



**Figure 2-6:** Image of graticule which is used to count mammospheres of greater than 50 µM diameter.

### 2.19. Assessment of self-renewal – secondary mammosphere generation

Media containing the known amount of mammospheres from the primary generation were collected into a 30 mL sterilin. The wells were washed with PBS to ensure collection of all mammospheres and centrifuged at 100 x g for 2 min. The supernatant was carefully removed, resuspended in trypsin (200 µL) and placed in incubator at 37°C

for 2 min. The mammospheres were disaggregated using a 25 gauge needle to form a single cell suspension. RPMI media supplemented with 10% FCS was added (1 mL) to neutralise the trypsin and centrifuged at 1000 x g for 2 min. Supernatant was removed and the appropriate amount of mammosphere media was added corresponding to the number of wells calculated from the primary generation, as follows:

$$\text{No of } 1^{\circ} \text{ mammospheres} \times 100 \text{ cells per mammosphere} / \text{No of cells seeded per well} = \\ \text{No of wells set up for secondary generation.}$$

Plates were incubated undisturbed for 5 days and the resulting secondary mammospheres were counted as per 2.18 and mammosphere self-renewal was calculated as follows: Total number of 2° mammospheres formed/ total number of 1° mammospheres formed. Any value under 1, was deemed a decrease in self renewal properties and a value above 1 was deemed an increase in self renewal properties.

## **2.20. Preparation of cell culture blocks as block donors**

SKBR3 parental cells were grown to 75-80% confluency, trypsinised and resuspended in 10 mL of media. Cells were pelleted by centrifugation at 75 x g for 3 min and the supernatant was removed. Cells were washed once in PBS, re-pelleted and the supernatant was removed. The cell pellet was fixed in 5 mL of a 10 % (v/v) neutral-buffered formalin solution, containing formaldehyde solution (Sigma, 252549), sodium dihydrogen phosphate (Fisher Scientific, 7558-79-4) and disodium hydrogen phosphate (Fisher Scientific, 7558-80-7), and incubated overnight at room temperature. Cells were pelleted by centrifugation at 75 x g for 3 min, washed with PBS and re-pelleted. Cells were re-suspended in 200 µL of a 0.8 % agarose (Sigma, A9539) solution and transferred to a 1.5 ml microcentrifuge tube, from which the tapered end had been

removed. The agarose plug was left to solidify within the tube, removed via the cap end and transferred to an embedding cassette (Fisher Scientific, 15-200-402E). The cassettes were placed in a slide bath and were washed for 1 hour each in the following solutions: ultra-high purity (UHP) water, 50 % ethanol (Merck, 100983), 70 % ethanol, 90 % ethanol, 100 % ethanol. This was followed by 2 x 1 hour washes in 100 % xylene (Applichem, A0663), before being placed into melted paraffin (McCormick Scientific, 561006) for 2 hours. Using the Leica EG1150H machine the cassettes were placed in plastic moulds (SKS Science, M475), embedded with paraffin and left to cool. Once the paraffin was set the cell culture blocks were stored at 4 °C with desiccant prior to sectioning.

#### **2.21. Sectioning and coring of cell culture donor blocks**

Sectioning of cell culture blocks was carried out on a Reichert-Jung 2030 microtome. Briefly, 10 µM sections were cut from the cell blocks, sections were floated out in a water bath at 40 °C, mounted on super frost slides (Thermo Scientific, 10143560WCUT) and allowed to dry at room temperature. Once dry, the sections were trimmed of any excess paraffin and scraped into a microcentrifuge tube (1.5 mL). Cores of 1.0 mm and 1.5 mm were taken using biopsy punches (Brymill Cyrogenic Systems, BPP-10F, BPP-15F) and immediately placed into a microcentrifuge tube (1.5 mL). Both sections and cores were stored at 4°C.

#### **2.22. De-paraffinisation and H & E staining of sections**

Sections were placed into an oven at 60°C for 20 min. Once paraffin had melted thoroughly, sections were transferred to a slide bath and washed for 5 min each in the following solutions; xylene (Applichem, A0663), 100 % ethanol (Merck, 100983), 90 % ethanol, 70 % ethanol and running tap water. Sections were then transferred to bath of

Haematoxylin (Reactifs Ral, 361070) for 4 min and rinsed in running tap water until a purple colour developed, differentiated in 0.3% acid alcohol until a blue colour developed and rinsed in running tap water for 4 min. Sections were then stained with Eosin (Acros Organics, 409430250) for 2 min and underwent dehydration, clearing and mounting. Briefly, sections were washed for 5 min each in the following solutions; 70% ethanol, 90% ethanol, 100% ethanol and xylene. Sections were mounted using Di-n-butyl phthalate (Dpx) mounting liquid (Sigma Aldrich, 44581), coverslips and allowed to dry at room temperature. Images were captured using the Nikon Eclipse TS100 microscope with attached Olympus DP70 digital microscope camera.

### **2.23. HER2 Immunohistochemistry**

Automated immunohistochemistry was performed using the DAKO Autostainer system. Antibodies against HER2 (c-eRBB2) (Dako, A0485) were used in this study. Previously HER2 positive breast samples were scored by a pathologist and only sections with a 2+–3+ score were used as positive controls for IHC experiments (**Table 2-15**). A representative image showing the scoring system for HER2 is detailed in **Figure 2-7**. Antigen retrieval and dewaxing was performed using automated Dako PT Link in Target Retrieval Solution pH6 (Dako S1699). Slides were placed in Dako PT link at 65 °C and heated to 97 °C and maintained at 97 °C for 20 minutes. The slides are cooled to 65 °C and removed. After de-paraffinisation, the slides were placed in the DAKO Autostainer, which performed the programmed application of reagents in order as listed in **Table 2-16**. The dilution of HER2 antibody was 1 in 250. Washes were performed, with DAKO wash buffer, before and after the application of the each reagent, except in the case of the Real HP Block, where a blow step was performed. Slides were subsequently dehydrated in grading alcohols 70 %, 90 %, and 100 %, cleared in xylenes (2 x 3 minutes each) and mounted in Di(nbutyl) Phthalate in Xylene (DPX).

**Table 2-15:** Overview of the scoring system guidelines for Herceptin in tumour tissues. Adapted from [258].

Score	HER2 Over-expression assessment	Staining Pattern
<b>0</b>	Negative	No staining observed or membrane staining is observed in <10% of tumour cells
<b>1+</b>	Negative	Faint membrane staining is detected in more than 10% of tumour cells
<b>2+</b>	Weakly Positive*	A weak to moderate complete membrane staining is observed in more than 10% of tumour cells
<b>3+</b>	Strongly Positive **	A strong complete membrane staining is observed in more than 10% of cells

\*May be analysed further using fluorescence in situ hybridisation (FISH).

\*\*FISH analysis may be used as a complementary test in these cases.

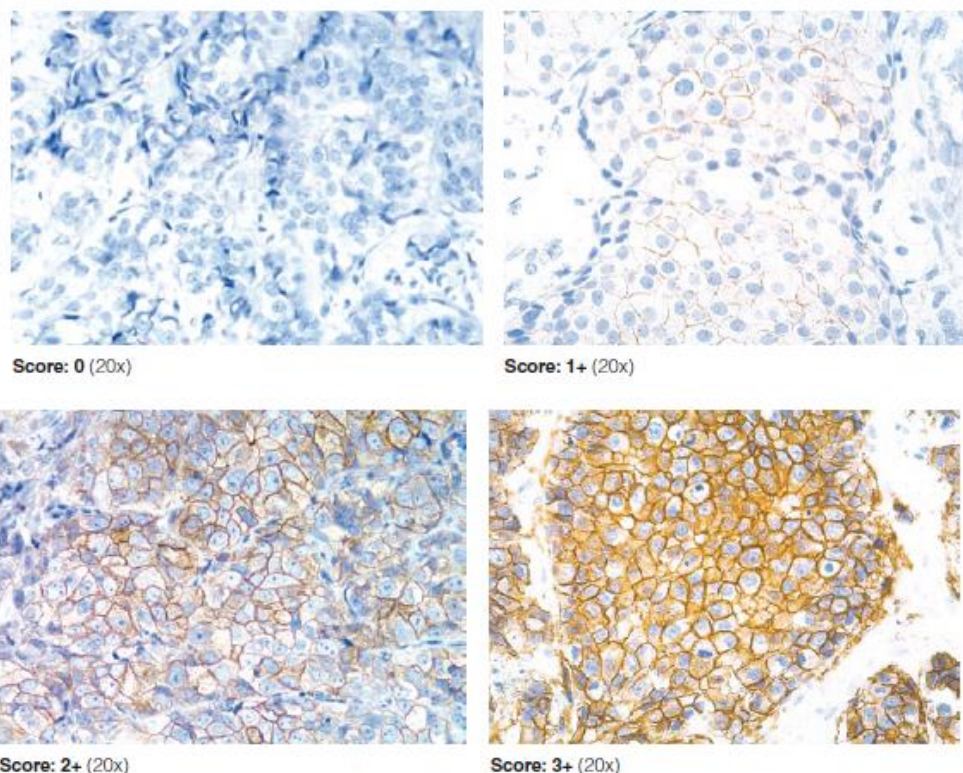


**Figure 2-7:** Illustration of the scoring system 0-3+ in breast tumour tissues. Images are adapted from [258]

**Table 2-16:** Dako autostainer programmed steps for HER2 immunohistochemistry

<b>Reagent</b>	<b>Time (mins)</b>
Real HP Block (DAKO)	10
Antibody	30
Real EnVision (Dako)	30
Real DAB (DAKO)	5
Real HP Block (DAKO)	5

**2.24. Formalin Fixed Paraffin Embedded (FFPE) - miRNA extraction**

Total RNA/miRNA was extracted from the above sections/cores using three commercially available kits, Recoverall Total Nucleic Acid Isolation Kit (Ambion), High Pure miRNA Isolation Kit (Roche) and miRNeasy FFPE Kit (Qiagen) according to manufacturer's instructions as per **Table 2-17**. Experiments were carried out in triplicate.

**Table 2-17:** Summary of protocols for RNA extraction using the 3 commercially available kits.

	<b>Roche- High Pure miRNA Isolation Kit</b>	<b>Ambion- RecoverAll Total Nucleic Acid Isolation Kit</b>	<b>Qiagen-miRNeasy FFPE kit</b>
<b>Sample input</b>	One 10 $\mu$ M FFPE section or 1.0 mm/1.5 mm Core		
<b>Deparaffinisation</b>	Xylene & 2 Ethanol Steps with a drying step of 55°C for 10 mins	Xylene & 2 Ethanol steps with a melting step of 50°C for 3 mins and an air-dry step of 45 mins	Xylene & Ethanol step with a drying incubation at RT
<b>Lysis conditions</b>	55 °C overnight	50°C for 15 mins and 80 °C for 15 mins	56 °C for 15 mins and 80°C for 15 mins
<b>Proteinase K step</b>	Included in Lysis step	-	Included in Lysis Step
<b>DNase digest step</b>	Optional	Included in protocol	Included in protocol
<b>Elution volume</b>	50 $\mu$ L	60 $\mu$ L	14-30 $\mu$ L

### 2.25. RNA evaluation

The Nanodrop ND 1000 (Thermo Scientific) was used to determine concentration (ng/ $\mu$ L) and quality (A260/280). To determine RNA integrity, the Agilent RNA 6000 Nano Assay protocol was used for the Agilent 2100 Bioanalyser (Agilent Technologies) according to manufacturers' instructions.

## **2.26. qRT-PCR analysis**

Estimation of miRNA and mRNA recovery was determined by quantification of expression levels of the endogenous controls RNU48 and GAPDH respectively. Reverse transcriptase was carried out as per 2.6 for the miRNA endogenous control RNU48. qRT-PCR experiments were performed as per 2.8. Experiments were carried out in biological and technical triplicate.

## **2.27. Patient population**

Sixteen FFPE tumour samples from the ICORG-12-09 pilot retrospective laboratory-based cohort study investigating durable complete response following trastuzumab treatment were included for miRNA expression analysis. All patients were diagnosed at St Vincent's University Hospital (SVUH), Dublin between 1995 and 2011 and ethical approval to conduct the study was granted by SVUH Ethics and Medical Research Committee in June 2012. Patient sera from the neoadjuvant phase II TCHL clinical trial (ICORG-10-05) investigating TCH (Docetaxel, Carboplatin and Trastuzumab) and TCHL (Docetaxel, Carboplatin, Trastuzumab and Lapatinib treatment in HER2 positive breast cancer patients were assessed for circulating miRNAs. Ethical approval for the TCHL trial was granted by the UCC Clinical Research Ethics Committee. Ethical approval has also been obtained from the DCU Research Ethics Committee for each of the studies.

## **2.28. Statistical analysis**

Drug IC<sub>50</sub> values were calculated using CalcuSyn (version 1.1.0.0) software. Analysis of the differences between the control and treated cell lines and changes in expression of miRNAs was performed using the Student t-test (two tailed with unequal variance). The cut-off for statistical significance was set at  $p \leq 0.05$ .

## **Chapter Three**

# **Characterisation of acquired trastuzumab and lapatinib resistant cell lines**

### **3.1. Introduction**

The monoclonal antibody, trastuzumab, and lapatinib, the dual EGFR and HER2 tyrosine kinase inhibitor are both approved treatments for HER2 positive breast cancer. Trastuzumab has clinical efficacy, however, between 66-88 % of metastatic HER2 positive breast cancer patients are innately resistant to treatment [25, 259]. Those who do initially respond, the majority will develop resistance to trastuzumab usually develops within 1-2 years [260]. In the adjuvant setting approximately 15 % of patients with early stage breast cancer relapse and develop metastatic disease despite trastuzumab based treatment [261]. Lapatinib treatment in combination with capecitabine was approved for the treatment of patients who relapsed on trastuzumab treatment due to achieving significant response in a phase III clinical trial [262, 263]. However, acquired resistance to lapatinib is also an emerging clinical problem. The problem of acquired resistance is still poorly understood. Cell line models of acquired trastuzumab and lapatinib resistance were previously developed in our laboratory by Dr. Browne and Dr. Mc Dermott using the HER2 positive SKBR3 [246] and HCC-1954 [247] cell lines. We characterised these acquired resistant cell lines in relation to drug sensitivity, doubling time, migration and stem cell populations.

### **3.2. Sensitivities of SKBR3-P and SKBR3-T cells to trastuzumab and lapatinib**

The SKBR3-T cell line was established by continuous exposure to trastuzumab (10 µg/mL) for 6 months and represents a model of acquired trastuzumab resistance. The SKBR3-L cell line was established by continuous exposure to lapatinib (250 nM) for 6 months and represents a model of acquired trastuzumab and lapatinib resistance. An

aged matched parental cell line, SKBR3-P was also created alongside these cell lines for comparison. Trastuzumab treatment (10  $\mu\text{g}/\text{mL}$ ) significantly inhibited proliferation by  $40.4 \pm 7.2 \%$  in the SKBR3-P cells compared to  $5.1 \pm 2.8 \%$  in the SKBR3-T cells ( $p=0.0007$ ) and  $9.7 \pm 3.9 \%$  in the SKBR3-L cells ( $p=0.0000002$ ) (**Figure 3-1**).

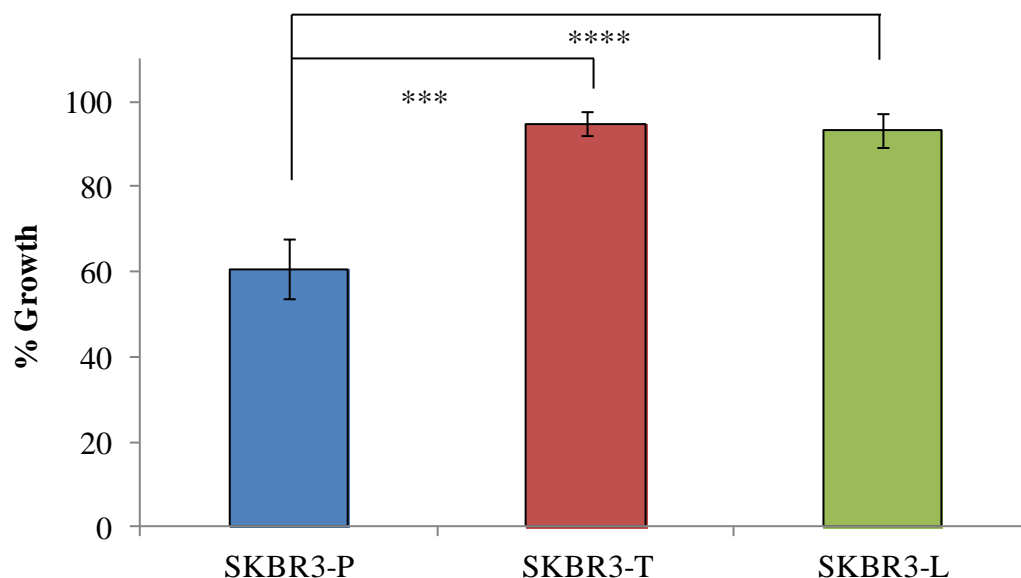


**Figure 3-1:** Determination of trastuzumab sensitivity in the SKBR3 cell line and the acquired resistant variants; SKBR3-T and SKBR3-L after trastuzumab treatment (10  $\mu\text{g}/\text{mL}$ ). Proliferation was measured by acid phosphatase method after 5 days, and is expressed relative to untreated control. Error bars denote the standard deviation of triplicate experiments. Student's t-test was performed to compare response in the resistant and parental cell lines: \*\*\* denotes  $p < 0.0005$ , \*\*\*\* denotes  $p < 0.00005$ .

We encountered a loss of resistance in the SKBR3-T cells in a new batch of FBS Gold (PAA) (Serum B). Previously, most experiments for this study were carried out in Serum A. We examined the resistant phenotype with three different batches of serum (serum A, B and C) (**Figure 3-2**). We found there was a significant difference in growth inhibition 19.6 % ( $p=0.02$ ) when treated with trastuzumab (10  $\mu\text{g}/\text{mL}$ ), when cultured in serum A and B (2 different batches from the same company). Serum from two different companies (serum B vs C) also showed a significant effect on response to trastuzumab

(14.8 %,  $p=0.02$ ). These results suggest that serum is an extremely important factor in acquired resistant cell lines. It is also a point to note that serum screens do not account for long term culture and the loss of resistance over time.

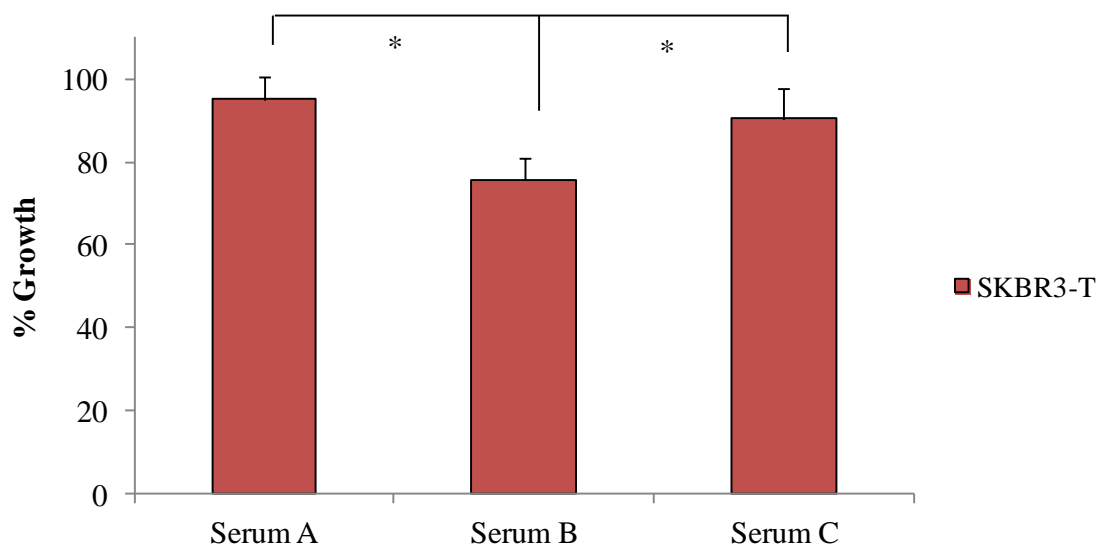


**Figure 3-2:** Determination of trastuzumab sensitivity in the SKBR3-T cell line after culture in different batches of serum (A, B, C). Proliferation was measured by acid phosphatase method after 5 days, and is expressed relative to untreated control. Error bars denote the standard deviation of triplicate experiments. Student's t-test was performed to compare response: \* denotes  $p<0.05$ .

The lapatinib  $IC_{50}$  for the SKBR3-P was  $0.05 \pm 0.008 \mu\text{M}$  compared to that of the SKBR3-T  $0.13 \pm 0.05 \mu\text{M}$  and the SKBR3-L  $4.04 \pm 0.46 \mu\text{M}$  cell lines (**Figure 3-3**). Cells are classified as resistant to lapatinib if the  $IC_{50}$  is greater than  $1\mu\text{M}$  [123]. The SKBR3-L cells are significantly resistant to lapatinib treatment compared to the SKBR3-P ( $p=0.01$ ) whereas the SKBR3-T cells are not lapatinib resistant.

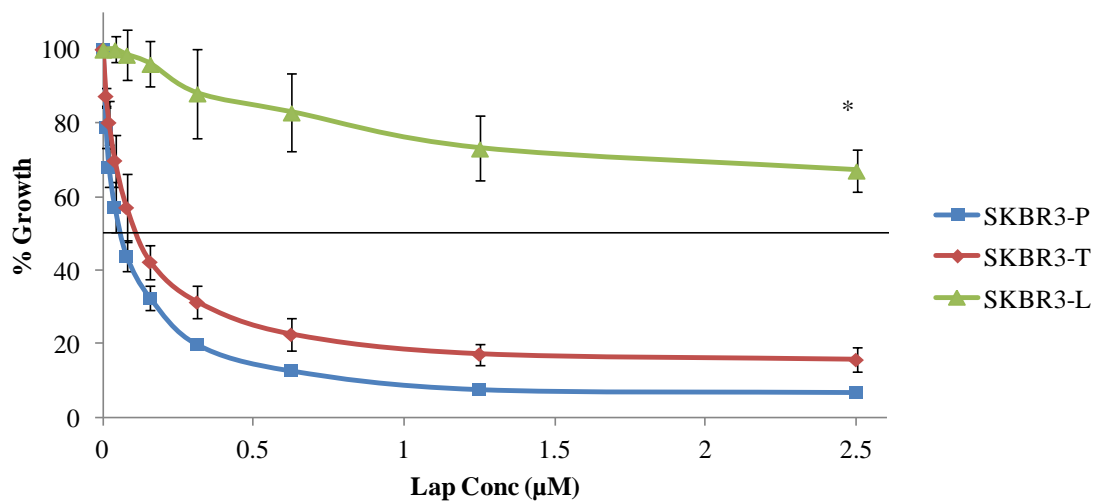


**Figure 3-3:** Determination of lapatinib sensitivity in the SKBR3-P cell line and the acquired resistant variants; SKBR3-T and SKBR3-L. Proliferation was measured by acid phosphatase method after 5 days, and is expressed relative to untreated control. Line represents 50% growth. Error bars denote the standard deviation of triplicate experiments. Student’s t-test was performed to determine statistical significance: \* denotes  $p < 0.05$ .

### 3.3. Doubling times

We determined the doubling times of the SKBR3-P, SKBR3-T and SKBR3-L cell lines. The SKBR3-L cells have a significantly longer doubling time  $67.0 \pm 9.8$  h than the SKBR3-P;  $32.2 \pm 2.2$  h ( $p = 0.02$ ) and the SKBR3-T;  $32.6 \pm 2.5$  h ( $p = 0.02$ ) (**Table 3-1**) (**Figure 3-4**).

**Table 3-1:** Average doubling time (h) for the SKBR3-P, SKBR3-T and SKBR3-L cell lines. Proliferation was measured by acid phosphatase at Day 0, 3, 5 and 7.

Doubling time (h)	
SKBR3-P	$32.2 \pm 2.2$
SKBR3-T	$32.6 \pm 2.5$
SKBR3-L	$67.0 \pm 9.8$

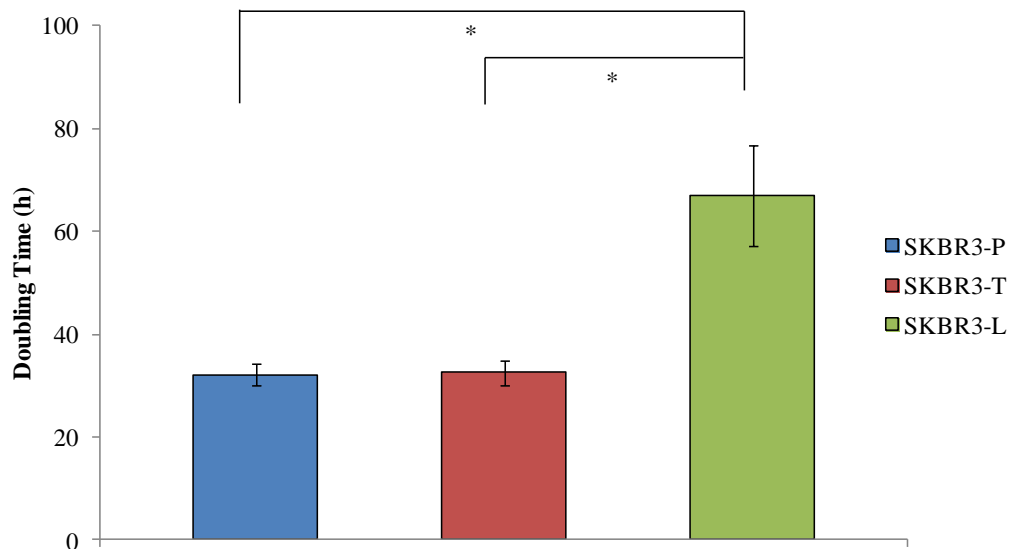


**Figure 3-4:** Average doubling times (h) of the SKBR3-P, SKBR3-T and SKBR3-L cell lines. Proliferation was measured by acid phosphatase at Day 0, 3, 5 and 7. Error bars denote the standard deviation of triplicate experiments. \* denotes  $p < 0.05$  determined by Students t-test.

### 3.4. Migratory properties of the acquired resistant cell lines

We examined migration of the cell lines using a wound scratch assay after 24 h and 48 h (Figure 3-5). No significant differences were seen in migration after 24 h (**Figure 3-5 A**). The SKBR3-T cell line is more migratory than the SKBR3-P cell line ( $p=0.0001$ ) after 48 h (**Figure 3-5 A**). The SKBR3-L ( $93.3 \pm 4.0$  %) cell line is significantly more migratory than the SKBR3-P ( $12.3 \pm 1.0$  %) ( $p=0.02$ ) cell line after 48 h (**Figure 3-5 A**). Representative images of the triplicate assays at each time point is shown in **Figure 3-5 B**.

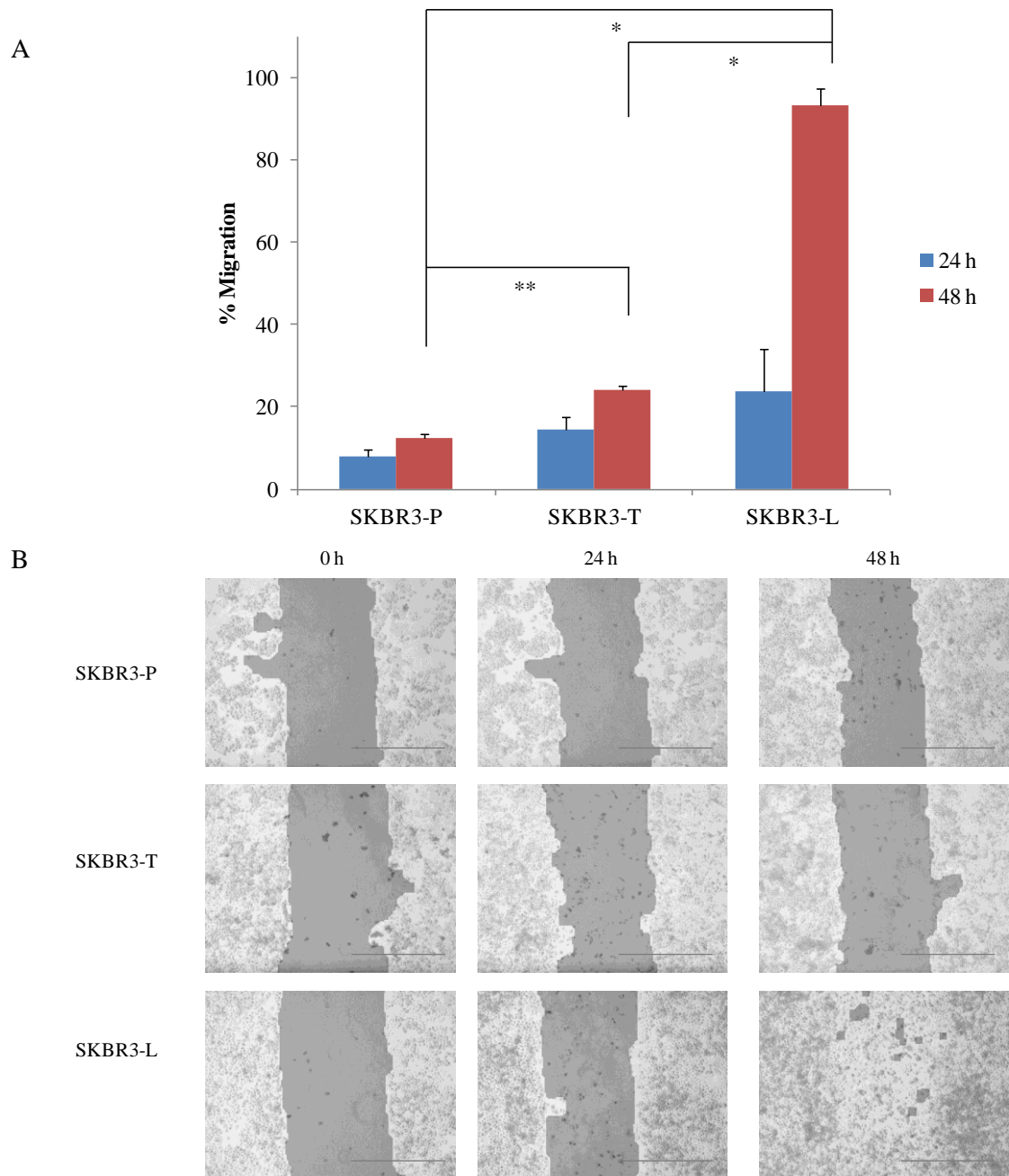


**Figure 3-5:** Average migration in the SKBR3-P, SKBR3-T and SKBR3-L cell lines after 24 h and 48 h time points graphical representation (A) and wound scratch images (B). Open space (%) was calculated using the TScratch program and migration was then calculated (100% - open space %). Error bars denote the standard deviation of triplicate experiments. Student's t-test was performed to determine significant difference between the SKBR3-P, SKBR3-T and SKBR3-L cell lines: \* denotes  $p < 0.05$  and \*\*\* denotes  $p < 0.005$ .

### 3.5. Sensitivity of BT474-Tr acquired trastuzumab resistance cell line model

Previously, an acquired trastuzumab variant of the BT474 cells, BT474-Tr was created in UCLA [123]. Treatment of the BT474-P cells with 10  $\mu\text{g}/\text{mL}$  trastuzumab inhibited growth by  $59.5 \pm 8.6 \%$ ; however treatment of the BT474-Tr cells with 10  $\mu\text{g}/\text{mL}$  trastuzumab has no significant effect on growth ( $1.1 \pm 3.3 \%$ ) (**Figure 3-6**). We also investigated the sensitivity of these cell lines to lapatinib treatment. These cell lines are extremely sensitive to lapatinib treatment with  $\text{IC}_{50}$  values of  $0.02 \pm 0.006 \mu\text{M}$  for the BT-474-P and  $0.03 \pm 0.002 \mu\text{M}$  for the BT-474-Tr (**Figure 3-7**).

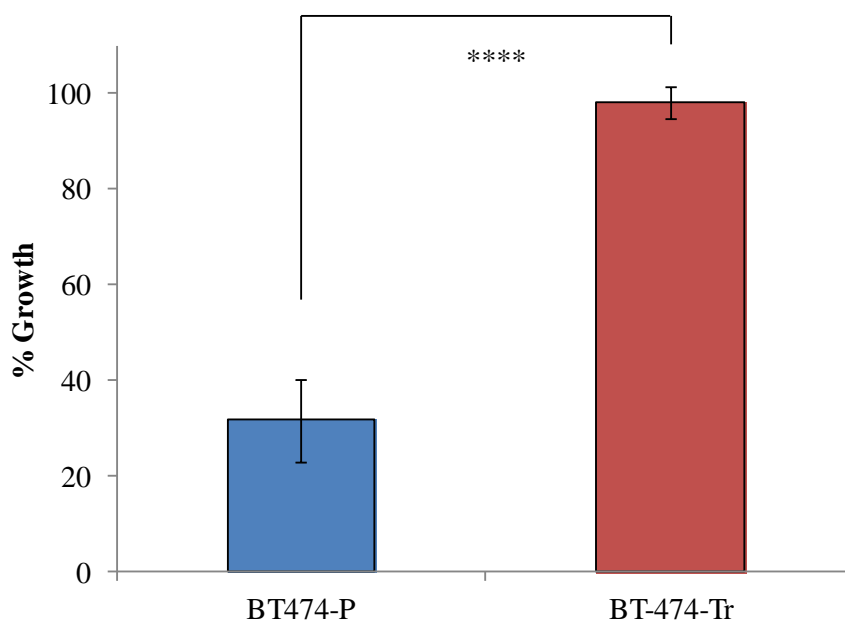


**Figure 3-6:** Determination of trastuzumab sensitivity in the BT474-P and acquired trastuzumab resistant BT474-Tr cell line after trastuzumab treatment (10  $\mu\text{g}/\text{mL}$ ). Proliferation was measured by acid phosphatase method after 5 days, and is expressed relative to untreated control. Error bars denote the standard deviation of triplicate experiments. Student's t-test was performed to determine significant difference: \*\*\*\* denotes  $p < 0.00005$ .

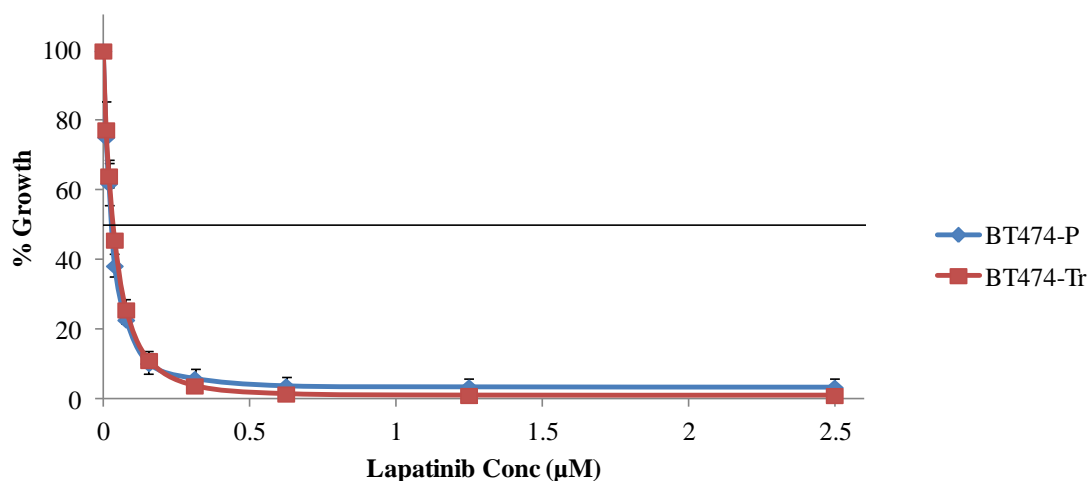


**Figure 3-7:** Determination of lapatinib sensitivity in the BT-474-P cell line and the acquired resistant variant; BT-474-Tr. Proliferation was measured by acid phosphatase method after 5 days, and is expressed relative to untreated control. Line represents 50% growth. Error bars denote the standard deviation of triplicate experiments.

### 3.6. HCC-1954-L acquired lapatinib resistance cell line model

Previously, an acquired lapatinib resistant variant of the HCC-1954 cell line, HCC-1954-L was created by continuous conditioning with increasing doses of lapatinib by Dr. Martina McDermott [247]. Resistance to lapatinib is classified when the  $IC_{50}$  is above 1  $\mu M$ , as defined by O'Brien *et al.* [103]. Both the HCC-1954-P ( $3.16 \pm 2.9\%$ ) and the HCC-1954-L ( $2.64 \pm 4.3\%$ ) are resistant to trastuzumab (**Figure 3-8**). The HCC-1954-L ( $2.7 \pm 0.1\ \mu M$ ) ( $p = 0.01$ ) were previously determined resistant to lapatinib when compared to the HCC-1954-P ( $0.42 \pm 0.02\ \mu M$ ) cells by Dr. Martina McDermott. We confirmed lapatinib resistance of the HCC-1954-L cells ( $24.5 \pm 6.2\%$ ) compared to its parent ( $55.0 \pm 4.4\%$ ) at a concentration of 1  $\mu M$  (**Figure 3-9**).

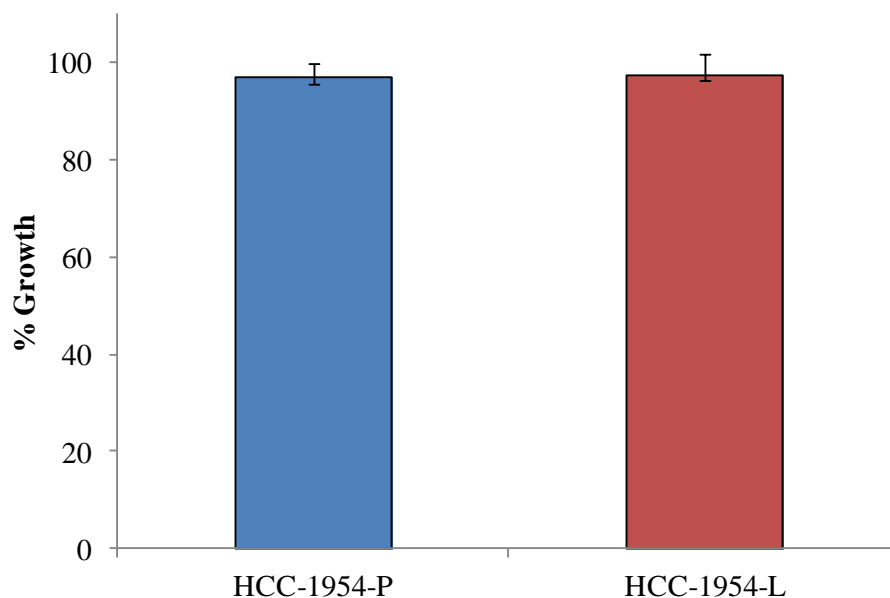


**Figure 3-8:** Determination of trastuzumab sensitivity in the HCC-1954-P and acquired lapatinib resistant HCC-1954-L cell line after trastuzumab treatment (10  $\mu\text{g}/\text{mL}$ ). Proliferation was measured by acid phosphatase method after 5 days, and is expressed relative to untreated control. Error bars denote the standard deviation of triplicate experiments.

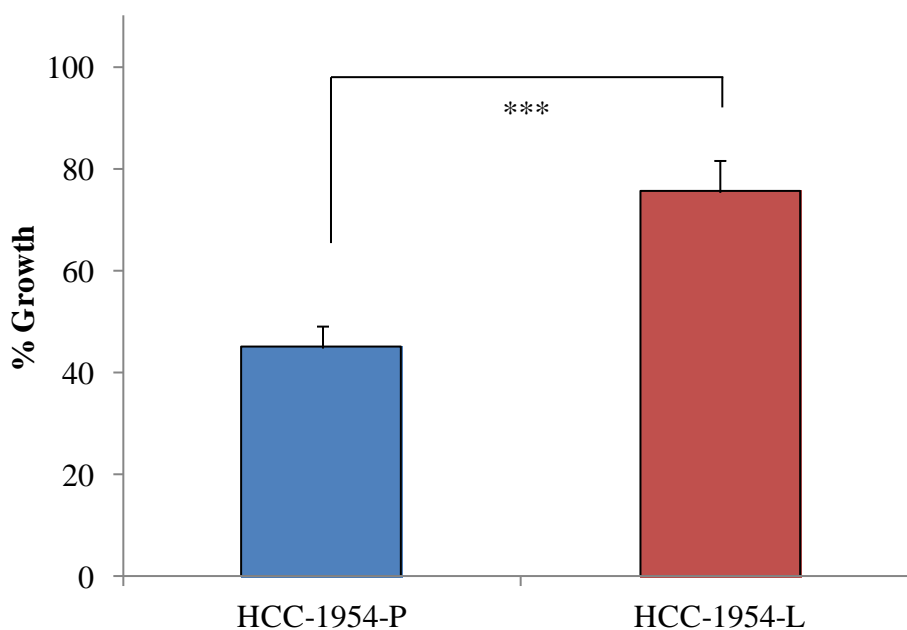


**Figure 3-9:** Confirmation of lapatinib resistance at 1  $\mu\text{M}$  in the HCC-1954-L cell line compared to its parental, HCC-1954-P. Proliferation was measured by acid phosphatase method after 5 days, and is expressed relative to untreated control. Error bars denote the

standard deviation of triplicate experiments. Student's t-test was performed to determine significant difference: \*\*\* denotes  $p < 0.0005$ .

### 3.7. Microarray data analysis of the SKBR3-T and SKBR3-L cell lines

Previously, gene expression analysis (microarrays) were performed for the SKBR3-P, SKBR3-T and SKBR3-L cell lines in UCLA (n=1). We analysed the data and identified significantly altered genes in the SKBR3-T cell line compared to its parent when applying a  $p < 0.05$  and a  $\pm 1.5$  fold change cut-off. As breast cancer stem cells have been implicated in resistance to chemotherapy and trastuzumab [264, 265] we investigated a list of putative stem cell markers in our microarray in collaboration with Dr. Michael O'Gallagher, Trinity College Dublin (TCD). This list was cross compared with our microarray data for the SKBR3-T (**Table 3-2**) and SKBR3-L (**Table 3-3**) cell lines.

**Table 3-2:** Significantly altered putative stem cell markers in the SKBR3-T cell line microarray data (UCLA, n=1) compared with the SKBR3-P cell line. Targets were selected using a 1.5 fold cut-off and  $p < 0.05$ .

Gene Name	Sequence Description	Fold Change	P-value	Accession #	Sequence Code
SFRP1	secreted frizzled-related protein 1	1.6	0.0009	BC036503	A_23_P10121
JAG2	jagged 2	1.6	0.0011	NM_002226	A_23_P106024
MYC	v-myc myelocytomatosis viral oncogene homolog (avian)	1.6	0.0000	NM_002467	A_23_P215956
KLF4	Kruppel-like factor 4 (gut)	1.5	0.0107	NM_004235	A_23_P32233
GLI3	GLI family zinc finger 3	-1.5	0.0071	NM_000168	A_23_P111531
YY1	YY1 transcription factor	-1.5	0.0034	AK026497	A_24_P916288
FOXO1	forkhead box O1	-1.6	0.0018	NM_002015	A_23_P151426
LTBP1	latent transforming growth factor beta binding protein 1	-1.6	0.0013	NM_000627	A_23_P43810
WNT4	wingless-type MMTV integration site family, member 4	-1.9	0.0001	NM_030761	A_23_P11787
BMP7	bone morphogenetic protein 7	-2.2	1.08E-06	NM_001719	A_23_P68487
BMP7	bone morphogenetic protein 7	-2.3	2.11E-07	AK094784	A_23_P154643
WNT6	wingless-type MMTV integration site family, member 6	-3.3	2.87E-11	NM_006522	A_23_P119916

**Table 3-3:** Significantly altered stem cell markers in the SKBR3-L cell line microarray data (UCLA, n=1) compared with the SKBR3-P cell line. Targets were selected using a 1.5 fold cut-off and  $p < 0.05$ .

Gene Name	Sequence Description	Fold Change	P-value	Accession #	Sequence Code
ALDH1A1	aldehyde dehydrogenase 1 family, member A1	5.0	4.55E-15	NM_000689	A_23_P83098
BMP7	bone morphogenetic protein 7	4.0	3.99E-13	NM_001719	A_24_P91566
BMP7	bone morphogenetic protein 7	3.4	1.40E-11	AK094784	A_23_P154643
KLF4	Kruppel-like factor 4 (gut)	3.3	2.51E-11	NM_004235	A_23_P32233
BMP7	bone morphogenetic protein 7	3.1	1.64E-10	NM_001719	A_23_P68487
CTNNB1	catenin (cadherin-associated protein), beta 1, 88kDa	2.9	4.14E-21	NM_001904	A_23_P29495
CTNNB1	catenin (cadherin-associated protein), beta 1, 88kDa	2.2	8.21E-07	NM_001904	A_23_P29499
WNT7B	wingless-type MMTV integration site family, member 7B	2.1	1.43E-06	NM_058238	A_23_P320054
BMP1	bone morphogenetic protein 1	2.0	8.65E-06	NM_006128	A_23_P33277
LTBP1	latent transforming growth factor beta binding protein 1	1.9	0.00003	NM_000627	A_23_P43810
BMP1	bone morphogenetic protein 1	1.8	0.00005	NM_001199	A_24_P129417
ADAM17	ADAM metalloproteinase domain 17	1.7	0.0003	NM_003183	A_23_P143120
JAG1	jagged 1 (Alagille syndrome)	1.7	0.0003	NM_000214	A_23_P210763
JAK1	Janus kinase 1	1.5	0.00	NM_002227	A_23_P97005
MYC	v-myc myelocytomatosis viral oncogene homolog (avian)	1.5	0.0003	NM_002467	A_23_P215956
JAG2	jagged 2	1.5	0.0078	NM_002226	A_23_P106024
WNT7B	wingless-type MMTV integration site family, member 7B	1.5	0.01	NM_058238	A_24_P911607
FOXO1A	CDNA FLJ12289 fis, clone MAMMA1001788	-1.7	0.00026	AK022351	A_24_P930391
PTCH1	patched homolog 1 (Drosophila)	-1.8	0.00017	AK124593	A_24_P106910
BMP8A	bone morphogenetic protein 8a	-2.2	4.98E-07	NM_181809	A_23_P115118
WNT4	wingless-type MMTV integration site family, member 4	-2.3	1.45E-07	NM_030761	A_23_P382607
FOXO1	forkhead box O1	-2.6	1.48E-08	NM_002015	A_23_P151426
POU5F1	POU class 5 homeobox 1	-2.8	1.71E-09	NM_002701	A_23_P59138
JAK3	Janus kinase 3	-2.9	5.39E-10	BC028068	A_24_P59667
WNT4	wingless-type MMTV integration site family, member 4	-3.4	1.38E-11	NM_030761	A_23_P11787

Interestingly, ALDH1A1 was significantly up-regulated in the SKBR3-L (5.0 fold,  $p=4.55E-15$ ) compared to the SKBR3-P cell line. ALDH1A1 was slightly down-regulated in the SKBR3-T (-1.3 fold,  $p=0.04$ ). We investigated the expression and activity of ALDH1A1 in our SKBR3 cell lines by immunoblotting. ALDH1A1 is decreased in the SKBR3-T compared to the SKBR3-P, however it is not significantly altered (**Figure 3-10**). We detected a significant up-regulation of ALDH1A1 in the SKBR3-L cell lines compared to the parental ( $p=0.003$ ) which is consistent with the microarray data (**Figure 3-10**).

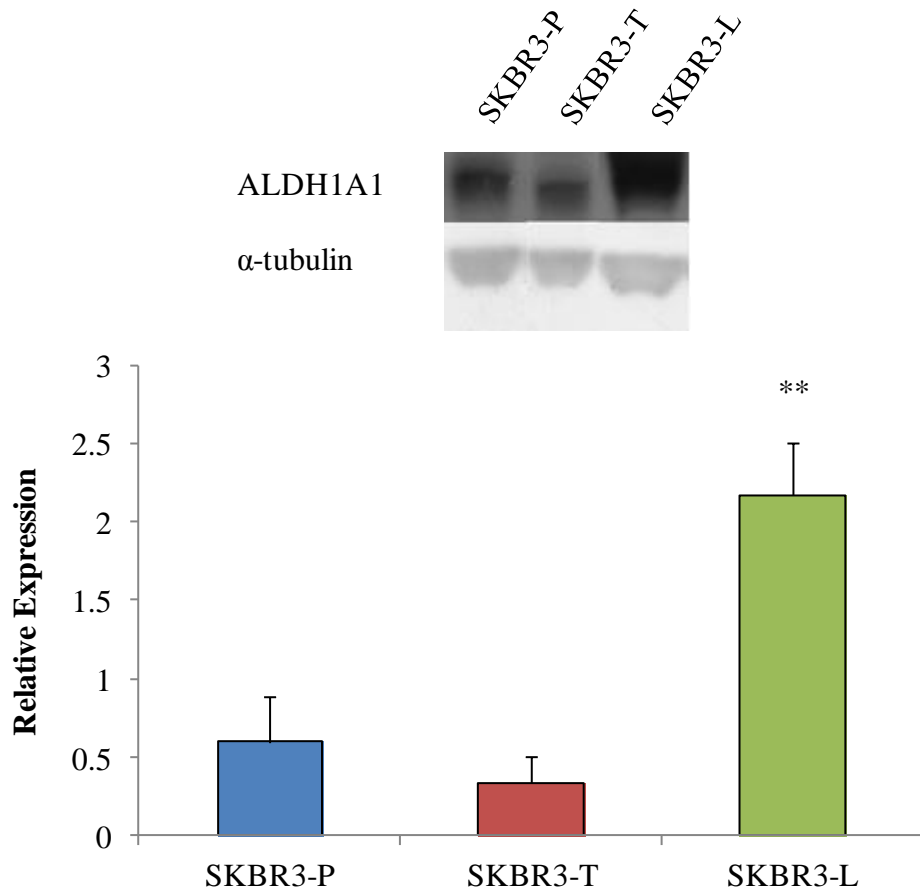


**Figure 3-10:** ALDH1A1 expression in the SKBR3-P, SKBR3-T and SKBR3-L cell lines.  $\alpha$ -tubulin was used as a loading control on each gel. Images are representative of triplicate experiments. Densitometry analysis of triplicate immunoblots was performed using ImageJ software.

### 3.8. ALDEFLUOR analysis of SKBR3-P & SKBR3-L cell lines

The ALDEFLUOR assay is a non-immunological assay which identifies putative stem and progenitor cells based on ALDH (aldehyde dehydrogenase) enzyme activity. The assay is based on expression of ALDH in cells which converts its substrate BAAA (Bodipy aminoacetaldehyde) into a negatively charged product, BAA<sup>-</sup>. This product is retained within the cells causing cells with ALDH<sup>+</sup> expression to fluoresce. The putative cancer stem cells (pCSCs) can be discriminated from non-pCSCs based on the

fluorescent intensity. In Dr. Gallagher's group, they find the diethylamino-benzaldehyde (DEAB) negative control insufficient when a cell contains >80 % ALDH+ cells. They use a mixed population control which contains known ALDH- cells and the query cell line which can then be used to discriminate between the ALDH+ and ALDH- cells in the query cell line. They utilise three technical flow cytometry controls; discrimination of debris, discrimination of single cells from doublets and/or clusters and discrimination of live cells from dead cells.

Initially, Dr. Gallagher's group (TCD) carried out the ALDEFLUOR assay on pellets of the SKBR3-P and SKBR3-L cell lines to determine the amount of putative cancer stem cells (pCSCs) in these cell lines. The samples were analysed and the technical controls were applied to determine the mixed population, the ALDH+ stained population and the optimal ALDH+ stained population for the SKBR3-P (**Figure 3-11 A**) and the SKBR3-L (**Figure 3-11 B**) cell lines. The results from the ALDEFLUOR assay show a high level of ALDH+ stained population within the SKBR3-P cell line ( $95.4 \pm 0.9\%$ ) (Figure 3-11) (**Table 3-4**). The SKBR3-L cell line had a significantly reduced level of ALDH+ stained cells ( $78.2 \pm 6.0\%$ ) compared to the SKBR3-P ( $p=0.04$ ).

These results conflict with our microarray data and our western data which show the SKBR3-L cells have significantly higher expression of ALDH1A1 than the SKBR3-P (**Figure 3-10**). The western blotting data may not be a true representative of ALDH1A1 expression as it may be present within a subpopulation of the cells.

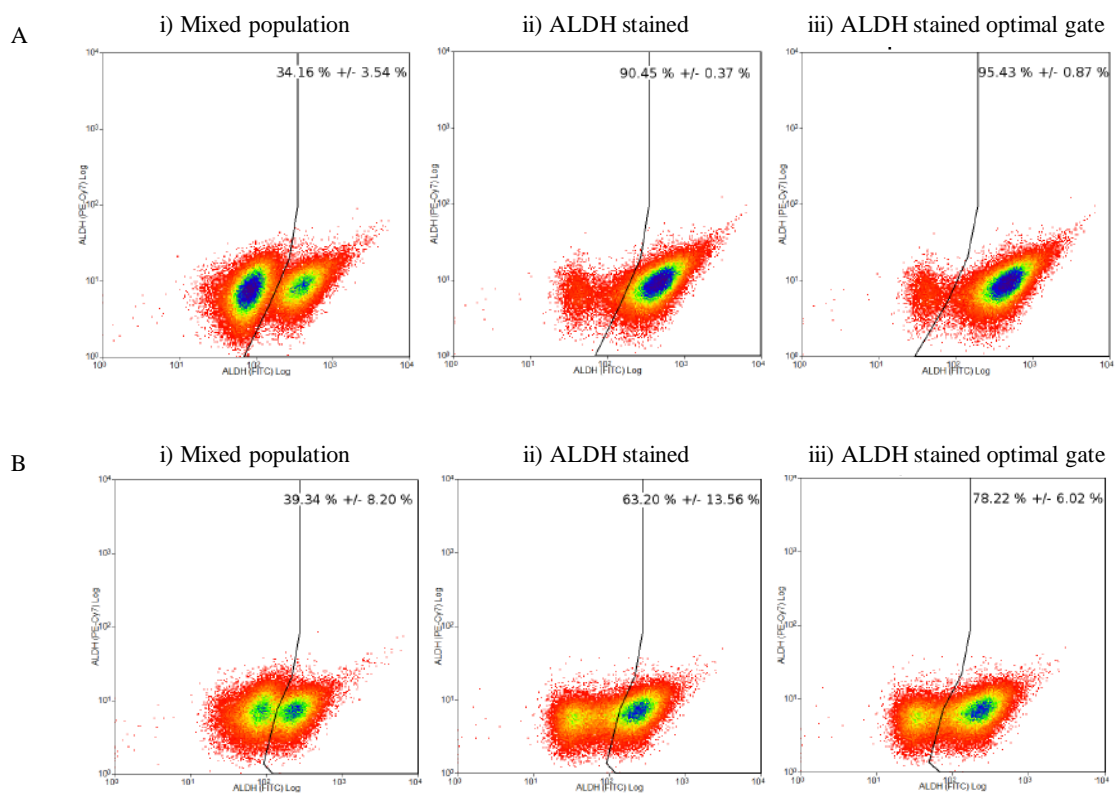


**Figure 3-11:** ALDEFLUOR FACS profiles for the (A) SKBR3-Par and (B) SKBR3-L cell lines. The mixed population consists of known ALDH- A2780 cells and SKBR3-Par cells. This allowed for a gate (black line) to be set between the ALDH- and ALDH+ populations. B) The ALDH Stained sample uses the Mixed Population gate to identify ALDH+ cells. This has a certain degree of false negatives. C) Due to the clear distinction between the ALDH- and ALDH+ fractions in the SKBR3-Par cell line a more optimal gate can be drawn.

**Table 3-4:** Overall mean ALDH+ cell population within the SKBR3-P and SKBR3-L cell lines. Standard deviation is representative of triplicate experiments.

	Mix Population	ALDH Stained	ALDH St. Opt. Gate
SKBR3-P	34.2 ± 3.5	90.5 ± 0.4	95.4 ± 0.9
SKBR3-L	39.3 ± 8.2	63.2 ± 13.6	78.2 ± 6.0

### **3.9. Summary**

The SKBR3-T and SKBR3-L were confirmed as acquired trastuzumab and lapatinib resistant cell lines. Interestingly, the SKBR3-L also shows cross resistance to trastuzumab treatment. We also confirmed the SKBR3-P and SKBR3-T are lapatinib sensitive cell lines. Over time, we identified that changes in serum batches can have drastic effects on resistance. Serum screens can indicate if a cell line will lose resistance; however, this is a short-term assay (7 days). There is a large variation in resistance to trastuzumab upon culturing in serum from different batches and different suppliers.

The doubling time of the SKBR3-L cell line is significantly longer than the SKBR3-P and SKBR3-T cell lines. This suggests that acquired lapatinib resistance has a significant effect on the growth rate of these cells. The SKBR3-T cell line is more migratory than the SKBR3-P cell line after 48 h. The SKBR3-L cell line after 48 h was significantly more migratory than both the SKBR3-P and SKBR3-T cell lines.

We confirmed the BT-474-Tr cells are resistant to trastuzumab. Determination of lapatinib sensitivity of these cell lines showed they are extremely sensitive to lapatinib. The HCC-1954-L cell line, another model of acquired lapatinib resistance was also confirmed as lapatinib resistant and innately resistant to trastuzumab. These resistant cell line models will be the focus of our microRNA profiling in Chapter Four.

Previously, gene expression analysis was carried out on the SKBR3-P, SKBR3-T and SKBR3-L cell lines in UCLA. We identified that ALDH1A1 is up-regulated in the SKBR3-L cell line. Protein expression analysis by western blotting confirmed the

microarray results. Further analysis of our cell lines by the ALDEFLUOR assay indicated the SKBR3-P cell line had a high population of pCSCs. The SKBR3-L cell line had a significantly lower pCSC population compared to the SKBR3-P. The ALDEFLUOR results contradict the results seen in our microarray and protein expression analysis and suggest that there is not an increase in the pCSC population within the lapatinib resistant cell line. Further analysis of ALDH1A1 using immunocytochemistry may indicate the subpopulations that are expressing this putative stem cell marker.

## **Chapter Four**

### **miRNA expression in trastuzumab and lapatinib resistant cell lines**

#### **4.1. Introduction**

As previously mentioned, miRNAs have been shown to play a role in regulating genes involved in drug resistance [266, 267]; therefore we chose to investigate miRNAs and their differential expression in acquired and innate trastuzumab and lapatinib resistant HER2 positive breast cancer cells.

#### **4.2. miRNA expression analysis (Taqman Low Density arrays)**

To identify differentially expressed miRNAs in the acquired trastuzumab and lapatinib resistant cells compared to the parental cell line, TaqMan Low Density Arrays (TLDA- Applied Biosystems) were performed previously by Salima Souahli at the NICB, DCU. Expression values were calculated using the comparative threshold cycle (Ct) method where the SKBR3-T (**Table 4-1**) and SKBR3-L (**Table 4-2**) cell lines were normalised to the endogenous control RNU48 and compared to the SKBR3-P cell line. A fold change cut-off of  $\pm 1.5$  fold change and  $p < 0.05$  cut-off was applied to the data.

**Table 4-1:** Significantly altered miRNAs from TLDA analysis in the SKBR3-T cell line compared to the SKBR3-P cell line that met the cut off criteria of a  $\pm 1.5$  fold change cut-off and a p-value of  $< 0.05$ . Fold changes were calculated using the comparative Ct method. Student's t-test was performed to determine significant differences.

	<b>Fold Change <math>\pm</math> std dev</b>	<b>p-value</b>
<b>miR-149</b>	1.9 $\pm$ 0.5	0.03
<b>miR-192</b>	-2.8 $\pm$ 0.5	0.03
<b>miR-205</b>	3.4 $\pm$ 0.5	0.02
<b>miR-221</b>	3.2 $\pm$ 0.2	0.02
<b>miR-222</b>	2.4 $\pm$ 0.7	0.04
<b>miR-301</b>	-1.5 $\pm$ 0.2	0.03
<b>miR-342</b>	1.6 $\pm$ 0.2	0.02
<b>miR-362</b>	1.6 $\pm$ 0.4	0.02
<b>miR-550</b>	-2.2 $\pm$ 0.8	0.03
<b>miR-9</b>	2.4 $\pm$ 0.0	0.00001

**Table 4-2:** Significantly altered miRNAs from TLDA analysis in the SKBR3-L cell line compared to the SKBR3-P cell line that met the cut off criteria of a  $\pm 1.5$  fold change cut-off and a p-value of  $<0.05$ . Fold changes were calculated using the comparative Ct method. Student's t-test was performed to determine significant differences.

	<b>Fold Change <math>\pm</math> std dev</b>	<b>p-value</b>
<b>miR-135a</b>	7.7 $\pm$ 1.3	0.03
<b>miR-181b</b>	-1.6 $\pm$ 0.1	0.04
<b>miR-192</b>	3.7 $\pm$ 0.2	0.0003
<b>miR-194</b>	4.7 $\pm$ 1.4	0.05
<b>miR-221</b>	-1.5 $\pm$ 0.4	0.03
<b>miR-224</b>	-4.3 $\pm$ 1.2	0.04
<b>miR-26b</b>	-1.6 $\pm$ 0.3	0.03
<b>miR-30a-3p</b>	-3.0 $\pm$ 0.8	0.05
<b>miR-30e-3p</b>	-2.3 $\pm$ 0.1	0.02
<b>miR-375</b>	-4.1 $\pm$ 0.1	0.0006
<b>miR-550</b>	-2.2 $\pm$ 0.7	0.03
<b>miR-92a</b>	-2.2 $\pm$ 0.4	0.01
<b>miR-9</b>	1.6 $\pm$ 0.1	0.001

### 4.3. RNA extraction

RNA extracted from the SKBR3-P, SKBR3-T and SKBR3-L cell lines was separated on an agarose gel to determine RNA integrity. Bands representing total RNA (28S and 18S) and miRNA (small RNA) were assessed in all samples (**Figure 4-1**).

Concentration ( $\mu\text{g}/\mu\text{l}$ ) and purity ( $A_{260/280}$ ) of RNA was determined by analysis on a Nanodrop (Thermo Scientific).

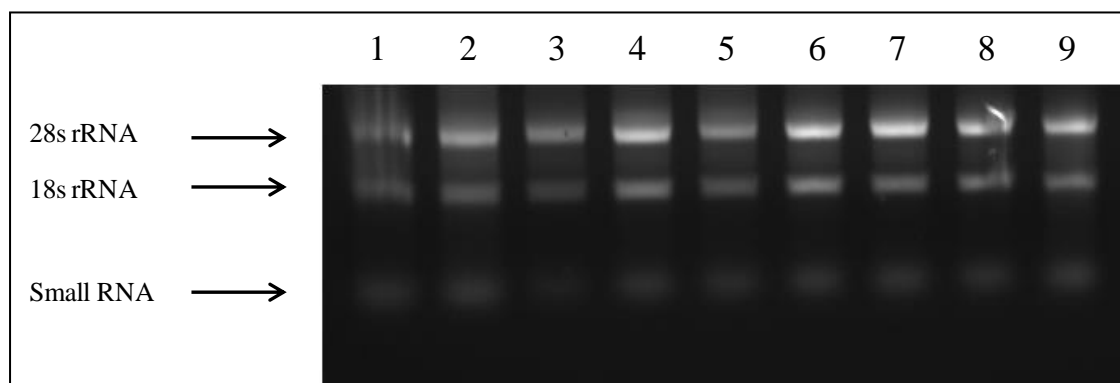


**Figure 4-1:** RNA extractions for SKBR3-P (1-3), SKBR3-T (4-6) and SKBR3-L (7-9).

#### **4.4. qRT-PCR validation of miRNA targets in trastuzumab and lapatinib resistant cells**

Validation of the differentially expressed miRNAs from the TLDA analysis was carried out by individual qRT-PCR. Six miRNAs plus miR-224 out of the ten altered miRNAs in the SKBR3-T cell line were selected for further validation. We confirmed that miR-221 ( $p=0.04$ ), miR-222 ( $p=0.01$ ) and miR-9 ( $p=0.04$ ) were significantly up-regulated and miR-224 ( $p=0.01$ ) was significantly down-regulated in the SKBR3-T cell line compared to the SKBR3-P cell line (**Table 4-3**).

**Table 4-3:** Validation of miRNAs identified in TLDA analysis was carried out using individual qRT-PCR analysis in the SKBR3-T cell line compared to the parental cell line. Fold changes were calculated using the comparative Ct method. Student's t-test was performed to determine significant differences (highlighted in bold).

	<b>Fold Change <math>\pm</math> std dev</b>	<b>p-value</b>
miR-192	-1.5 $\pm$ 0.6	0.33
miR-205	1.1 $\pm$ 0.3	0.60
<b>miR-221</b>	<b>5.8 <math>\pm</math> 0.8</b>	<b>0.04</b>
<b>miR-222</b>	<b>3.8 <math>\pm</math> 0.4</b>	<b>0.01</b>
<b>miR-224</b>	<b>-1.6 <math>\pm</math> 0.2</b>	<b>0.01</b>
miR-550	1.1 $\pm$ 0.2	0.45
<b>miR-9</b>	<b>2.2 <math>\pm</math> 0.8</b>	<b>0.04</b>

In the SKBR3-L cell line, ten miRNAs plus miR-222 were selected for further validation. We confirmed that miR-221 (p=0.02), miR-222 (p=0.04), miR-224 (p=0.01), were significantly down-regulated and miR-9 (p=0.01) was the only significantly up-regulated miRNA in the SKBR3-L cell line compared to the SKBR3-P cell line. miR-30a-3p was significantly altered, however, it was the opposite trend as seen in the TLDA analysis (**Table 4-4**).

**Table 4-4:** Validation of miRNA targets identified in TLDA analysis was carried out using individual qRT-PCR analysis in the SKBR3-L cell line compared to the parental cell line. Fold changes were calculated using the comparative Ct method. Student's t-test was performed to determine significant differences (highlighted in bold).

	<b>Fold Change <math>\pm</math> std dev</b>	<b>p-value</b>
miR-135a	-1.3 $\pm$ 0.2	0.21
miR-192	2.1 $\pm$ 0.8	0.08
<b>miR-221</b>	<b>-2.7 <math>\pm</math> 1.1</b>	<b>0.02</b>
<b>miR-222</b>	<b>-2.0 <math>\pm</math> 1.0</b>	<b>0.04</b>
<b>miR-224</b>	<b>-5.2 <math>\pm</math> 0.3</b>	<b>0.01</b>
<b>miR-30a-3p</b>	<b>2.3 <math>\pm</math> 0.3</b>	<b>0.01</b>
miR-30e-3p	-1.7 $\pm$ 0.1	0.14
miR-375	-1.5 $\pm$ 0.3	0.02
miR-550	-1.6 $\pm$ 0.6	0.04
miR-92a	-1.9 $\pm$ 0.5	0.02
<b>miR-9</b>	<b>2.7 <math>\pm</math> 0.7</b>	<b>0.01</b>

We selected miR-221 and -222 for validation in both SKBR3-T and SKBR3-L despite miR-222 not being altered in the TLDA data. They are clustered genes located in an intergenic region which contain identical seed sequences and suggest that these miRNAs are expressed together and function on the same target mRNAs [268]. miR-224 was validated in the SKBR3-T cell line despite only being significantly altered in the SKBR3-L TLDA data due to the large decrease in expression seen in SKBR3-L cell lines.

#### 4.5. Validation of miRNA targets in the BT474-Tr acquired trastuzumab resistance cell line model

The miRNA targets identified in the acquired trastuzumab resistant cell line, SKBR3-T were validated in the BT474-Tr cell line to determine if any of the alterations were cell line specific. miR-221 (p=0.02) and miR-222 (p=0.004) were significantly up-regulated and miR-224 expression was switched off in the BT474-Tr cell line compared to that of its parent (**Table 4-5**). However, miR-9 expression was not significantly altered in this model of acquired resistance (**Table 4-5**).

**Table 4-5:** Validation of miRNA expression in BT-474-Tr cells compared to BT474 cells. Fold changes were calculated using the comparative Ct method. Student's t-test was performed to determine significant differences (highlighted in bold). \*On - Off fold change denotes Ct values < 36 to Ct values of > 36 in the BT474-TR resistant cell lines respectively.

	Fold Change $\pm$ std dev	p-value
<b>miR-221</b>	<b>5.7 <math>\pm</math> 0.9</b>	<b>0.02</b>
<b>miR-222</b>	<b>5.3 <math>\pm</math> 0.8</b>	<b>0.004</b>
<b>miR-224</b>	<b>On-Off* <math>\pm</math> 1.5</b>	<b>0.0004</b>
miR-9	-1.1 $\pm$ 0.6	0.65

#### 4.6. Validation of miRNA targets in the HCC-1954-L acquired lapatinib resistance cell line model

miRNA expression analysis of the HCC-1954 and HCC-1954-L cells identified that; miR-222 (p=0.05) was significantly down-regulated and miR-9 (p=0.04) were significantly up-regulated in the HCC1954-L cell line compared to the HCC-1954 cell line (**Table 4-6**).

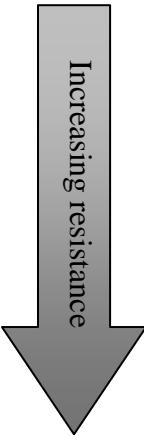
**Table 4-6:** Validation of miRNA expression in HCC-1954-L cells compared to HCC-1954 cells. Fold changes were calculated using the comparative Ct method. Student’s t-test was performed to determine significant differences (highlighted in bold).

	<b>Fold Change ± std dev</b>	<b>p-value</b>
miR-221	1.0 ± 0.7	0.98
<b>miR-222</b>	<b>-1.9 ± 0.4</b>	<b>0.05</b>
miR-224	1.7 ± 0.7	0.17
<b>miR-9</b>	<b>1.9 ± 0.3</b>	<b>0.04</b>

#### **4.7. Analysis of miRNA targets in a cell line panel of innate trastuzumab and lapatinib resistance**

miRNA was extracted from cell lines that were previously characterised as innately sensitive or resistant to trastuzumab and lapatinib by Dr Neil O’Brien (refer to **Table 2-2**) [103]. Expression values for the innate trastuzumab resistant cell lines were compared to a pooled trastuzumab sensitive control sample (BT474-P and SKBR3-P). In the innate trastuzumab setting (**Table 4-7**); miR-221 expression was significantly higher in 5/6 innately resistant cell lines compared to the sensitive cell lines. miR-222 expression was significantly higher in 3/6, however, was significantly lower in 3/6 innately resistant cell lines compare to the sensitive cell lines. miR-224 expression was significantly lower in 5/6 innately resistant cell lines compared to the sensitive cell lines. miR-9 was significantly higher in 1/6 innately resistant cell lines compared to the sensitive. However, opposing the trend seen in the acquired resistance setting, miR-9 is significantly lower in 5/6 innately resistant cell lines compared to the sensitive cell lines.

**Table 4-7:** miRNA expression analysis of miR-221, -222, -224 and -9 in the innate trastuzumab resistant cell lines compared to innate trastuzumab sensitive cell lines; SKBR3-P and BT-474-P. Arrow indicates increasing levels of resistance. Fold changes were calculated using the comparative Ct method and represented with  $\pm$  std dev. Student's t-test was performed to determine significant differences (highlighted in bold).



	<b>miR-221</b>	<b>miR-222</b>	<b>miR-224</b>	<b>miR-9</b>
<b>UACC-732</b>	<b>3.4 <math>\pm</math> 0.6</b>	<b>-5.6 <math>\pm</math> 0.2</b>	<b>-7.1 <math>\pm</math> 0.6</b>	<b>-2.9 <math>\pm</math> 0.4</b>
<b>HCC-1419</b>	<b>7.9 <math>\pm</math> 0.4</b>	<b>-28.2 <math>\pm</math> 0.5</b>	<b>-5.3 <math>\pm</math> 0.5</b>	<b>-7.7 <math>\pm</math> 0.3</b>
<b>JIMT-1</b>	<b>45.4 <math>\pm</math> 0.9</b>	<b>283.8 <math>\pm</math> 0.3</b>	<b>-5.8 <math>\pm</math> 0.2</b>	<b>-3.4 <math>\pm</math> 0.3</b>
<b>HCC-1954</b>	<b>964.5 <math>\pm</math> 0.3</b>	<b>687.2 <math>\pm</math> 0.5</b>	<b>15.7 <math>\pm</math> 0.4</b>	<b>-1.2 <math>\pm</math> 0.2</b>
<b>HCC-1569</b>	-1.6 $\pm$ 0.8	2.1 $\pm$ 0.5	-5.5 $\pm$ 0.3	45.0 $\pm$ 0.2
<b>MDA-MB-453</b>	<b>5.7 <math>\pm</math> 0.6</b>	<b>-11.1 <math>\pm</math> 1.1</b>	<b>-7.1 <math>\pm</math> 0.4</b>	<b>-2.4 <math>\pm</math> 0.4</b>

Expression values for the innate lapatinib resistant cell lines were compared to a pooled trastuzumab sensitive control sample (SKBR3-P, BT-474-P, HCC-1419 and HCC-1954). In the innate lapatinib resistance setting; miR-221 expression is significantly lower in 2/4 and significantly higher in 1/4 innately lapatinib resistant cell lines compared to the sensitive cell lines (**Table 4-8**). miR-221 expression is unaltered in the MDA-MB-453 cell line. miR-222 expression is significantly lower in 2/4 and significantly higher in 1/4 innately resistant cell lines compared to the sensitive pool. miR-222 expression is unaltered in the HCC-1569 cell line. miR-224 expression is significantly lower in 4/4 innately lapatinib resistant cell lines compared to the sensitive pool. miR-9 expression levels are significantly higher in 1/4 and significantly lower in

1/4 innately lapatinib resistant cell lines compared to the sensitive pool. However, miR-9 expression is unaltered in the UACC-732 and MDA-MB-453 cell lines.

**Table 4-8:** miRNA expression analysis of miR-221, -224 and -9 in the innate lapatinib resistant cell lines compared to innate lapatinib sensitive cell lines; SKBR3-P, BT-474-P, HCC-1419 and HCC-1954. Arrow indicates increasing levels of resistance Fold changes were calculated using the comparative Ct method and represented with  $\pm$  std dev. Student's t-test was performed to determine significant differences (highlighted in bold).

	miR-221	miR-224	miR-9
UACC-732	-2.3 $\pm$ 0.7	-7.5 $\pm$ 0.3	-1.2 $\pm$ 0.3
JIMT-1	<b>5.2 <math>\pm</math> 0.8</b>	<b>-7.1 <math>\pm</math> 0.2</b>	<b>-1.6 <math>\pm</math> 0.4</b>
HCC-1569	<b>-10.1 <math>\pm</math> 0.5</b>	<b>-4.9 <math>\pm</math> 0.0</b>	<b>122.1 <math>\pm</math> 0.1</b>
MDA-MB-453	-1.9 $\pm$ 0.6	<b>-10.5 <math>\pm</math> 0.5</b>	-1.3 $\pm$ 0.3



#### 4.8. Short-term trastuzumab treatment of SKBR3-P cell line

SKBR3-P cells were treated for 24 h and 48 h with media, trastuzumab (10  $\mu$ g/mL) or lapatinib (250 nM) after which time cells were harvested for miRNA extraction. Fold changes were calculated as treated compared to untreated controls. However, no significant changes were observed after 24 h or 48 h short-term trastuzumab treatment in the miRNA expression (**Table 4-9**). However, lapatinib induced significant down-regulation of miR-221,-222 and -224 after 24 h (**Table 4-10**). No alterations in miRNA expression were seen after 48 h treatment with lapatinib.

**Table 4-9:** miRNA expression analysis after short-term treatment (24 h & 48 h) with 10 µg/mL trastuzumab.

	<b>24 h ± std dev</b>	<b>48 h ± std dev</b>
<b>miR-9</b>	1.3 ± 0.3	1.7 ± 0.6
<b>miR-221</b>	1.0 ± 0.5	1.7 ± 1.0
<b>miR-222</b>	1.1 ± 0.7	1.5 ± 1.3
<b>miR-224</b>	1.2 ± 0.9	1.2 ± 0.1

**Table 4-10:** miRNA expression analysis after short-term treatment (24 h & 48 h) with lapatinib (250 nM). Significant fold changes are highlighted in **bold**. \* denotes p<0.05 and \*\* denotes p<0.005.

	<b>24 h ± std dev</b>	<b>48 h ± std dev</b>
<b>miR-9</b>	-3.0 ± 0.8	1.1 ± 0.5
<b>miR-221</b>	<b>-14.2 ± 0.5 **</b>	-2.5 ± 0.9
<b>miR-222</b>	<b>-20.1 ± 0.7 *</b>	1.4 ± 0.4
<b>miR-224</b>	<b>-7.6 ± 1.2 **</b>	-1.2 ± 0.5

#### 4.9. Target prediction for microRNAs

We utilised miRWalk to identify potential targets and cross compared this with the UCLA dataset for miR-221 (Table 4-11) (Table 4-12), miR-222 (Table 4-13) (Table 4-14), miR-224 (Table 4-15) (Table 4-16) and miR-9 (Table 4-17) (Table 4-18) in both SKBR3-T and SKBR3-L cell lines respectively. We applied a fold change cut-off of  $\pm 2.0$  and  $p < 0.05$ .

**Table 4-11:** Potential targets for miR-221 in the SKBR3-T cell lines. miRWalk identified targets related to miR-221 and these were cross compared with our UCLA dataset (n=1). Fold change cut-off of  $\pm 2.0$  and  $p < 0.05$  were applied.

Gene Name	Sequence Description	Fold Change	p-value	Accession #	Sequence Code
ANG	Homo sapiens angiogenin, ribonuclease, RNase A family, 5 (ANG), transcript variant 1, mRNA.	-2.2	1.23E-06	NM_001145	A_23_P428738
CDKN1C	cyclin-dependent kinase inhibitor 1C (p57, Kip2)	-2.0	0.00001	NM_000076	A_23_P428129

**Table 4-12:** Potential targets for miR-221 in the SKBR3-L cell lines. miRWalk identified targets related to miR-221 and these were cross compared with our UCLA dataset (n=1). Fold change cut-off of  $\pm 2.0$  and  $p < 0.05$  were applied.

Gene Name	Sequence Description	Fold Change	P-value	Accession #	Sequence Code
CCL2	chemokine (C-C motif) ligand 2	3.3	3.09E-26	NM_002982	A_23_P89431
PPARG	peroxisome proliferator-activated receptor gamma	2.6	1.15E-17	NM_015869	A_23_P252062
CSK	c-src tyrosine kinase	2.3	0.000000211	NM_004383	A_23_P152024
CXCR4	chemokine (C-X-C motif) receptor 4	2.1	1.12E-10	NM_003467	A_23_P102000
ITGAV	integrin, alpha V (vitronectin receptor, alpha polypeptide, antigen CD51)	2.0	0.00001	NM_002210	A_23_P381992
TPM1	tropomyosin 1 (alpha)	2.0	0.00001	L02922	A_24_P924721
MET	met proto-oncogene (hepatocyte growth factor receptor)	2.0	0.00001	NM_000245	A_23_P145844

**Table 4-13:** Potential targets for miR-222 in the SKBR3-T cell lines. miRWalk identified targets related to miR-222 and these were cross compared with our UCLA dataset (n=1). Fold change cut-off of  $\pm 2.0$  and  $p < 0.05$  were applied.

Gene Name	Sequence Description	Fold Change	p-value	Accession #	Sequence Code
ANG	Homo sapiens angiogenin, ribonuclease, RNase A family, 5 (ANG), transcript variant 1, mRNA.	-2.2	1.23E-06	NM_001145	A_23_P428738
CDKN1C	cyclin-dependent kinase inhibitor 1C (p57, Kip2)	-2.0	0.00001	NM_000076	A_23_P428129

**Table 4-14:** Potential targets for miR-222 in the SKBR3-L cell lines. miRWalk identified targets related to miR-222 and these were cross compared with our UCLA dataset (n=1). Fold change cut-off of  $\pm 2.0$  and  $p < 0.05$  were applied.

Gene Name	Sequence Description	Fold Change	p-value	Accession #	Sequence Code
FGFR3	fibroblast growth factor receptor 3	3.9	6.59E-13	NM_000142	A_23_P500501
CCL2	chemokine (C-C motif) ligand 2	3.3	3.09E-26	NM_002982	A_23_P89431
PPARG	peroxisome proliferator-activated receptor gamma	2.6	1.15E-17	NM_015869	A_23_P252062
MMP1	matrix metalloproteinase 1 (interstitial collagenase)	2.5	1.24E-15	NM_002421	A_23_P1691
CSK	c-src tyrosine kinase	2.3	0.000000211	NM_004383	A_23_P152024
FGFR3	fibroblast growth factor receptor 3	2.2	0.00000114	NM_000142	A_23_P212830
PPP2R2A	protein phosphatase 2 (formerly 2A), regulatory subunit B, alpha isoform	2.0	0.00000727	NM_002717	A_23_P123539
SOD2	superoxide dismutase 2, mitochondrial	2.0	0.00000759	NM_000636	A_23_P134176
TPM1	tropomyosin 1 (alpha)	2.0	0.00001	L02922	A_24_P924721
MET	met proto-oncogene (hepatocyte growth factor receptor)	2.0	0.00001	NM_000245	A_23_P145844

**Table 4-15:** Potential targets for miR-224 in the SKBR3-T cell lines. miRWalk identified targets related to miR-224 and these were cross compared with our UCLA dataset (n=1). Fold change cut-off of  $\pm 2.0$  and  $p < 0.05$  were applied.

Gene Name	Sequence Description	Fold Change	p-value	Accession #	Sequence Code
FOSB	FBJ murine osteosarcoma viral oncogene homolog B	2.8	1.57E-09	NM_006732	A_23_P429998
JUNB	jun B proto-oncogene	2.2	0.00000112	NM_002229	A_24_P241815
RARA	retinoic acid receptor, alpha	2.0	0.00000709	NM_000964	A_23_P207842

**Table 4-16:** Potential targets for miR-224 in the SKBR3-L cell lines. miRWalk identified targets related to miR-224 and these were cross compared with our UCLA dataset (n=1). Fold change cut-off of  $\pm 2.0$  and  $p < 0.05$  were applied.

Gene Name	Sequence Description	Fold Change	p-value	Accession #	Sequence Code
JUNB	jun B proto-oncogene	3.3	2.33E-11	NM_002229	A_24_P241815
CTNNB1	catenin (cadherin-associated protein), beta 1, 88kDa	2.9	4.14E-21	NM_001904	A_23_P29495
PAK2	p21 protein (Cdc42/Rac)-activated kinase 2	2.6	1.50E-08	NM_002577	A_23_P327307
AP2M1	adaptor-related protein complex 2, mu 1 subunit	2.3	0.000000241	NM_004068	A_23_P155624
CTNNB1	catenin (cadherin-associated protein), beta 1, 88kDa	2.2	0.000000821	NM_001904	A_23_P29499
CXCR4	chemokine (C-X-C motif) receptor 4	2.1	1.12E-10	NM_003467	A_23_P102000
JUNB	jun B proto-oncogene	2.0	0.00000908	NM_002229	A_23_P4821

**Table 4-17:** Potential targets for miR-9 in the SKBR3-T cell lines. miRWalk identified targets related to miR-9 and these were cross compared with our UCLA dataset (n=1). Fold change cut-off of -1.5 and p<0.05 were applied.

Gene Name	Sequence Description	Fold Change	p-value	Accession #	Sequence Code
RARA	CDNA clone IMAGE:5162874	-2.8	2.13E-09	BC038432	A_24_P551302
DDIT3	DNA-damage-inducible transcript 3	-2.0	0.00000599	NM_004083	A_23_P21134

**Table 4-18:** Potential targets for miR-9 in the SKBR3-L cell lines. miRWalk identified targets related to miR-9 and these were cross compared with our UCLA dataset (n=1). Fold change cut-off of -1.5 and p<0.05 were applied.

Gene Name	Sequence Description	Fold Change	p-value	Accession #	Sequence Code
BACE1	beta-site APP-cleaving enzyme 1	-4.8	1.07E-14	NM_012104	A_23_P52806
CDK6	cyclin-dependent kinase 6	-3.2	6.15E-11	NM_001259	A_24_P166663
PROM1	prominin 1	-2.8	1.77E-09	NM_006017	A_23_P258463
PTBP2	polypyrimidine tract binding protein 2	-2.8	1.88E-09	NM_021190	A_23_P46396
JUN	jun oncogene	-2.7	7.41E-19	NM_002228	A_23_P201538
ELAVL1	ELAV (embryonic lethal, abnormal vision, Drosophila)-like 1 (Hu antigen R)	-2.7	5.40E-09	NM_001419	A_32_P200165
PTBP2	CDNA clone IMAGE:4797534	-2.6	1.49E-08	BC030757	A_24_P136711
FOXO1	forkhead box O1	-2.6	1.48E-08	NM_002015	A_23_P151426
CEBPA	CCAAT/enhancer binding protein (C/EBP), alpha	-2.5	1.55E-08	NM_004364	A_24_P216165
BCL6	B-cell CLL/lymphoma 6 (zinc finger protein 51)	-2.4	9.26E-08	NM_138931	A_23_P57856
MYCN	v-myc myelocytomatosis viral related oncogene, neuroblastoma derived (avian)	-2.3	1.50E-07	AF320053	A_23_P303390
FOXP1	CDNA FLJ12381 fis, clone MAMMA1002566	-2.3	3.16E-07	AK022443	A_24_P460763
NEUROG3	neurogenin 3	-2.1	2.28E-06	NM_020999	A_23_P35534
CDKN2A	cyclin-dependent kinase inhibitor 2A (melanoma, p16, inhibits CDK4)	-2.0	8.49E-10	NM_058197	A_23_P43484
CEBPB	CCAAT/enhancer binding protein (C/EBP), beta	-2.0	9.62E-10	NM_005194	A_23_P411296

#### **4.10. Summary**

TLDA analysis yielded ten potential miRNAs that were differentially expressed in the acquired trastuzumab SKBR3-T cell line and thirteen potential miRNAs in the acquired lapatinib resistant SKBR3-L cell line when compared to their aged parental controls. We also included miR-224 in the analysis for the SKBR3-T cell line and miR-222 in the SKBR3-L cell line due to the close linkages between these miRNAs as explained previously.

Validation of these findings by individual qRT-PCR in biological and technical triplicates in the SKBR3-T cells confirmed miR-221, -222 and -9 were significantly up-regulated and miR-224 was down-regulated. Further validation in the SKBR3-L cell line confirmed that; miR-9 was significantly up-regulated and miR-221, -222 and -224 were all significantly down-regulated.

To determine if these alterations were cell line specific, we examined the selected miRNAs in other cell line models of acquired resistance; BT474-Tr (an acquired trastuzumab resistant cell line model from UCLA) and the HCC-1954-L (an acquired lapatinib resistant cell line model). We determined that miR-221 and -222 are significantly up-regulated in the BT474-Tr cell line compared to the BT-474-P which follows the same trend as seen in the SKBR3-T cell line. Interestingly, miR-224 expression is switched off in the BT-474-Tr cells as it is undetectable by qRT-PCR (Ct values >39) in the BT-474-Tr cells compared to its parental cell line. In the HCC-1954-L cell lines; miR-222 is significantly down-regulated and miR-9 is significantly up-regulated in these cells.

miR-221, -222 and -224 are involved in trastuzumab resistant cell lines whereas miR-222 and -9 are involved in acquired lapatinib resistant cell lines. There is one common miRNA in the acquired trastuzumab and lapatinib setting; miR-222.

From these results we focused on the miR-221, -222, -224 and -9 in the innate trastuzumab resistant setting and found: miR-221 expression was significantly higher in 5/6; miR-222 expression was significantly higher in 3/6; miR-224 was significantly lower in 5/6; and miR-9 was significantly higher in only 1/6 innately resistant cell line models tested compared to a innately sensitive cell lines. There are alterations in miRNAs in the innate setting and while miR-221 and miR-224 seem to follow the trend observed in the acquired resistance setting, miR-222 and miR-9 follow opposing trends. We focused on miR-221, -224 and miR-9 in the innate lapatinib resistance setting and found: miR-221 expression is significantly lower in 2/4; miR-224 is significantly down regulated in 4/4; and miR-9 is significantly higher in 1/4 innately resistant cell lines compared to innately sensitive cell lines.

We also investigated the short term treatment effects of trastuzumab and lapatinib in the SKBR3-P cell line to determine if there were any changes in miRNA expression. After 24 h treatment with trastuzumab (10  $\mu\text{g}/\text{mL}$ ) no significant changes were seen in the miRNA expression levels. However, after 24 h treatment with lapatinib (250 nM), there were significant alterations in miR-221, -222 and -224 expression levels. This suggests that the miRNAs we identified in the trastuzumab acquired resistant are specific to long term resistance and not short-term resistance. In the lapatinib setting, we identified that after 24 h treatment, miR-221, -222 and -224 are significantly down-regulated in the SKBR3-P cell line.

Target prediction is a useful tool to identify potential mRNA targets for specific miRNAs. We utilised the miRWalk database and the UCLA microarray analysis that was carried out on our SKBR3-P, SKBR3-T and SKBR3-L cell lines to identify potential druggable targets. Cross comparison yielded a small list of potential targets including; retinoic acid receptor alpha (RARA), met proto-oncogene (MET), angiogenin (ANG), cyclin dependent kinase 6 (CDK6) and beta-site APP cleaving enzyme 1 (BACE1).

## **Chapter Five**

# **miR-9 and retinoic acid receptors in trastuzumab and lapatinib resistant cells**

## 5.1 Introduction

miR-9 was identified as up-regulated in the SKBR3-T, SKBR3-L and HCC-1954-L trastuzumab and lapatinib resistant cell lines. Target prediction utilising miRWalk to identify potential down-regulated targets for miR-9 was carried out.

## 5.2 Identification of potential miR-9 targets

Microarray analysis performed on the SKBR3, SKBR3-T and SKBR3-L cell lines was previously carried out in UCLA (n=1). This UCLA dataset was compared with a miRWalk validated target list for miR-9 (159 targets) thus yielding targets that are altered in the resistant cell lines compared to their parental cell line. Briefly, as miR-9 was up-regulated, only messenger RNA (mRNA) targets that were significantly down-regulated were selected ( $> 2$  fold change,  $p < 0.05$ ) as potential targets. Only two statistically significant mRNA targets for miR-9 were identified in the SKBR3-T; retinoic acid receptor alpha (RAR $\alpha$ ) and DNA-damage-inducible-transcript-3 (DDIT3) as shown in **Table 4-17**. We focused on RAR $\alpha$  expression as it has been previously associated with tamoxifen resistance [269] and HER2 positive breast cancer [270, 271]. Three different RAR $\alpha$  probes were included on the array. Two showed significant up-regulation while one showed down-regulation in the microarray analysis in both the SKBR3-T and SKBR3-L cell lines (**Table 5-1**). We examined sensitivity to all-trans retinoic acid in the resistant cells and measured the expression of RAR $\alpha$ . All-trans retinoic acid (ATRA), commonly known as vesanoid (tretinoin) is most commonly used for the treatment of promyelocytic leukemia [272].

**Table 5-1:** RAR $\alpha$  microarray expression data for SKBR3-T and SKBR3-L versus SKBR3-P cell lines including all probes on the microarray (UCLA, n=1).

Array	Sequence Name	Fold Change	p-value	Accession #	Sequence Code
SKBR3-T	RARA	1.5	0.01	NM_000964	A_32_P5251
	RARA	2.0	7.09E-06	NM_000964	A_23_P207842
	RARA	-2.8	2.13E-09	BC038432	A_24_P551302
SKBR3-L	RARA	1.2	0.26932	NM_000964	A_32_P5251
	RARA	1.8	0.0001	NM_000964	A_23_P207842
	RARA	-1.5	0.01	BC038432	A_24_P551302

### 5.3 All-trans retinoic acid (ATRA) treatment

#### 5.3.1 SKBR3-P, SKBR3-T and SKBR3-L cell lines

We investigated the effect of ATRA treatment on the SKBR3-P, SKBR3-T and SKBR3-L cell lines with a range of ATRA concentrations (0.2-0.5  $\mu$ M). The SKBR3-T cells displayed significant resistance to ATRA at 2  $\mu$ M compared with the SKBR3-P (p=0.01), whereas, the SKBR3-L cells show similar sensitivity to the SKBR3-P cells (Figure 5-1) (Table 5-2).

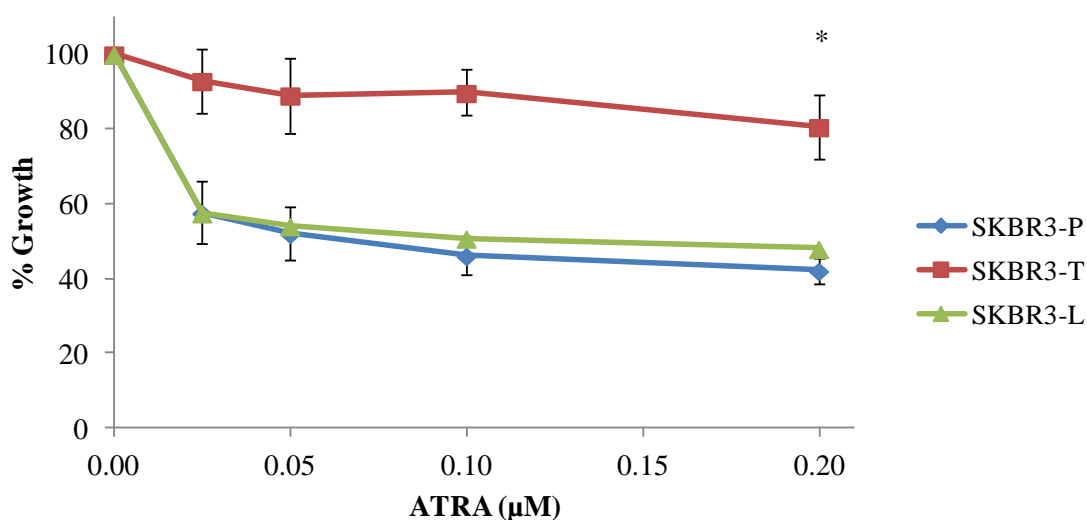


**Figure 5-1:** Determination of ATRA sensitivity in the SKBR3-P cell line and the acquired resistant variants; SKBR3-T and SKBR3-L. Proliferation was measured by acid phosphatase method after 5 days, and is expressed relative to untreated control. Student's t-test was performed to determine significance of the difference in response to treatment: \* denotes  $p < 0.05$  when comparing ATRA treatment ( $2 \mu\text{M}$ ) in the SKBR3-T to the SKBR3-P cell line. Error bars denote the standard deviation of triplicate experiments.

**Table 5-2:** Growth inhibition (%) of the SKBR3-P, SKBR3-T and SKBR3-L cell lines upon ATRA treatment ( $2 \mu\text{M}$ ). Proliferation was measured by acid phosphatase method after 5 days, and is expressed relative to untreated control.

Cell Line	% Growth Inhibition $\pm$ std dev
SKBR3-P	$57.9 \pm 3.3$
SKBR3-T	$19.4 \pm 8.6$
SKBR3-L	$52.0 \pm 4.9$

### 5.3.2 *Other cell line models –BT-474, HCC-1954 and EFM-192A*

To determine if ATRA resistance is linked to trastuzumab resistance we examined ATRA sensitivity in three other cell lines. The BT-474-P and its acquired trastuzumab resistant variant BT-474-Tr were both insensitive to ATRA treatment (**Figure 5-2 A**). The HCC-1954 and its acquired lapatinib resistant variant, HCC-1954-L were also both insensitive to ATRA treatment (**Figure 5-2 B**). The EFM-192A cell line has been previously classed as sensitive to trastuzumab [103], however, we found it was moderately sensitive showing  $28.6 \pm 4.8$  % growth inhibition upon trastuzumab treatment (10  $\mu\text{g/mL}$ ). This cell line showed slight sensitivity to ATRA treatment with maximum growth inhibition of  $12.8 \pm 3.2$  % at 0.2  $\mu\text{M}$  (**Figure 5-2 C**).

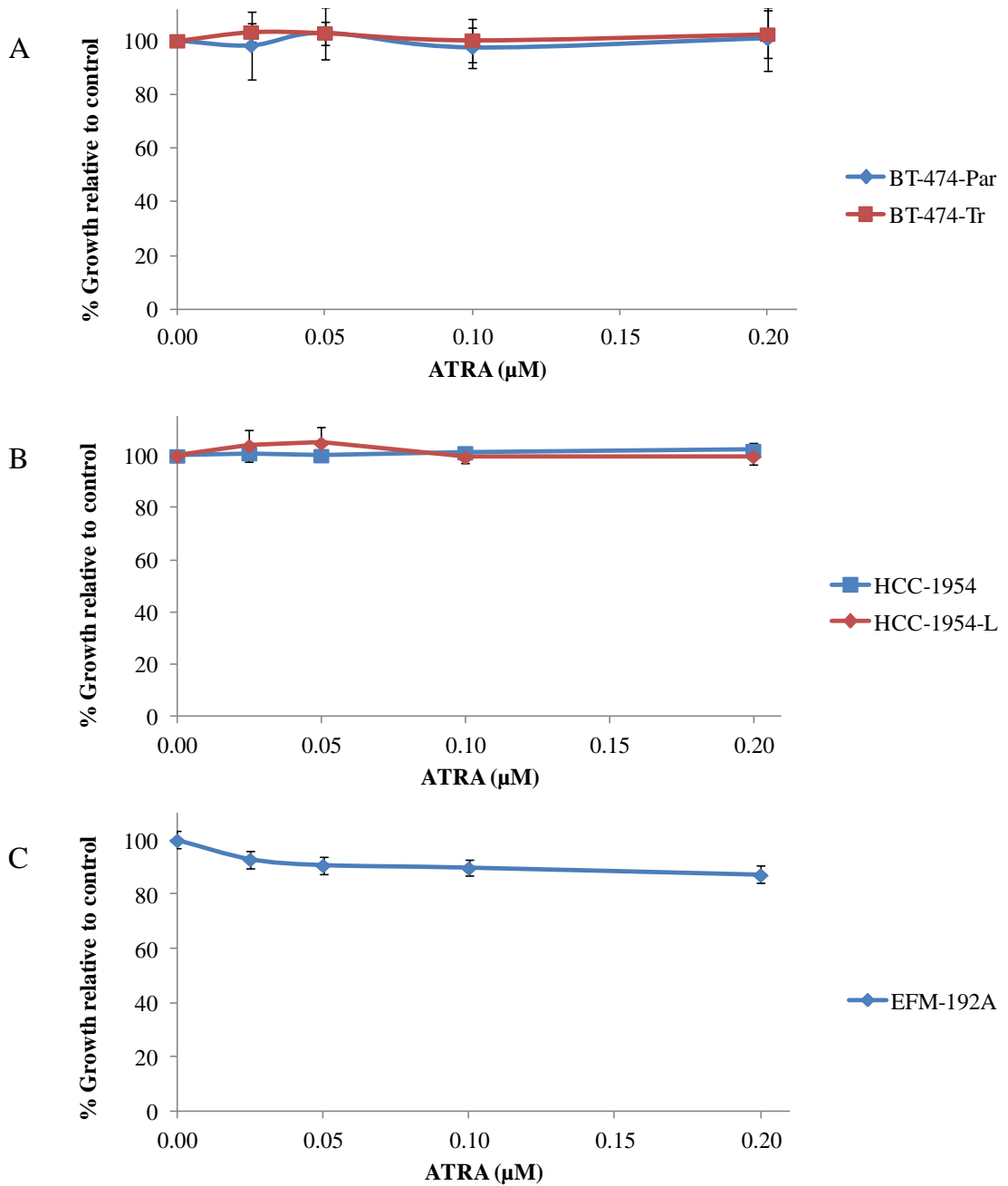


**Figure 5-2:** Determination of ATRA sensitivity in the (A) BT-474-P and BT-474-Tr and (B) HCC-1954-P and HCC-1954-L and (C) EFM-192A cell lines. Proliferation was measured by acid phosphatase method after 5 days, and is expressed relative to untreated control. Error bars denote the standard deviation of triplicate experiments.

## 5.4 All-*trans* retinoic acid (ATRA) and trastuzumab combination treatment

### 5.4.1 SKBR3-P, SKBR3-T and SKBR3-L

We also examined the effect of ATRA in combination with trastuzumab on proliferation using a fixed concentration of trastuzumab (10 µg/mL). In the SKBR3-P cells, combined treatment with ATRA and trastuzumab significantly enhanced growth inhibition compared to ATRA (p=0.0002) or trastuzumab (p=0.0002) treatment alone (**Figure 5-3 A**). The SKBR3-T cells are insensitive to ATRA alone, however, combined treatment with ATRA and trastuzumab significantly inhibited cell growth (p=0.003) when compared to ATRA (p=0.002) or trastuzumab (p=0.003) alone (**Figure 5-3 B**). The SKBR3-L cells are sensitive to ATRA inhibition alone similar to the SKBR3-P cells. Combined treatment with ATRA and trastuzumab significantly enhanced growth inhibition compared to ATRA (p=0.01) or trastuzumab (p=0.001) alone (**Figure 5-3 C**).

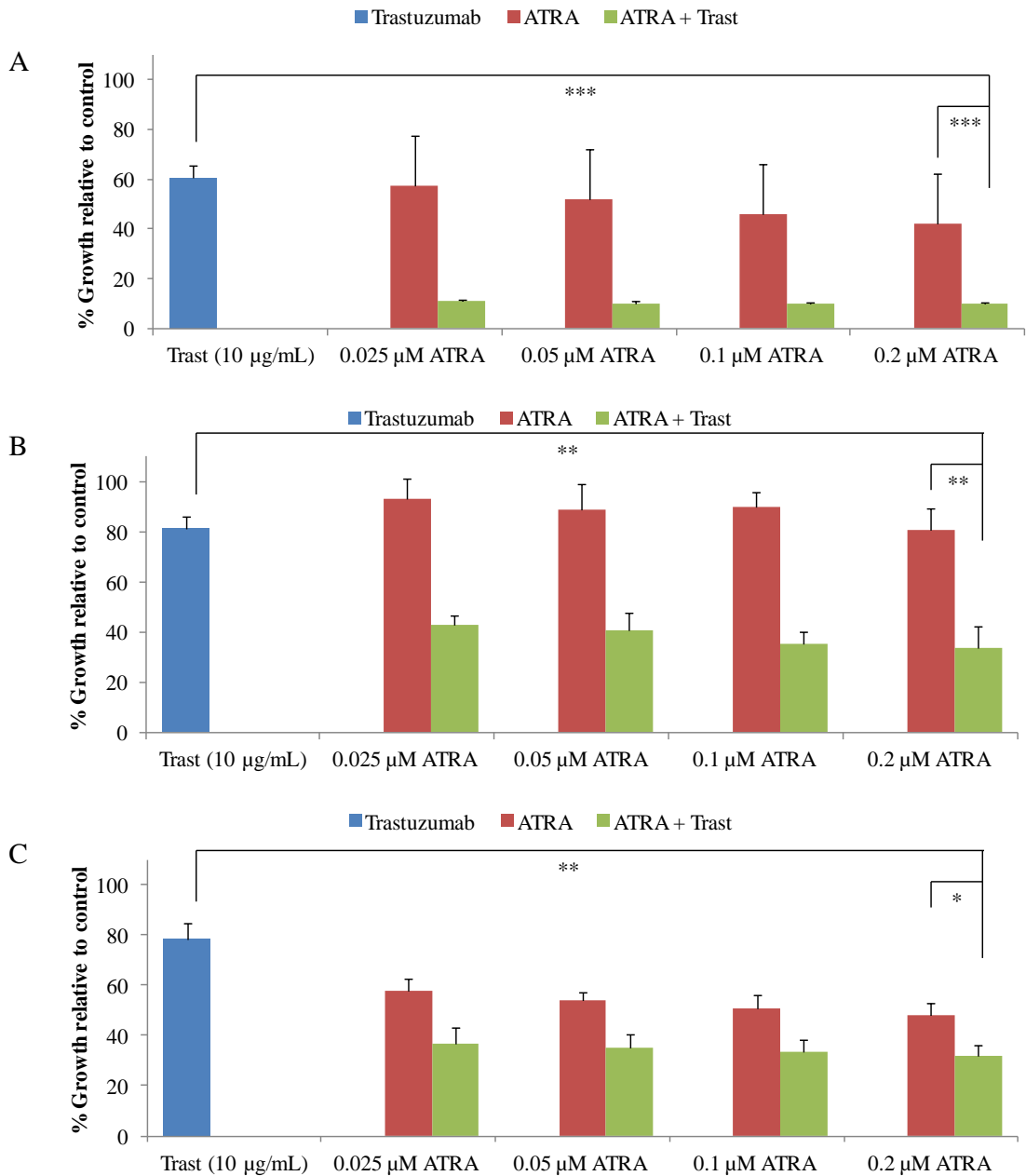


**Figure 5-3:** Proliferation of (A) SKBR3-P, (B) SKBR3-T and (C) SKBR3-L cells treated with trastuzumab (Trast) (10 µg/mL) or ATRA (0.025 µM - 2 µM) as single agents and the combination. Proliferation was measured after five days by the acid phosphatase method. Percent proliferation is expressed relative to untreated control. Student's t-test was performed to compare the combination to the single agents.\* denotes p < 0.05, \*\* denotes p < 0.005 and \*\*\* denotes p < 0.0005. Error bars represent standard deviation of triplicate experiments.

#### 5.4.2 Other cell line models –BT-474, HCC-1954 and EFM-192A

We also examined the effect of ATRA in combination with trastuzumab in other cell lines. Combined treatment of ATRA and trastuzumab did not enhance growth inhibition compared to trastuzumab alone in the BT-474-P ( $p=0.14$ ) and the BT-474-Tr ( $p=0.11$ ) cells (**Figure 5-4**). Similarly, combined treatment did not enhance response compared to trastuzumab alone in either the HCC-1954-P ( $p=0.37$ ) or HCC-1954-L ( $p=0.22$ ) cells (**Figure 5-5**).

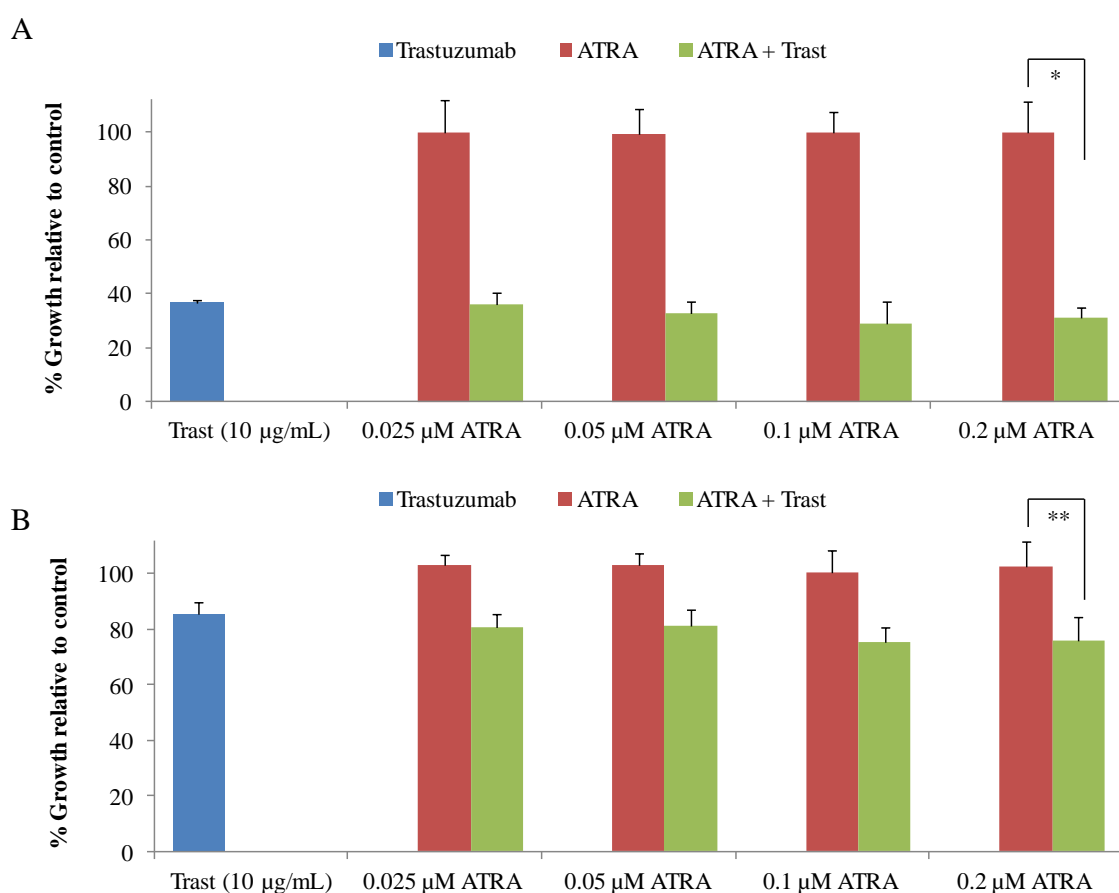


**Figure 5-4:** Proliferation of (A) BT-474 and (B) BT-474-Tr treated with trastuzumab (Trast) (10 µg/mL) or ATRA (0.025 µM - 2 µM) and the combination. Proliferation was measured after five days by the acid phosphatase method. Percent proliferation is expressed relative to untreated control. Student's t-test was performed to compare the combination to the single agents.\* denotes  $p < 0.05$  and \*\* denotes  $p < 0.005$ . Error bars represent standard deviation of triplicate experiments.

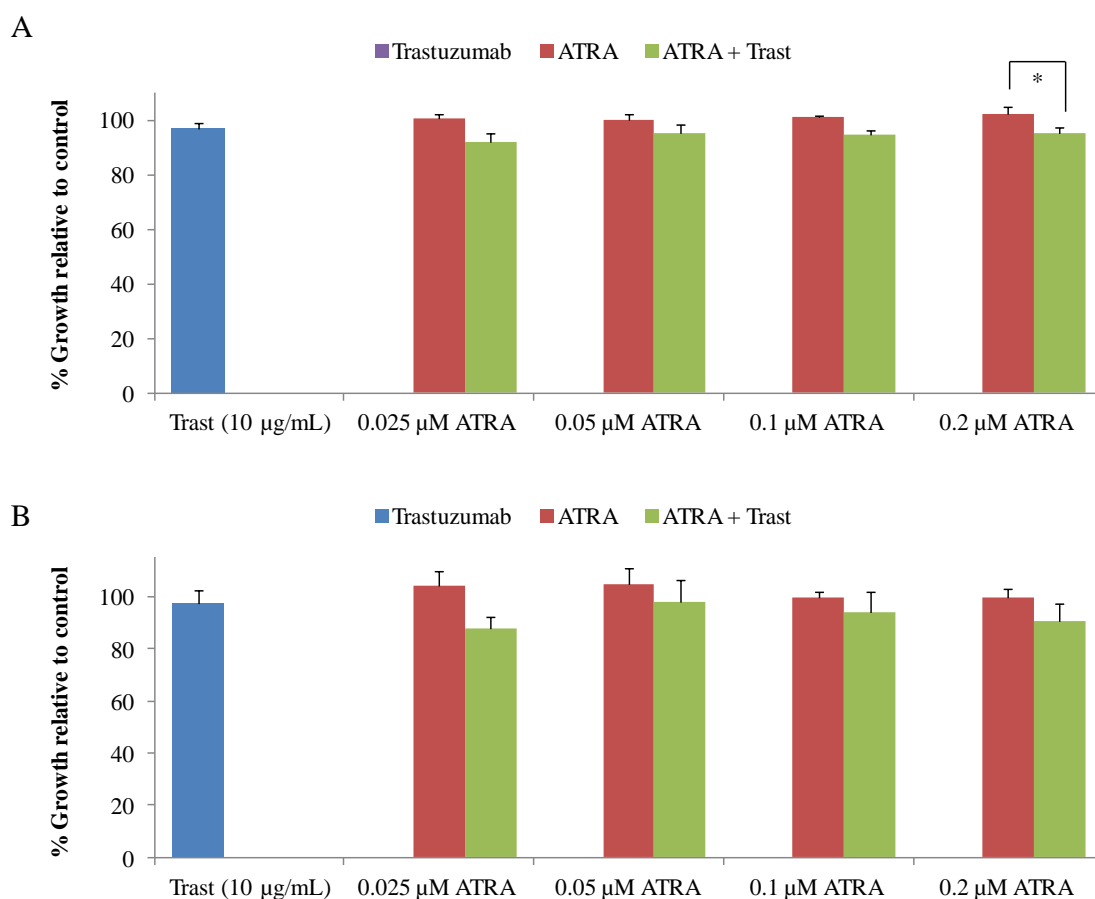


**Figure 5-5:** Proliferation of (A) HCC-1954 and (B) HCC-1954-L treated with trastuzumab (Trast) (10 µg/mL) or ATRA (0.025 µM - 2 µM) and the combination. Proliferation was measured after five days by the acid phosphatase method. Percent proliferation is expressed relative to untreated control. Student's t-test was performed to compare the combination to the single agents.\* denotes  $p < 0.05$ . Error bars represent standard deviation of triplicate experiments.

In the slightly sensitive cell line, EFM-192A, combined treatment enhanced response to trastuzumab treatment when compared to trastuzumab ( $p=0.003$ ) or ATRA ( $p=0.0001$ ) alone (**Figure 5-6**).

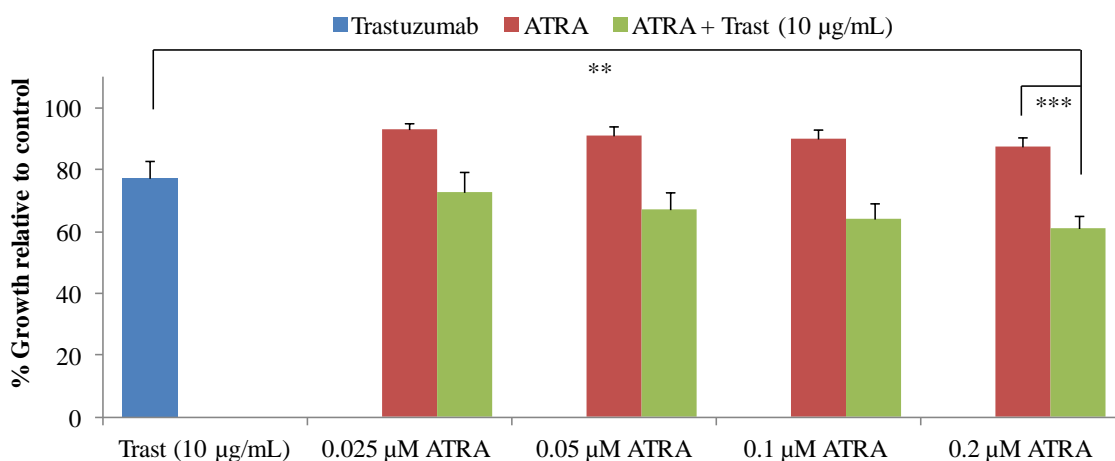


**Figure 5-6:** Proliferation of EFM-192A cells treated with trastuzumab (Trast) (10 µg/mL), ATRA (0.025 µM - 2 µM) and the combination. Proliferation was measured after five days by the acid phosphatase method. Percent proliferation is expressed relative to untreated control. Student's t-test was performed to compare the combination to the single agents. \*\* denotes  $p < 0.005$  and \*\*\* denotes  $p < 0.0005$ . Error bars represent standard deviation of triplicate experiments.

## 5.5 All-trans retinoic acid (ATRA) treatment - Lapatinib combinations

### 5.5.1 SKBR3, SKBR3-T and SKBR3-L cell lines

We examined the effect of ATRA in combination with lapatinib in the SKBR3 cell line panel, using a fixed concentration of 50 nM lapatinib in the SKBR3-P and SKBR3-T cell lines and 1 µM in the SKBR3-L cell line. In the SKBR3 cells, combined treatment with ATRA and lapatinib significantly enhanced growth inhibition compared to ATRA ( $p=0.003$ ) or lapatinib (50 nM) ( $p=0.0009$ ) alone (**Figure 5-7 A**). The combined treatment in the SKBR3-T cell line was also more effective compared to ATRA ( $p=0.002$ ) or lapatinib (50 nM) (0.001) alone (**Figure 5-7 B**). The SKBR3-L cells are resistant to lapatinib (1 µM) treatment, however, the combined treatment enhanced response compared to ATRA ( $p=0.0004$ ) or lapatinib ( $p=0.01$ ) alone (**Figure 5-7 C**).

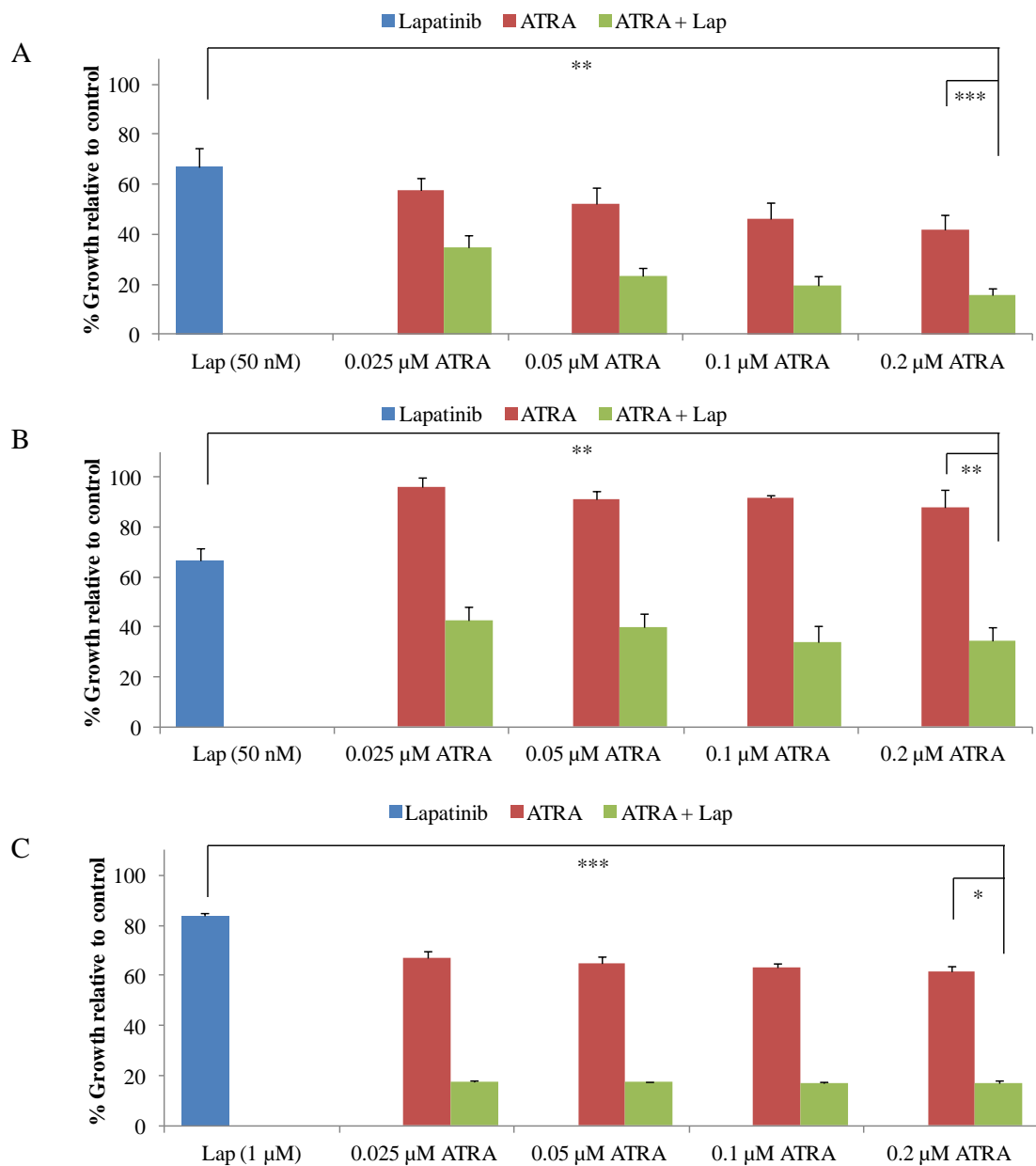


**Figure 5-7:** Proliferation of (A) SKBR3, (B) SKBR3-T and (C) SKBR3-L cells treated with and without lapatinib (50 nM or 1 μM) and ATRA (0.025 μM- 2 μM) as single agents or in combination. Proliferation was measured after five days by the acid phosphatase method. Percent proliferation is expressed relative to untreated control. Student's t-test was performed to determine significance of the difference in response to treatment: \* denotes  $p < 0.05$ , \*\* denotes  $p < 0.005$  and \*\*\* denotes  $p < 0.0005$  when comparing ATRA treatment or combined treatment with lapatinib alone. Error bars represent standard deviation of triplicate experiments.

### **5.5.2 Other cell line models –BT-474, HCC-1954 and EFM-192A**

We examined the effect of ATRA in combination with lapatinib using a fixed concentration of 50 nM in the BT-474-P and BT-474-Tr and EFM-192A and 1  $\mu$ M in the HCC1954 and HCC-1954-L cell lines. In the BT-474-P cells, the combined treatment did not enhance growth inhibition compared to lapatinib alone ( $p=0.86$ ) (**Figure 5-8 A**). Similarly, the combined treatment did not enhance growth inhibition in the BT-474-Tr compared to lapatinib alone ( $p=0.14$ ) (**Figure 5-8 B**). In the HCC-1954-P and HCC-1954-L cells, combined treatment did not enhance growth inhibition compared to lapatinib alone ( $p=0.89$  and  $p=0.27$  respectively) (**Figure 5-9**). Similarly combined treatment did not enhance growth inhibition in the EFM-192A cell line compared to lapatinib treatment alone ( $p=0.12$ ) (**Figure 5-10**)

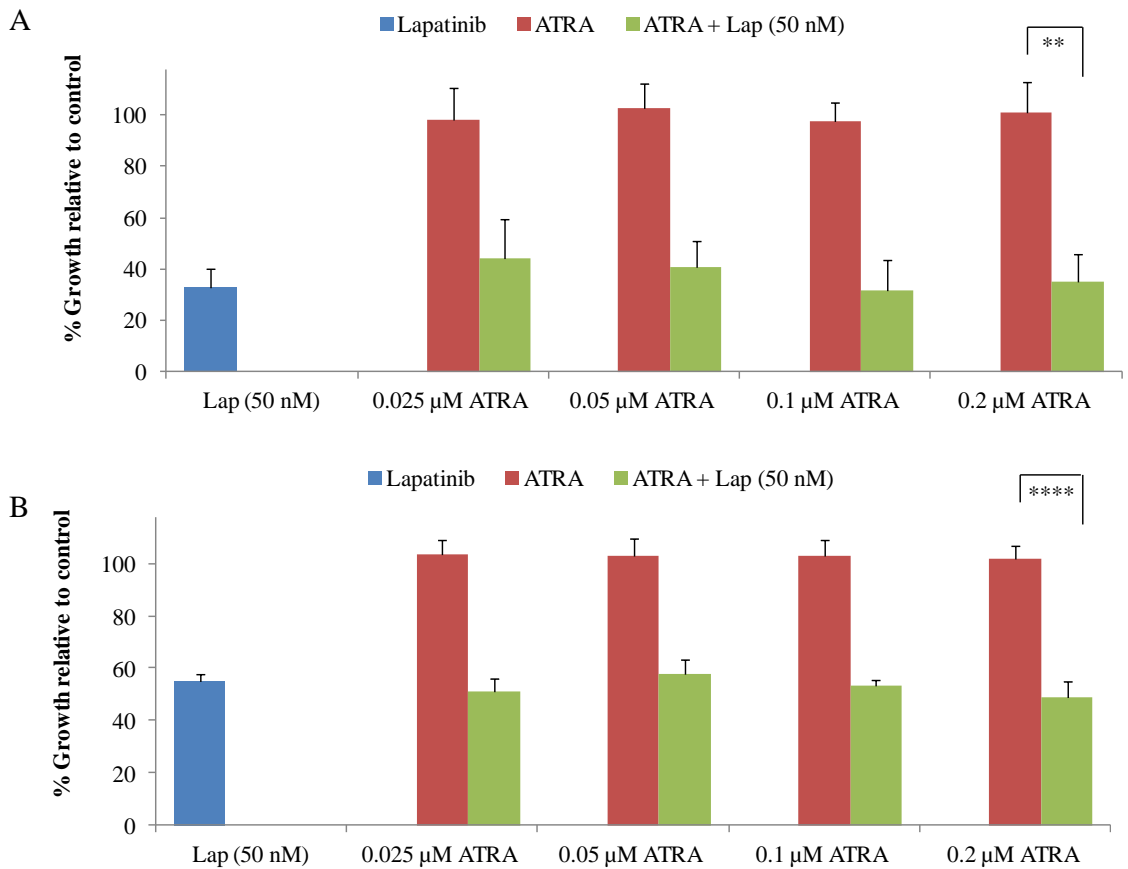


**Figure 5-8:** Proliferation of (A) BT-474 and (B) BT-474-Tr treated with lapatinib (Lap) (50 nM), ATRA (0.025  $\mu$ M - 2  $\mu$ M) and the combination. Proliferation was measured after five days by the acid phosphatase method. Percent proliferation is expressed relative to untreated control. Student's t-test was performed to compare the combination to the single agents.\* denotes  $p < 0.05$  and \*\* denotes  $p < 0.005$ . Error bars represent standard deviation of triplicate experiments.

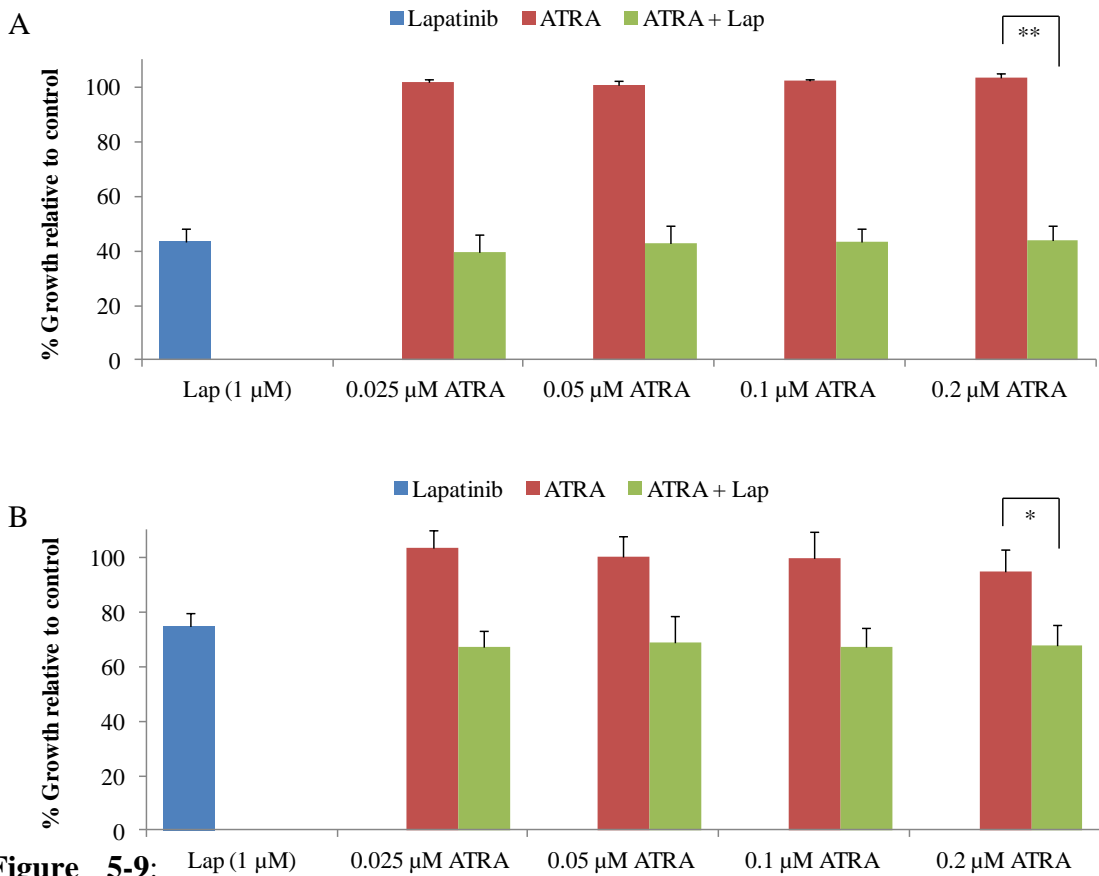


**Figure 5-9:** Proliferation of (A) HCC-1954 and (B) HCC-1954-L treated with lapatinib (Lap) (1  $\mu$ M), ATRA (0.025  $\mu$ M - 2  $\mu$ M) and the combination. Proliferation was measured after five days by the acid phosphatase method. Percent proliferation is expressed relative to untreated control. Student's t-test was performed to compare the combination to the single agents.\* denotes  $p < 0.05$  and \*\* denotes  $p < 0.005$ . Error bars represent standard deviation of triplicate experiments.

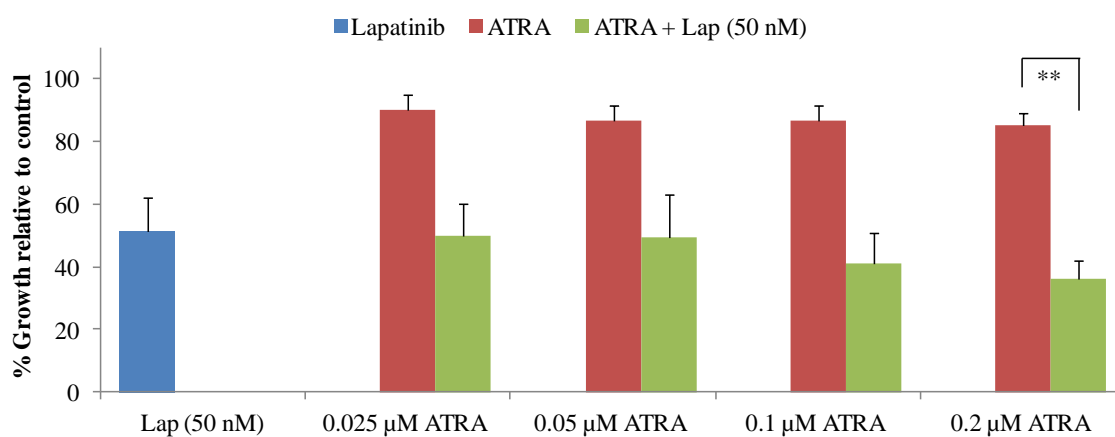


**Figure 5-10:** Proliferation of the EFM-192A cell line treated with lapatinib (Lap) (50 nM), ATRA (0.025 μM - 2 μM) and the combination. Proliferation was measured after five days by the acid phosphatase method. Percent proliferation is expressed relative to untreated control. Student's t-test was performed to compare the combination to the single agents. \*\* denotes  $p < 0.005$ . Error bars represent standard deviation of triplicate experiments.

## 5.6 RAR $\alpha$ expression analysis

### 5.6.1 RAR $\alpha$ mRNA expression

We investigated the expression of RAR $\alpha$  mRNA in our SKBR3-T and SKBR3-L cell lines compared to the SKBR3-P. Gene expression analysis was carried out by qRT-PCR using RAR $\alpha$  specific primers. GAPDH was used as the endogenous control. RAR $\alpha$  mRNA expression levels were not significantly altered in the SKBR3-T and SKBR3-L cell lines compared to the SKBR3-P cell line (**Table 5-3**).

**Table 5-3:** mRNA expression analysis of RAR $\alpha$  in the SKBR3-T and SKBR3-L acquired resistant cell lines. Fold changes were calculated using the comparative Ct method and is expressed relative to expression in the SKBR3-P cells. Student's t-test was performed to determine significant difference.

Cell line	Fold change $\pm$ stdev	p-value
SKBR3-T	-1.2 $\pm$ 0.5	0.5
SKBR3-L	-1.4 $\pm$ 0.2	0.2

### 5.6.2 RAR $\alpha$ protein expression

We examined RAR $\alpha$  protein expression in our acquired resistant cell lines by Western blotting. We found no significant changes in the RAR $\alpha$  protein expression between the SKBR3 and the SKBR3-T (p=0.3) cell line and the BT-474-P and BT-474-Tr (p=0.4) cell lines (**Figure 5-11**).

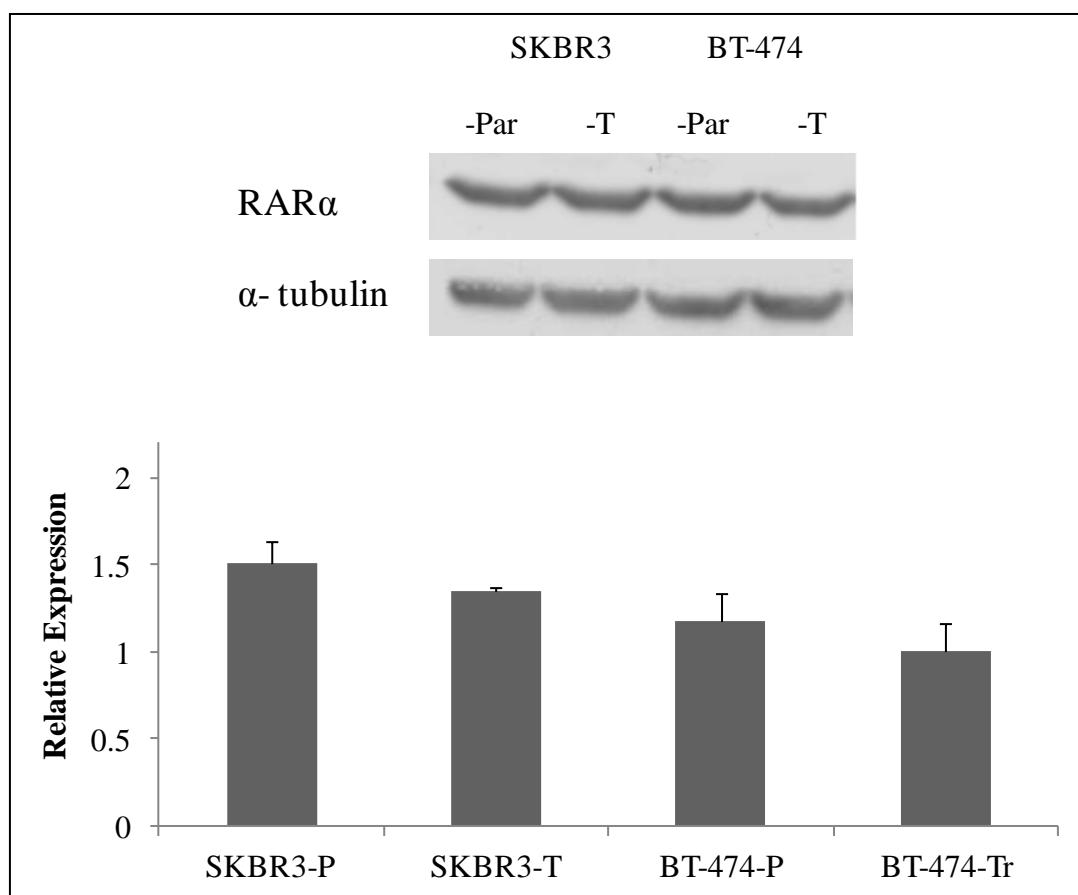


**Figure 5-11:** RAR $\alpha$  protein expression in the SKBR3-P, SKBR3-T, BT-474-P and BT-474-Tr cell lines.  $\alpha$ -tubulin was used as a loading control for each gel. Images are representative of triplicate experiments. Densitometry analysis of triplicate immunoblots was performed using ImageJ software.

### 5.7 RAR $\beta$ , RAR $\gamma$ and RxR $\alpha$ protein expression

As we saw no significant change in the levels of RAR $\alpha$  protein between the parental and the acquired resistant variants, altered RAR $\alpha$  protein expression does not contribute to the decreased ATRA sensitivity in the SKBR3-T cells. Further investigation on miRWalk using the predictive miRNA targets algorithms identified RAR $\beta$ , RAR $\gamma$ , RxR $\alpha$  and RXR $\beta$  as potential targets of miR-9 (**Table 5-4**).

**Table 5-4:** miRNA Predicted Targets on mRNA 3' UTR Region produced by miRWalk and other programs. Hsa-miR-9-1, -2 and -3 refer to the 3 miR-9 seed sequences.

MicroRNA	Gene	miRanda	miRDB	miRWalk	RNA22	Targetscan	SUM
hsa-miR-9-1	RARB	1	0	1	0	1	3
hsa-miR-9-2	RARB	1	0	1	0	1	3
hsa-miR-9-3	RARB	1	0	1	0	1	3
hsa-miR-9-1	RARG	1	0	0	0	0	1
hsa-miR-9-2	RARG	1	0	0	0	0	1
hsa-miR-9-3	RARG	1	0	0	0	0	1
hsa-miR-9-1	RXRA	1	0	1	0	1	3
hsa-miR-9-2	RXRA	1	0	1	0	1	3
hsa-miR-9-3	RXRA	1	0	1	0	1	3
hsa-miR-9-1	RXRB	1	0	0	0	0	1
hsa-miR-9-2	RXRB	1	0	0	0	0	1
hsa-miR-9-3	RXRB	1	0	0	0	0	1

As both RAR $\beta$  and RAR $\gamma$  are targeted by ATRA, we examined their mRNA expression in the UCLA microarray data (**Table 5-5**) and measured protein expression by western blotting. RAR $\beta$  mRNA was unaltered in the SKBR3-T cell line microarray (**Table 5-5**) and protein expression was not significantly altered ( $p=0.57$ ) (**Figure 5-12**). RAR $\beta$  expression was not significantly altered in the BT-474-Tr cells compared to the BT-474-P ( $p=0.93$ ) (**Figure 5-12**). RAR $\gamma$  expression was up-regulated in the microarray data (**Table 5-5**), however; its protein expression was not significantly altered in either the SKBR3-T or BT-474-Tr cell lines (**Figure 5-13**).

**Table 5-5:** RAR $\beta$ , RAR $\gamma$ , RXR $\alpha$  and RXR $\beta$  expression in the SKBR3-T cell lines compared to SKBR3-P from UCLA microarray (n=1). Significant altered proteins are highlighted in bold.

Primary Sequence Name	Fold Change	P-value	Sequence Description	Accession #
RARB	-1.1	0.49	retinoic acid receptor, beta	NM_000965
RARB	-1.1	0.47	retinoic acid receptor, beta	NM_000965
<b>RARG</b>	<b>1.4</b>	<b>0.02</b>	<b>retinoic acid receptor, gamma</b>	<b>NM_000966</b>
RARG	1.2	0.14	retinoic acid receptor, gamma	NM_000966
<b>RARG</b>	<b>1.6</b>	<b>0.001</b>	<b>retinoic acid receptor, gamma</b>	<b>NM_000966</b>
<b>RARG</b>	<b>1.4</b>	<b>0.02</b>	<b>retinoic acid receptor, gamma</b>	<b>NM_000966</b>
<b>RXRA</b>	<b>-1.3</b>	<b>0.04</b>	<b>retinoid X receptor, alpha</b>	<b>NM_002957</b>
RXRA	1.1	0.45	retinoid X receptor, alpha	NM_002957
RXRA	1.0	0.75	retinoid X receptor, alpha	AK090416
RXRA	1.1	0.61	retinoid X receptor, alpha	NM_002957
RXRA	-1.1	0.37	retinoid X receptor, alpha	AK090416
<b>RXRA</b>	<b>-2.2</b>	<b>7.18E-07</b>	<b>retinoid X receptor, alpha</b>	<b>NM_002957</b>
<b>RXRB</b>	<b>1.3</b>	<b>0.04</b>	<b>retinoid X receptor, beta</b>	<b>NM_021976</b>
<b>RXRB</b>	<b>1.5</b>	<b>0.00</b>	<b>retinoid X receptor, beta</b>	<b>NM_021976</b>

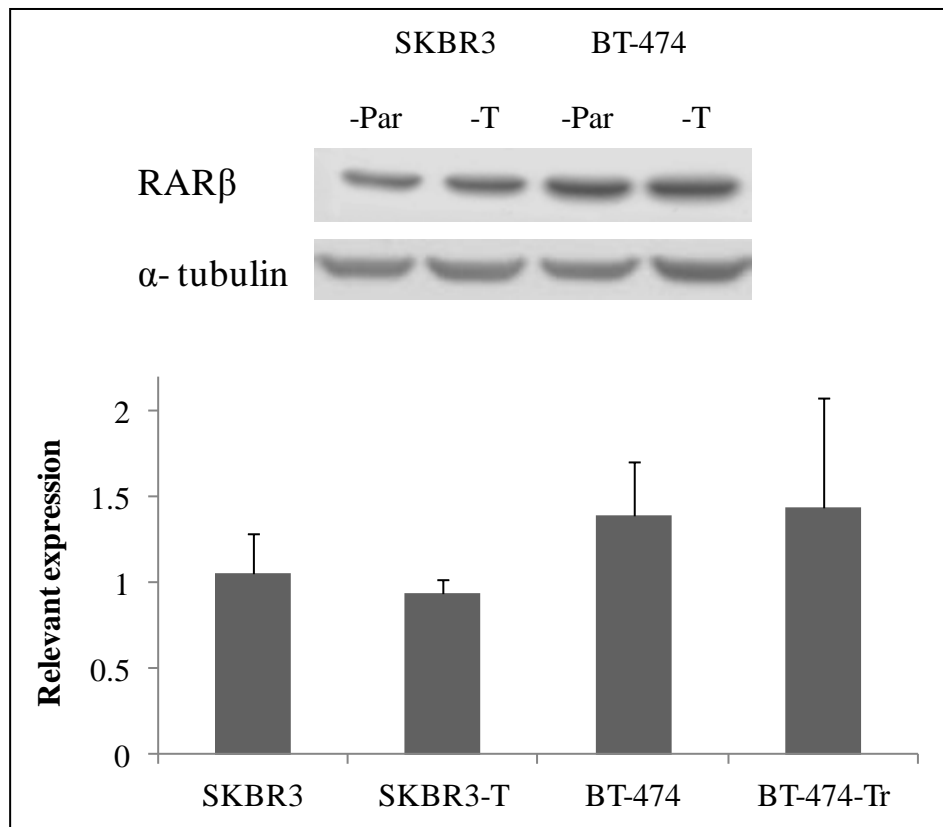


**Figure 5-12:** RAR $\beta$  protein expression in the SKBR3-P, SKBR3-T, BT-474-P and BT-474-Tr cell lines.  $\alpha$ -tubulin was used as a loading control for each gel. Images are representative of triplicate experiments. Densitometry analysis of triplicate immunoblots was performed using ImageJ software.

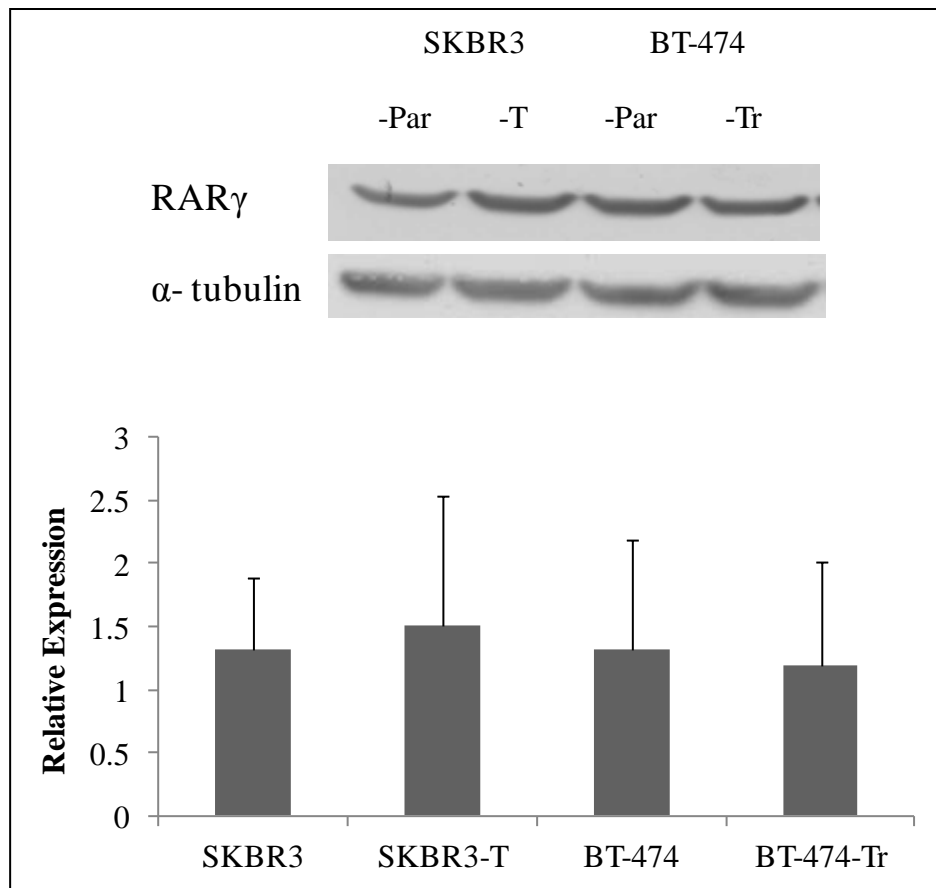


**Figure 5-13:** RAR $\gamma$  protein expression in the SKBR3-P, SKBR3-T, BT-474-P and BT-474-Tr cell lines.  $\alpha$ -tubulin was used as a loading control for each gel. Images are representative of triplicate experiments. Densitometry analysis of triplicate immunoblots was performed using ImageJ software.

RxR $\alpha$  was significantly down-regulated in the microarray data (**Table 5-5**) however; no changes in RxR $\alpha$  protein levels were observed in the SKBR3-T cells compared to the SKBR3-P (**Figure 5-14**). The BT-474-P cells have a higher level of RxR $\alpha$  expression than the SKBR3-P or SKBR3-T cell line, however, no significant changes were observed in the levels of RxR $\alpha$  between the BT-474-Tr and BT-474-P cell line ( $p=0.22$ ) (**Figure 5-14**).

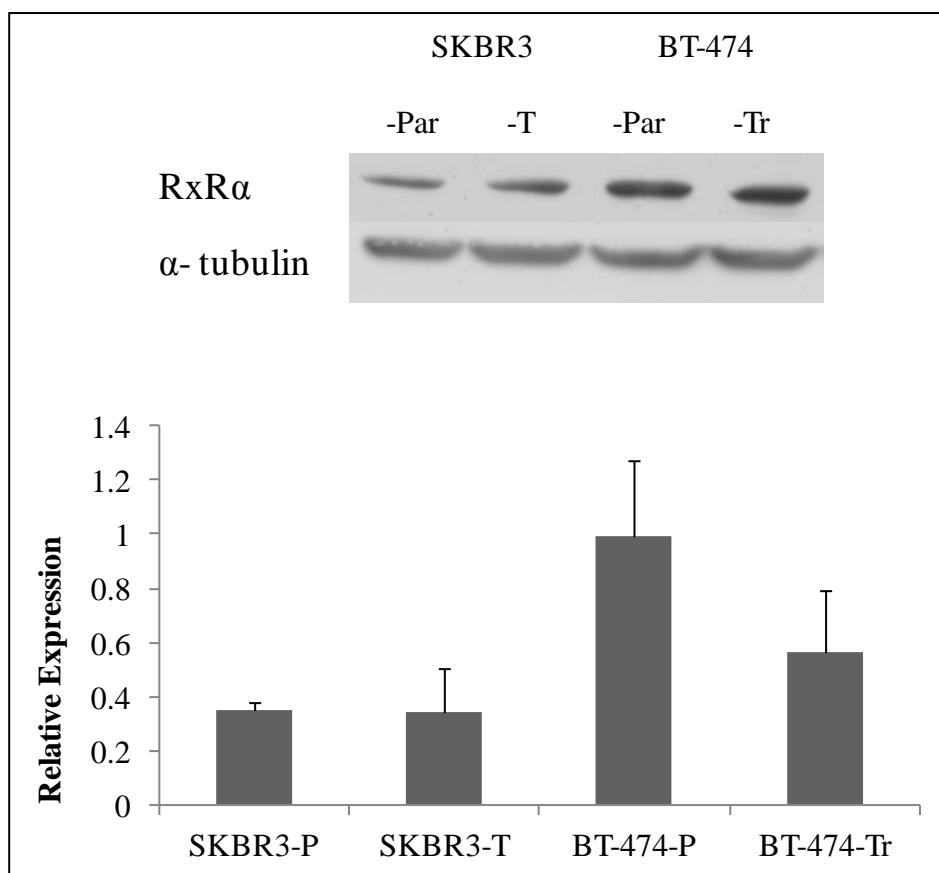


**Figure 5-14:** RxR $\alpha$  protein expression in the SKBR3-P, SKBR3-T, BT-474-P and BT-474-Tr cell lines.  $\alpha$ -tubulin was used as a loading control for each gel. Images are representative of triplicate experiments. Densitometry analysis of triplicate immunoblots was performed using ImageJ software.

### 5.8 24 hour ATRA treatment and the effect on the retinoic acid receptors

We investigated the expression levels of RAR $\alpha$ , RAR $\beta$ , RAR $\gamma$  and RxR $\alpha$  after a 24 hour treatment with trastuzumab (10  $\mu$ g/mL). We used the SKBR3 (ATRA sensitive) and the SKBR3-T, BT-474 and BT-474-Tr (ATRA insensitive) cell lines for these experiments. No significant differences were seen in the expression levels of receptors in the SKBR3-P or SKBR3-T cell line upon trastuzumab treatment (**Figure 5-15**).

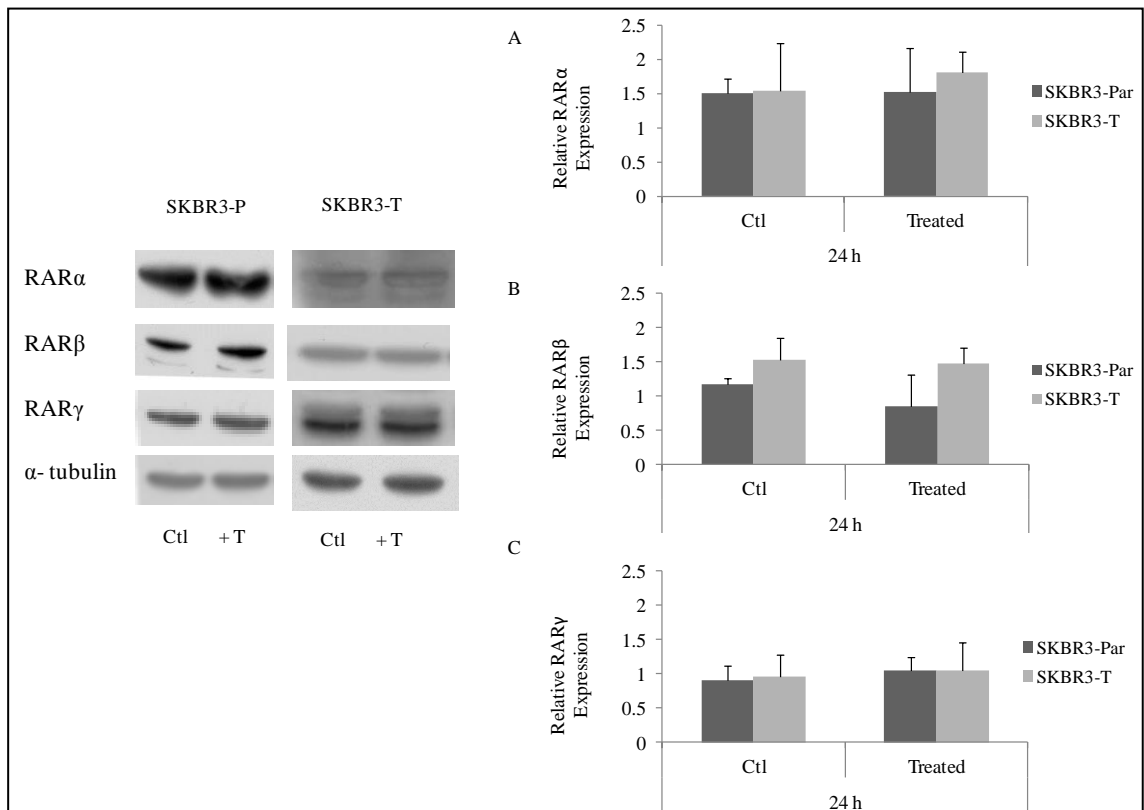


**Figure 5-15:** Expression analysis of retinoic acid receptors after 24 h treatment with trastuzumab (10 μg/mL) in the SKBR3-P and SKBR3-T cell lines. Densitometry was carried out to determine relative expression of (A) RARα, (B) RARβ and (C) RARγ to the loading control, α-tubulin. Experiments were carried out in triplicate.

No significant differences were observed in the BT-474-P cell line for the RARs (**Figure 5-16**). A small but statistically significant increase in RARγ expression ( $p=0.05$ ) was observed in the BT-474-Tr cell line upon trastuzumab treatment compared to its untreated control.

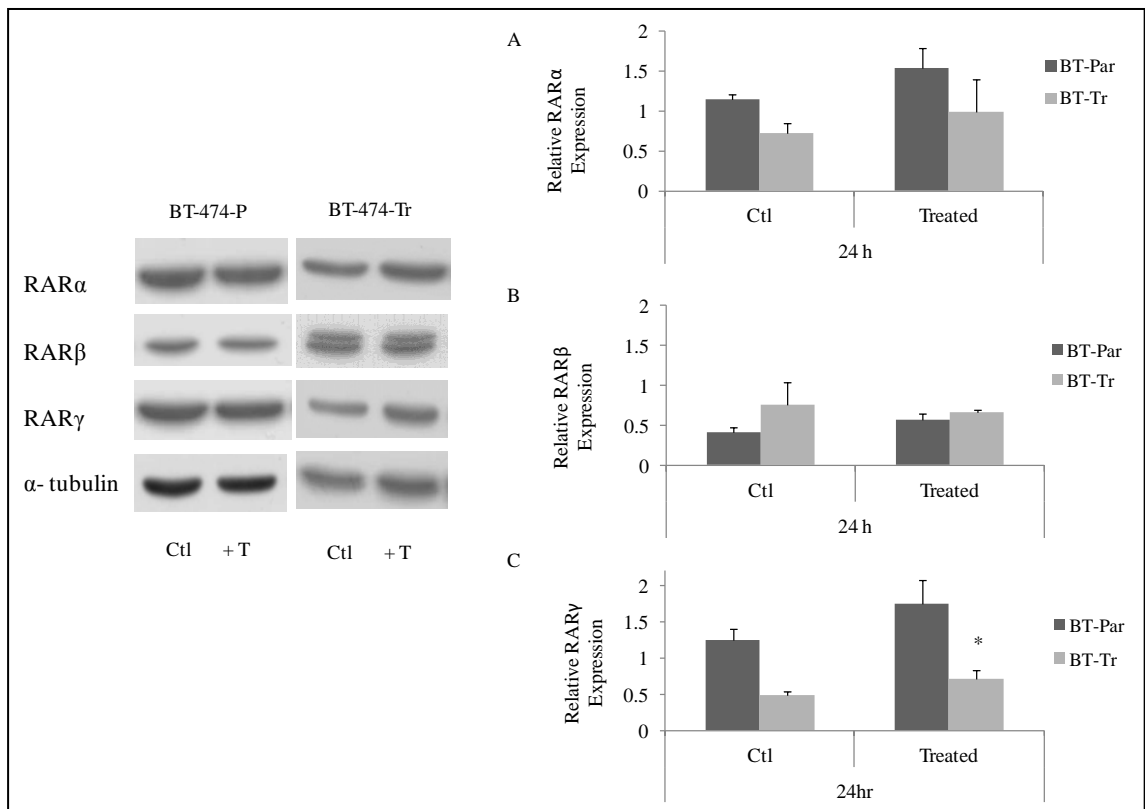


**Figure 5-16:** Expression analysis of retinoic acid receptors after 24 h treatment with trastuzumab (10 μg/mL) in the BT-474-P and BT-474-Tr cell lines. Densitometry was carried out to determine relative expression of (A) RARα, (B) RARβ and (C) RARγ to the loading control, α-tubulin. Experiments were carried out in triplicate. \* denotes p < 0.05.

## 5.9 Summary

Utilising the miRWalk database we identified RAR $\alpha$  as a potential target for miR-9. RAR $\alpha$  was differently altered in the SKBR3-T and SKBR3-L cell line compared to the SKBR3-P cell lines in the microarray dataset.

Interestingly, the SKBR3-P and SKBR3-L cell lines were sensitive to ATRA inhibition however, the SKBR3-T were less sensitive. Combination treatment with trastuzumab and/or lapatinib was significantly more effective than either trastuzumab or lapatinib treatment alone.

The BT-474-P, BT-474-Tr, HCC1954-P, and HCC-1954-L cell lines are insensitive to ATRA inhibition, while the EFM-192A cells show slight sensitivity. Combined trastuzumab and ATRA treatment in the BT-474-P, BT-474-Tr, HCC-1954-P and HCC-1954-L cell lines does not enhance growth inhibition compared to trastuzumab treatment alone. Combined trastuzumab and ATRA treatment in the EFM-192A cell line enhances growth inhibition compared to trastuzumab alone.

Combined treatment with lapatinib in the BT-474-P, BT-474-Tr, HCC-1954-P, HCC-1954-L and EFM-192A cells does not enhance the growth inhibition compared to lapatinib treatment alone.

In the cell lines that show response to ATRA alone, the combinations with trastuzumab and lapatinib enhance response. However, in the cell lines that are innately ATRA resistant i.e.: no growth inhibition, no enhancement on growth inhibition was observed.

We found no alterations in RAR $\alpha$  mRNA or protein expression in the resistant cell lines compared to the parental cell lines. As RAR $\alpha$  expression is unchanged in the SKBR3-T cells it does not account for the resistance to ATRA observed in the SKBR3-T. We identified that RAR $\gamma$  and RxR $\alpha$  showed altered expression in the microarray data; however we also investigated RAR $\beta$  expression. RAR $\beta$  and RAR $\gamma$  expression were unchanged in both the acquired resistant cell lines compared to their parental. This suggests that RAR $\beta$  and RAR $\gamma$  expression do not contribute to the decreased sensitivity seen in the SKBR3-T cell line. RxR $\alpha$  expression was also unchanged in the SKBR3-T cell line.

We also investigated the expression of the RARs upon trastuzumab treatment in our cell lines. No significant alterations were seen in the SKBR3-P, SKBR3-T and BT-474-P cell lines. However, RAR $\gamma$  expression was significantly up-regulated in the BT-474-Tr cell line after 24 h treatment.

The results observed suggest that RAR $\alpha$ , RAR $\beta$ , RAR $\gamma$  or RxR $\alpha$  do not contribute to the decreased sensitivity in the SKBR3-T cell line and do not predict response or resistance to ATRA treatment.

## **Chapter Six**

### **The role of miR-221 & -222 in resistance, migration and ‘stemness’**

## **6.1 Introduction**

We previously identified that expression of miR-221 and -222 is increased in acquired trastuzumab resistant cell lines. miR-221 and -222 have been implicated in epithelial-to-mesenchymal transition (EMT) in basal-like breast cancers through a reduction in E-cadherin abundance [273]. They also have reported roles in tamoxifen, [274] and fulvestrant [275] resistance and in cancer stem cells [276, 277]. To investigate the role of mi-221 and -222 in trastuzumab response in HER2 positive breast cancer we generated SKBR3-P cells stably transfected with miR-221, miR-222 and both miRNAs.

## **6.2 Characterisation of the stable transfected SKBR3-P cell line**

### ***6.2.1 Confirmation of transfection in the SKBR3-P cell line***

Lentiviral transfected SKBR3-P cell lines expressing pre-miR-221, -222 or both -221 and -222 were created by Dr. Laoighse Mulrane UCD (Chapter 2.11). A pre-scrambled control (SKBR3-P-Scramble) was also established. Over-expression of miR-221 and miR-222 was determined by qRT-PCR using the SKBR3-P-Scramble as the calibrator sample (which was comparable in Ct values to the SKBR3 cell line). We confirmed that levels of miR-221 were significantly increased in the SKBR3-P-221 and SKBR3-P-221-222 cell lines and not in the SKBR3-P-222 (**Table 6-1**). We also confirmed that miR-222 levels were highly over-expressed in only the SKBR3-P-222 and SKBR3-P-221-222 cell lines (**Table 6-1**). As the lentiviral vector contained a GFP-gene we also used fluorescent microscopy to confirm successful transfection. The stably transfected cell lines were green fluorescent protein (GFP) positive as shown in (**Figure 6-1**).

**Table 6-1:** miR-221 and miR-222 expression levels by qRT-PCR in the stably transfected SKBR3 cell lines. SKBR3-P-Scramble was used as a calibrator and RNU48 was used as the endogenous control. \* indicates  $p < 0.05$  by Student's t-test.

	Fold change in expression $\pm$ std dev		
	SKBR3-P-221	SKBR3-P-222	SKBR3-P-221_222
miR-221	$139.0 \pm 0.7$ *	$-2.8 \pm 0.6$	$72.2 \pm 0.3$ *
miR-222	$1.7 \pm 0.3$	$1175.5 \pm 0.2$ *	$746.7 \pm .04$ *

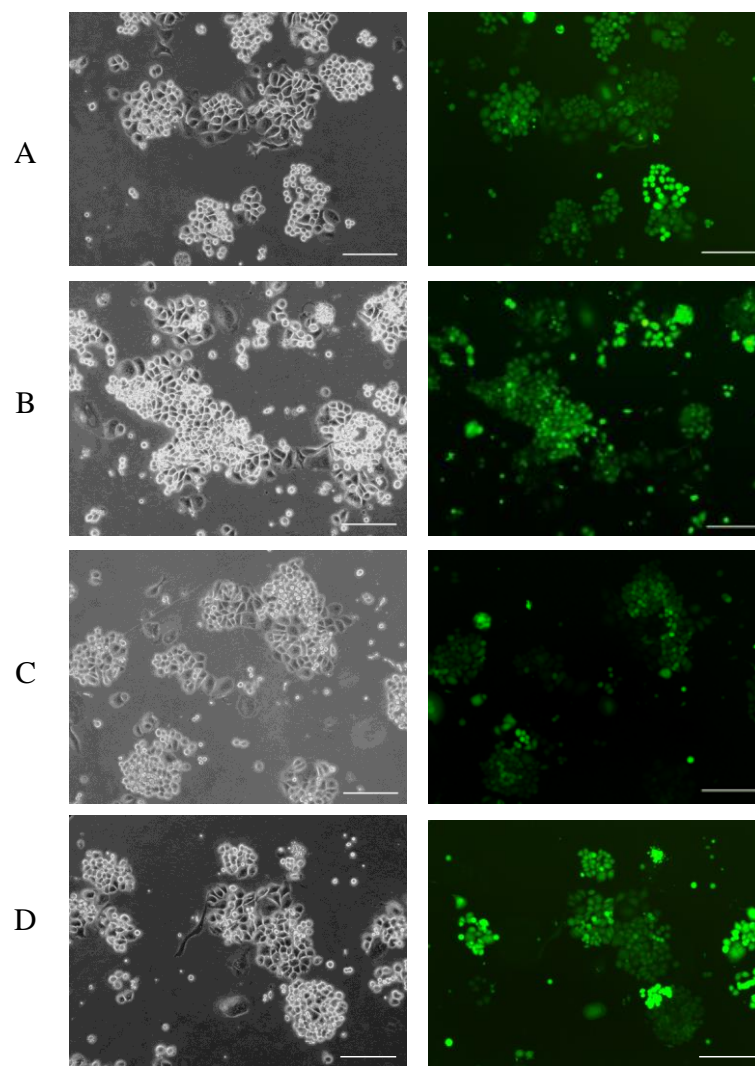


**Figure 6-1:** Phase contrast and fluorescent images of the stably transfected cell lines; SKBR3-P-Scramble (A), SKBR3-P-221 (B), SKBR3-P-222 (C) and SKBR3-P-221-222 (D). Images were captured using the Leica DFC 500 microscope Nikon TS100 microscope at 10X magnification. Scale bar represents 200  $\mu\text{m}$ .

### 6.2.2 Effect of miR-221 and -222 over-expression on morphology and doubling time

No morphological changes were observed between the SKBR3, SKBR3-T and the stably transfected cell lines (**Figure 6-2**).

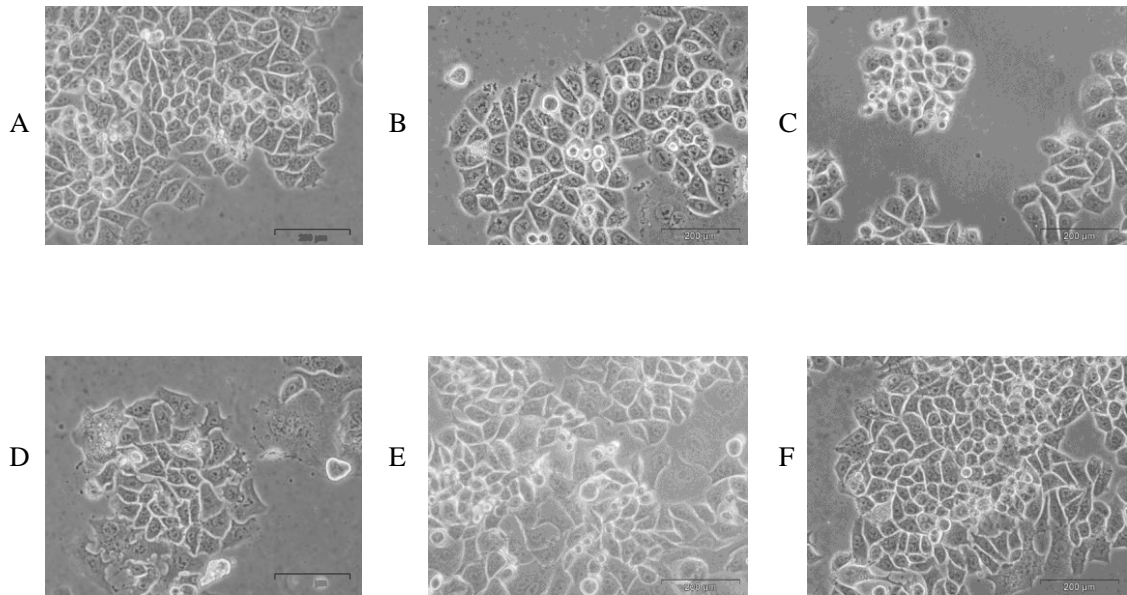


**Figure 6-2:** Phase contrast images observing the morphology of the SKBR3-P (A), SKBR3-T (B), SKBR3-Scrm (C), SKBR3-221 (D), SKBR3-222 (E) and SKBR3-221-222 (F). Images were captured at 20X magnification using the (Nikon TS100) at 20X magnification. Scale bar = 200 µM.

We investigated the effect of over-expression of miR-221 and miR-222 on the doubling time of the cells (**Figure 6-3**) (**Table 6-2**). The lentiviral transduction showed no significant effect on the doubling time of the SKBR3-Scrm compared to the SKBR3-P cell lines ( $p=0.3$ ).

Trastuzumab treatment increased the doubling times i.e: slowed down cell growth in most of the cell lines investigated. The SKBR3-P-221 ( $31.8 \pm 0.2$ ) and SKBR3-P-221-222 ( $29.1 \pm 1.8$ ) cell lines showed slightly reduced doubling times compared to the SKBR3-P-Scrm ( $34.9 \pm 3.0$ ), however, the reductions were not statistically significant

( $p=0.3$ ,  $p=0.1$  respectively) (**Figure 6-3**). Trastuzumab treatment significantly increased the doubling time of the SKBR3-P ( $p=0.01$ ), SKBR3-P-Scrm ( $p=0.04$ ), SKBR3-P-221 ( $p=0.01$ ), SKBR3-221-222 ( $p=0.001$ ), but not the SKBR3-T ( $p=0.1$ ) and SKBR3-P-222 ( $p=0.08$ ) cell lines (**Table 6-2**).

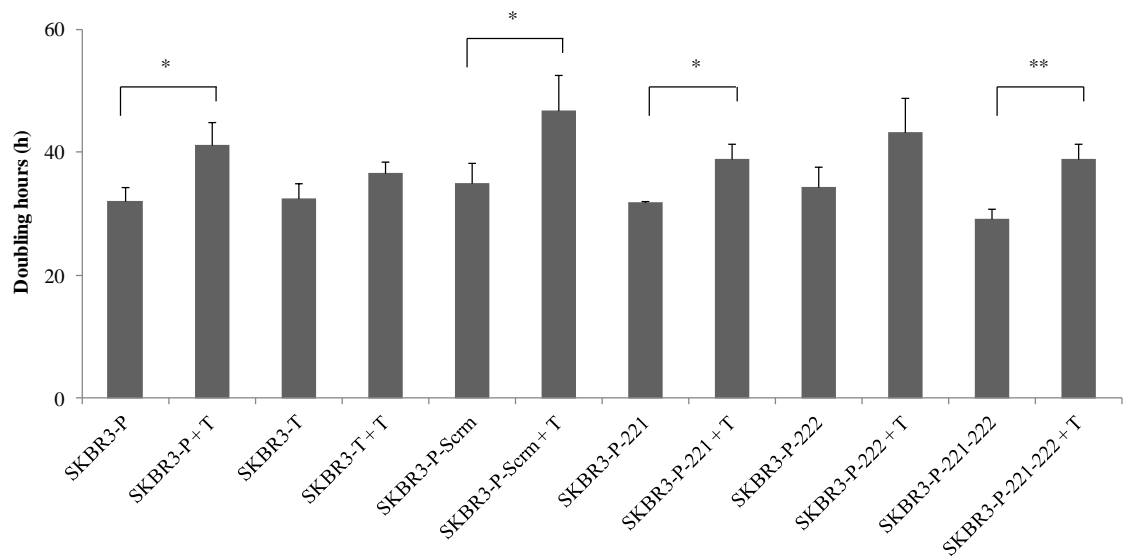


**Figure 6-3:** Average doubling times (h)  $\pm$  stdev for the SKBR3-P, SKBR3-T and stably transfected cells with or without trastuzumab treatment. Doubling time was assessed by the acid phosphatase method on Day 0, 3, 5 and 7. Error bars represent the standard deviation of triplicate experiments. Student's t-test was performed to determine significant effects of trastuzumab on doubling time. \* denotes  $p<0.05$  and \*\* denotes  $p<0.005$ .

**Table 6-2:** Average doubling times (h)  $\pm$  stdev for the SKBR3-P, SKBR3-T and stably transfected cells with or without trastuzumab treatment. Student's t-tests were carried out to determine significant effects of trastuzumab on doubling times. \* denotes  $p < 0.05$  and \*\* denotes  $p < 0.005$ .

<b>Doubling Time (h) <math>\pm</math> std dev</b>		
	<b>Ctl</b>	<b>Trast</b>
SKBR3-P	$32.2 \pm 2.2$	$41.2 \pm 3.6$ *
SKBR3-T	$32.6 \pm 2.5$	$36.6 \pm 2.0$
SKBR3-P-Scrm	$34.9 \pm 3.0$	$46.7 \pm 5.9$ *
SKBR3-P-221	$31.8 \pm 0.2$	$38.8 \pm 2.6$ *
SKBR3-P-222	$34.5 \pm 3.2$	$43.2 \pm 5.7$
SKBR3-P-221-222	$29.1 \pm 1.8$	$38.9 \pm 2.6$ **

### 6.2.3 Effect of miR-221 and -222 on trastuzumab sensitivity

As miR-221 and -222 were up-regulated in the acquired trastuzumab resistant cell lines, we investigated the trastuzumab sensitivity of the stably cell lines. The SKBR3-P-Scrm cell line is growth inhibited by  $34.7 \pm 6.3$  % upon treatment with  $4 \mu\text{g/mL}$  trastuzumab compared with a  $43.0 \pm 1.2$  % growth inhibition in the SKBR3-P cell line (**Figure 6-4**). However, this is not a significant difference ( $p=0.15$ ) which suggests the lentiviral transduction has a small but non-significant effect on the resistance profile of the cells. The SKBR3-P-221, SKBR3-P-222 and the SKBR3-P-221-222 cell lines show growth inhibition of  $33.8 \pm 4.1$  %,  $37.4 \pm 4.6$  % and  $35.8 \pm 2.9$  %, not statistically different compared to the SKBR3-P-Scrm ( $p=0.85$ ,  $0.37$  and  $0.80$  respectively) (**Figure 6-4**) (**Table 6-3**).

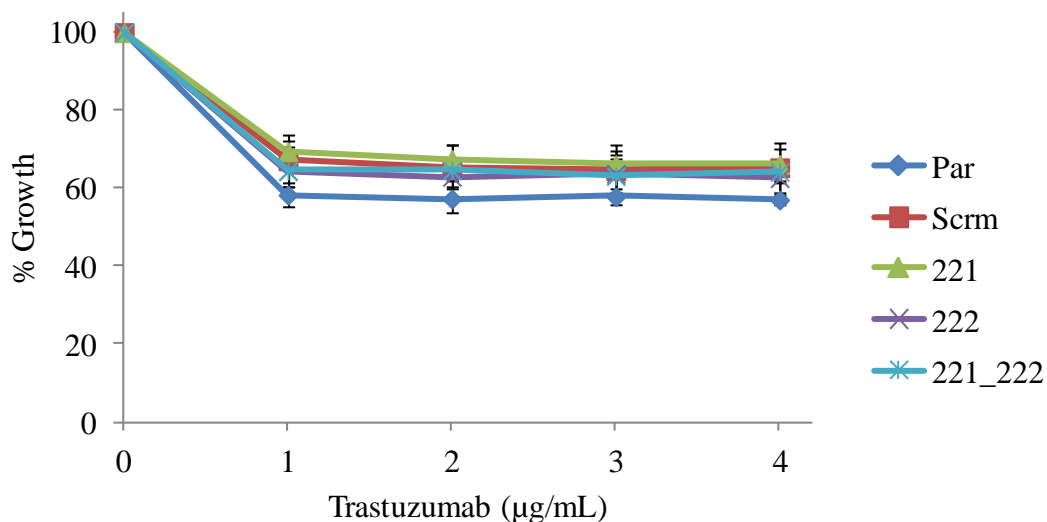


**Figure 6-4:** Determination of trastuzumab sensitivity in the SKBR3-P and SKBR3-P-stably transfected cell lines. Proliferation was measured by acid phosphatase assay after 5 days, and is expressed relative to untreated control. Error bars denote the standard deviation of triplicate experiments.

**Table 6-3:** Growth inhibition of the SKBR3-P and the SKBR3-P-stably transfected cell lines after trastuzumab treatment (4 µg/mL) ± std dev.

	Growth Inhibition (% ± std dev)
SKBR3-P	43.0 ± 1.2
SKBR3-P-Scrm	34.7 ± 6.3
SKBR3-P-221	33.8 ± 4.1
SKBR3-P-222	37.4 ± 4.6
SKBR3-P-221-222	35.8 ± 2.9

#### 6.2.4 Effect of miR-221 and -222 on migration

We examined the effect of over-expression of these miRNAs on migration at 24 h and 48 h time-points by wound scratch assay as they have both been previously reported to

increased migration in basal-like breast cancer (**Figure 6-5**) [278]. When we compared the SKBR3-P to the SKBR3-P-Scrm, we noticed the lentiviral transduction had a significant effect on migration at 24 h ( $p=0.02$ ) and 48 h ( $p=0.01$ ) (**Table 6-4**) (**Figure 6-6**). The SKBR3-P-221 ( $45.2 \pm 5.6$  %,  $61.5 \pm 9.4$  %) cell line is significantly more migratory than the SKBR3-P-Scrm ( $28.7 \pm 6.4$  %,  $36.5 \pm 4.3$  %) after both 24 and 48 h ( $p=0.03$ ,  $0.03$ ) respectively (**Table 6-4**) (**Figure 6-6**). The SKBR3-P-221-222 ( $59.1 \pm 6.7$  %) cell line is also significantly more migratory than the SKBR3-P-Scrm ( $36.5 \pm 4.3$  %) cell line after 48 h ( $p=0.01$ ) (**Table 6-4**) (**Figure 6-6**). No significant change in migration was observed for the SKBR3-P-222 compared to the SKBR3-P-Scrm after 24 h ( $p=0.47$ ) and 48 h ( $p= 0.67$ ) (**Table 6-4**) (**Figure 6-6**).

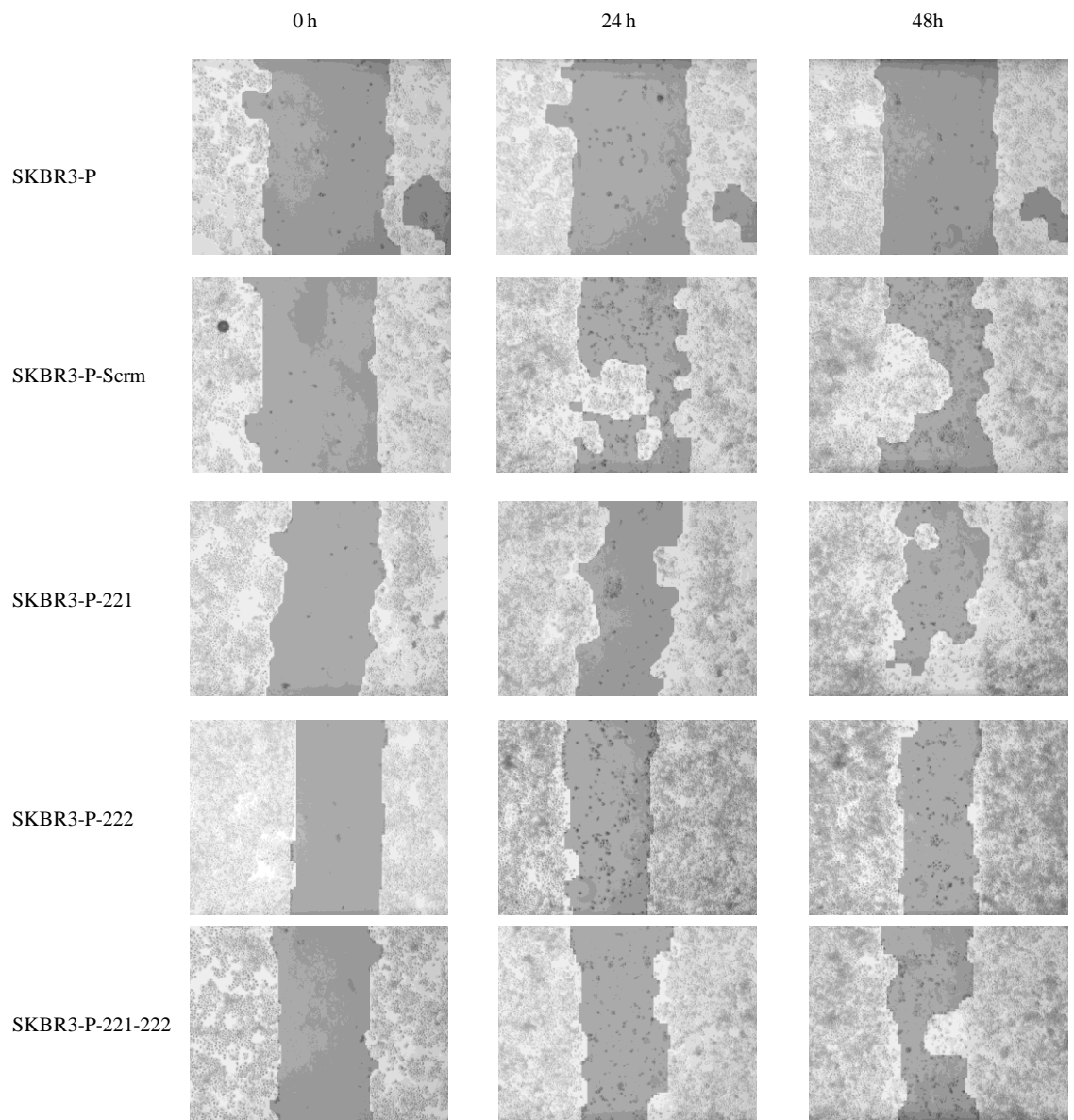


**Figure 6-5:** Representative images of the TScratch analysed wound scratch images of the SKBR3-P, SKBR3-P-Scrm, SKBR3-P-221, SKBR3-P-222 and SKBR3-P-221-222 at 0 h, 24 h and 48 h timepoints using the Nikon TS100 microscope.

**Table 6-4:** Average migration in the SKBR3-P, SKBR3-P -221, SKBR3-P -222 and SKBR3-P -221-222 cell lines after 24 h and 48 h timepoints. Open space (%) was calculated using the TScratch program and migration was then calculated (100% - open space %).

	24 hr	48 hr
SKBR3-P	8.0 ± 1.7	12.3 ± 1.0
SKBR3-P-Scrm	28.7 ± 6.4	36.5 ± 4.3
SKBR3-P-221	45.2 ± 5.6	61.5 ± 9.4
SKBR3-P-222	21.8 ± 12.9	41.6 ± 17.6
SKBR3-P-221-222	37.8 ± 16.0	59.1 ± 6.7

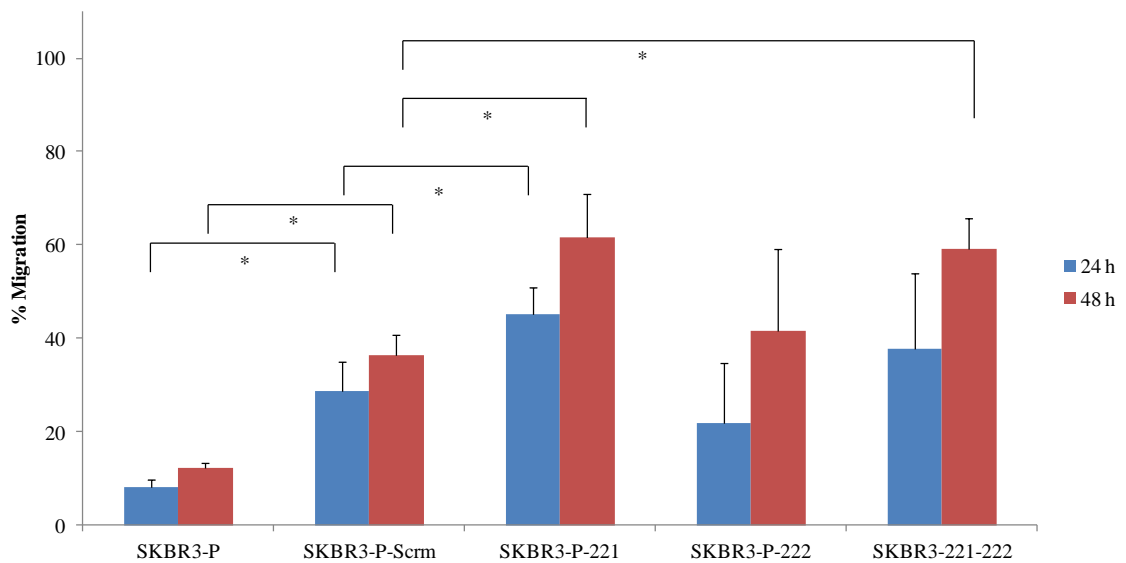


**Figure 6-6:** Average migration in the SKBR3-P, SKBR3-P-Scrm, SKBR3-P-221, SKBR3-P-222 and SKBR3-P-221-222 cell lines after 24 h and 48 h time points. Open space (%) was calculated using the TScratch program and migration was then calculated (100 % - open space %). Error bars denote the standard deviation of triplicate experiments. Student's t-test was performed to determine significant difference: \* denotes p<0.05.

### 6.3 Target Prediction for miR-221 and miR-222

We identified a study which involved transfection of MCF-7 cells with miR-221 and miR-222 [279] and a freely accessible microarray dataset (E-TABM-601) was available. Using R software hierarchical cluster analysis showed that the samples types separated out into control and transfected groups (**Figure 6-7**).

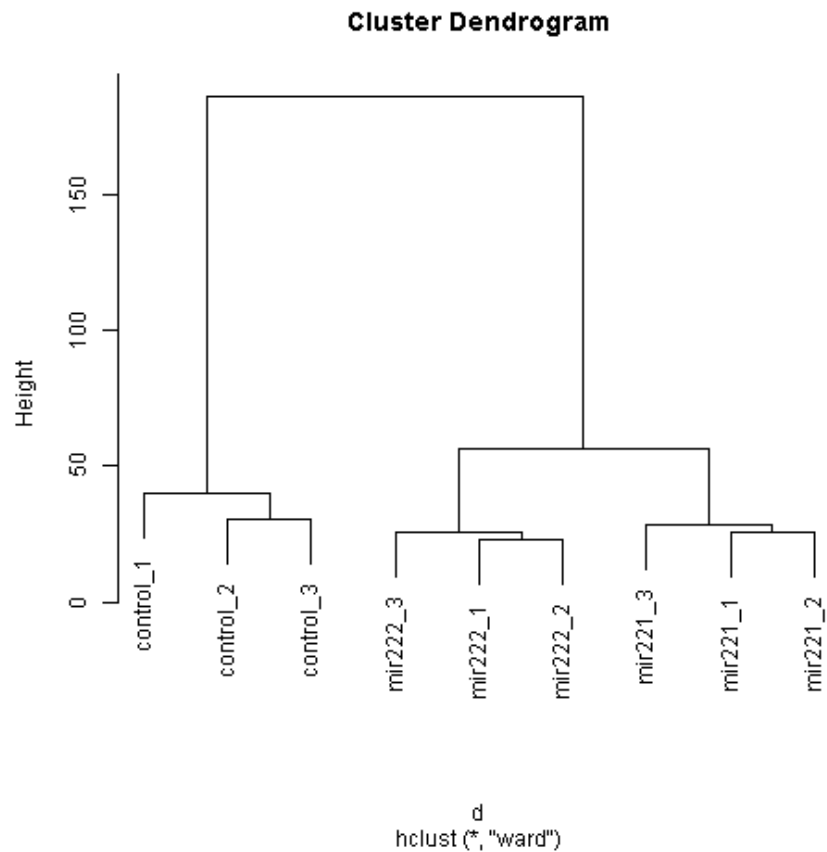


**Figure 6-7:** Hierarchical cluster analysis was carried out on the freely accessible GEO dataset E-TABM-601. The high level quality control shows the control groups and the transfected miR-221 and -222 groups clustering together.

Differential expression of the data was calculated using a  $\pm 1.2$  fold change and a BH (Benjamini Hochberg) adjusted p-value of  $< 0.05$ . A list of differentially expressed targets was identified (886) and compared against predicted targets for miR-221 and -

222 using Target Scan. This identified 73 potential down-regulated targets that are predicted to be targeted by miR-221 and/or -222 in MCF-7 cells. This was cross-compared to our microarray UCLA dataset and targets that were significantly down-regulated were identified. We identified seven potential down-regulated targets from this array dataset (**Table 6-5**). As p27<sup>kip1</sup> has previously been linked with trastuzumab resistance we tested the stably transfected cell lines for p27<sup>kip1</sup> expression (**Figure 6-8**). p27<sup>kip1</sup> expression was significantly down-regulated in the SKBR3-222 (p=0.03) and -221-222 (p=0.03) cell lines suggesting that p27<sup>kip1</sup> is a target for miR-222. p27<sup>kip1</sup> levels were also reduced in the SKBR3-P-221 cell line although this did not achieve statistical significance (p=0.09).

**Table 6-5:** Potential targets for miR-221 and -222 identified from microarray analysis of a freely accessible microarray, E-TABM-601 and cross comparison with a microarray dataset from UCLA (n=1) of the SKBR3-T cell line compared with the SKBR3-P.

Gene Name	Sequence Description	Fold Change	p-value	Accession #	Sequence Code
HNRNPA3	heterogeneous nuclear ribonucleoprotein A3	-1.9	0.00005	NM_194247	A_24_P488588
HIPK2	homeodomain interacting protein kinase 2	-1.7	0.0003	AK074291	A_24_P500621
MED1	mediator complex subunit 1	-1.5	0.003	NM_004774	A_23_P425704
RALGAPA1	Ral GTPase activating protein, alpha subunit 1 (catalytic)	-1.5	0.007	AL834362	A_23_P151565
TMCC1	transmembrane and coiled-coil domain family 1	-1.4	0.02	NM_015008	A_23_P170986
CDKN1B	cyclin-dependent kinase inhibitor 1B (p27, Kip1)	-1.3	0.01	NM_004064	A_24_P81841
ARL6IP1	ADP-ribosylation factor-like 6 interacting protein 1	-1.3	0.05	NM_015161	A_23_P118150

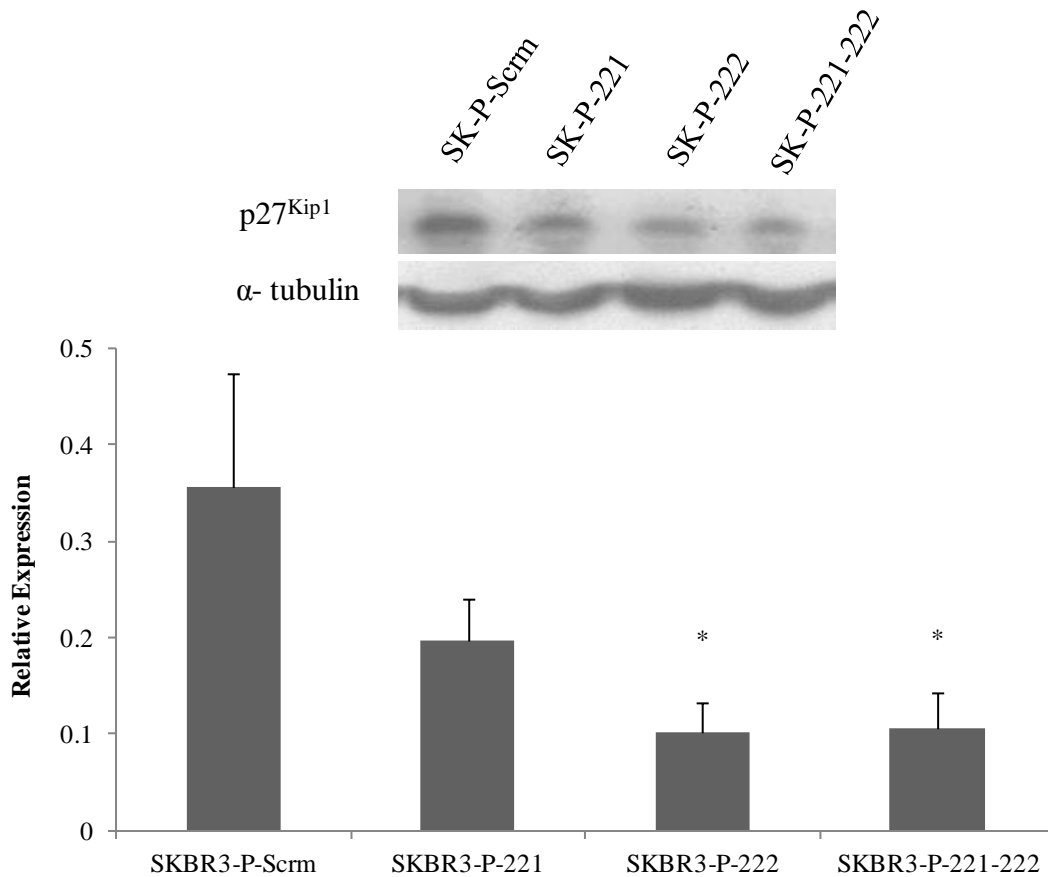


**Figure 6-8:** p27<sup>kip1</sup> expression in the stable transfected cell line.  $\alpha$ -tubulin was used as a loading control on each gel. Images are representative of triplicate experiments. Densitometry analysis of triplicate immunoblots was performed using ImageJ software. \* denotes  $p < 0.05$ .

p27<sup>kip1</sup> [280] along with SOCS1 [278] have previously been identified as a potential targets for miR-221 and -222. Miller *et al.*, discovered that miR-221 and -222 play a role in tamoxifen resistance through their targeting of p27<sup>kip1</sup> and Li *et al.* discovered miR-221 and -222 were involved in migration through SOCS1 and p27<sup>kip1</sup>. We have confirmed p27<sup>kip1</sup> expression is altered in our miR-222 over-expressing cell line (**Figure 6-8**). We investigated SOCS1 expression in our stably transfected cell lines. We determined a slight decrease in the expression levels in the SKBR3-P-221 cell line

compared to the scramble control; however, it was not significantly altered ( $p=0.34$ ) (Figure 6-9).

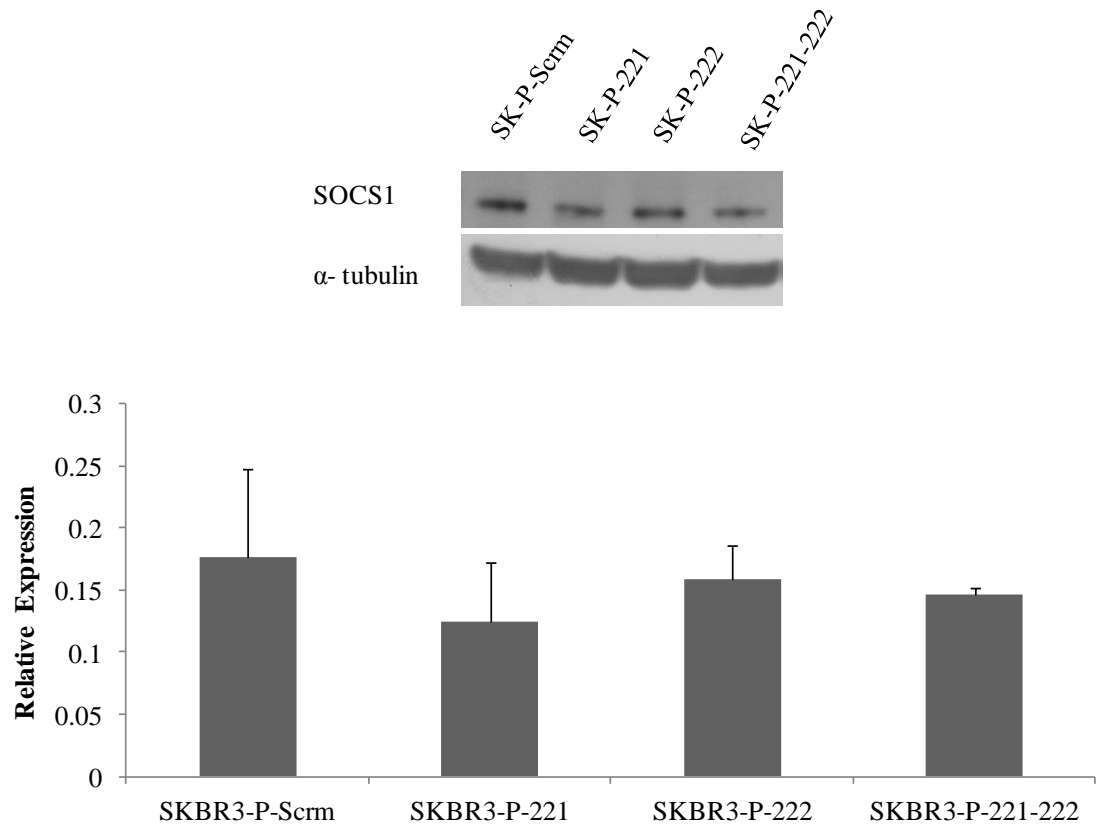


**Figure 6-9:** SOCS1 expression in the stable transfected cell line.  $\alpha$ -tubulin was used as a loading control on each gel. Images are representative of triplicate experiments. Densitometry analysis of triplicate immunoblots was performed using ImageJ software.

#### 6.4 miR-221 and -222 and their involvement in stemness

Based on previously published associations between miR-221 and miR-222 and stem cells [281], we used an established mammosphere assay to examine alterations in stemness. Mammosphere assays are sphere-forming assays which are utilised for the quantification of stem cell activity and self renewal. An assay protocol was previously published and optimised by Shaw *et al.* [282]. We investigated the mammosphere forming efficiency (MFE) of the SKBR3-P, the trastuzumab resistant variant, SKBR3-T

and the stably transfected cell line panel (**Figure 6-10**). We determined no significant difference in the MFE of the SKBR3-T ( $1.3 \pm 0.4$  %) cells compared to the SKBR3-P ( $1.5 \pm 0.2$  %) cell line ( $p=0.7$ ). MFE comparison between the SKBR3-P and SKBR3-P-Scrm cell line shows that the lentiviral transduction had no significant effect on the MFE of the cell lines (SKBR3-P-Scrm ( $2.1 \pm 0.4\%$ ) and SKBR3-Par ( $1.5 \pm 0.2$  %) cell line,  $p=0.03$ ). Mammosphere assays of the stably transfected cell line show that over-expression of miR-221 in the SKBR3-P-221 cell line has no effect on MFE when compared to the scrambled control, SKBR3-P-Scrm ( $p=0.4$ ). Over-expression of miR-222 has no significant effect on the MFE of the SKBR3-P cells when compared to the SKBR3-P-Scrm ( $p=0.9$ ). Over-expression of both miRNAs together also does not have a significant effect on the MFE of the SKBR3-P-221-222 cell line compared to the SKBR3-P ( $p=0.3$ ) and the SKBR3-P-Scrm ( $p=0.4$ ) cell lines.

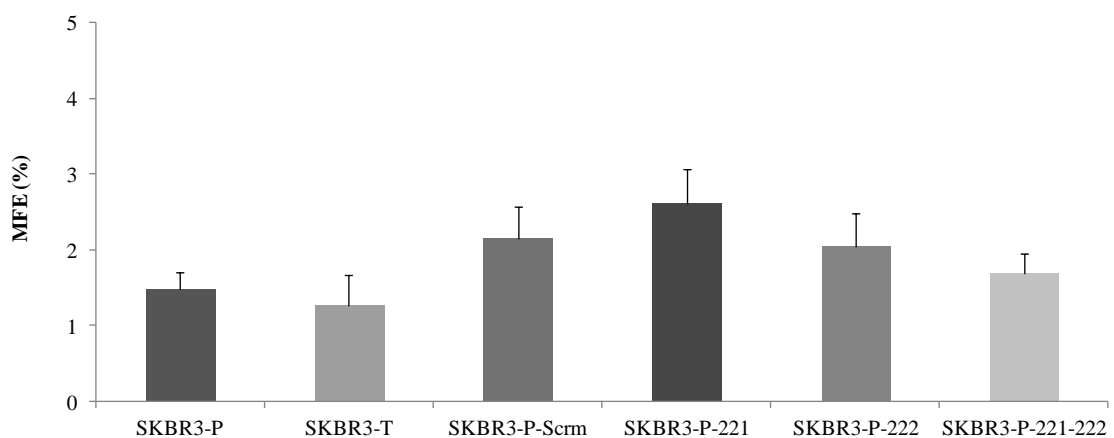


**Figure 6-10:** Mammosphere forming efficiency (MFE %) of the SKBR3-P, SKBR3-T and the stably transfected cell lines. MFE was determined as the number of mammospheres  $>50$   $\mu\text{m}$  after 5 days culture in mammosphere media relative to the number of cells seeded initially. Error bars denote the standard deviation of triplicate experiments. Student's t-test was performed to determine significant difference between the SKBR3-P and the stable transfected cell lines. \* denotes  $p<0.05$ .

We also investigated the effect of trastuzumab (10  $\mu\text{g}/\text{mL}$ ) and lapatinib (50 nM) on the MFE of the cell lines (**Figure 6-11**). Lapatinib treatment significantly decreased MFE in the SKBR3-T cell lines ( $p=0.02$ ), however trastuzumab or lapatinib treatment had no significant effect on the MFE of the other cell lines tested. The SKBR3-P cell line is sensitive to both trastuzumab and lapatinib inhibition but the MFE of the SKBR3-P cell line is unchanged to treatment with either agent.

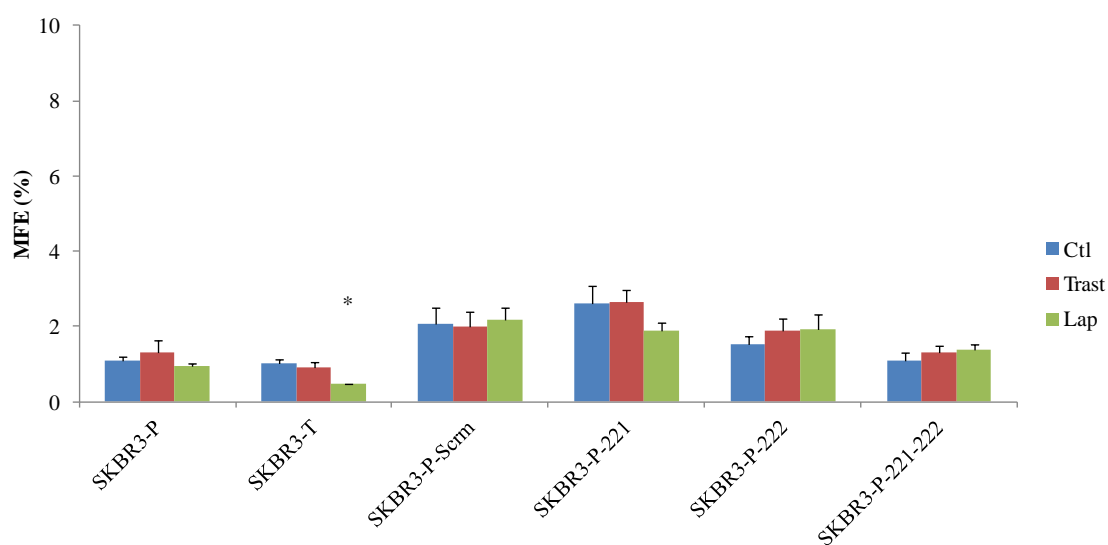


**Figure 6-11:** Mammosphere forming efficiency (MFE %) of the SKBR3-P, SKBR3-T and the stably transfected cell lines following trastuzumab (10  $\mu\text{g}/\text{mL}$ ) and lapatinib (50 nM) treatment. MFE was determined as the number of mammospheres  $>50 \mu\text{m}$  after 5 days culture in mammosphere media relative to the number of cells seeded initially. Error bars denote the standard deviation of duplicate experiments.

## 6.5 Summary

We successfully created stably transduced over-expressing SKBR3-P cell lines for miR-221 and -222 (in collaboration with Dr. Mulrane). We observed no morphological differences between the SKBR3-P, SKBR3-T and the stably transfected cell lines. We investigated the effect of over-expressing miR-221 and -222 on doubling times and found no significant changes. However, trastuzumab treatment significantly increased the doubling time of the SKBR3-P, SKBR3-P-Scrm, SKBR3-P-221 and SKBR3-P-221-222 cell lines when compared to the untreated controls. However, there was no significant effect on doubling time of the stably transfected cell lines compared to the scrambled control. The stably transfected cell lines do not show a significant change in trastuzumab sensitivity using a 2D proliferation assay. We investigated the effect of these miRNAs on migration and found the lentiviral transduction increased migration. When we compared the migratory potential of the stably transfected cell line to the scrambled control, SKBR3-P-Scrm, we observed that the SKBR3-P-221 is significantly more migratory than the scrambled control after 24 and 48 h. The SKBR3-221-222 cell line also was more migratory after 48 h than the SKBR3-P-Scrm.

p27<sup>kip1</sup> (CDKN1B) was altered in the SKBR3-T cell line and is a previously validated target for miR-221 and -222. We determined that p27<sup>kip1</sup> expression is down-regulated in the SKBR3-P-222 and SKBR3-P-221-222 cell lines.

miR-221 and -222 have been previously reported in stem cell activity and promotion. We examined the stemness potential of our stably transfected cells by the mammosphere assays. We observed no significant changes in the MFE of the stable

transduced cell lines compared to the SKBR3-P. Trastuzumab and lapatinib treatment had no significant effect on mammosphere formation in the stable transfected cell lines.

In summary, miR-221 and/or miR-222 do not appear to play a significant role in the acquired trastuzumab phenotype. However, they appear to increase the migratory capacity of the cells which may contribute to a more aggressive phenotype.

## **Chapter Seven**

### **miRNA expression in HER2 positive breast tumours**

## **7.1 Introduction**

Formalin fixation is the standard method of preserving patient tissue samples. However upon formalin fixation, cross-linking of DNA and degradation occur which can cause difficulties in extracting intact DNA. miRNAs are more stable than DNA and mRNA and therefore are ideal candidates for investigating biomarkers in archival patient samples [283]. For this study, we obtained tumour samples from a cohort of patients (n=16) with metastatic HER2 positive breast cancer, who either progressed on trastuzumab treatment (PFS <12 months) (n=10) or had a durable response to trastuzumab treatment (PFS >36 months) (n=6) [101]. Initially, we investigated a number of commercially available kits for the extraction of miRNA from formalin fixed paraffin embedded (FFPE) samples, using cell culture donor blocks. Based on the results obtained, miRNA was extracted from the FFPE tumour samples for miRNA analysis of the four miRNAs; miR-221, -222,-224 and -9 previously identified in Chapter Four.

## **7.2 Assessment of FFPE miRNA extraction kits**

### **7.2.1 Cell culture donor block preparation**

Cell culture donor blocks (CCDB) were prepared from SKBR3-P cells. Sections (5 µM) were cut from the CCDB and were Hematoxylin & Eosin (H&E) stained to ensure sufficient cell numbers and quality as shown in **Figure 7-1**.

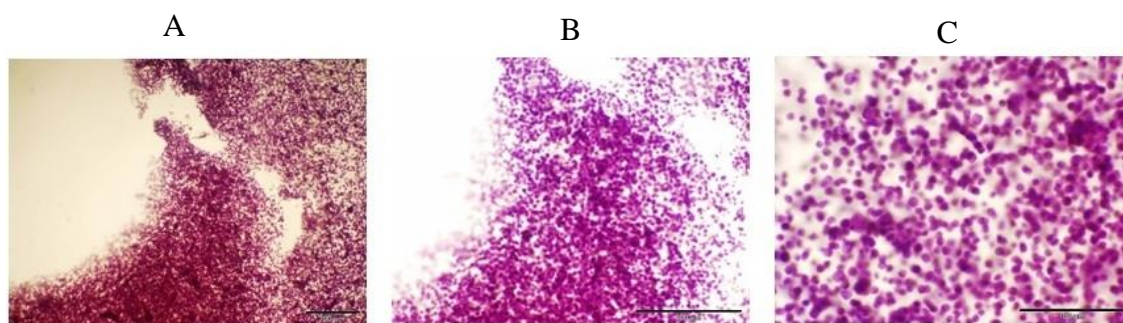


**Figure 7-1:** H&E stained sections from SKBR3-P cell culture donor blocks. Images were captured at 10X (A), 20X (B) and 40X (C) magnification using the Nikon TS100 microscope. Scale bars represent 500  $\mu\text{m}$  (A), 200  $\mu\text{m}$  (B) and 100  $\mu\text{m}$  (C).

### 7.2.2 Comparison of miRNA extraction methods

We tested miRNA extraction using three commercially available kits; RecoverAll™ Total Nucleic Acid Isolation Kit (Ambion) which extracts total RNA, High Pure miRNA Isolation kit (Roche) which extracts miRNAs and total RNA and miRNeasy FFPE Kit (Qiagen) which extracts miRNA and total RNA. We also investigated different sources of starting material; full-face sections (10  $\mu\text{m}$ ) and cores (1.0 mm and 1.5 mm). miRNA was analysed by Nanodrop (Thermo Scientific) and the RNA quantity ( $\mu\text{g}$ ) and  $A_{260/280}$  (~ 1.8-2.2) were determined (**Table 7-1**).

**Table 7-1:** Total amount ( $\mu\text{g}$ ) of RNA,  $A_{260/280}$  ratios using the Nanodrop (Thermo Scientific) extracted from sections (10  $\mu\text{M}$ ), cores; 1.0 mm and 1.5 mm using three commercially available kits.

	RecoverAll™ Total Nucleic Acid Isolation Kit		High Pure miRNA Isolation Kit		miRNeasy FFPE Kit	
	$\mu\text{g}$	$A_{260/280}$	$\mu\text{g}$	$A_{260/280}$	$\mu\text{g}$	$A_{260/280}$
Section (10 $\mu\text{M}$ )	2.3	2.0	3.7	2.1	4.4	2.0
Core (1 mm)	2.4	2.0	2.4	2.1	1.2	2.0
Core (1.5 mm)	3.7	2.1	6.0	2.0	2.6	2.0

The miRNA extracts were also analysed using the Agilent 2100 Bioanalyzer. The Bioanalyzer yields electropherograms (peaks) which can identify intact small (5S-fragments) and total RNA (18S and 28S – fragments) (**Figure 7-2 A**). It also determines the integrity of RNA by RNA Integrity Number (RIN). RNA extracted using the RecoverAll™ Total Nucleic Acid Isolation Kit yielded small RNA peaks at 5S in all of the starting material, however, no total RNA was detected at 18S and 28S (**Figure 7-2 B**). miRNA extracted using the High Pure miRNA Isolation kit from Riche yielded no small RNA peaks in any of the sample (**Figure 7-2 B**). miRNA extracted from the miRNeasy FFPE Kit from Qiagen yielded small RNA peaks from all of starting material (**Figure 7-2 B**). RNA integrity is assessed using the RIN, the intactness of the sample is graded from 1 to 10, 10 being the most intact. RIN values for FFPE samples are generally lower than cell line RNA, ranging from values of 1.0 upwards [284]. The RIN values for the RecoverAll™ Total Nucleic Acid Isolation Kit ranged from 1.2 – 2.1 (**Table 7-2**). The RIN values for the Roche kit are comparable between sections and 1.5 mm cores. The 1.0 mm cores had a slighter lower value of 1.2 (**Table 7-2**). Sections

extracted using the RecoverAll kit had a higher RIN value than the cores of either size. The RIN values for the miRNeasy kit were lower than the other two kits however; the 1.5 mm cores had a higher RIN value than sections or 1.0 mm cores (**Table 7-2**).

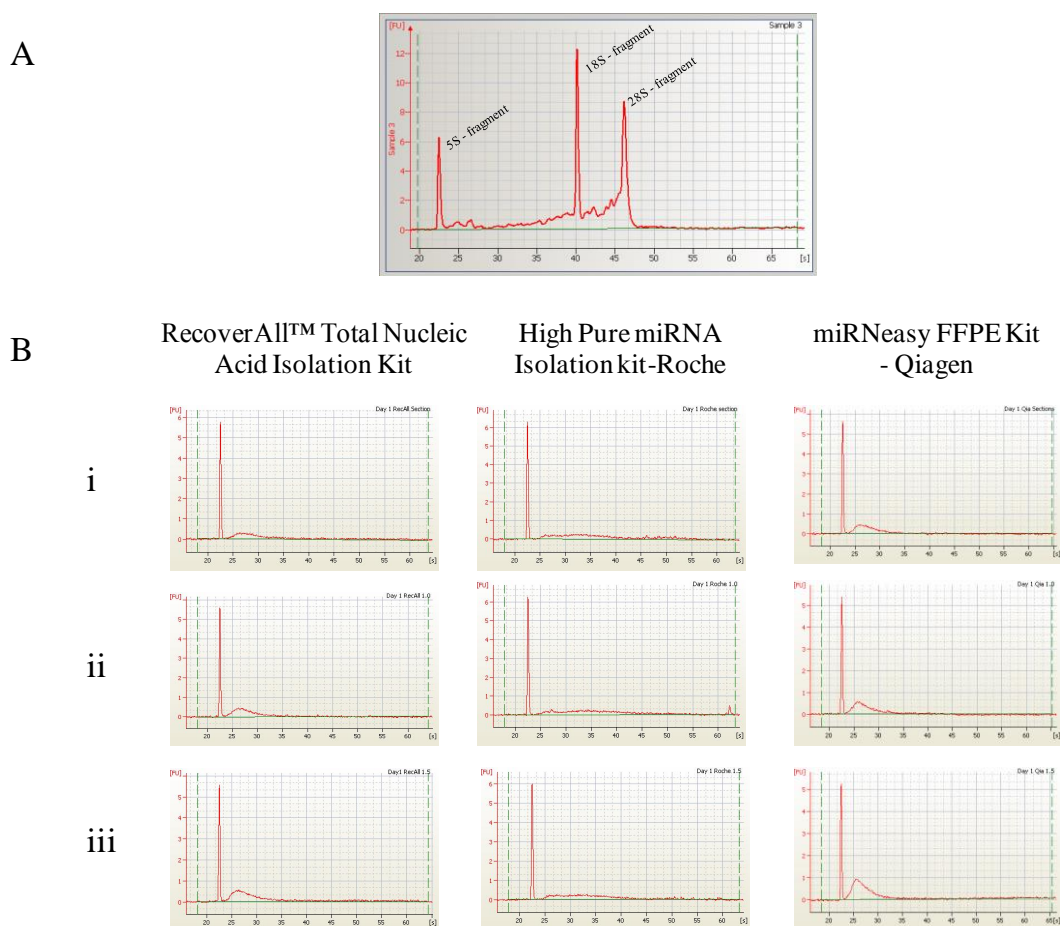


**Figure 7-2:** (A) An electropherogram from the Agilent 2100 Bioanalyzer with small RNA peaks indicated by the 5S fragment and total RNA peaks indicated by the 18S and 28S fragments. (B) miRNA extracts from (i) sections (10  $\mu$ M), (ii) 1.0 mm core and (iii) 1.5 mm core using the RecoverAll, High Pure and Qiagen kit were analysed using the Agilent Bioanalyzer. Electropherograms shown are representative of triplicate RNA extractions.

**Table 7-2:** RIN values determined by the Agilent Bioanalyzer for miRNA extracts from sections (10  $\mu$ M), 1.0 mm core and 1.5 mm core using the three commercially available kits.

		RIN
<b>RecoverAll™ Total Nucleic Acid Isolation Kit</b>	Section (10 $\mu$ M)	1.8 $\pm$ 0.6
	Core (1.0 mm)	1.2 $\pm$ 0.1
	Core (1.5 mm)	2.1 $\pm$ 0.7
<b>High Pure miRNA Isolation Kit</b>	Section (10 $\mu$ M)	1.4 $\pm$ 0.2
	Core (1.0 mm)	1.2 $\pm$ 0.1
	Core (1.5 mm)	1.4 $\pm$ 0.3
<b>miRNeasy FFPE Kit</b>	Section (10 $\mu$ M)	1.0 $\pm$ 0.0
	Core (1.0 mm)	1.1 $\pm$ 0.6
	Core (1.5 mm)	1.8 $\pm$ 0.4

CCDB RNA extracts were tested by qRT-PCR to determine if miRNA extracted from FFPE samples are detectable by qRT-PCR. Taqman qRT-PCR assays using an endogenous control assay for RNU48 was carried out. The resulting threshold cycle (Ct) values were comparable to those seen in cell line miRNA extracts (Ct values ~ 25) (**Table 7-3**).

**Table 7-3:** Cycle threshold (Ct) values determined from qRT-PCR analysis for the endogenous control RNU48 using miRNA extracted from CCDB. Standard deviations are representative of triplicate experiments.

		Ct
<b>RecoverAll™ Total Nucleic Acid Isolation Kit</b>	Section (10 µM)	25.1 ± 0.1
	Core (1.0 mm)	25.1 ± 0.2
	Core (1.5 mm)	24.6 ± 0.1
<b>High Pure miRNA Isolation Kit</b>	Section (10 µM)	26.4 ± 0.1
	Core (1.0 mm)	24.6 ± 0.1
	Core (1.5 mm)	24.8 ± 0.1
<b>miRNeasy FFPE Kit</b>	Section (10 µM)	25.0 ± 0.2
	Core (1.0 mm)	25.0 ± 0.2
	Core (1.5 mm)	24.7 ± 0.6
<b>miRVana Kit</b>	Cell line – SKBR3	25.4 ± 0.3

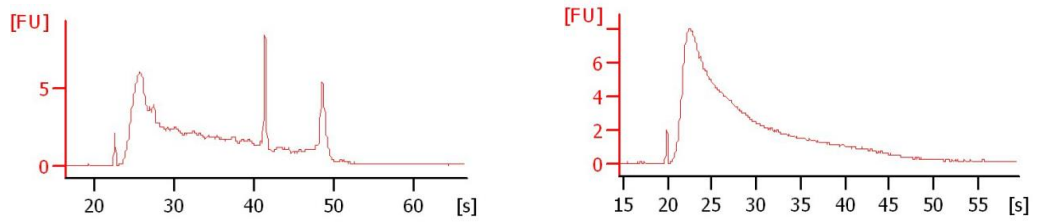
The High Pure kit yielded no visible small RNA peaks (5S-fragments) in the Bioanalyzer analysis; we decided to focus on the RecoverAll and miRNeasy kits. miRNA extraction was carried out on two tumour samples (the SKBR3-T cell line was used as a positive control) using the RecoverAll™ Total Nucleic Acid Isolation Kit and miRNeasy FFPE Kit. We successfully extracted RNA from FFPE tumours using both kits as seen in **Table 7-4**. The  $A_{260/280}$  and  $A_{260/230}$  results were comparable to that seen in the cell line positive control (**Table 7-4**)

**Table 7-4:** Quantification of concentration (ng/  $\mu$ L), total RNA ( $\mu$ g) and assessment of RNA purity by  $A_{260/280}$  and  $A_{260/230}$  ratios of RNA extracts from FFPE patient samples and SKBR3-T cell line.

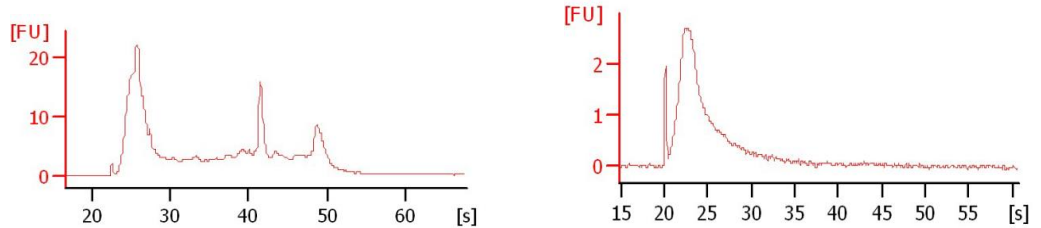
	Sample	Conc (ng/ $\mu$ L)	Total RNA ( $\mu$ g)	$A_{260/280}$	$A_{260/230}$
<b>RecoverAll™ Total Nucleic Acid Isolation Kit</b>	Tumour No.1	376.8	11.3	2.0	1.8
	SKBR3-T	244.0	2.5	2.1	1.8
<b>miRNeasy FFPE Kit</b>	Tumour No.2	84.2	2.5	1.9	1.8
	SKBR3-T	1233.4	37.0	2.1	2.0

RNA was further analysed using the Agilent Bioanalyzer. The cell line positive controls using either the RecoverAll (**Figure 7-3 A**) or miRNeasy extraction (**Figure 7-3 B**) kits resulted in intact small RNA peaks at the 5S fragment and total RNA peaks at the 18S and 28S- fragments. In comparison, the tumour samples yielded no intact total RNA peaks, however, a large peak at the small RNA 5S fragment. Therefore both kits were successful in the extraction of miRNA from FFPE tumour samples.

A



B



SKBR3-T

Tumour Samples

**Figure 7-3:** miRNA extracted from SKBR3-T cell line as a positive control and FFPE patient samples using the (A) RecoverAll™ Total Nucleic Acid Isolation Kit and (B) miRNeasy FFPE Kit extraction kits and extracts were analysed on the Agilent Bioanalyzer.

Based on the results and combined with the cost and ease of handling, we chose the miRNeasy FFPE kit for this study.

### 7.3 Primary tumour miRNA analysis in a FFPE HER2 positive breast cancer cohort

A cohort of patient samples from St. Vincent's University Hospital (n=16) that are classified as DCR (> 36 months in remission) and non-DCR (progressed < 12 months) were used for miRNA expression analysis in HER2 positive breast cancer (outlined in Section 2.27). Normal breast FFPE sections (Insight Biotechnology Ltd, Cat No: CS802489) were used for calculations and comparison.

### 7.3.1. Patient characteristics

The HER2 status of all the patients included in this study were previously scored by a pathologist as HER-2 positive with membrane staining and a 3+ score and whenever necessary (Scoring 2+/1+) HER2 amplification was confirmed by fluorescent in situ hybridisation (FISH).

**Table 7-5:** Patient characteristics from ICORG-12-09 study. \* indicates HER2 amplification was confirmed by further FISH analysis.

		DCR (n = 6)	Non-DCR (n = 10)
<b>Median Age</b>		69.5 yrs	58.5 yrs
<b>ER status</b>	Positive	1/6	7/10
	Negative	5/6	1/10
	Unknown	-	2/10
<b>PR status</b>	Positive	1/6	3/10
	Negative	3/6	2/10
	Unknown	2/6	5/10
<b>Histology</b>	IDC	6/6	7/10
	DCIS	-	-
	Unknown	-	3/10
<b>Grade</b>	1+	-	1/10 *
	2+	-	2/10 *
	3+	6/6	6/10
	Unknown	-	1/10

ER: Estrogen Receptor, PR: Progesterone Receptor, IDC: Invasive ductal carcinoma, DCIS: Ductal carcinoma in situ, \* patients were confirmed HER2 amplified by FISH.

### 7.3.2. *HER2 immunohistochemistry and miRNA extraction*

As these patients had previously been identified as HER2 positive by a pathologist, sections (4  $\mu\text{M}$ ) were HER2 stained using the DAKO autostainer to identify HER2 positive tumour tissue for coring from DCR as illustrated in **Figure 7-4** and non-DCR as illustrated in **Figure 7-5**. Two 1.0 mm cores were punched and subsequently extracted using the miRNeasy FFPE kit. The miRNA extracts were analysed using the Nanodrop (Thermo Scientific) (**Table 7-6**) and subsequently used for further downstream reactions.

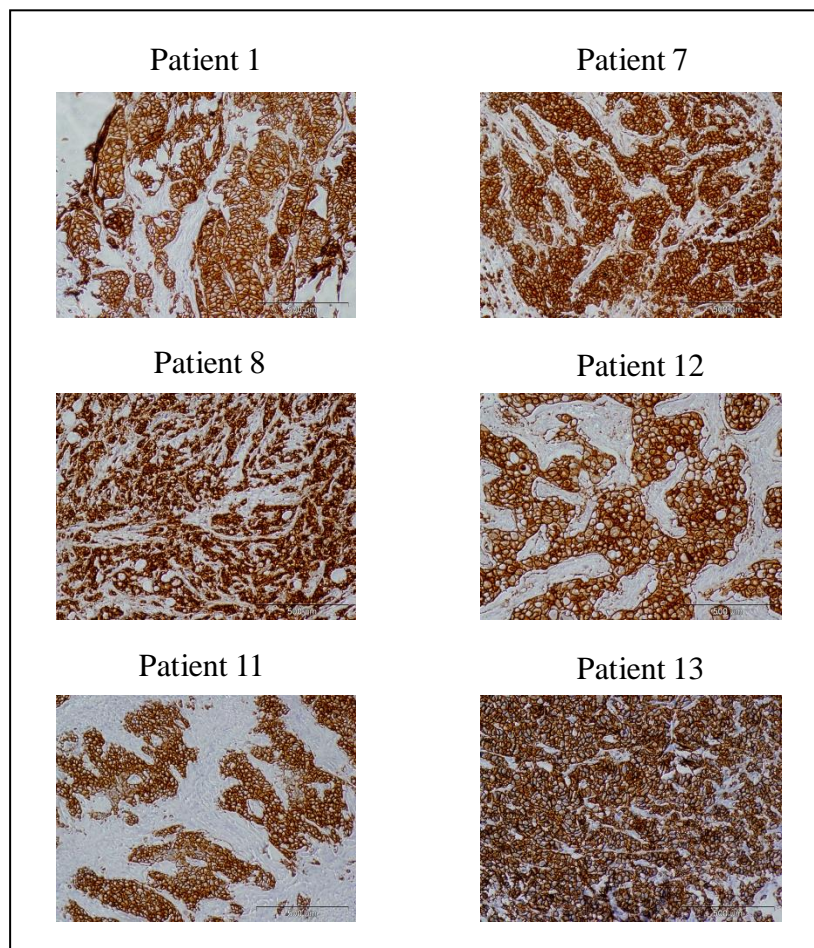


**Figure 7-4:** Immunohistochemical analysis of HER2 protein expression in the cohort of durable complete responders (DCR). Scale bar = 500  $\mu\text{m}$ . Images were captured at 10X magnification using the Nikon TS100 Microscope.

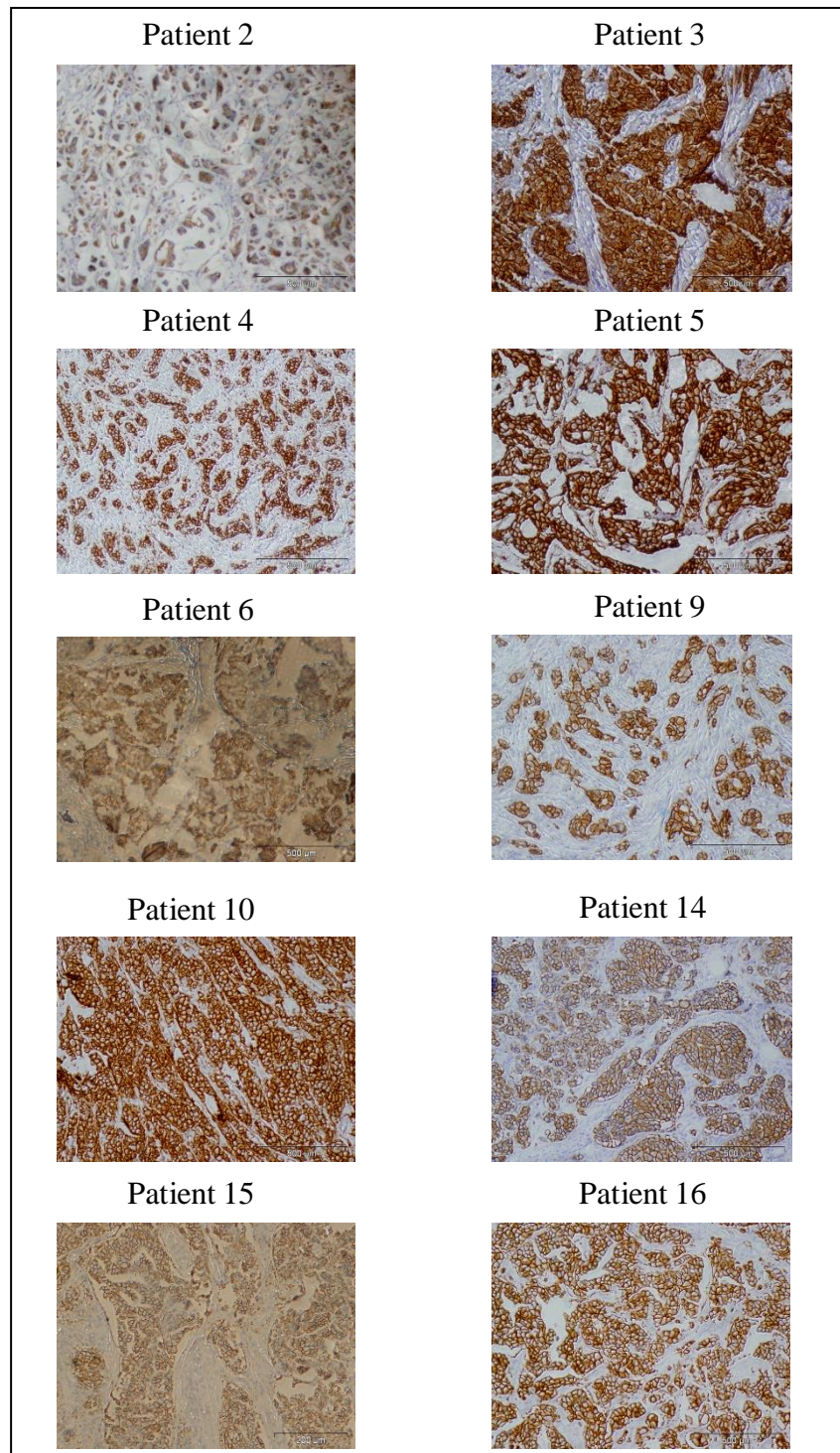


**Figure 7-5:** Immunohistochemical analysis of HER2 protein expression in the cohort of non-durable complete responders (non-DCR). Scale bar=500  $\mu$ m. Images were captured at 10X magnification using the Nikon TS100 Microscope.

**Table 7-6:** miRNA extracted from FFPE patient samples using the miRneasy kit was analysed by Nanodrop to determine concentration (ng/ $\mu$ l) and  $A_{260/280}$ .

Response	Patient No	Conc (ng/ $\mu$ l)	Total Conc ( $\mu$ g)	$A_{260/280}$	$A_{260/230}$
DCR	1	25.7	0.8	1.8	1.5
Non-DCR	2	54.6	1.6	1.9	1.7
Non-DCR	3	31.7	1.0	1.8	1.5
Non-DCR	4	16.8	0.5	1.4	1.1
Non-DCR	5	17.3	0.5	1.5	1.1
Non-DCR	6	18.9	0.6	1.5	1.0
DCR	7	60.9	1.8	2.0	2.7
DCR	8	68.3	2.0	1.9	1.9
Non-DCR	9	24.0	0.7	1.8	2.3
Non-DCR	10	25.8	0.8	1.7	1.7
DCR	11	18.4	0.6	1.8	1.5
DCR	12	42.5	1.3	1.9	1.8
DCR	13	66.3	2.0	1.8	0.9
Non-DCR	14	100.5	3.0	2.2	2.3
Non-DCR	15	85.0	2.6	2.1	3.2
Non-DCR	16	70.5	2.1	2.3	3.6
Normal Breast Section		20.3	0.6	1.7	1.2

### 7.3.3. *qRT-PCR analysis*

The miRNAs identified from the cell line analysis (miR-221, -222, -224 and -9) were tested in this patient cohort. RNU48 was used as the endogenous control and normal breast tissue was a calibrator sample. The fold changes were calculated using the comparative method. The average fold change of each group (DCR or non-DCR) was

calculated (**Table 7-7**). miR-221 expression was higher in the non-DCR (2.4 fold change) group in comparison to the DCR group (1.8 fold change) (**Figure 7-6**). miR-222 expression was also higher in the non-DCR group (3.2 fold change) compared to the DCR (1.7 fold change) (**Figure 7-6**). miR-224 expression was lower in the non-DCR group (-6.3 fold change) in comparison to the DCR group (1.8 fold change) (**Figure 7-6**). miR-9 expression was higher in the non-DCR group compared to the DCR group (**Figure 7-6**). However, statistical testing using a Mann Whitney test yielded no significance between the DCR and non-DCR groups for miR-221 (p=0.74), miR-222 (p=0.74), miR-224 (p=0.51) and miR-9 (p=0.79).

**Table 7-7:** Mean miRNA expression values (range) for miR-221, -222, -224 and -9 in DCR (n=6) and non-DCR (n=10) cohort. Fold changes were calculated relative to normal FFPE breast tissue.

	DCR	Non-DCR
miR-221	2.0 (-1.9 - 4.7 )	2.4 ( -2.8 - 13.8)
miR-222	1.8 (-1.3 - 4.2)	3.2 (-2.7 - 13.8)
miR-224	2.0 (-9.7 – 14.2)	-6.3 (-64.3 – 26.3)
miR-9	4.3 (-1.6 – 14.8)	11.2 (-1.7 – 48.6)

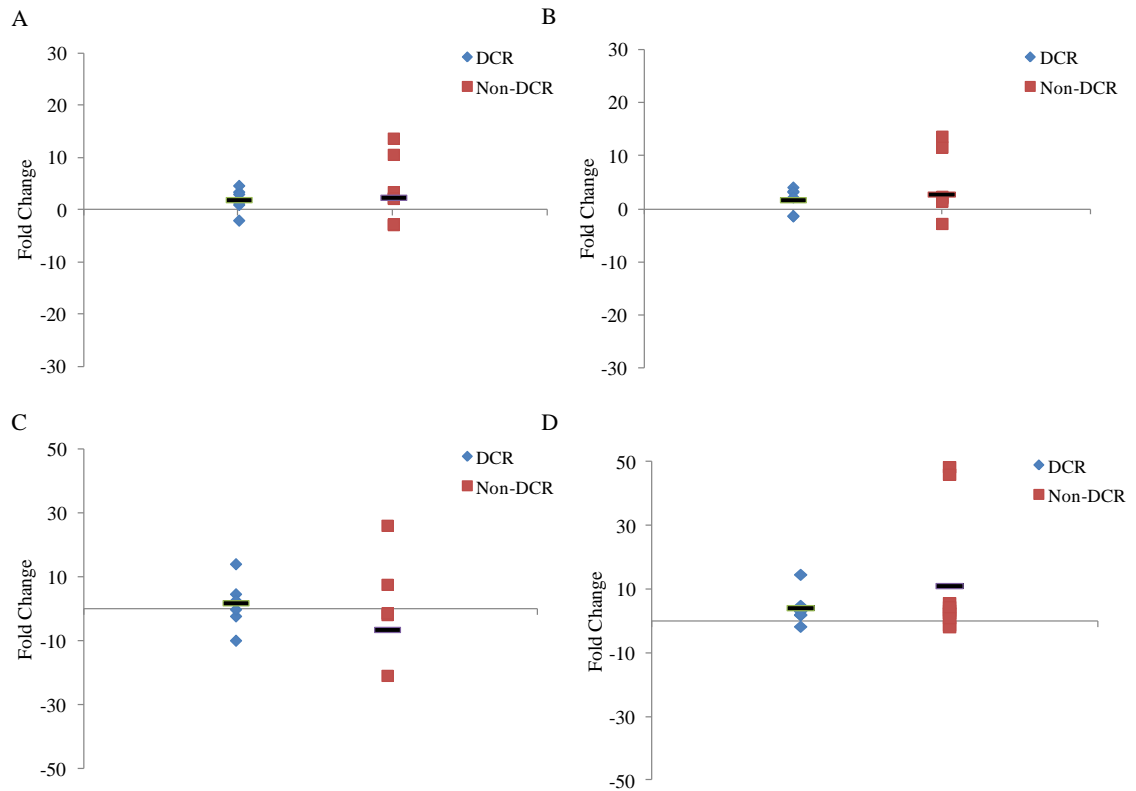


**Figure 7-6:** miRNA expression analysis for miR-221 (A), -222 (B), -224 (C) and -9 (D) in DCR  $\blacklozenge$  (n=6) and non-DCR  $\blacksquare$  (n=10) cohort. Fold changes were calculated relative to normal FFPE breast tissue. The average fold change for each group is plotted as a black line.

#### 7.4 Conditioned media study

CmiRNAs are potential non-invasive biomarkers of disease [285, 286], clinical outcome [287] and resistance [288]. To determine if the miRNAs identified in Chapter 4 may be detected in patient sera, we initially analysed miRNAs in conditioned media from cell lines.

##### 7.4.1. miRNA analysis from conditioned media

miRNA was extracted from conditioned media from the SKBR3-P, SKBR3-T and SKBR3-L cell lines as previously described [255] and extracts were analysed using the Nanodrop (**Table 7-8**). We observed high variability in the  $A_{260/230}$  values. We carried

out qRT-PCR analysis for the miRNAs using 100 ng RNA (instead of 10 ng) for the RT-PCR step and RNU48 endogenous control. The standard deviations between the biological replicates were quite high (**Table 7-9**) which could be due to the variability seen in the  $A_{260/230}$ . The endogenous control RNU48 also had variable Ct values suggesting it is not an appropriate control for this experiment (**Table 7-9**). We observed detectable Ct values for all miRNAs tested in this study qRT-PCR analysis (**Table 7-9**) (**Figure 7-7**). Fold changes were calculated using the comparative Ct method using the SKBR3-P CM as a control. No significant alterations were seen in the miRNAs tested (**Table 7-10**) but this possibly due to the high deviations between the samples.

**Table 7-8:** Quantification of concentration (ng/  $\mu$ L), total RNA ( $\mu$ g) and assessment of RNA purity by  $A_{260/280}$  and  $A_{260/230}$  ratios of RNA extracts from conditioned media from SKBR3, SKBR3-T and SKBR3-L cell lines.

Sample	Conc (ng/ $\mu$ L)	Total RNA ( $\mu$ g)	$A_{260/280}$	$A_{260/230}$
SKBR3-P #1	67.7	2.0	2.0	6.9
SKBR3-P #2	69.8	2.1	2.0	0.5
SKBR3-P #3	66.0	2.0	2.0	1.0
SKBR3-T #1	64.3	1.9	2.0	4.5
SKBR3-T #2	72.6	2.2	2.0	5.7
SKBR3-T #3	70.2	2.1	2.0	0.5
SKBR3-L #1	63.6	1.9	2.0	3.7
SKBR3-L #2	67.8	2.0	2.0	5.1
SKBR3-L #3	68.5	2.1	2.0	1.0

**Table 7-9:** miR-9, -221, -222, -224 and RNU48 Ct values for each biological replicate for the SKBR3-P, SKBR3-T and SKBR3-L conditioned media. Average Ct values (AVG) and standard deviations (std dev) for each cell line.

		Replicate 1	Replicate 2	Replicate 3	AVG	std dev
<b>SKBR3-P-CM</b>	miR-9	38.9	38.7	39.7	39.1	0.5
	miR-221	34.0	29.0	30.5	35.3	2.6
	miR-222	29.4	28.6	30.3	38.4	0.9
	miR-224	32.2	32.4	32.7	31.2	0.3
	RNU48	30.5	31.0	32.8	31.6	1.2
<b>SKBR3-T-CM</b>	miR-9	34.0	34.1	38.0	32.5	2.3
	miR-221	30.5	32.6	31.7	29.4	1.1
	miR-222	28.1	29.7	30.0	29.3	1.0
	miR-224	28.9	30.2	32.4	28.9	1.8
	RNU48	26.4	29.6	31.7	32.4	2.7
<b>SKBR3-L-CM</b>	miR-9	36.4	38.9	40.0	30.5	1.8
	miR-221	33.1	32.6	31.7	32.0	0.7
	miR-222	29.1	28.3	29.4	31.4	0.6
	miR-224	31.0	32.6	32.4	29.3	0.9
	RNU48	29.6	29.8	31.7	30.4	1.2

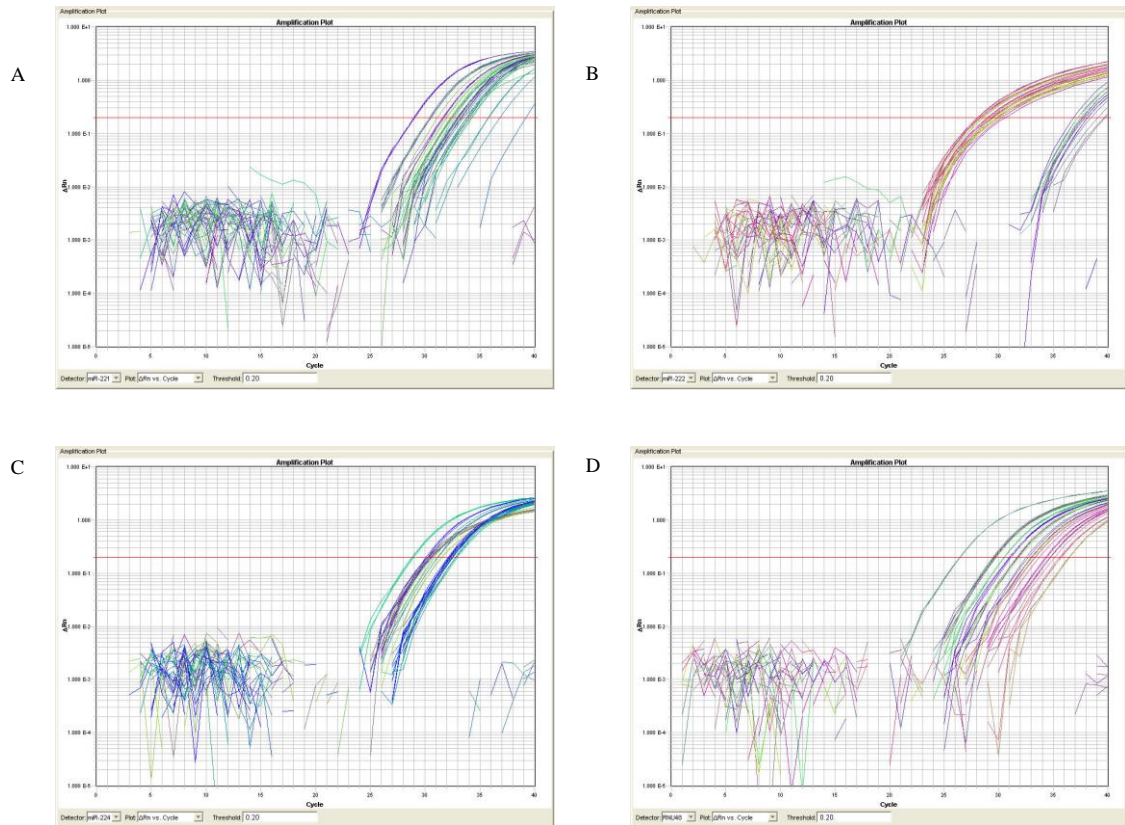


**Figure 7-7:** Amplification plots for (A) miR-221, (B) -222, (C) -224 (D) RNU48 for the SKBR3-P-CM, SKBR3-T-CM and SKBR3-L-CM.

**Table 7-10:** Expression analysis of miRNA in conditioned media from SKBR3-T and SKBR3-L cell line compared to the parental cell line. Fold changes were calculated using the comparative Ct method.

	<b>miR-9</b>	<b>miR-221</b>	<b>miR-222</b>	<b>miR-224</b>
SKBR3-T	3.0 ± 1.4	-6.1 ± 2.3	-4.1 ± 1.2	-1.2 ± 0.9
SKBR3-L	-1.3 ± 1.7	-5.2 ± 2.5	-1.5 ± 0.5	-1.6 ± 0.9

### 7.5 miRNA analysis from serum samples

As shown previously, miRNAs are stable and can be successfully extracted from conditioned media. Using pre- and post-treatment serum samples from the TCHL trial (outlined in Section 2.27) (neoadjuvant trial comparing trastuzumab and/or lapatinib with chemotherapy in HER2 positive breast cancer), we extracted miRNAs using the miRCURY RNA Isolation Kit - Biofluids (Exiqon). We initially extracted two samples; patient #09 from the TCH arm A and patient #082 from the TCHL arm B (**Table 7-11**). miR-9, -221 and -222 were detectable in both sets of patient sera, however, miR-224 was not detectable (**Table 7-12**) (**Figure 7-8**). RNU48 was undetermined for patient #082 and quite variable for patient #09 (**Table 7-12**). We calculated the fold change differences between pre- and post-treatment in patient no 09 and determined the miR-9, -221 and -222 expression are elevated post treatment (**Table 7-13**).

**Table 7-11:** Nanodrop analysis of serum extracted from pre and post TCHL samples

Sample	ng/ul	A <sub>260/280</sub>	A <sub>260/230</sub>
082 pre	4.8	0.7	0.1
082 post	4.7	0.7	0.1
09 pre	3.6	0.9	0.2
09 post	3.9	0.9	0.2

**Table 7-12:** Ct values for TCHL serum samples, pre- and post-surgery, for miR-9, -221, -222, -224 and the endogenous control RNU48. Ct values are represented  $\pm$  standard deviation of technical triplicates. Undet represents undetermined values i.e. > 40 cycle thresholds.

	<b>09 Pre</b>	<b>09 Post</b>	<b>082 Pre</b>	<b>082 Post</b>
miR-9	38.1 $\pm$ 0.6	37.8 $\pm$ 0.9	39.2 $\pm$ 0.1	38.9 $\pm$ 0.8
miR-221	28.1 $\pm$ 0.0	28.7 $\pm$ 0.1	29.9 $\pm$ 0.0	29.5 $\pm$ 0.1
miR-222	27.2 $\pm$ 0.1	29.0 $\pm$ 0.1	28.2 $\pm$ 0.1	30.0 $\pm$ 0.2
miR-224	Undet	Undet	Undet	Undet
RNU48	33.7 $\pm$ 0.4	39.6 $\pm$ 0.5	Undet	Undet

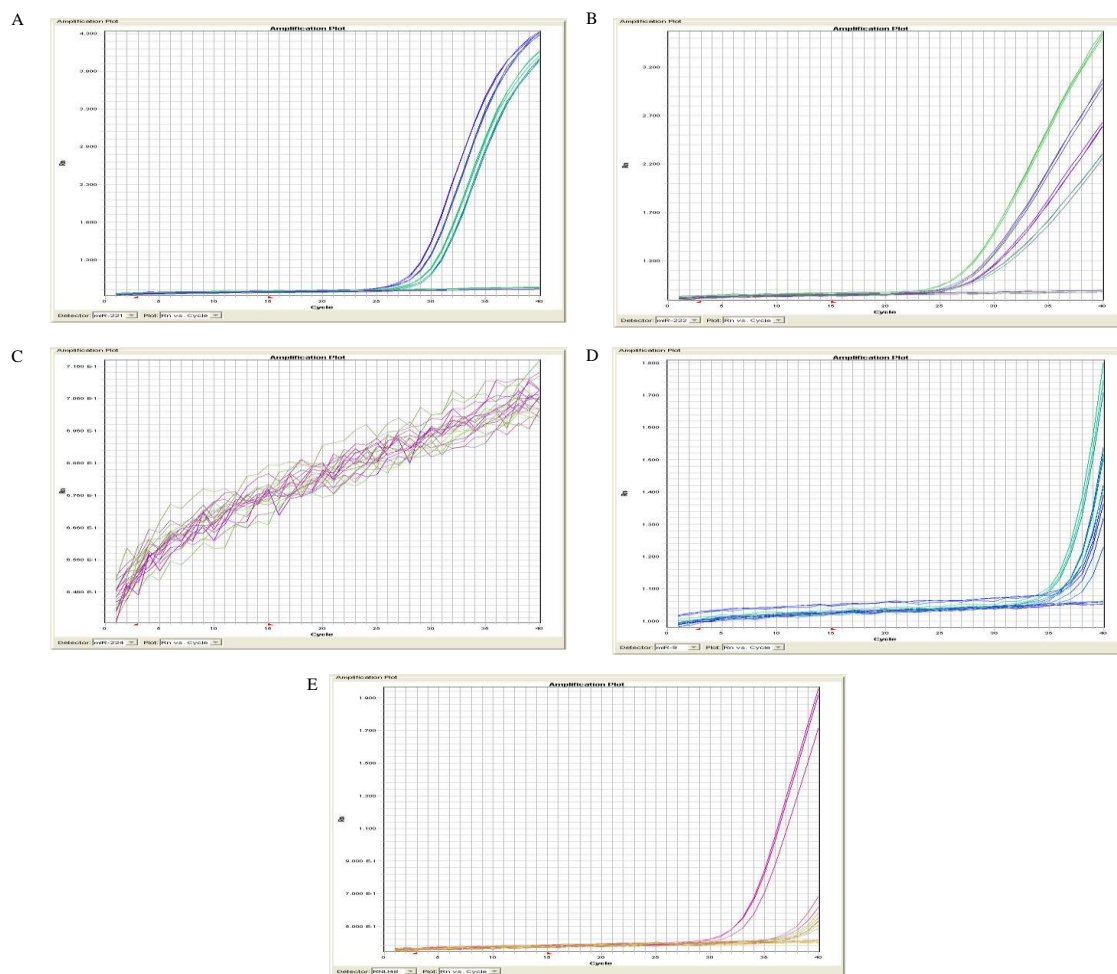


**Figure 7-8:** Amplification plots for (A) miR-221, (B) -222, (C) -224 (D) -9 and (E) RNU48 in TCHL serum samples (Patient #082 and #09).

**Table 7-13:** Expression analysis of miR-9, -221 and -222 in serum from Patient #09 (complete response) after treatment on the TCH arm A. Fold changes were calculated using the comparative Ct method.

Patient #09	Fold Change $\pm$ Std Dev
miR-9	74.5 $\pm$ 0.9
miR-221	39.8 $\pm$ 0.1
miR-222	17.0 $\pm$ 0.1

## 7.6 Summary

In this study, we optimised the extraction of miRNA from FFPE derived tissues. Analysis of miRNA extracted from HER2 positive tumour tissues in FFPE patient samples by Nanodrop, Bioanalyzer and qRT-PCR shows that intact miRNA was successfully extracted and is suitable for use in down-stream expression analysis. Using this information, we examined miRNA expression of miR-221, -222,-224 and -9 in a cohort of HER2 positive breast cancer patients who either achieved a DCR or who relapsed (non-DCR). Interestingly, we observed the same trends in expression of miR-221, -222,-224 and -9 as observed in the acquired resistant cell lines. miR-221, -222 and -9 expression is elevated in the non-DCR cohort compared to the DCR cohort and miR-224 is decreased in the non-DCR cohort compared to the DCR cohort. With regards innate trastuzumab resistance, the results seen in the non-DCR cohort follow the same elevated trend observed in miR-221 and -224 expression. These preliminary results confirm the trends in miRNA expression seen in the acquired trastuzumab resistant cell lines and in two of the miRNAs in the innate trastuzumab resistant cell lines. However the differences in expression levels were not statistically significant. This may be due to the small number ( $n = 16$ ) of samples in this study and a larger patient study would be required to confirm that these miRNAs may have potential as biomarkers of trastuzumab resistance.

We also successfully extracted miRNAs from conditioned media. The  $A_{260/280}$  ratio of 2.0 suggest 'pure' RNA [289]. However, the  $A_{260/230}$  ratios were extremely variable between samples and this suggests contamination from the extraction procedure or the starting material. Low  $A_{260/230}$  ratios are related to phenol carryover from the extraction procedure which may account for the low ratio seen in SKBR3-P #2, SKBR3-T #3,

SKBR3-P #3 and SKBR3-L #3. High  $A_{260/230}$  ratios are generally associated with problems in the measurement e.g.: a dirty pedestal or using a different pH solution to blank the samples initially. However, the samples were eluted in nuclease free H<sub>2</sub>O and the Nanodrop was blanked using the same so this does not account for the high ratios observed in the SKBR3-P #1, SKBR3-T #1, SKBR3-T #2, SKBR3-L #1 and SKBR3-L #2. We also collected the conditioned media in media with added serum. The protein in serum may have carried through the reaction. The variability in the samples may account for the variability seen downstream in the Ct values and the high standard deviations in the qRT-PCR analysis. Despite this, all four miRNAs were successfully detected in the conditioned medium which suggests that they are secreted and thus may have potential as extracellular biomarkers that may be detected in patient sera.

We initially examined 2 patient serum samples from the TCHL trial. Similar to the conditioned media RNU48 does not appear to be a suitable endogenous control for these studies. However, 3 of the 4 miRNAs tested were successfully detected.

This provides proof in principle that miR-221, -222 and -9 can be detected in patient sera. Further work using a more appropriate endogenous control, one that is stable in normal healthy sera, will be required to determine their predictive biomarker potential and the possibility of looking at miRNAs in serum samples as predictive biomarkers for trastuzumab treatment.

## **Chapter Eight**

### **Discussion**

## 8.1. Introduction

Trastuzumab is a monoclonal antibody approved for the treatment of HER2 positive breast cancer. It has become a standard of care for the treatment of HER2 positive tumours in both the metastatic and adjuvant settings. Lapatinib, a dual HER2/EGFR tyrosine kinase inhibitor, in combination with capecitabine is an approved treatment for HER2 positive advanced or metastatic breast cancer that has previously been treated with anthracyclines, taxanes and trastuzumab. However, some patients do not respond initially (*de novo* or innate resistance), and those who initially respond frequently develop resistance within 1-2 years (acquired resistance). Resistance to HER2 targeted therapies has been extensively investigated [145, 247, 290, 291]. However, biomarkers of resistance and strategies to overcome resistance have yet to be approved. miRNAs are potential biomarkers that may possess valuable information regarding resistance and prognosis [292]. In recent years, their expression and alterations have been linked with diseases including breast cancer [184, 293]. As access to fresh tissues is difficult the most common patient material is archived FFPE tumour blocks [283]. The process of formalin fixation and paraffin embedding has degradative effects upon tissue components including DNA and RNA; however, miRNAs remain stable after this process [294]. Therefore miRNAs may hold potential as predictive biomarkers of resistance to trastuzumab and lapatinib. They may also lead to the identification of new targets to overcome resistance.

Initially in this study, a panel of previously generated acquired resistant cell lines were characterised with regard to drug sensitivities, doubling times and migratory potential. Furthermore, identification of miRNAs associated with acquired trastuzumab and lapatinib resistance in HER2 positive breast cancer cells and determination if these

miRNAs are also involved in innate resistance. In parallel, a number of FFPE miRNA extraction methods were investigated to identify optimal extraction of miRNA from these precious tissue sources. Expression analysis was carried out of the miRNAs identified from the cell lines in a cohort of FFPE samples from HER2 positive breast cancer patients who are classified as durable complete responders (DCR > 36 months in remission) and non-DCR (progression < 12 months) to trastuzumab-based therapy. Preliminary miRNA expression analysis in patient sera was carried out using samples obtained from a neoadjuvant clinical trial (TCHL).

## **8.2. Characterisation of acquired trastuzumab and lapatinib resistant cell lines**

An acquired trastuzumab resistant cell line SKBR3-T and lapatinib resistant cell line, SKBR3-L were previously created by continuous exposure to trastuzumab or lapatinib for 6 months (Figure 2-1). The SKBR3-T cell line was confirmed as resistant to trastuzumab treatment (Figure 3-1) compared to the parental and the SKBR3-L cell line is resistant to both lapatinib and trastuzumab (Figure 3-1) (Figure 3-3). One of the issues encountered while working with the resistant cell lines was instability of the resistant phenotype. A potential explanation is culturing in different sera. The resistant cell line models were tested in two different batches of serum and a significant difference in resistance was determined (Figure 3-2). Serum is a vital ingredient for the growth of cells *in vitro* and is an extremely complex mixture. It is comprised of growth factors, transport proteins, trace elements and hormones which are essential for active cellular proliferation [295]. Proteomic analysis by Zheng *et al.* identified that protein concentrations and abundance were relatively stable among all sera tested, however, the levels of growth factors varied between samples. Interestingly, serum which promoted

cell proliferation contained the highest levels of growth factors [296]. Previously, growth factors such as transforming growth factor 1 (TGF1) [297] and insulin-like growth factor binding protein 2 (IGFBP2) [298] have been implicated in multidrug and chemotherapy resistance respectively. The significant loss of resistance in the acquired resistant cell lines is potentially due to the levels growth factors present in different batches of serum. Future proteomic analysis of the serum the cells were conditioned in compared to the new batches of serum may identify the main growth factor that is causative in the loss of the resistant phenotype.

One way to avoid this issue would be to work with the same batch of serum that the cell lines were conditioned in, however, this is difficult to achieve. Another option would be to culture in batchless 'chemically defined' serum. This serum contains no proteins, hydroslyates or components of unknown composition and is animal origin free [299]. Each component in this serum is known and this eliminates the variability seen between batches of serum. Another option is to use a defined growth factor composition such as those used for primary culture. Chemically defined serum or primary culture growth factors may be advantageous but would need to be tested with respect growth, morphology, doubling times, miRNA, mRNA and protein expression profiles and drug sensitivity to determine if they cause any significant alterations in the cell lines.

The doubling times of our panel of acquired resistant SKBR3 cell lines was investigated and lapatinib conditioning of the SKBR3 was determined to significantly increase the doubling time of the SKBR3-L compared to the SKBR3-P cells (Table 3-1) (Figure 3-4). This suggests lapatinib resistance is associated with a slower growth rate which is later discussed in relation to CDKN1A expression in 8.3.3. The migratory properties of

the cell lines were also investigated by wound scratch assay [253], using two time points, 24 and 48 h. The SKBR3-T cell line was significantly more migratory than the parental after 48 h (Figure 3-5). Interestingly, the SKBR3-L cell line is significantly more migratory than the SKBR3-P and SKBR3-T cell lines at 48 h (Figure 3-5). Therefore, although the SKBR3-L cells have a slower growth rate they are highly migratory. It has previously been reported that lapatinib treatment in triple negative cell lines increases the aggressive phenotype of these cells through down-regulation of miR-7 [212]. Enhancement of migration and invasion in the TNBC cells was due to over-expression of cyclooxygenase-2 (COX2) and EGFR and down-regulation of miR-7. Interestingly, the SKBR3-L cell lines have increased levels of EGFR and pEGFR compared to the SKBR3-P [300]. This may contribute to the increased migratory potential of these cells compared to the parental cells. Further work would be required to determine if this increase in the EGFR pathway is associated with increased migration.

Another acquired trastuzumab resistant cell line, BT-474-Tr and its parental BT474-P were generously gifted from UCLA [123] and another lapatinib acquired resistant cell line, HCC1954-L was previously created by Dr. Mc Dermott [247]. The BT-474-Tr cell line was confirmed as resistant to trastuzumab treatment (Figure 3-6) but extremely sensitive to lapatinib inhibition (Figure 3-7). The HCC-1954-P and HCC-1954-L cell lines are both innately resistant to trastuzumab treatment (Figure 3-8) and the HCC-1954-L cells were confirmed as resistant to lapatinib inhibition (Figure 3-9). Previously, microarray analysis of the SKBR3-P, SKBR3-T and SKBR3-L cell lines was carried out in UCLA (one replicate each). This data was used for potential target gene identification. Previously, breast cancer stem cells (BCSCs) have been reported as

chemo-resistant [301, 302] and therefore a panel of stem cell markers were examined in our microarray data and significantly altered stem cell markers were identified in the SKBR3-T (Table 3-2) and SKBR3-L (Table 3-3) cell lines. Interestingly, ALDH1A1 was altered in both resistant cell lines. Consistent with the microarray data, ALDH1A1 protein expression is slightly decreased in the SKBR3-T and is significantly increased in the SKBR3-L cell line (Figure 3-10). The ALDH1 enzyme family is comprised of ALDH1A1, ALDH1A2 and ALDH1A3. It was previously assumed that ALDH1A1 was the primary determinant of ALDEFLUOR activity, however; other ALDH family members including ALDH1A3, ALDH2, ALDH4A1, ALDH5A1, ALDH6A1 and ALDH7A1 also determine activity [303]. Duru *et al.* have previously shown that HER2 positive breast cancer stem cells are associated with increased ALDH activity and aggressiveness [304].

A collaboration with Dr. Gallagher's 'Stemness' group in Trinity College Dublin examined the ALDH activity of the SKBR3-P and SKBR3-L cell lines. This assay can identify stem and progenitor cells as the enzyme ALDH is highly expressed in these cell types [305]. ALDH positivity identifies a stem cell population and using the fluorescence nature of this assay ALDH+ cells can be identified and sorted from ALDH- cells. Initially the ALDH expression of the SKBR3-P and SKBR3-L cell lines was examined. A high population of ALDH+ cells in the SKBR3-P cell line was identified and a significantly lower population in the SKBR3-L cell line (Figure 3-11) (Table 3-4). This conflicts with the results observed in the microarray and immunoblotting. However, as the ALDEFLUOR assay detects activity of a number of different isoforms and the immunoblotting focused on ALDH1A1 expression this may account for the difference in results. The microarray data also suggests that there are

alterations in multiple members of the ALDH family including, ALDH2, ALDH5A1, ALDH6A1, and ALDH7A1 which have also been associated with ALDEFLUOR activity [303]. However, the ALDEFLUOR results suggest that an increase in a stem cell population is not likely to play a causative role in the resistant phenotype of the SKBR3-L cells.

### **8.3. microRNA expression analysis**

#### **8.3.1. Cell line analysis**

miRNA profiling was carried out on the acquired trastuzumab and lapatinib resistant SKBR3 breast cancer cells. Analysis of TLDA identified ten (Table 4-1) and thirteen (Table 4-2) miRNAs that were altered in the acquired trastuzumab and lapatinib resistant cell lines, respectively. Validation of these miRNAs by individual qRT-PCR confirmed that miR-221, miR-222 and miR-9 were significantly up-regulated in the SKBR3-T cell line (Table 4-3). miR-224 was included in the validation due to its position on the same chromosome as miR-221 and -222 and observed it was significantly down-regulated (Table 4-3). Validation in the SKBR3-L cell line determined miR-30a-3p and miR-9 were significantly up-regulated and miR-221, miR-224, miR-375, miR-550 and miR-92a were down-regulated (Table 4-4). However, miR-30a-3p was excluded as it followed an opposite trend from the TLDA analysis. miR-221 and -222 were selected for validation in the SKBR3-L despite miR-222 not being altered in the TLDA data. As miR-221 and -222 are clustered genes located which contain identical seed sequences suggesting that these miRNA are expressed together and function on the same target mRNAs (356).

To determine that these alterations were not specific to the SKBR3 cell line, expression of these miRNAs in other cell line models of acquired trastuzumab (BT474-Tr) and lapatinib (HCC-1954-L) resistance was investigated. miR-9 expression was unaltered and miR-224 expression was turned off in the acquired trastuzumab resistant BT-474-Tr cells compared to the parental cells (Table 4-5). miR-221 and miR-222 were significantly up-regulated in the BT-474-Tr cells (Table 4-5). miR-9 was significantly up-regulated and miR-222 was significantly down-regulated in the HCC-1954-L cell line (Table 4-6).

The miRNA profiles for each drug were different as miR-221, -222, -224 and -9 are associated with acquired trastuzumab resistant cell lines. miR-222 and -9 are associated with acquired lapatinib resistance. However, miR-222 is a common alteration in both the acquired trastuzumab and lapatinib cell lines.

The expression of the altered miRNAs was also investigated in a panel of innately sensitive and resistant HER2 positive cell lines. The trastuzumab sensitive cell lines (SKBR3 and BT-474) were used for the comparative calculations. miR-221 expression was significantly higher in 5/6 innately resistance cell lines tested and miR-222 was higher only in 3/6 of the innately resistant cell lines compared to the sensitive cell lines (Table 4-7). miR-224 was lower in 5/6 of the innately resistant cell lines compared to the sensitive cell lines. miR-9 expression was lower in 5/6 of the innately resistant cell lines in contrast with the up-regulated expression in the acquired resistant cell lines (Table 4-7). These results show that altered expression of miR-221 and miR-224 is not only seen in the acquired resistant cell lines but also in the innate resistant cell lines and suggest that these miRNAs could be possible biomarkers of trastuzumab resistance.

Low expression of miR-9 may be a predictive biomarker of specifically innate trastuzumab resistance. miR-222 is not a marker of innate trastuzumab resistance but could be used as an indicator of acquired trastuzumab resistance.

miR-221, miR-224 and miR-9 expression was also investigated in the innate lapatinib resistant cell lines. The SKBR3, BT-474, HCC-1419 and HCC-1954 cell lines are classed as sensitive cell lines and were used for the comparative calculations. miR-221 expression was lower in 2/4 innately resistant cell lines, miR-224 was lower in all 4 innately lapatinib resistant cell lines and miR-9 expression was higher in 1/4 innately resistant cell lines (Table 4-8). Low expression of miR-224 maybe an indicator of innate lapatinib resistance.

Ye *et al.* determined that miR-221 expression may promote trastuzumab resistance by targeting PTEN [207], which has been previously reported as a mechanism of trastuzumab resistance [103]. They also observed that miR-221 over-expression in the SKBR3 cell lines conferred trastuzumab resistance and increased the migratory and invasive properties of this cell line. This is the only reported miRNA involved in trastuzumab and/or lapatinib resistance from our panel of miRNAs identified.

The effect of a short term treatment of trastuzumab and lapatinib on the SKBR3-P cells was investigated. This experiment also investigated if the miRNA alterations are caused by long term exposure or also occur following short-term exposure of drug. No changes were seen in the expression of the miRNAs after 24 and 48 h treatment with trastuzumab (10 µg/mL) (Table 4-9). A significant down-regulation of miR-221, miR-222 and miR-224 was observed in the SKBR3-P cell lines after lapatinib treatment (24

h) (Table 4-10). Thus, the miRNAs identified in the trastuzumab acquired resistant SKBR3-T cell line are specifically associated with long term exposure and not short term drug treatment. The short term treatment with lapatinib however, has a significant effect on the miRNAs after 24 h but these changes are reversed after 48 hours. This reversal in miRNA expression needs to be explored further.

### **8.3.2. Comparison of FFPE miRNA extraction kits**

During the FFPE process, from collection and fixation and to the dehydration and embedding process each step can impact the quality of the final embedded sample. Integrity of DNA and RNA from FFPE samples is affected by the fixation length and cross-linking that can occur from formalin [306]. Other factors that may result in fragmented DNA and RNA are the temperature at which the sample is embedded and the length of storage [306]. RNA can become oxidised at the exposed surface of the FFPE sample [306]. The optimal storage conditions for FFPE after one year was 4°C as intact RNA was still detectable [306]. Formalin and the chemical modifications it has upon RNA negatively impact on RT-PCR. The degree of formalin modifications on RNA is dependent on fixation time and the RNA isolation procedure. Cross-linking occurs at the 5' and 3' ends of RNA and efficiency of PCR is greatly reduced. PCR amplification of FFPE RNA samples is best suited to short targets [306] which is why miRNAs are suitable for investigation. Gene expression analysis utilises TaqMan PCR which can be carried out on as little as 1 ng of starting material [307]. This overcomes one of the problems frequently encountered in FFPE as the RNA yields can be quite low.

Recent improvements in RNA extraction kits include a proteinase K step which solubilised the FFPE tissue completely, promoting breakdown of the formalin cross-

links, inhibiting RNases that may still be stable and successfully extracting RNA [307, 308]. Extraction methods with a column DNase digestion step were found to yield detectable RNA from FFPE samples [307]. Increasing the temperature of the formalin free buffer removed the methylol groups from the bases which restored template activity to RNA from FFPE samples [308]. FFPE sections were susceptible to RNA degradation by light and air, however, storage of the FFPE blocks in the open or protected from both light and air did not affect the RNA quality if the sample for extraction was not taken directly from the top of the block [306].

FFPE extraction kits were assessed; firstly using CCDB generated using SKBR3-P cells. Three commercially available kits that are most commonly used for miRNA extraction were used; RecoverAll (Ambion), miRNeasy (Qiagen) and High Pure FFPE RNA Micro Kit (Roche). A previous comparison of these 3 kits showed that miRNA extracted from FFPE tissues is more stable and easily recovered than mRNA and the RecoverAll kit was the preferred extraction kit for miRNA [294]. Another important criterion for extraction of miRNA is the specimen size. Previous investigations into the optimal thickness of sections for miRNA extraction from FFPE samples suggested that the optimal section thickness was 10  $\mu\text{M}$  or greater for optimal miRNA analysis. In addition to testing 10  $\mu\text{M}$  sections we also investigated cores of 1.0 mm and 1.5 mm. The reasoning for isolating cores from tissue samples is disease specific areas e.g.: HER2 positive can be isolated areas of tumour as sections which should minimise the amount of normal tissue in the sample. In comparison with Doleshal *et al.*, we found that the RecoverAll kit had good overall yields of RNA as did the RNeasy kit (Table 7-1). The Roche kit had high variability in yields of RNA (Table 7-1). When comparing the sections (10  $\mu\text{M}$ ) and cores, sections produced greater yields. As the cores focus on

a smaller more specific area of FFPE block than a section, it is not surprising to find smaller yields in our core samples.

Bioanalyser analysis of all samples in comparison to a cell line positive control showed that the RecoverAll and miRNeasy kit yielded small peaks at the small RNA positions but no evidence of 18S and 28S peaks for total RNA (Figure 7-2). As the RNA is degraded from the embedding process, RIN values tend to be lower in FFPE samples even as low as 1.4 [309]. In this study, the RIN values ranged from 1.1-1.8 suggesting the RNA has been degraded in the overall embedding process but is acceptable for acceptable for downstream qRT-PCR analysis. The RIN value has been suggested as superior over the A260/280 ratio in breast cancer samples [310] so it is best to focus on Bioanalyser (Agilent) analysis for determination of intact RNA and the Nanodrop (Thermo scientific) for determination of concentration. The conclusion from this study was sufficient miRNA could be extracted from two 1.0 mm cores in HER2 positive specific areas using the miRNeasy kit.

### **8.3.3. *miRNA analysis in the HER2 positive FFPE tumour samples***

In collaboration with Dr. Giuseppe Gullo and ICORG, access was obtained to a cohort of patients (n=16) from St. Vincent's Hospital, Dublin. The study consists of two cohorts of HER2 positive metastatic breast cancer patients who received trastuzumab-based treatment; cohort one includes patients who are classed trastuzumab sensitive (durable complete responders, DCR as defined by RECIST 1.0 [311]) (n=6) and cohort two included patients who are classed trastuzumab resistant (non-durable complete responders, non-DCR) (n=10). Approximately, 9% of patients who received first line chemotherapy and trastuzumab achieved DCR lasting for more than 36 months [101]. DCR was more frequently observed in ER negative patients (DCR-14%) and in those

with liver metastases [101]. The DCR rate for patients who received trastuzumab with first line chemotherapy was 16 %, however, DCR was completely absent in patients who received trastuzumab in second line of chemotherapy. These patient samples were chosen for miRNA investigation as a follow up of the previous cell line work as they may lead to potential biomarkers of response to trastuzumab based therapy and early identification of responders or patients who are likely to achieve DCR. The tumour sample available are FFPE specimens and the RNA extraction procedure described in section 2.24 was used.

Initially, the miRNAs identified in Chapter Four were examined in this FFPE study. HER2 staining was used to identify the HER2 positive areas in the tumour specimens from normal tissue. miRNA was successfully extracted from these difficult tissue specimens. Interestingly, the miRNA expression profiles followed the same trend as observed seen in the acquired trastuzumab resistant cell line (Figure 7-6). miR-221, -222 and -9 expression is higher and miR-224 is lower in the non-DCR tumours compared to the DCR tumours. Although this is a very small cohort these preliminary data suggest that these miRNAs maybe predictive biomarkers of trastuzumab resistance. Recently, miR-221 has been associated with PTEN expression and trastuzumab resistance in HER2 breast cancer cell lines [207]. The authors suggest that miR-221 may be a biomarker of progression and poor overall survival in HER2 positive breast cancer. miR-222 expression is reportedly involved in resistance to adriamycin and docetaxel in breast cancer [312]. Both miR-221 and -222 have been associated with tamoxifen resistance [274]. miR-9 has previously been shown to predict nasopharyngeal carcinoma (NPC) metastasis in plasma samples [313] and is a potential biomarker for local recurrence in ER positive breast cancer [314]. miR-224 expression has been

associated with cisplatin resistance in lung adenocarcinomas [315] and ovarian papillary serous carcinoma [316]. Further miRNA microarrays and microarrays should be carried out on these two cohorts to identify other key miRNAs or mRNAs that are involved in trastuzumab resistance.

In summary, elevated levels of miR-221, -222 and decreased levels of miR-224 may be predictive of acquired trastuzumab resistance. Elevated levels of miR-221 and low levels of miR-224 may be potential predictive biomarkers of both innate and acquired trastuzumab resistance. Elevated levels of miR-9 and low levels of miR-222 may be predictive of acquired lapatinib resistance. Lower levels of miR-221 and -222 are predictive of innate lapatinib resistance. Further exploration of these miRNA signatures in a larger cohort of trastuzumab responders and non-responders is needed to confirm their predictive potential. To the best of our knowledge, this is the first report of miR-9, miR-222 and miR-224 and their potential roles as predictive biomarkers of trastuzumab resistance in HER2 positive metastatic disease.

#### **8.3.4. *miRNA analysis in conditioned media***

Circulating miRNAs have come to the fore-front of translational research as non-invasive biomarkers of disease. As we identified potentially novel biomarkers of resistance in patient tumours, we decided to investigate miRNA expression in patient sera samples from the TCHL trial. To determine if these miRNAs are potentially secreted from HER2 positive breast cancer cells we initially tested conditioned media from cell lines. We successfully isolated RNA from conditioned media and carried out miRNA analysis for the 4 miRNAs (miR-221,-222,-224 and -9) (Table 7-8). We observed high variability within the  $A_{260/230}$  values for the RNA extracted from the

conditioned media which may account for the variability observed in the Ct values obtained in the qRT-PCR (Table 7-9). This suggests that further optimisation of the miRNA extraction of conditioned media is required to eliminate potential sources of contamination such as protein or phenol. Another potential contaminant is serum and further experiments should be carried out under serum reduced conditions to examine the serum affects on conditioned media miRNAs. Despite the variation in the Ct values obtained, all 4 miRNAs were detected in the conditioned media, providing evidence that they are indeed secreted from the HER2 positive breast cancer cells and thus may be potential circulating biomarkers in HER2 positive breast cancer patients.

#### **8.3.5. *miRNA analysis in patient sera***

Utilising a new miRNA extraction kit specific for biofluids, we extracted miRNAs from two pre- and post- neoadjuvant treatment (TCH or TCHL) serum samples. Nanodrop analysis of the miRNA extracts showed low ratios for both  $A_{260/280}$  and  $A_{260/230}$  (Table 7-11). miR-9, -221 and -222 were detectable, however miR-224 was undetected in both patient sera (Table 7-12). miR-221 has previously been identified in prostate cancer [317], malignant melanoma [318] and together with miR-222 in hepatocellular carcinoma [319] patients serum samples. miR-222 was one of three altered miRNAs in case samples compared to controls within the Sister Study cohort in breast cancer serum samples [320]. Previously, miR-224 serum expression was identified as down-regulated in prostate cancer serum samples [321] and was correlated with predicting survival and reflects stage in hepatocellular carcinoma [322]. miR-9 has been reported as a potential prognostic and diagnostic serum miRNA in osteosarcoma [323] and is associated with prediction of metastases in NPC [324]. RNU48 was detected in only one patient sample.

We observed the same variability in RNU48 expression as seen in the conditioned media samples.

The endogenous control used in the previous miRNA analysis RNU48, may not be ideally suited to the conditioned media and patient sera studies as we saw large variation between the replicates and the Ct values ranged from 26.4-32.8. RNU48 is a small nucleolar non-coding RNA (snoRNAs) approximately 70 nucleotides in length [325]. It has also been show that U6, another endogenous control is not suitable for circulating miRNAs [326]. However, there are 19 human control miRNA assays available [327] and further optimisation studies should be performed to identify an appropriate control for extracellular miRNAs. From this pilot experiment we can conclude that 3 of the 4 miRNAs are detectable in patient serum and following optimisation of the control further analysis of their expression in the pre- and post-treatment samples should be performed to determine if they are predictive of response to HER2 targeted therapies in the neoadjuvant setting.

#### **8.4. Evidence of miRNA value in resistance**

A meta- analysis of all previously published data for miR-221 and -222 in PubMed, Embase, Cochrane, and CNKI databases which included 17 studies involving 1,204 subjects analysed their prognostic potential for OS and DFS [328]. Elevated expression of miR-221 and -222 was associated with poor OS in cancer patients when stratified by ethnicity, cancer type, statistical methodology, sample, and quality assessment.

Previously, miR-224 has been identified in cisplatin resistant lung adenocarcinomas and CDKN1A is a direct target [315]. They determined that miR-224 is up-regulated in

cisplatin resistant lung cancer cell and it regulates the G1/S phase transition of the cell cycle. They concluded that the miR-224:CDKN1A signalling pathway could be a potential target in overcoming cisplatin resistance in lung cancer. Cyclin-dependent kinase inhibitor 1A (CDKN1A/p21<sup>Cip1</sup>) is an important factor in cell cycle progression and is up-regulated in both the SKBR3-T and SKBR3-L cell lines. CDKN1A inhibits cyclin-dependent kinase 2 and/or cyclin dependent kinase 4 (CDK2/CDK4) and inhibits progression of the cell cycle at the G1 phase and is also involved in cellular senescence [329]. The increase in CDKN1A may contribute to the increase in doubling time in the SKBR3-L cell lines (Table 3-1). In our cell lines, miR-224 expression is down-regulated in the SKBR3-T and -L cells and turned off in the BT-474-Tr cell line. This would indicate that if miR-224 was a direct target for CDKN1A, then its expression would be increased therefore having a higher level of cell cycle arrest and senescence. This could potentially account for the increased doubling time seen in the SKBR3-L cells (Figure 3-4). Altered CDKN1A expression could contribute to the slower growth rate we see in the SKBR3-L cell line. Zhu *et al.* determined that decreased miR-224 expression is a potentially diagnostic and prognostic tool in non-small cell lung cancer (NSCLC) cell lines and primary tissues [330].

miR-9 expression has been identified as a prognostic marker in osteosarcoma in both tissue [331] and serum [323] samples. More recently, miR-9 has been associated with epithelial-mesenchymal transition (EMT) and breast cancer stem cell (BCSC) phenotypes [332]. Gwak *et al.* observed higher expression levels of miR-9 in HER2 positive and triple negative breast cancer subtypes. miR-9 was associated with higher stage and grade, p53 over-expression and a high proliferation index. Interestingly, high levels of miR-9 was found in tumours exhibiting CD44+/CD24- phenotype, vimentin

expression and E-cadherin loss which are involved in the EMT pathway. In a study by Liu *et al.*, they determined that erbin (ErbB2 Interacting Protein) was down-regulated in HER2 over-expressing breast cancer cell lines [333]. They also concluded that erbin mediates trastuzumab resistance by activation of AKT and that it is essential for the regulation of migration. Interestingly, utilising miRWalk miR-9 is predicted to target erbin which could be a potential miRNA:mRNA interaction that could be a key player in trastuzumab resistance.

The miRNAs which were identified in the innate trastuzumab (miR-221 and miR-224) and lapatinib (miR-224) resistant cell lines have predictive potential and could be used to screen HER2 positive breast cancer patients prior to therapy to determine innate resistance. In the clinic, carrying out miRNA analysis on biopsy specimens could identify a subset of patients who will not respond or go on to relapse on trastuzumab based therapy. These patients could be placed on a different regimen of alternative HER2 targeted therapies.

Biomarkers of acquired resistance may be of value in the neoadjuvant setting. An increase in miR-221,-222 and -9 and /or decreased levels of miR-224 in a surgical tumour specimen following neoadjuvant therapy could be indicative of acquired resistance and suggest that alternative therapies should be administered post-surgery rather than continuing trastuzumab therapy as is the current practice. Similarly these biomarkers could also be used to monitor disease progression in patients with metastatic disease.

## 8.5. Target prediction for miRNAs

Utilising the miRWalk database potential gene targets were identified for the altered miRNAs (miR-221, -222, -224, -9). Cross comparison of the miRWalk results with the UCLA microarray dataset narrowed down the potential targets specific to the resistant cell lines. miR-221 and miR-222 belong to a miRNA cluster located on chromosome X [334]. A common target was identified for miR-221 and -222; angiogenin (ANG) which is up-regulated in the SKBR3-T cell lines according to the microarray data (Table 4-11). ANG is a pro-angiogenic secreted protein which has been previously associated with invasion and metastasis in breast cancer [335]. Chemokine (C-C motif) ligand 2 (CCL2) is a potential target for miR-221 in the SKBR3-L cell lines (Table 4-12). CCL2 is a chemokine that has stimulatory and migratory effects on mononuclear cells [336] and elevated expression has been previously associated with poor prognosis in breast cancer patients [337]. miR-224 has reported roles in cellular migration, invasion [338], and metastasis in breast cancer cells [339]. In a study by Zhu *et al.*, they found that down-regulation of miR-224 (anti-miR-224) in MDA-MB-231 cells (triple negative breast cancer cells) that over-express Ubc9 (E2-conjugating enzyme that promotes cell invasion and metastasis) enhanced their invasive potential [340]. miR-224 targets included FBJ murine osteosarcoma viral oncogene homolog B (FOSB) in the acquired trastuzumab SKBR3 cell line (Table 4-15) and jun B proto-oncogene (JUNB) in the acquired lapatinib SKBR3 cell line (Table 4-16). FOSB has previously been associated with poor differentiation of breast carcinomas [341] and JUNB expression has been negatively correlated with tumour stage in breast cancer [342].

In the acquired trastuzumab SKBR3 cell line retinoic acid receptor alpha (RARA) was identified as a potential target for miR-9. RAR $\alpha$  is mainly associated with acute

promyelocytic leukemia (APL) [343]. Interestingly, HER2 and RAR $\alpha$  are located on the same chromosome, 17q12-q21. Co-amplification of RARA $\alpha$  was identified in 23-32% of HER2 positive breast cancers [344]. Combination treatment with lapatinib and ATRA caused synergistic growth inhibition and apoptosis. In 2013, Alsafadi *et al.*, reported that RAR $\alpha$  is amplified in 27 % of HER2 positive breast cancers and in the SKBR3 cell line [345]. RAR $\alpha$  was selected in this study as a potentially druggable target for further evaluation in the resistant cells.

### ***8.5.1 miR-9 and Retinoic acid receptor alpha***

miR-9 has reported roles in epithelial and breast carcinoma cells. It has been associated with induction of epithelial mesenchymal transition (EMT) by targeting E-cadherin [346] and increased motility and migration in breast cancer cells by activation of MYC and MYCN [346]. Thus miR-9 may play a role in the increased migration we see in the SKBR3-L acquired resistant cell line. It also plays a role in: (i) metastases and promotion of cell motility [347], (ii) induction of VEGF and tumour angiogenesis [346], (iii) cell growth [348] and (iv) negative regulation of NF $\kappa$ B-1 [349]. Recent studies have also identified miR-9 as a potential marker of local recurrence in ER positive breast cancer patients [350]. Hyper-methylation of miR-9 can be used as an independent prognostic factor for DFS in acute lymphoblastic leukaemia [351].

RAR $\alpha$  was identified as an altered target gene in SKBR3-T cells and a potential target for miR-9 from miRWalk database cross compared with the microarray (UCLA) (Table 5-1). RAR $\alpha$  was included as a validated target for miR-9, however, the reference cited does not specifically link miR-9 and RAR $\alpha$  [352]. According to that study RAR $\alpha$  is a potential target for miR-27a.

Initially, the effect of ATRA treatment was investigated in the SKBR3-P, SKBR3-T and SKBR3-L cell lines. ATRA is an active metabolite of vitamin A and is also a differentiating agent of cancer stem cells [353]. It is primarily and routinely used in the treatment of acute promyelocytic leukemia [354]. The SKBR3-P and SKBR3-L were sensitive to ATRA treatment; however, interestingly the SKBR3-T cell line was insensitive to ATRA inhibition (Figure 5-1) (Table 5-2). The other cell line models of resistance were also investigated and determined the BT-474-P, BT-474-Tr, HCC-1954-P, HCC-1954-L are insensitive to ATRA treatment (Figure 5-2). The EFM-192A cell lines are moderately sensitive to ATRA treatment (Figure 5-2).

Combination treatment of these cell lines with ATRA and trastuzumab was also investigated further. Combination treatment was significantly more effective than either ATRA or trastuzumab treatment alone in the SKBR3-P, -L and -T cell lines despite the SKBR3-T cells displaying acquired resistance to ATRA alone (Figure 5-3). Combined treatment in the BT-474 (Figure 5-4) and HCC-1954 (Figure 5-5) cell lines showed no significant enhancement on growth inhibition. The EFM-192A cells showed an enhanced growth inhibition upon combined treatment with ATRA and trastuzumab (Figure 5-6).

The effect of combined treatment of ATRA with lapatinib was investigated in our cell line models of acquired resistance. We identified that the combination treatment in the SKBR3-P, -T and -L cell lines was significantly more effective than either agent alone (Figure 5-7). Combined treatment in the BT474 (Figure 5-8), HCC-1954 (Figure 5-9)

and EFM-192A (Figure 5-10) cell lines showed no enhanced growth inhibition compared to lapatinib treatment alone.

These results suggest that combination treatment with ATRA and anti-HER2 therapies is only effective in HER2 positive breast cancer cells that show some sensitivity to single agent ATRA. The results also suggest that combined treatment may overcome trastuzumab and/or lapatinib resistance in some cases as we see enhanced growth inhibition in the acquired trastuzumab and lapatinib SKBR3 cell lines.

mRNA expression of RAR $\alpha$  was examined in the SKBR3-T and SKBR3-L cell lines; however RAR $\alpha$  mRNA is not significantly altered in these cell lines (Table 5-3). RAR $\alpha$  protein expression is also unaltered in these cell lines (Figure 5-11). Thus we see no significant change in the mRNA or protein expression of RAR $\alpha$ . As the expression of RAR $\alpha$  is unaltered it therefore does not account for the ATRA insensitivity observed in the SKBR3-T cell line, we investigated further into predicted targets of miR-9 from miRWalk. RAR $\beta$ , RAR $\gamma$ , RxR $\alpha$  and RxR $\beta$  are listed as predicted targets for miR-9 and cross comparison with the UCLA dataset for the SKBR3-T cell line showed alterations in these proteins (Table 5-5). However RAR $\beta$  (Figure 5-12), RAR $\gamma$  (Figure 5-13) and RxR $\alpha$  (Figure 5-14) protein expression is unaltered in the SKBR3-T and BT-474-Tr cell lines compared to the parental cell lines. Thus none of these receptors account for the difference in sensitivity in the SKBR3-T cell line.

To identify potential alterations that may contribute to the reduced ATRA sensitivity in SKBR3-T cells, we examined the retinoic acid receptor signalling pathway. We identified significantly altered mRNAs in the SKBR3-T and SKBR3-L cell line

microarrays (Table 8-1). There were overlapping targets between the cell lines; however we did not identify any unique targets that were altered in the SKBR3-T cell line compared to the SKBR3-L cell line that could account for the difference in ATRA sensitivities.

**Table 8-1:** Significantly altered genes of the retinoic acid receptor pathway in the SKBR3-T and SKBR3-L cell line microarray data.

SKBR3-T microarray			SKBR3-L microarray		
Gene Name	Fold Change	p-value	Gene Name	Fold Change	p-value
RARA	2.0	7.09E-06	PRAME	3.3	2.06E-11
CDKN1A	1.6	0.00003	PPARG	2.6	1.15E-17
RARA	1.5	0.00532	PRAME	2.0	0.00001
AKR1B1	-1.5	0.00609	RARA	1.8	0.00011
AKR1B10	-1.9	0.00004	RARG	1.6	0.00086
AKR1B10	-2.3	1.93E-07	CDKN1A	1.5	0.00012
CRABP2	-2.3	2.09E-07	RXRΒ	1.5	0.00349
RARA	-2.8	2.13E-09	RARA	-1.5	0.01031
			AKR1B1	-1.6	0.00154
			RARRES3	-2.0	9.65E-06
			STRA8	-2.0	0.00001
			RXRA	-2.2	7.18E-07
			AKR1B10	-3.0	3.22E-10
			AKR1B10	-3.5	6.43E-12
			CRABP2	-4.0	3.62E-13

### 8.5.2 *ATRA response, estrogen receptor status and RAR $\alpha$ amplification*

ATRA resistance has been previously linked with lack of ER $\alpha$  expression and low expression of RARs [355, 356]. This is supported by Rishi *et al.* who discovered that RAR $\alpha$  is significantly increased in ER positive cell lines [357]. In the cell lines we have tested, the SKBR3 and HCC-1954 cell lines are ER negative and show different sensitivities to ATRA inhibition. Details of the cell lines examined in this study regarding their origin, receptor status and sensitivities to the drugs tested are provided in Table 8-2. The SKBR3-P and SKBR3-L cell line are sensitive to ATRA inhibition alone. The HCC-1954 and HCC-1954-L cells are ER negative and ATRA resistant. The BT-474 and EFM-192A cells are ER positive and resistant to ATRA inhibition. This disagrees with the findings of van der Leede *et al.* regarding the association between ER status and ATRA sensitivity [356].

Examination of HER2 and RARA co-amplification, in 5 ER negative and 5 ER positive cell lines showed that all cell lines with HER2 over-expression showed amplification of RAR $\alpha$  [344]. All ER positive cell lines contained more RAR $\alpha$  than the ER negative cell lines and SKBR3 was the only ER negative cell line that has HER2/RAR $\alpha$  co-amplification. This agrees with the findings that SKBR3 cell lines are more sensitive to ATRA inhibition than the BT474 cells. Alsafadi *et al.*, determined the SKBR3 cell lines as HER2 and RAR $\alpha$  co-amplified and the BT-474 cell line as HER2 amplified and RAR $\alpha$  non-amplified [345]. The SKBR3 cell line was more sensitive to ATRA inhibition than the BT-474 cell line, which is consistent with our results. The HCC-1954 cell line is also RAR $\alpha$  non-amplified and was insensitive to ATRA inhibition alone or combined treatments. The EFM-192A cell line, which was moderately sensitive to ATRA inhibition is also RAR $\alpha$  amplified which suggests the differences in sensitivities

could be due to differences in co-amplification of RAR $\alpha$  in our cell lines. This co-amplification warrant further investigation in our resistant cell line models.

**Table 8-2:** Summary of cell lines used in this study. The origin of tissue, cancer type, receptor and RARA amplification status ( $\pm$ ) and sensitivity (S), moderate sensitivity (M) or resistance (R) to trastuzumab (trast), lapatinib (lap) and all-trans retinoic acid (ATRA) and enhancement ( $\pm$ ) with combined treatment is detailed.

Cell line	Original tissue	Cancer type	HER2 status	ER/PR status	p53 status	RARA amplification	Trast	Lap	ATRA	ATRA + Trast	ATRA + Lap
SKBR3							S	S	S	+	+
SKBR3-T	Pleural effusion	Metastatic invasive ductal carcinoma	+	-	+	+	R	S	R	+	+
SKBR3-L							R	R	S	+	+
BT474	Primary tumour	Invasive ductal carcinoma	+	+	+	-	S	S	R	-	-
BT-474-Tr							R	S	R	-	-
HCC1954	Primary tumour	Ductal carcinoma	+	-	$\pm$	-	R	S	R	-	-
HCC-1954-L							R	R	R	-	-
EFM192A	Pleural effusion	Invasive ductal carcinoma	+	+	+	+	R	S	M	+	-

Koay *et al.*, examined the levels of apoptosis upon single and combination treatments with trastuzumab and ATRA and determined that only the combination induced apoptosis in the BT-474 cells [358]. However, in the SKBR3 cells apoptosis was induced upon single ATRA treatment and only a small apoptotic induction with the combination treatment. They also investigated the effect of single and combined treatment on the retinoic acid receptors. They identified a small decrease in RAR $\alpha$  in the BT-474 upon ATRA, trastuzumab and combination treatment. They also identified a slight decrease in RAR $\beta$  expression upon trastuzumab and combination treatment. No alterations in RAR $\alpha$  or RAR $\beta$  expression were determined after 24 h trastuzumab treatment in the SKBR3-P and SKBR3-T cell line (Figure 5-15) or in the BT-474-P and BT-474-Tr cell line (Figure 5-16). They also investigated ATRA response in a

trastuzumab resistant BT-474 variant and found these cells were resistant to ATRA growth inhibition alone or in combination with trastuzumab. This agrees with the observations for ATRA alone in the BT-474-Tr cell line, however we did see a significant response in combined treatment with trastuzumab compared to ATRA treatment alone (Figure 5-8).

These results suggest that although miR-9 is up-regulated, expression of retinoic acid receptors is not altered in the resistant cell lines. However, sensitivity to ATRA is significantly reduced in the SKBR3-T cells. Further analysis of signalling pathways altered in response to ATRA in both the SKBR3-P and SKBR3-T would be required to elucidate the mechanism of cross resistance to ATRA alone in the SKBR3-T cells.

However, from a clinical perspective the SKBR3-T cells remain sensitive to combined trastuzumab and ATRA treatment suggesting that this may be a rationale combination to overcome resistance, perhaps in RAR $\alpha$  co-amplified HER2 positive tumours.

### ***8.5.3 miR-221 and -222 expression***

miR-221 and -222 are both up-regulated in both of the acquired trastuzumab resistant cell lines, SKBR3-T (Table 4-3) and BT-474-T (Table 4-5). This up-regulation appears to be specific to acquired trastuzumab resistance as miR-221 is down-regulated and miR-222 is unaltered in the SKBR3-L (Table 4-4) and HCC-1954-L cell lines (Table 4-6).

miR-221 expression has previously been associated with triple negative breast cancer (TNBC) [359]. Nassirpour *et al.* identified that miR-221 is an oncogene and functions in

cell proliferation, apoptosis, cell migration, invasion and tumour progression by its target p27<sup>kip1</sup>. They found that miR-221 expression is down-regulated and p27<sup>kip1</sup> mRNA expression is up-regulated in the SKBR3 cell line compared to normal breast tissue. Upon knockdown of miR-221 in the TNBC, they identified an induction of apoptosis, decrease in proliferation and suppression of tumorigenicity in mice. Li *et al.*, determined that miR-221 and miR-222 promote cellular migration in basal-like breast cancer (BLBC) cells [278]. They focused on this subtype of breast cancer and found that miR-221 and -222 expressions were higher in the highly invasive BLBC compared to non-invasive cell lines. They also determined that miR-221 and -222 inhibition slows down would closure in the three BLBC cell lines.

The role of miR-221 and -222 was investigated in the acquired trastuzumab resistance setting. Initially, transient transductions were carried out to examine the functionality of these miRNAs but they were unsuccessful due to increased growth with the scrambled controls. In collaboration with Dr. Mulrane, stably transduced cell lines were established. The SKBR3-P cell line was used as the model to determine if over-expression of these miRNAs induced resistance to trastuzumab. The morphology of the cell lines after transduction was similar to the non-transduced SKBR3-P (Figure 6-2). Over-expression of the miRNAs does not have any effect on the doubling time of the cell lines, however, upon trastuzumab treatment the doubling times were significantly increased in the SKBR3-P, SKBR3-P-Scrm, SKBR3-P-221 and SKBR3-P-221-222 (Table 6-2). The resistance profile of these cells was examined by proliferation assays and the stably transfected cell lines showed slightly reduced sensitivity to trastuzumab, however this was not a statistically significant difference compared to the SKBR3-P cell

line. Therefore, these results suggest that miR-221 and miR-222 on their own do not cause a resistant phenotype in the SKBR3 cells.

miR-221 and -222 have been previously reported to be involved in migration [278, 360]. Using the wound scratch assay, an increase in migration was observed in the SKBR3-P-Scrm at both 24 and 48 h time points suggesting the stable transduction has an effect (Figure 6-6). Over-expression of miR-221 significantly increased the migration potential at both 24 and 48 h. miR-222 over-expression did not have a significant effect on migration. The co-transfected cell line SKBR3-P-221-222 also showed a significant increase in migration after 48 h (Figure 6-6). No significant effect of miR-222 was observed on migration; however this could be due to the large standard deviations. Migration is an important feature in the ability of cancer cells to spread from the primary tumour and metastasise [361]. Although miR-221 does not appear to confer trastuzumab resistance in 2D proliferation assays, it enhances migration which could contribute to a more aggressive tumour phenotype in breast cancers that progress on trastuzumab. Thus targeting miR-221 or relevant downstream targets may be beneficial to prevent further metastatic spread.

To identify potential targets for miR-221 and -222, a freely accessible microarray data set (n=3) of over-expression of miR-221 and -222 in MCF-7 cells was utilised [279]. Bioinformatic analysis of this data identified a number of potential targets and cross comparison with the SKBR3-T microarray yielded seven potential targets (Table 6-5). Cyclin-dependent kinase inhibitor 1B (CDKN1B/p27<sup>kip1</sup>) was identified and expression was examined in our panel of transfected cell lines. CDKN1B expression was confirmed as significantly down-regulated in the SKBR3-P-222 and SKBR3-P-221-222

cell lines (Figure 6-8). This miRNA:mRNA interaction is also supported by a previous study that identified this relationship by sequence alignment (Figure 8-1) and luciferase reporter assay [278]. This study also led to the investigation of expression in suppressor of cytokine signalling (SOCS1) as they also confirmed direct target interaction with miR-221 and -222. However, no differences in SOCS1 expression were observed in our stable cell lines (Figure 6-9).

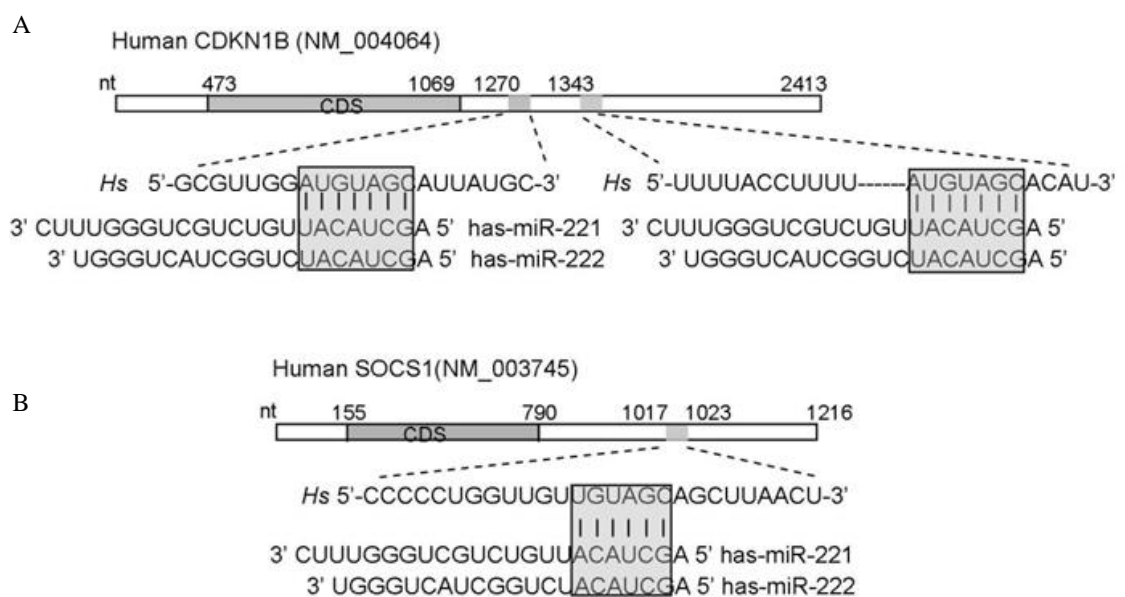


**Figure 8-1:** The binding sites of miR-221 and -222 seed sequences in (A) CDKN1B and (B) SOCS1 3' UTR [278].

p27<sup>kip1</sup> is a cell cycle regulator and can exert its function by halting the G1 phase progression [362]. It has been previously shown that knockdown of miR-221 has the ability to increase the levels of p27<sup>kip1</sup> and cause a subsequent increase in apoptosis in hepatocellular carcinoma [363]. HER2 over-expression in breast tumours correlated with low levels of p27<sup>kip1</sup> [364]. HER2 exerts its suppressive abilities on p27<sup>kip1</sup> through enhanced degradation of p27<sup>kip1</sup> by the Grb2/MAPK pathway [365]. Nahta *et al.*, have

previously reported that decreased levels of p27<sup>kip1</sup> are associated with trastuzumab resistance [290]. More recently, knockdown of a p27 phosphatase; protein phosphatase, Mg<sup>2+</sup>/Mn<sup>2+</sup> dependent, 1H (PPM1H) confers resistance to trastuzumab by decreasing levels of p27<sup>kip1</sup>[366]. Lee-Hoeflich *et al.* also determined that in HER2 positive tumours low levels of PPM1H is a poor prognostic marker in this subtype treated with trastuzumab. In the miR-221 and -222 over-expressing SKBR3-T cell line, p27<sup>kip1</sup> mRNA expression is down-regulated (-1.5, p=0.06). miR-221 and -222 mediated down-regulation of p27<sup>kip1</sup> levels may occur in trastuzumab resistant cells, although the fact that trastuzumab resistance is not induced in the 221/222 transfected cells suggests that down-regulation of p27<sup>kip1</sup> does not play a causative role in the development of resistance, at least in this cell line model.

#### ***8.5.4 miR-221 and -222 expression and 'stemness'***

As miR-221 and -222 have previously been implicated in cancer stem cells [367], the mammosphere assay was used to investigate the stem cell potential of our cell lines. Mammosphere forming efficiency (MFE) is an important property of cancer stem cells that possess tumour regeneration properties [368]. The stemness potential of the SKBR3-P, SKBR3-T and the stably transfected cell lines was investigated. Unfortunately, the SKBR3-L cell lines were not tested due to difficulties encountered with the stability of the resistant phenotype. There were no significant differences in the MFE of the SKBR3-T cell line compared to its parental (Figure 6-10). Over-expression of miR-221 significantly increased the MFE of the SKBR3-P cell line (Figure 6-10). We also investigated the effect of trastuzumab and lapatinib treatment on the MFE. Lapatinib (50 nM) treatment on the SKBR3-T mammospheres significantly decreased the MFE of this cell line (Figure 6-11). Trastuzumab treatment had no effect on the MFE of any of

the cell lines tested. This appears to suggest that trastuzumab is unable to block mammosphere formation. The fold change of miR-221 in the SKBR3-T cells is lower than the over-expression levels achieved in the SKBR3-P-221 cell line. This may account for the lack of an increase in MFE in the SKBR3-T cells. Also, as the SKBR3 cell lines are mostly a homogenous population, it is perhaps difficult to identify putative cancer stem cells in an *in vitro* situation.

Breast cancer stem cells (BCSCs) have been characterised by the expression of stem cell surface markers CD44, epithelial surface antigen (ESA), epithelial cell adhesion molecule (EpCAM) and integrin subunit  $\alpha 6$  (CD49f) and the absence of CD24 (Figure 8-2A). Liu *et al.*, described two stem cell states that breast cancer stem cells can exist in. Firstly an epithelial to mesenchymal transition (EMT)-like state which is characterised by CD24-/CD44+ expression and secondly a mesenchymal to epithelial transition (MET)-like state which is ALDH positive. EMT is characterised by a loss of E-cadherin, increased expression of transcription factors; slug, snail and twist and an increase in mesenchymal proteins such as vimentin [369]. EMT is a key player in cell metastasis and invasion of breast cancer [370]. Liu *et al.* proposed that the two stem cell states are inter-convertible and this is regulated by miRNA expression (Figure 8-2 B). Interestingly, miR-221 and miR-9 are suggested to induce the EMT-like stem cell state in association with miR-100 and miR-155. With regard to the trastuzumab acquired resistant cell line, miR-9 and miR-221 expression is up-regulated which could suggest the acquired cells are driven toward a more EMT stem cell state. The SKBR3-P cell line may be driven towards a MET-stem cell state due to the high levels of ALDH+ cells. Potentially, the driver behind acquired trastuzumab resistance is a shift towards an EMT stem cell state. This would also suggest the SKBR3-T cell line should be more

migratory and invasive. In our assays they showed enhanced migration but not invasion (Figure 3-5). To investigate this hypothesis further, future work involving other markers of the EMT and MET-like stem cell phenotypes would need to be explored in these cells lines.

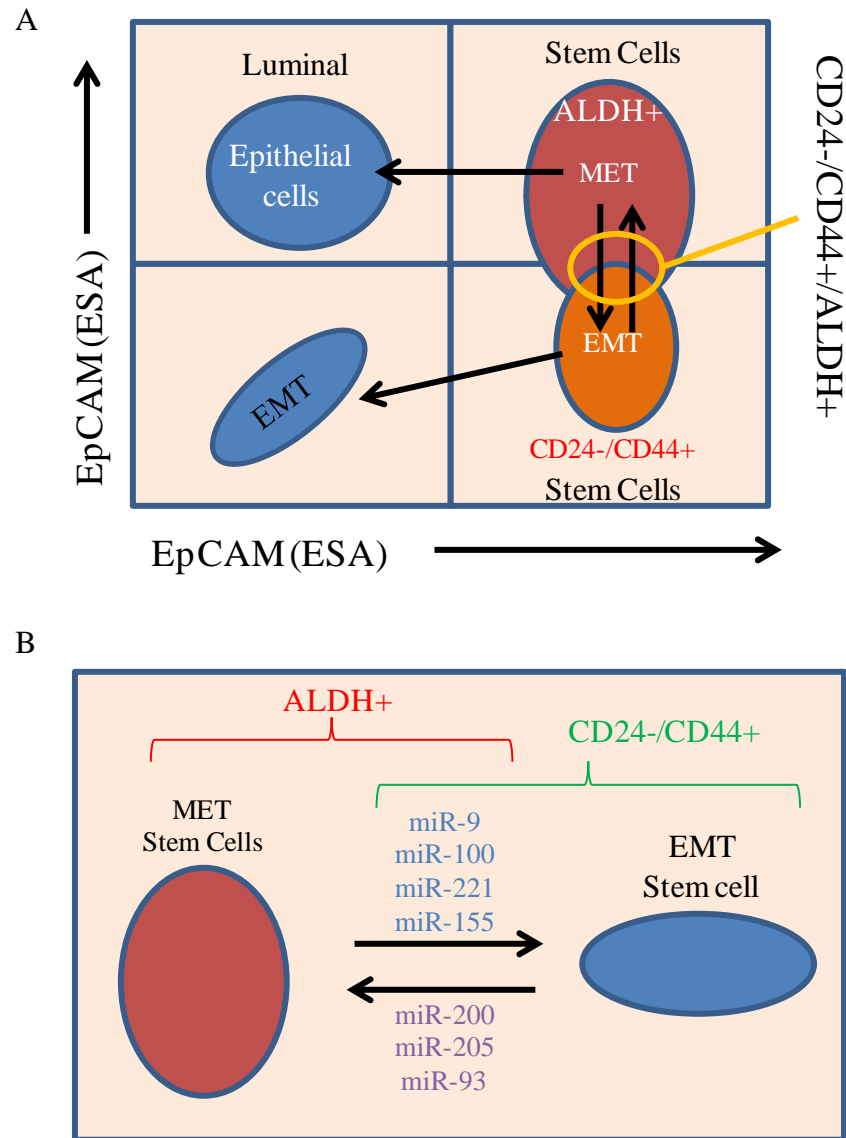


**Figure 8-2:** Illustration of two stem cell states breast cancer stem cells (BCSC) can exist in. (A) BCSC EMT-like state which is EpCAM-CD49f+ and CD24-/CD44+ and a MET-like state which is EpCAM+ and ALDH+ (B) The two stem cell states are interconvertible which are governed by miRNA expression; miR-9,-100,-221 and -155 can promote EMT-like stem cells and miR-200, -205 and -93 can induce MET-like stem cells [367].

## **8.6. Summary and conclusions**

miRNA expression is altered within the acquired trastuzumab and lapatinib resistant cell lines. We identified a miRNA profile of increased miR-221 and -222 expression with decreased miR-224 expression is associated with acquired trastuzumab resistance. Altered miR-9 expression is relevant to both acquired trastuzumab and lapatinib resistance in the SKBR3-T, SKBR3-L and HCC-1954-L cell line models. The miRNA profile of decreased miR-221 and -224 expression with increase miR-9 expression is associated with acquired lapatinib resistance. These miRNAs may be used as predictive markers of resistance. Elevated expression of miR-221 and decreased expression of miR-224 is also associated with innate trastuzumab resistance and could be potentially used as predictive biomarkers of response to trastuzumab. Through analysis of potential targets of miR-9, we identified that ATRA treatment enhances response to trastuzumab treatment and overcomes trastuzumab resistance in selected HER2 positive breast cancer cell lines. RAR $\alpha$  co-amplification may be a potential predictive biomarker of response to ATRA to identify the patients who might benefit from this combination treatment. Preliminary analysis of the miRNAs identified in the cell line models of resistance, in patient samples, suggest that they may have potential as biomarkers of resistance in HER2 positive tumours or as circulating biomarkers in serum specimens.

## **Chapter Nine**

### **Bibliography**

1. Rudden, R.W., *Cancer Biology*. 4th edn ed2007: Oxford University Press (NY).
2. *Breast Cancer Home Page - National Cancer Institute*. 2010; Information about breast cancer treatment, prevention, genetics, causes, screening, clinical trials, research and statistics from the National Cancer Institute.]. Available from: <http://www.cancer.gov/>.
3. Ireland, T.N.C.R., *Cancer in Ireland 1994-2012: Annual Report of the National Cancer Registry*, 2014.
4. Staff, M.C. *Risk Factors*. Diseases and Conditions: Breast cancer 2014; Available from: <http://www.mayoclinic.org/diseases-conditions/breast-cancer/basics/risk-factors/con-20029275>.
5. Polyak, K., *Breast cancer: origins and evolution*. J Clin Invest, 2007. **117**(11): p. 3155-63.
6. *What is cancer?* 22/04/2010 26/10/10]; Available from: <http://www.cancer.ie/cancerInfo/whatis.php>.
7. Pusztai, L., et al., *Molecular classification of breast cancer: limitations and potential*. Oncologist, 2006. **11**(8): p. 868-77.
8. Ellis, P., *Invasive breast carcinoma*, in *WHO classification of tumours pathology and genetics of tumours of the breast and female genital organs* 2003, Lyon Press, Lyon.
9. Perou, C.M., et al., *Molecular portraits of human breast tumours*. Nature, 2000. **406**(6797): p. 747-52.
10. Sorlie, T., et al., *Gene expression patterns of breast carcinomas distinguish tumor subclasses with clinical implications*. Proc Natl Acad Sci U S A, 2001. **98**(19): p. 10869-74.
11. Sotiriou, C. and L. Pusztai, *Gene-expression signatures in breast cancer*. N Engl J Med, 2009. **360**(8): p. 790-800.
12. Schneider, B.P., et al., *Triple-negative breast cancer: risk factors to potential targets*. Clin Cancer Res, 2008. **14**(24): p. 8010-8.
13. Perou, C.M. and A.L. Borresen-Dale, *Systems Biology and Genomics of Breast Cancer*. Cold Spring Harb Perspect Biol.
14. Borresen, A.L., et al., *TP53 mutations and breast cancer prognosis: particularly poor survival rates for cases with mutations in the zinc-binding domains*. Genes Chromosomes Cancer, 1995. **14**(1): p. 71-5.
15. Gauthier, M.L., et al., *Abrogated response to cellular stress identifies DCIS associated with subsequent tumor events and defines basal-like breast tumors*. Cancer Cell, 2007. **12**(5): p. 479-91.
16. Foulkes, W.D., et al., *Germline BRCA1 mutations and a basal epithelial phenotype in breast cancer*. J Natl Cancer Inst, 2003. **95**(19): p. 1482-5.
17. Venkitaraman, A.R., *Cancer susceptibility and the functions of BRCA1 and BRCA2*. Cell, 2002. **108**(2): p. 171-82.
18. Peppercorn, J., C.M. Perou, and L.A. Carey, *Molecular subtypes in breast cancer evaluation and management: divide and conquer*. Cancer Invest, 2008. **26**(1): p. 1-10.
19. Taylor-Papadimitriou, J., et al., *Keratin expression in human mammary epithelial cells cultured from normal and malignant tissue: relation to in vivo phenotypes and influence of medium*. J Cell Sci, 1989. **94** ( Pt 3): p. 403-13.
20. Sorlie, T., et al., *Gene expression patterns of breast carcinomas distinguish tumor subclasses with clinical implications*. Proc Natl Acad Sci USA, 2001. **98**: p. 10869 - 10874.

21. Dollinger, M.R., E., Tempero, M., *Everyone's guide to cancer therapy: how cancer is diagnosed, treated and managed day to day*. Fifth ed 2008: Andrews McMeel.
22. Lawrence TS, T.H.R., Giaccia A., *Principles of Radiation Oncology*, in *Cancer Principles and Practice of Oncology* 2008, Lippincott Williams and Wilkins.
23. FDA, *Drugs @ FDA Herceptin*. 1998.
24. FDA, *Drugs @ FDA Pertuzumab*. 2012.
25. Vogel, C.L., et al., *Efficacy and Safety of Trastuzumab as a Single Agent in First-Line Treatment of HER2-Overexpressing Metastatic Breast Cancer*. *Journal of Clinical Oncology*, 2002. **20**(3): p. 719-726.
26. Richard Pazdur, M.D.N.C.I. *FDA Approval for Lapatinib Ditosylate*. 2011 25/07/21012]; Available from: <http://www.cancer.gov/cancertopics/druginfo/fda-lapatinib>.
27. Trials.gov, C. *Neratinib AND HER2*. 2012 27/07/2012]; Available from: <http://clinicaltrials.gov/ct2/results?term=Neratinib+AND+HER2>.
28. Trials.gov, C. *Afatinib and HER2*. 2012 27/07/2012]; Available from: <http://clinicaltrials.gov/ct2/results?term=Afatinib+and+HER2>.
29. Ioannou, N., et al., *Anti-tumour activity of afatinib, an irreversible ErbB family blocker, in human pancreatic tumour cells*. *Br J Cancer*, 2011. **105**(10): p. 1554-62.
30. FDA, *FDA approves new treatment for late-stage breast cancer*. 2013.
31. Shih, C., et al., *Transforming genes of carcinomas and neuroblastomas introduced into mouse fibroblasts*. *Nature*, 1981. **290**(5803): p. 261-4.
32. Bargmann, C.I., M.C. Hung, and R.A. Weinberg, *The neu oncogene encodes an epidermal growth factor receptor-related protein*. *Nature*, 1986. **319**(6050): p. 226-30.
33. Schechter, A.L., et al., *The neu oncogene: an erb-B-related gene encoding a 185,000-Mr tumour antigen*. *Nature*, 1984. **312**(5994): p. 513-6.
34. Slamon, D.J., et al., *Human breast cancer: correlation of relapse and survival with amplification of the HER-2/neu oncogene*. *Science*, 1987. **235**(4785): p. 177-82.
35. Slamon, D.J., et al., *Studies of the HER-2/neu proto-oncogene in human breast and ovarian cancer*. *Science*, 1989. **244**(4905): p. 707-12.
36. Pegram, M.D., G. Pauletti, and D.J. Slamon, *HER-2/neu as a predictive marker of response to breast cancer therapy*. *Breast Cancer Res Treat*, 1998. **52**(1-3): p. 65-77.
37. Browne, B.C., et al., *HER-2 signaling and inhibition in breast cancer*. *Curr Cancer Drug Targets*, 2009. **9**(3): p. 419-38.
38. Muthuswamy, S.K., et al., *ErbB2, but not ErbB1, reinitiates proliferation and induces luminal repopulation in epithelial acini*. *Nat Cell Biol*, 2001. **3**(9): p. 785-92.
39. Woods Ignatoski, K.M., et al., *p38MAPK induces cell surface alpha4 integrin downregulation to facilitate erbB-2-mediated invasion*. *Neoplasia*, 2003. **5**(2): p. 128-34.
40. Woods Ignatoski, K.M., et al., *The role of phosphatidylinositol 3'-kinase and its downstream signals in erbB-2-mediated transformation*. *Mol Cancer Res*, 2003. **1**(7): p. 551-60.
41. Kokai, Y., et al., *The role of the neu oncogene product in cell transformation and normal development*. *Princess Takamatsu Symp*, 1988. **19**: p. 45-57.

42. Ullrich, A. and J. Schlessinger, *Signal transduction by receptors with tyrosine kinase activity*. Cell, 1990. **61**(2): p. 203-12.
43. Brennan, P.J., et al., *HER2/neu: mechanisms of dimerization/oligomerization*. Oncogene, 2000. **19**(53): p. 6093-101.
44. Berasain, C., et al., *New molecular targets for hepatocellular carcinoma: the ErbB1 signaling system*. Liver Int, 2007. **27**(2): p. 174-85.
45. Yarden, Y., *The EGFR family and its ligands in human cancer. signalling mechanisms and therapeutic opportunities*. Eur J Cancer, 2001. **37 Suppl 4**: p. S3-8.
46. Fornaro, L., et al., *Anti-HER agents in gastric cancer: from bench to bedside*. Nat Rev Gastroenterol Hepatol, 2011. **8**(7): p. 369-383.
47. Kapeller, R. and L.C. Cantley, *Phosphatidylinositol 3-kinase*. Bioessays, 1994. **16**(8): p. 565-76.
48. Peles, E., et al., *Regulated coupling of the Neu receptor to phosphatidylinositol 3'-kinase and its release by oncogenic activation*. J Biol Chem, 1992. **267**(17): p. 12266-74.
49. Kelly, V., *How growth factors tell the cell to grow*, in *Growth & Cell Cycle Lecture Series 2009*, Trinity College Dublin: Dublin.
50. Ignatoski, K.M.W., et al., *ERBB-2 overexpression confers PI 3[prime] kinase-dependent invasion capacity on human mammary epithelial cells*. Br J Cancer, 2000. **82**(3): p. 666-674.
51. Li, N., et al., *Guanine-nucleotide-releasing factor hSos1 binds to Grb2 and links receptor tyrosine kinases to Ras signalling*. Nature, 1993. **363**(6424): p. 85-8.
52. Lange-Carter, C.A., et al., *A divergence in the MAP kinase regulatory network defined by MEK kinase and Raf*. Science, 1993. **260**(5106): p. 315-9.
53. Pearson, G., et al., *Mitogen-Activated Protein (MAP) Kinase Pathways: Regulation and Physiological Functions*. Endocr Rev, 2001. **22**(2): p. 153-183.
54. Noh, D.Y., S.H. Shin, and S.G. Rhee, *Phosphoinositide-specific phospholipase C and mitogenic signaling*. Biochim Biophys Acta, 1995. **1242**(2): p. 99-113.
55. Koch, C.A., et al., *SH2 and SH3 domains: elements that control interactions of cytoplasmic signaling proteins*. Science, 1991. **252**(5006): p. 668-74.
56. Marmor, M.D., K.B. Skaria, and Y. Yarden, *Signal transduction and oncogenesis by ErbB/HER receptors*. Int J Radiat Oncol Biol Phys, 2004. **58**(3): p. 903-13.
57. Matsumoto, E., et al., *PKC pathway and ERK/MAPK pathway are required for induction of cyclin D1 and p21Waf1 during 12-o-tetradecanoylphorbol 13-acetate-induced differentiation of myeloleukemia cells*. Kobe J Med Sci, 2006. **52**(6): p. 181-94.
58. Citri, A., K.B. Skaria, and Y. Yarden, *The deaf and the dumb: the biology of ErbB-2 and ErbB-3*. Exp Cell Res, 2003. **284**(1): p. 54-65.
59. Eccles, S.A., *The role of c-erbB-2/HER2/neu in breast cancer progression and metastasis*. J Mammary Gland Biol Neoplasia, 2001. **6**(4): p. 393-406.
60. Nahta, R. and F.J. Esteva, *HER-2-targeted therapy: lessons learned and future directions*. Clin Cancer Res, 2003. **9**(14): p. 5078-84.
61. Niehans, G.A., et al., *Stability of HER-2/neu expression over time and at multiple metastatic sites*. J Natl Cancer Inst, 1993. **85**(15): p. 1230-5.
62. O'Brien, N., et al., *HER2 Targeted Monoclonal Antibodies and Tyrosine Kinase Inhibitors in Frontiers in Anti-Cancer Drug Discovery*, Atta-ur-Rahman, Editor 2014, Bentham Science. p. 293-382.

63. Padhy, L.C., et al., *Identification of a phosphoprotein specifically induced by the transforming DNA of rat neuroblastomas*. Cell, 1982. **28**(4): p. 865-71.
64. Hudziak, R.M., et al., *p185HER2 monoclonal antibody has antiproliferative effects in vitro and sensitizes human breast tumor cells to tumor necrosis factor*. Mol Cell Biol, 1989. **9**(3): p. 1165-72.
65. Fendly, B.M., et al., *Characterization of murine monoclonal antibodies reactive to either the human epidermal growth factor receptor or HER2/neu gene product*. Cancer Res, 1990. **50**(5): p. 1550-8.
66. Sarup, J.C., et al., *Characterization of an anti-p185HER2 monoclonal antibody that stimulates receptor function and inhibits tumor cell growth*. Growth Regul, 1991. **1**(2): p. 72-82.
67. Shepard, H.M. and G.D. Lewis, *Resistance of tumor cells to tumor necrosis factor*. J Clin Immunol, 1988. **8**(5): p. 333-41.
68. Baselga, J. and J. Mendelsohn, *Receptor blockade with monoclonal antibodies as anti-cancer therapy*. Pharmacol Ther, 1994. **64**(1): p. 127-54.
69. Miller, R.A., et al., *Monoclonal antibody therapeutic trials in seven patients with T-cell lymphoma*. Blood, 1983. **62**(5): p. 988-95.
70. Carter, P., et al., *Humanization of an anti-p185HER2 antibody for human cancer therapy*. Proc Natl Acad Sci U S A, 1992. **89**(10): p. 4285-9.
71. Harries, M. and I. Smith, *The development and clinical use of trastuzumab (Herceptin)*. Endocr Relat Cancer, 2002. **9**(2): p. 75-85.
72. Slamon, D.J., et al., *Use of chemotherapy plus a monoclonal antibody against HER2 for metastatic breast cancer that overexpresses HER2*. N Engl J Med, 2001. **344**(11): p. 783-92.
73. Romond, E.H., et al., *Trastuzumab plus adjuvant chemotherapy for operable HER2-positive breast cancer*. N Engl J Med, 2005. **353**(16): p. 1673-84.
74. Roche. [cited 2013; Herceptin Product Information]. Available from: <http://www.roche-australia.com/fmfiles/re7229005/downloads/oncology/herceptin-pi.pdf>.
75. Hudis, C.A., *Trastuzumab--mechanism of action and use in clinical practice*. N Engl J Med, 2007. **357**(1): p. 39-51.
76. Ross, J.S., et al., *Targeted therapy in breast cancer: the HER-2/neu gene and protein*. Mol Cell Proteomics, 2004. **3**(4): p. 379-98.
77. De Santes, K., et al., *Radiolabeled antibody targeting of the HER-2/neu oncoprotein*. Cancer Res, 1992. **52**(7): p. 1916-23.
78. Klapper, L.N., et al., *Tumor-inhibitory antibodies to HER-2/ErbB-2 may act by recruiting c-Cbl and enhancing ubiquitination of HER-2*. Cancer Res, 2000. **60**(13): p. 3384-8.
79. Christianson, T.A., et al., *NH2-terminally Truncated HER-2/neu Protein: Relationship with Shedding of the Extracellular Domain and with Prognostic Factors in Breast Cancer*. Cancer Research, 1998. **58**(22): p. 5123-5129.
80. Molina, M.A., et al., *Trastuzumab (herceptin), a humanized anti-Her2 receptor monoclonal antibody, inhibits basal and activated Her2 ectodomain cleavage in breast cancer cells*. Cancer Res, 2001. **61**(12): p. 4744-9.
81. Fornier, M.N., et al., *Serum HER2 extracellular domain in metastatic breast cancer patients treated with weekly trastuzumab and paclitaxel: association with HER2 status by immunohistochemistry and fluorescence in situ hybridization and with response rate*. Ann Oncol, 2005. **16**(2): p. 234-9.

82. Kostler, W.J., et al., *Monitoring of serum Her-2/neu predicts response and progression-free survival to trastuzumab-based treatment in patients with metastatic breast cancer*. Clin Cancer Res, 2004. **10**(5): p. 1618-24.
83. Junttila, T.T., et al., *Ligand-independent HER2/HER3/PI3K complex is disrupted by trastuzumab and is effectively inhibited by the PI3K inhibitor GDC-0941*. Cancer cell, 2009. **15**(5): p. 429-40.
84. Delord, J.P., et al., *Selective inhibition of HER2 inhibits AKT signal transduction and prolongs disease-free survival in a micrometastasis model of ovarian carcinoma*. Ann Oncol, 2005. **16**(12): p. 1889-97.
85. Nagata, Y., et al., *PTEN activation contributes to tumor inhibition by trastuzumab, and loss of PTEN predicts trastuzumab resistance in patients*. Cancer cell, 2004. **6**(2): p. 117-127.
86. Lane, H.A., et al., *Modulation of p27/Cdk2 complex formation through 4D5-mediated inhibition of HER2 receptor signaling*. Ann Oncol, 2001. **12 Suppl 1**: p. S21-2.
87. Le, X.F., et al., *The role of cyclin-dependent kinase inhibitor p27Kip1 in anti-HER2 antibody-induced G1 cell cycle arrest and tumor growth inhibition*. J Biol Chem, 2003. **278**(26): p. 23441-50.
88. Varchetta, S., et al., *Elements related to heterogeneity of antibody-dependent cell cytotoxicity in patients under trastuzumab therapy for primary operable breast cancer overexpressing Her2*. Cancer Res, 2007. **67**(24): p. 11991-9.
89. Clynes, R.A., et al., *Inhibitory Fc receptors modulate in vivo cytotoxicity against tumor targets*. Nat Med, 2000. **6**(4): p. 443-6.
90. Beano, A., et al., *Correlation between NK function and response to trastuzumab in metastatic breast cancer patients*. J Transl Med, 2008. **6**: p. 25.
91. Cuello, M., et al., *Down-Regulation of the erbB-2 Receptor by Trastuzumab (Herceptin) Enhances Tumor Necrosis Factor-related Apoptosis-inducing Ligand-mediated Apoptosis in Breast and Ovarian Cancer Cell Lines that Overexpress erbB-2*. Cancer Research, 2001. **61**(12): p. 4892-4900.
92. Dubska, L., L. Andera, and M.A. Sheard, *HER2 signaling downregulation by trastuzumab and suppression of the PI3K/Akt pathway: an unexpected effect on TRAIL-induced apoptosis*. FEBS Lett, 2005. **579**(19): p. 4149-58.
93. Pegram, M.D., et al., *Rational combinations of trastuzumab with chemotherapeutic drugs used in the treatment of breast cancer*. J Natl Cancer Inst, 2004. **96**(10): p. 739-49.
94. Yen, L., et al., *Heregulin selectively upregulates vascular endothelial growth factor secretion in cancer cells and stimulates angiogenesis*. Oncogene, 2000. **19**(31): p. 3460-9.
95. Izumi, Y., et al., *Tumour biology: herceptin acts as an anti-angiogenic cocktail*. Nature, 2002. **416**(6878): p. 279-80.
96. Epstein M , A.R., Tchekmedyan N , et al. , *HER2-overexpressing human breast cancer xenografts exhibit increased angiogenic potential mediated by vascular endothelial growth factor (VEGF)* Breast Cancer Res Treat, 2002. **76**(S143 Abstract 570).
97. Klos, K.S., et al., *Combined trastuzumab and paclitaxel treatment better inhibits ErbB-2-mediated angiogenesis in breast carcinoma through a more effective inhibition of Akt than either treatment alone*. Cancer, 2003. **98**(7): p. 1377-1385.
98. Wen, X.F., et al., *HER2 signaling modulates the equilibrium between pro- and antiangiogenic factors via distinct pathways: implications for HER2-targeted antibody therapy*. Oncogene, 2006. **25**(52): p. 6986-6996.

99. Nahta, R., *Molecular Mechanisms of Trastuzumab-Based Treatment in HER2-Overexpressing Breast Cancer*. ISRN Oncol, 2012. **2012**: p. 428062.
100. Baselga, J., et al., *Mechanism of action of trastuzumab and scientific update*. Semin Oncol, 2001. **28**(5 Suppl 16): p. 4-11.
101. Gullo, G., et al., *Durable complete response following chemotherapy and trastuzumab for metastatic HER2-positive breast cancer*. Annals of Oncology, 2012.
102. Nahta, R. and F.J. Esteva, *Trastuzumab: triumphs and tribulations*. Oncogene. **26**(25): p. 3637-3643.
103. O'Brien, N.A., et al., *Activated Phosphoinositide 3-Kinase/AKT Signaling Confers Resistance to Trastuzumab but not Lapatinib*. Molecular Cancer Therapeutics, 2010. **9**(6): p. 1489-1502.
104. Browne, B.C., et al., *Inhibition of IGF1R activity enhances response to trastuzumab in HER-2-positive breast cancer cells*. Ann Oncol, 2011. **22**(1): p. 68-73.
105. Shattuck, D.L., et al., *Met receptor contributes to trastuzumab resistance of Her2-overexpressing breast cancer cells*. Cancer Res, 2008. **68**(5): p. 1471-7.
106. Saez, R., et al., *p95HER-2 predicts worse outcome in patients with HER-2-positive breast cancer*. Clin Cancer Res, 2006. **12**(2): p. 424-31.
107. Molina, M.A., et al., *NH(2)-terminal truncated HER-2 protein but not full-length receptor is associated with nodal metastasis in human breast cancer*. Clin Cancer Res, 2002. **8**(2): p. 347-53.
108. Nagy, P., et al., *Decreased Accessibility and Lack of Activation of ErbB2 in JIMT-1, a Herceptin-Resistant, MUC4-Expressing Breast Cancer Cell Line*. Cancer Research, 2005. **65**(2): p. 473-482.
109. Citri, A., B.S. Kochupurakkal, and Y. Yarden, *The achilles heel of ErbB-2/HER2: regulation by the Hsp90 chaperone machine and potential for pharmacological intervention*. Cell Cycle, 2004. **3**(1): p. 51-60.
110. Huober J, L.S., Untch M, Darb-Esfahani S, Solbach C, Tesch H, Holms F, Fehm T, von Minckwitz G, Mehta K, and Denkert C. *New Molecular Biomarkers for Resistance to Trastuzumab in Primary HER2 Positive Breast Cancer — A Translational Investigation from the Neoadjuvant GeparQuattro Study*. in *Thirty-Third Annual CTRC-AACR San Antonio Breast Cancer Symposium*. 2010. San Antonio.
111. Ross, J.S., et al., *The HER-2 receptor and breast cancer: ten years of targeted anti-HER-2 therapy and personalized medicine*. Oncologist, 2009. **14**(4): p. 320-68.
112. Thery, J.-C., et al., *Resistance to human epidermal growth factor receptor type 2-targeted therapies*. European Journal of Cancer, (0).
113. Rani, S., et al., *Neuromedin U: a candidate biomarker and therapeutic target to predict and overcome resistance to HER-tyrosine kinase inhibitors*. Cancer Res, 2014. **74**(14): p. 3821-33.
114. Rusnak, D. and T.M. Gilmer, *The Discovery of Lapatinib (GW572016)*. Molecular Cancer Therapeutics, 2011. **10**(11): p. 2019.
115. Moy, B., et al., *Lapatinib*. Nat Rev Drug Discov, 2007. **6**(6): p. 431-432.
116. Nielsen, D.L., M. Andersson, and C. Kamby, *HER2-targeted therapy in breast cancer. Monoclonal antibodies and tyrosine kinase inhibitors*. Cancer Treat Rev, 2009. **35**(2): p. 121-36.

117. Burris, H.A., 3rd, *Dual kinase inhibition in the treatment of breast cancer: initial experience with the EGFR/ErbB-2 inhibitor lapatinib*. *Oncologist*, 2004. **9 Suppl 3**: p. 10-5.
118. Gril, B., et al., *Effect of lapatinib on the outgrowth of metastatic breast cancer cells to the brain*. *J Natl Cancer Inst*, 2008. **100**(15): p. 1092-103.
119. Pubchem. *Lapatinib*. Compound Summary for CID 208908]. Available from: <http://pubchem.ncbi.nlm.nih.gov/compound/Lapatinib#section=Top>.
120. Opdam, F.L., et al., *Lapatinib for Advanced or Metastatic Breast Cancer*. *The Oncologist*, 2012. **17**(4): p. 536-542.
121. Moy, B. and P.E. Goss, *Lapatinib: Current Status and Future Directions in Breast Cancer*. *Oncologist*, 2006. **11**(10): p. 1047-1057.
122. Xia, W., et al., *Anti-tumor activity of GW572016: a dual tyrosine kinase inhibitor blocks EGF activation of EGFR/erbB2 and downstream Erk1/2 and AKT pathways*. Vol. 21. 2002, Basingstoke, ROYAUME-UNI: Nature Publishing Group.
123. Konecny, G.E., et al., *Activity of the Dual Kinase Inhibitor Lapatinib (GW572016) against HER-2-Overexpressing and Trastuzumab-Treated Breast Cancer Cells*. *Cancer Research*, 2006. **66**(3): p. 1630-1639.
124. Xia, W., et al., *Anti-tumor activity of GW572016: a dual tyrosine kinase inhibitor blocks EGF activation of EGFR/erbB2 and downstream Erk1/2 and AKT pathways*. *Oncogene*, 2002. **21**(41): p. 6255-63.
125. Burris, H.A., 3rd, et al., *Phase I safety, pharmacokinetics, and clinical activity study of lapatinib (GW572016), a reversible dual inhibitor of epidermal growth factor receptor tyrosine kinases, in heavily pretreated patients with metastatic carcinomas*. *J Clin Oncol*, 2005. **23**(23): p. 5305-13.
126. Hegde, P.S., et al., *Delineation of molecular mechanisms of sensitivity to lapatinib in breast cancer cell lines using global gene expression profiles*. *Mol Cancer Ther*, 2007. **6**(5): p. 1629-40.
127. Xia, W., et al., *Regulation of survivin by ErbB2 signaling: therapeutic implications for ErbB2-overexpressing breast cancers*. *Cancer Res*, 2006. **66**(3): p. 1640-7.
128. Altieri, D.C., *Survivin, cancer networks and pathway-directed drug discovery*. *Nat Rev Cancer*, 2008. **8**(1): p. 61-70.
129. Tanizaki, J., et al., *Roles of BIM induction and survivin downregulation in lapatinib-induced apoptosis in breast cancer cells with HER2 amplification*. *Oncogene*, 2011. **30**(39): p. 4097-106.
130. Mitchell, C., et al., *Inhibition of MCL-1 in breast cancer cells promotes cell death in vitro and in vivo*. *Cancer Biol Ther*, 2010. **10**(9): p. 903-17.
131. Huang, H.-L., et al., *Lapatinib Induces Autophagy, Apoptosis and Megakaryocytic Differentiation in Chronic Myelogenous Leukemia K562 Cells*. *PLoS ONE*, 2011. **6**(12): p. e29014.
132. Zhu, X., et al., *Autophagy stimulates apoptosis in HER2-overexpressing breast cancers treated by lapatinib*. *J Cell Biochem*, 2013. **114**(12): p. 2643-53.
133. Gayle, S.S., et al., *Pharmacologic inhibition of mTOR improves lapatinib sensitivity in HER2-overexpressing breast cancer cells with primary trastuzumab resistance*. *Anticancer Agents Med Chem*, 2012. **12**(2): p. 151-62.
134. Xu, J., J. Ji, and X.H. Yan, *Cross-talk between AMPK and mTOR in regulating energy balance*. *Crit Rev Food Sci Nutr*, 2012. **52**(5): p. 373-81.
135. Shell, S.A., et al., *Activation of AMPK is necessary for killing cancer cells and sparing cardiac cells*. *Cell Cycle*, 2008. **7**(12): p. 1769-75.

136. Konecny, G.E., et al., *Activity of the dual kinase inhibitor lapatinib (GW572016) against HER-2-overexpressing and trastuzumab-treated breast cancer cells.* Cancer Res, 2006. **66**(3): p. 1630-9.
137. Blackwell, K.L., et al., *Randomized study of Lapatinib alone or in combination with trastuzumab in women with ErbB2-positive, trastuzumab-refractory metastatic breast cancer.* J Clin Oncol, 2010. **28**(7): p. 1124-30.
138. Blackwell, K.L., et al., *Overall survival benefit with lapatinib in combination with trastuzumab for patients with human epidermal growth factor receptor 2-positive metastatic breast cancer: final results from the EGF104900 Study.* J Clin Oncol, 2012. **30**(21): p. 2585-92.
139. O'Donovan, N., et al., *Synergistic interaction between trastuzumab and EGFR/HER-2 tyrosine kinase inhibitors in HER-2 positive breast cancer cells.* Invest New Drugs, 2011. **29**(5): p. 752-9.
140. Martine J. Piccart-Gebhart, A.P.H., Jose Baselga, Evandro De Azambuja, Amylou C. Dueck, Giuseppe Viale, Jo Anne Zujewski, Aron Goldhirsch, Sergio Santillana, Kathleen I. Pritchard, Antonio C. Wolff, Christian Jackisch, Istvan Lang, Michael Untch, Ian E. Smith, Frances Boyle, Binghe Xu, Henry Leonidas Gomez, Richard D. Gelber, Edith A. Perez;. *First results from the phase III ALTO trial (BIG 2-06; NCCTG [Alliance] N063D) comparing one year of anti-HER2 therapy with lapatinib alone (L), trastuzumab alone (T), their sequence (T→L), or their combination (T+L) in the adjuvant treatment of HER2-positive early breast cancer (EBC).* in ASCO. 2014. J Clin Oncol.
141. Baselga, J., et al., *Lapatinib with trastuzumab for HER2-positive early breast cancer (NeoALTTO): a randomised, open-label, multicentre, phase 3 trial.* Lancet, 2012. **379**(9816): p. 633-40.
142. Untch, M., et al., *Pathologic Complete Response After Neoadjuvant Chemotherapy Plus Trastuzumab Predicts Favorable Survival in Human Epidermal Growth Factor Receptor 2-Overexpressing Breast Cancer: Results From the TECHNO Trial of the AGO and GBG Study Groups.* Journal of Clinical Oncology, 2011.
143. Guarneri, V., et al., *Preoperative chemotherapy plus trastuzumab, lapatinib, or both in human epidermal growth factor receptor 2-positive operable breast cancer: results of the randomized phase II CHER-LOB study.* J Clin Oncol, 2012. **30**(16): p. 1989-95.
144. Robidoux, A., et al., *Lapatinib as a component of neoadjuvant therapy for HER2-positive operable breast cancer (NSABP protocol B-41): an open-label, randomised phase 3 trial.* Lancet Oncol, 2013. **14**(12): p. 1183-92.
145. Liu, L., et al., *Novel mechanism of lapatinib resistance in HER2-positive breast tumor cells: activation of AXL.* Cancer Res, 2009. **69**(17): p. 6871-8.
146. Chen, S., et al., *Autophagy facilitates the Lapatinib resistance of HER2 positive breast cancer cells.* Med Hypotheses, 2011. **77**(2): p. 206-8.
147. Martin, A.P., et al., *Inhibition of MCL-1 enhances lapatinib toxicity and overcomes lapatinib resistance via BAK-dependent autophagy.* Cancer Biol Ther, 2009. **8**(21): p. 2084-96.
148. Xia, W., et al., *A model of acquired autoresistance to a potent ErbB2 tyrosine kinase inhibitor and a therapeutic strategy to prevent its onset in breast cancer.* Proc Natl Acad Sci U S A, 2006. **103**(20): p. 7795-800.
149. Aird, K.M., et al., *X-linked inhibitor of apoptosis protein inhibits apoptosis in inflammatory breast cancer cells with acquired resistance to an ErbB1/2 tyrosine kinase inhibitor.* Mol Cancer Ther, 2010. **9**(5): p. 1432-42.

150. Rexer, B.N., et al., *Phosphoproteomic mass spectrometry profiling links Src family kinases to escape from HER2 tyrosine kinase inhibition*. *Oncogene*, 2011. **30**(40): p. 4163-4174.
151. Lee, R.C., R.L. Feinbaum, and V. Ambros, *The C. elegans heterochronic gene lin-4 encodes small RNAs with antisense complementarity to lin-14*. *Cell*, 1993. **75**(5): p. 843-854.
152. PILLAI, R.S., *MicroRNA function: Multiple mechanisms for a tiny RNA?* *RNA*, 2005. **11**(12): p. 1753-1761.
153. Bentwich, I., et al., *Identification of hundreds of conserved and nonconserved human microRNAs*. *Nat Genet*, 2005. **37**(7): p. 766-770.
154. Ambros, V., *MicroRNA Pathways in Flies and Worms: Growth, Death, Fat, Stress, and Timing*. *Cell*, 2003. **113**(6): p. 673-676.
155. Bartel, D.P., *MicroRNAs: Genomics, Biogenesis, Mechanism, and Function*. *Cell*, 2004. **116**(2): p. 281-297.
156. Cheng, A.M., et al., *Antisense inhibition of human miRNAs and indications for an involvement of miRNA in cell growth and apoptosis*. *Nucleic Acids Research*, 2005. **33**(4): p. 1290-1297.
157. Jamshidi-Adegani, F., et al., *Mir-302 cluster exhibits tumor suppressor properties on human unrestricted somatic stem cells*. *Tumor Biology*, 2014. **35**(7): p. 6657-6664.
158. He, L., et al., *A microRNA polycistron as a potential human oncogene*. *Nature*, 2005. **435**(7043): p. 828-833.
159. Lu, J., et al., *MicroRNA expression profiles classify human cancers*. *Nature*, 2005. **435**(7043): p. 834-838.
160. Brennecke, J., et al., *Principles of MicroRNA-Target Recognition*. *PLoS Biol*, 2005. **3**(3): p. e85.
161. Ligresti, G., et al., *Breast cancer: Molecular basis and therapeutic strategies (Review)*. *Mol Med Report*, 2008. **1**(4): p. 451-8.
162. Baselga, J. and S.M. Swain, *CLEOPATRA: A Phase III Evaluation of Pertuzumab and Trastuzumab for HER2-Positive Metastatic Breast Cancer*. *Clinical Breast Cancer*, 2010. **10**(6): p. 489-491.
163. Bucci, M.K., A. Bevan, and M. Roach, 3rd, *Advances in radiation therapy: conventional to 3D, to IMRT, to 4D, and beyond*. *CA Cancer J Clin*, 2005. **55**(2): p. 117-34.
164. Borchert, G.M., W. Lanier, and B.L. Davidson, *RNA polymerase III transcribes human microRNAs*. *Nat Struct Mol Biol*, 2006. **13**(12): p. 1097-1101.
165. Kim, V.N., *MicroRNA biogenesis: coordinated cropping and dicing*. *Nat Rev Mol Cell Biol*, 2005. **6**(5): p. 376-385.
166. Lund, E., et al., *Nuclear Export of MicroRNA Precursors*. *Science*, 2004. **303**(5654): p. 95-98.
167. Yi, R., et al., *Exportin-5 mediates the nuclear export of pre-microRNAs and short hairpin RNAs*. *Genes & Development*, 2003. **17**(24): p. 3011-3016.
168. Sontheimer, E.J., *Assembly and function of RNA silencing complexes*. *Nat Rev Mol Cell Biol*, 2005. **6**(2): p. 127-138.
169. Nelson, P.T., A.G. Hatzigeorgiou, and Z. Mourelatos, *miRNP:mRNA association in polyribosomes in a human neuronal cell line*. *RNA*, 2004. **10**(3): p. 387-94.
170. Huntzinger, E. and E. Izaurralde, *Gene silencing by microRNAs: contributions of translational repression and mRNA decay*. *Nat Rev Genet*, 2011. **12**(2): p. 99-110.

171. Wang, Y., et al., *MicroRNA: past and present*. Front Biosci, 2007. **12**: p. 2316-29.
172. Gu, S. and M.A. Kay, *How do miRNAs mediate translational repression?* Silence, 2010. **1**(1): p. 11.
173. Zhang, Y.X., et al., *AXL is a potential target for therapeutic intervention in breast cancer progression*. Cancer Res, 2008. **68**(6): p. 1905-15.
174. Perez, E.A., et al., *Cardiac safety of lapatinib: pooled analysis of 3689 patients enrolled in clinical trials*. Mayo Clin Proc, 2008. **83**(6): p. 679-86.
175. Lee, I., et al., *New class of microRNA targets containing simultaneous 5'-UTR and 3'-UTR interaction sites*. Genome Res, 2009. **19**(7): p. 1175-1183.
176. Zheng, Y., et al., *NGF-induced Tyro3 and Axl function as survival factors for differentiating PC12 cells*. Biochem Biophys Res Commun, 2009. **378**(3): p. 371-5.
177. Shukla, G.C., J. Singh, and S. Barik, *MicroRNAs: Processing, Maturation, Target Recognition and Regulatory Functions*. Mol Cell Pharmacol, 2011. **3**(3): p. 83-92.
178. Meister, G., et al., *Human Argonaute2 Mediates RNA Cleavage Targeted by miRNAs and siRNAs*. Mol Cell, 2004. **15**(2): p. 185-197.
179. Liu, J., et al., *Argonaute2 is the catalytic engine of mammalian RNAi*. Science, 2004. **305**(5689): p. 1437-41.
180. Appasan, K., *MicroRNAs: From Basic Science to Disease Biology* 2008: Cambridge University press.
181. Krol, J., I. Loedige, and W. Filipowicz, *The widespread regulation of microRNA biogenesis, function and decay*. Nat Rev Genet, 2010. **11**(9): p. 597-610.
182. Pillai, R.S., et al., *Inhibition of translational initiation by Let-7 MicroRNA in human cells*. Science, 2005. **309**(5740): p. 1573-6.
183. Morozova, N., et al., *Kinetic signatures of microRNA modes of action*. RNA, 2012. **18**(9): p. 1635-55.
184. Iorio, M.V., et al., *MicroRNA Gene Expression Deregulation in Human Breast Cancer*. Cancer Research, 2005. **65**(16): p. 7065-7070.
185. Moller, H.G., et al., *A systematic review of microRNA in glioblastoma multiforme: micro-modulators in the mesenchymal mode of migration and invasion*. Molecular Neurobiology, 2013. **47**(1): p. 131-44.
186. Lowery, A., et al., *MicroRNA signatures predict oestrogen receptor, progesterone receptor and HER2/neu receptor status in breast cancer*. Breast Cancer Research, 2009. **11**(3): p. R27.
187. Ma, L., J. Teruya-Feldstein, and R. Weinberg, *Tumour invasion and metastasis initiated by microRNA-10b in breast cancer*. Nature, 2007. **449**: p. 682 - 688.
188. Tavazoie, S.F., et al., *Endogenous human microRNAs that suppress breast cancer metastasis*. Nature, 2008. **451**(7175): p. 147-152.
189. Huang, Q., et al., *The microRNAs miR-373 and miR-520c promote tumour invasion and metastasis*. Nat Cell Biol, 2008. **10**(2): p. 202-210.
190. Lu, J., et al., *MicroRNA expression profiles classify human cancers*. Nature, 2005. **435**(7043): p. 834-8.
191. Ganepola, G.A., et al., *Novel blood-based microRNA biomarker panel for early diagnosis of pancreatic cancer*. World J Gastrointest Oncol, 2014. **6**(1): p. 22-33.
192. Zhu, C., et al., *A five-microRNA panel in plasma was identified as potential biomarker for early detection of gastric cancer*. Br J Cancer, 2014. **110**(9): p. 2291-2299.

193. Søren Jensby Nielsen, P.D. *Screening Tool Can Detect Colorectal Cancer from a Small Blood Sample*. 2010 22/12/10]; Available from: <http://www.aacr.org/home/public--media/aacr-press-releases.aspx?d=2068>.
194. Negrini, M. and G. Calin, *Breast cancer metastasis: a microRNA story*. *Breast Cancer Res*, 2008. **10**: p. 203.
195. Tsuda N, K.K., Efferson CL, Ioannides CG., *Synthetic microRNA and double-stranded RNA targeting the 3'-untranslated region of HER-2/neu mRNA inhibit HER-2 protein expression in ovarian cancer cells*. *Int J Oncol*, 2005. **27**(5): p. 1299-306.
196. Gary K. Scott, A.G., Dipa Bhaumik, Crystal E. Berger, Christopher S. Sullivan and Christopher C. Benz *Coordinate Suppression of ERBB2 and ERBB3 by Enforced Expression of Micro-RNA miR-125a or miR-125b*. *Journal of Biological Chemistry*, 2006. **282**: p. 1479-1486.
197. Chen, H., et al., *Preliminary validation of ERBB2 expression regulated by miR-548d-3p and miR-559*. *Biochemical and Biophysical Research Communications*, 2009. **385**(4): p. 596-600.
198. Le, X.F., et al., *Modulation of MicroRNA-194 and Cell Migration by HER2-Targeting Trastuzumab in Breast Cancer*. *PLoS ONE*, 2012. **7**(7): p. e41170.
199. Kim, J., et al., *MicroRNA signature for HER2-positive breast and gastric cancer*. *Anticancer Res*, 2014. **34**(7): p. 3807-10.
200. Newie, I., et al., *The HER2-encoded miR-4728-3p regulates ESR1 through a non-canonical internal seed interaction*. *PLoS ONE*, 2014. **9**(5): p. e97200.
201. Rehman, S.K. *MiR-21 upregulation in breast cancer cells leads to PTEN loss and Herceptin resistance*. 2010 22/12/10]; Available from: [http://www.breastcancer.org/treatment/targeted\\_therapies/new\\_research/201004\\_20.jsp](http://www.breastcancer.org/treatment/targeted_therapies/new_research/201004_20.jsp).
202. Gong, C., et al., *Up-regulation of miR-21 mediates resistance to trastuzumab therapy for breast cancer*. *J Biol Chem*, 2011. **286**(21): p. 19127-37.
203. Tzu-Hsuan Huang, F.W., Gabriel B. Loeb, Ruby Hsu, Amy Heidersbach, Allison Brincat, Dai Horiuchi, Robert J. Lebbink, Yin-Yuan Mo, Andrei Goga and Michael T. McManus, *Up-regulation of miR-21 by HER2/neu Signaling Promotes Cell Invasion*. *Journal of Biological Chemistry*, 2009. **284**: p. 18515-18524.
204. Nielsen, B.S., et al., *miR-21 Expression in Cancer Cells may Not Predict Resistance to Adjuvant Trastuzumab in Primary Breast Cancer*. *Front Oncol*, 2014. **4**: p. 207.
205. Jung, E.J., et al., *Plasma microRNA 210 levels correlate with sensitivity to trastuzumab and tumor presence in breast cancer patients*. *Cancer*, 2012. **118**(10): p. 2603-14.
206. Ye, X.M., et al., *Epigenetic silencing of miR-375 induces trastuzumab resistance in HER2-positive breast cancer by targeting IGF1R*. *BMC Cancer*, 2014. **14**: p. 134.
207. Ye, X., et al., *MiR-221 promotes trastuzumab-resistance and metastasis in HER2-positive breast cancers by targeting PTEN*. *BMB Rep*, 2014. **47**(5): p. 268-73.
208. Bai, W.D., et al., *MiR-200c suppresses TGF-beta signaling and counteracts trastuzumab resistance and metastasis by targeting ZNF217 and ZEB1 in breast cancer*. *Int J Cancer*, 2014. **135**(6): p. 1356-68.
209. Iorio, M.V., et al., *microRNA-205 regulates HER3 in human breast cancer*. *Cancer Res*, 2009. **69**(6): p. 2195-200.

210. Siziopikou, K.P. and M. Cobleigh, *The basal subtype of breast carcinomas may represent the group of breast tumors that could benefit from EGFR-targeted therapies*. *Breast*, 2007. **16**(1): p. 104-7.
211. Finn, R.S., et al., *Estrogen receptor, progesterone receptor, human epidermal growth factor receptor 2 (HER2), and epidermal growth factor receptor expression and benefit from lapatinib in a randomized trial of paclitaxel with lapatinib or placebo as first-line treatment in HER2-negative or unknown metastatic breast cancer*. *J Clin Oncol*, 2009. **27**(24): p. 3908-15.
212. Hsia, T.C., et al., *Lapatinib-mediated cyclooxygenase-2 expression via epidermal growth factor receptor/HuR interaction enhances the aggressiveness of triple-negative breast cancer cells*. *Mol Pharmacol*, 2013. **83**(4): p. 857-69.
213. Corcoran, C., et al., *miR-630 targets IGF1R to regulate response to HER-targeting drugs and overall cancer cell progression in HER2 over-expressing breast cancer*. *Mol Cancer*, 2014. **13**: p. 71.
214. Chen, X., et al., *Characterization of microRNAs in serum: a novel class of biomarkers for diagnosis of cancer and other diseases*. *Cell Res*, 2008. **18**(10): p. 997-1006.
215. Mitchell, P.S., et al., *Circulating microRNAs as stable blood-based markers for cancer detection*. *Proceedings of the National Academy of Sciences*, 2008. **105**(30): p. 10513-10518.
216. Shen, J., S.A. Stass, and F. Jiang, *MicroRNAs as potential biomarkers in human solid tumors*. *Cancer Lett*, 2013. **329**(2): p. 125-36.
217. Sand, M., et al., *Expression levels of the microRNA maturing microprocessor complex component DGCR8 and the RNA-induced silencing complex (RISC) components argonaute-1, argonaute-2, PACT, TARBP1, and TARBP2 in epithelial skin cancer*. *Mol Carcinog*, 2012. **51**(11): p. 916-22.
218. Guo, Y., et al., *Silencing the Double-Stranded RNA Binding Protein DGCR8 Inhibits Ovarian Cancer Cell Proliferation, Migration, and Invasion*. *Pharm Res*, 2013.
219. Park, N.J., et al., *Salivary microRNA: discovery, characterization, and clinical utility for oral cancer detection*. *Clin Cancer Res*, 2009. **15**(17): p. 5473-7.
220. Hanke, M., et al., *A robust methodology to study urine microRNA as tumor marker: microRNA-126 and microRNA-182 are related to urinary bladder cancer*. *Urol Oncol*, 2010. **28**(6): p. 655-61.
221. Weber, J.A., et al., *The microRNA spectrum in 12 body fluids*. *Clin Chem*, 2010. **56**(11): p. 1733-41.
222. Kosaka, N., et al., *Secretory mechanisms and intercellular transfer of microRNAs in living cells*. *J Biol Chem*, 2010. **285**(23): p. 17442-52.
223. Wang, K., et al., *Circulating microRNAs, potential biomarkers for drug-induced liver injury*. *Proceedings of the National Academy of Sciences*, 2009.
224. Ramachandran, K., et al., *Human miRNome profiling identifies microRNAs differentially present in the urine after kidney injury*. *Clin Chem*, 2013. **59**(12): p. 1742-52.
225. Zerneck, A., et al., *Delivery of microRNA-126 by apoptotic bodies induces CXCL12-dependent vascular protection*. *Sci Signal*, 2009. **2**(100): p. ra81.
226. Vickers, K.C., et al., *MicroRNAs are transported in plasma and delivered to recipient cells by high-density lipoproteins*. *Nat Cell Biol*, 2011. **13**(4): p. 423-33.

227. Arroyo, J.D., et al., *Argonaute2 complexes carry a population of circulating microRNAs independent of vesicles in human plasma*. Proc Natl Acad Sci U S A, 2011. **108**(12): p. 5003-8.
228. Wang, K., et al., *Export of microRNAs and microRNA-protective protein by mammalian cells*. Nucleic Acids Res, 2010. **38**(20): p. 7248-59.
229. Cheng, G., *Circulating miRNAs: Roles in cancer diagnosis, prognosis and therapy*. Advanced Drug Delivery Reviews, 2015. **81**(0): p. 75-93.
230. Heegaard, N.H., et al., *Circulating micro-RNA expression profiles in early stage nonsmall cell lung cancer*. Int J Cancer, 2012. **130**(6): p. 1378-86.
231. Nguyen, H.C., et al., *Expression differences of circulating microRNAs in metastatic castration resistant prostate cancer and low-risk, localized prostate cancer*. Prostate, 2013. **73**(4): p. 346-54.
232. Pu, X.X., et al., *Circulating miR-221 directly amplified from plasma is a potential diagnostic and prognostic marker of colorectal cancer and is correlated with p53 expression*. J Gastroenterol Hepatol, 2010. **25**(10): p. 1674-80.
233. Liu, A.M., et al., *Circulating miR-15b and miR-130b in serum as potential markers for detecting hepatocellular carcinoma: a retrospective cohort study*. BMJ Open, 2012. **2**(2): p. e000825.
234. Lawrie, C.H., et al., *Detection of elevated levels of tumour-associated microRNAs in serum of patients with diffuse large B-cell lymphoma*. Br J Haematol, 2008. **141**(5): p. 672-5.
235. van Schooneveld, E., et al., *Expression profiling of cancerous and normal breast tissues identifies microRNAs that are differentially expressed in serum from patients with (metastatic) breast cancer and healthy volunteers*. Breast Cancer Res, 2012. **14**(1): p. R34.
236. Sochor, M., et al., *Oncogenic microRNAs: miR-155, miR-19a, miR-181b, and miR-24 enable monitoring of early breast cancer in serum*. BMC Cancer, 2014. **14**: p. 448.
237. Cheng, H.H., et al., *Plasma Processing Conditions Substantially Influence Circulating microRNA Biomarker Levels*. PLoS ONE, 2013. **8**(6): p. e64795.
238. Muller, V., et al., *Changes in serum levels of miR-21, miR-210, and miR-373 in HER2-positive breast cancer patients undergoing neoadjuvant therapy: a translational research project within the Geparquinto trial*. Breast Cancer Res Treat, 2014. **147**(1): p. 61-8.
239. Health, N.I.o. *Stem cell information*. 25/07/2015]; Available from: <http://stemcells.nih.gov/info/basics/pages/basics1.aspx>.
240. McDermott, S.P. and M.S. Wicha, *Targeting breast cancer stem cells*. Mol Oncol, 2010. **4**(5): p. 404-19.
241. Al-Hajj, M., et al., *Prospective identification of tumorigenic breast cancer cells*. Proc Natl Acad Sci U S A, 2003. **100**(7): p. 3983-8.
242. Ginestier, C., et al., *ALDH1 is a marker of normal and malignant human mammary stem cells and a predictor of poor clinical outcome*. Cell Stem Cell, 2007. **1**(5): p. 555-67.
243. Balic, M., et al., *Most early disseminated cancer cells detected in bone marrow of breast cancer patients have a putative breast cancer stem cell phenotype*. Clin Cancer Res, 2006. **12**(19): p. 5615-21.
244. Li, X., et al., *Intrinsic resistance of tumorigenic breast cancer cells to chemotherapy*. J Natl Cancer Inst, 2008. **100**(9): p. 672-9.

245. Cufi, S., et al., *Metformin-induced preferential killing of breast cancer initiating CD44+CD24-/low cells is sufficient to overcome primary resistance to trastuzumab in HER2+ human breast cancer xenografts*. *Oncotarget*, 2012. **3**(4): p. 395-8.
246. Browne, B.C., *The role of receptor tyrosine kinase signalling in HER-2-positive cells and trastuzumab (Herceptin) resistance in breast cancer*, 2009, Dublin City University.
247. McDermott, M.S., et al., *PP2A inhibition overcomes acquired resistance to HER2 targeted therapy*. *Mol Cancer*, 2014. **13**: p. 157.
248. Chen, T.R., *In situ detection of mycoplasma contamination in cell cultures by fluorescent Hoechst 33258 stain*. *Experimental Cell Research*, 1977. **104**(2): p. 255-262.
249. Livak, K.J. and T.D. Schmittgen, *Analysis of relative gene expression data using real-time quantitative PCR and the 2(-Delta Delta C(T)) Method*. *Methods*, 2001. **25**(4): p. 402-8.
250. Dweep, H., et al., *miRWalk--database: prediction of possible miRNA binding sites by "walking" the genes of three genomes*. *J Biomed Inform*, 2011. **44**(5): p. 839-47.
251. Dweep, H., et al., *miRWalk – Database: Prediction of possible miRNA binding sites by “walking” the genes of three genomes*. *J Biomed Inform*. **44**(5): p. 839-847.
252. Mulrane, L., et al., *miR-187 Is an Independent Prognostic Factor in Breast Cancer and Confers Increased Invasive Potential In Vitro*. *Clinical Cancer Research*, 2012. **18**(24): p. 6702-6713.
253. Liang, C.C., A.Y. Park, and J.L. Guan, *In vitro scratch assay: a convenient and inexpensive method for analysis of cell migration in vitro*. *Nat Protoc*, 2007. **2**(2): p. 329-33.
254. Geback, T., et al., *TScratch: a novel and simple software tool for automated analysis of monolayer wound healing assays*. *Biotechniques*, 2009. **46**(4): p. 265-74.
255. Glynn, C.L., et al., *Isolation of Secreted microRNAs (miRNAs) from Cell-conditioned Media*. *MicroRNA*, 2013. **2**(1): p. 14-19.
256. Balicki, D., *Moving Forward in Human Mammary Stem Cell Biology and Breast Cancer Prognostication Using ALDH1*. *Cell Stem Cell*. **1**(5): p. 485-487.
257. Shaw, F.L., et al., *A detailed mammosphere assay protocol for the quantification of breast stem cell activity*. *Journal of Mammary Gland Biology and Neoplasia*, 2012. **17**(2): p. 111-7.
258. Dako, *Guidelines for scoring HercepTest™-Breast*.
259. Baselga, J., et al., *Phase II study of weekly intravenous recombinant humanized anti-p185HER2 monoclonal antibody in patients with HER2/neu-overexpressing metastatic breast cancer*. *J Clin Oncol*, 1996. **14**(3): p. 737-44.
260. Rita, N. and J.E. Francisco, *Herceptin: mechanisms of action and resistance*. *Cancer letters*, 2006. **232**(2): p. 123-138.
261. Nahta, R. and F.J. Esteva, *HER2 therapy: molecular mechanisms of trastuzumab resistance*. *Breast Cancer Res*, 2006. **8**(6): p. 215.
262. Schaller, G., et al., *Phase II study of capecitabine plus trastuzumab in human epidermal growth factor receptor 2 overexpressing metastatic breast cancer pretreated with anthracyclines or taxanes*. *J Clin Oncol*, 2007. **25**(22): p. 3246-50.

263. Cameron, D., et al., *A phase III randomized comparison of lapatinib plus capecitabine versus capecitabine alone in women with advanced breast cancer that has progressed on trastuzumab: updated efficacy and biomarker analyses*. Breast Cancer Res Treat, 2008. **112**(3): p. 533-43.
264. Samanta, D., et al., *Hypoxia-inducible factors are required for chemotherapy resistance of breast cancer stem cells*. Proc Natl Acad Sci U S A, 2014.
265. Diessner, J., et al., *Targeting of preexisting and induced breast cancer stem cells with trastuzumab and trastuzumab emtansine (T-DM1)*. Cell Death Dis, 2014. **5**: p. e1149.
266. Ge, X., et al., *MicroRNA expression profiles associated with acquired gefitinibresistance in human lung adenocarcinoma cells*. Mol Med Rep, 2015. **11**(1): p. 333-40.
267. Lv, J., et al., *miRNA expression patterns in chemoresistant breast cancer tissues*. Biomed Pharmacother, 2014.
268. Zhang, C., et al., *PUMA is a novel target of miR-221/222 in human epithelial cancers*. Int J Oncol, 2010. **37**(6): p. 1621-6.
269. Johansson, H.J., et al., *Retinoic acid receptor alpha is associated with tamoxifen resistance in breast cancer*. Nat Commun, 2013. **4**.
270. Tari, A.M., et al., *Her2/neu induces all-trans retinoic acid (ATRA) resistance in breast cancer cells*. Oncogene, 2002. **21**(34): p. 5224-32.
271. Mendoza-Gamboa, E., D.R. Siwak, and A.M. Tari, *The HER2/Grb2/Akt pathway regulates the DNA binding activity of AP-1 in breast cancer cells*. Oncol Rep, 2004. **12**(4): p. 903-908.
272. Ablain, J. and H. de Thé, *Retinoic acid signaling in cancer: The parable of acute promyelocytic leukemia*. International Journal of Cancer, 2014: p. n/a-n/a.
273. Stinson, S., et al., *TRPS1 targeting by miR-221/222 promotes the epithelial-to-mesenchymal transition in breast cancer*. Sci Signal, 2011. **4**(177): p. ra41.
274. Gan, R., et al., *Downregulation of miR-221/222 enhances sensitivity of breast cancer cells to tamoxifen through upregulation of TIMP3*. Cancer Gene Ther, 2014. **21**(7): p. 290-6.
275. Rao, X., et al., *MicroRNA-221/222 confers breast cancer fulvestrant resistance by regulating multiple signaling pathways*. Oncogene, 2011. **30**(9): p. 1082-97.
276. Wang, M., et al., *Deregulated microRNAs in gastric cancer tissue-derived mesenchymal stem cells: novel biomarkers and a mechanism for gastric cancer*. Br J Cancer, 2014. **110**(5): p. 1199-210.
277. Storci, G., et al., *Slug/beta-catenin-dependent proinflammatory phenotype in hypoxic breast cancer stem cells*. Am J Pathol, 2013. **183**(5): p. 1688-97.
278. Li, Y., et al., *miR-221/222 promotes S-phase entry and cellular migration in control of basal-like breast cancer*. Molecules, 2014. **19**(6): p. 7122-37.
279. Di Leva, G., et al., *MicroRNA cluster 221-222 and estrogen receptor alpha interactions in breast cancer*. J Natl Cancer Inst, 2010. **102**(10): p. 706-21.
280. Miller, T., et al., *MicroRNA-221/222 confers tamoxifen resistance in breast cancer by targeting p27(Kip1)*. J Biol Chem, 2008. **283**: p. 29897 - 29903.
281. Li, J., et al., *MicroRNA-221 is Required for Proliferation of Mouse Embryonic Stem Cells via P57 Targeting*. Stem Cell Rev, 2014.
282. Shaw, F.L., et al., *A detailed mammosphere assay protocol for the quantification of breast stem cell activity*. J Mammary Gland Biol Neoplasia, 2012. **17**(2): p. 111-7.

283. Liu, A., et al., *MicroRNA expression profiling outperforms mRNA expression profiling in formalin-fixed paraffin-embedded tissues*. *Int J Clin Exp Pathol*, 2009. **2**(6): p. 519-27.
284. Abramovitz, M., et al., *Optimization of RNA extraction from FFPE tissues for expression profiling in the DASL assay*. *Biotechniques*, 2008. **44**(3): p. 417-23.
285. Abue, M., et al., *Circulating miR-483-3p and miR-21 is highly expressed in plasma of pancreatic cancer*. *Int J Oncol*, 2014.
286. Zi, Y., et al., *Circulating MicroRNA as Potential Source for Neurodegenerative Diseases Biomarkers*. *Molecular Neurobiology*, 2014: p. 1-10.
287. Wu, X., et al., *De novo sequencing of circulating miRNAs identifies novel markers predicting clinical outcome of locally advanced breast cancer*. *J Transl Med*, 2012. **10**: p. 42.
288. Wang, H., et al., *Circulating MiR-125b as a marker predicting chemoresistance in breast cancer*. *PLoS ONE*, 2012. **7**(4): p. e34210.
289. Scientific, T., *T042 TECHNICAL BULLETIN: Assessment of Nucleic Acid Purity*.
290. Nahta, R., et al., *P27kip1 Down-Regulation Is Associated with Trastuzumab Resistance in Breast Cancer Cells*. *Cancer Research*, 2004. **64**(11): p. 3981-3986.
291. White, C.D., et al., *IQGAP1 protein binds human epidermal growth factor receptor 2 (HER2) and modulates trastuzumab resistance*. *J Biol Chem*, 2011. **286**(34): p. 29734-47.
292. Sarkar, F.H., et al., *Implication of microRNAs in drug resistance for designing novel cancer therapy*. *Drug Resist Updat*, 2010. **13**(3): p. 57-66.
293. Gao, Y., et al., *MiR-335 inhibits migration of breast cancer cells through targeting oncoprotein c-Met*. *Tumour Biol*, 2014.
294. Doleshal, M., et al., *Evaluation and validation of total RNA extraction methods for microRNA expression analyses in formalin-fixed, paraffin-embedded tissues*. *J Mol Diagn*, 2008. **10**(3): p. 203-11.
295. Ferruzza, S., et al., *Serum-reduced and serum-free media for differentiation of Caco-2 cells*. *ALTEX*, 2013. **30**(2): p. 159-68.
296. Zheng, X., et al., *Proteomic Analysis for the Assessment of Different Lots of Fetal Bovine Serum as a Raw Material for Cell Culture. Part IV. Application of Proteomics to the Manufacture of Biological Drugs*. *Biotechnology Progress*, 2006. **22**(5): p. 1294-1300.
297. Shen, A., et al., *Pien Tze Huang Overcomes Multidrug Resistance and Epithelial-Mesenchymal Transition in Human Colorectal Carcinoma Cells via Suppression of TGF-beta Pathway*. *Evid Based Complement Alternat Med*, 2014. **2014**: p. 679436.
298. Han, S., et al., *Exogenous IGFBP-2 promotes proliferation, invasion, and chemoresistance to temozolomide in glioma cells via the integrin beta1-ERK pathway*. *Br J Cancer*, 2014. **111**(7): p. 1400-9.
299. Jayme, D.W. and S.R. Smith, *Media formulation options and manufacturing process controls to safeguard against introduction of animal origin contaminants in animal cell culture*. *Cytotechnology*, 2000. **33**(1-3): p. 27-36.
300. M, M.D., *Mechanisms of resistance to lapatinib in HER2-positive breast cancer*, in *School of Biotechnology 2012*, Dublin City University.
301. Cole, J.M., et al., *Enrichment for chemoresistant ovarian cancer stem cells from human cell lines*. *J Vis Exp*, 2014(91): p. 51891.

302. Suzuki, S., et al., *JNK suppression of chemotherapeutic agents-induced ROS confers chemoresistance on pancreatic cancer stem cells*. *Oncotarget*, 2014.
303. Marcato, P., et al., *Aldehyde dehydrogenase: Its role as a cancer stem cell marker comes down to the specific isoform*. *Cell Cycle*, 2011. **10**(9): p. 1378-1384.
304. Duru, N., et al., *HER2-associated radioresistance of breast cancer stem cells isolated from HER2-negative breast cancer cells*. *Clin Cancer Res*, 2012. **18**(24): p. 6634-47.
305. Petrosino, J., D. DiSilvestro, and O. Ziouzenkova, *Aldehyde Dehydrogenase IAI: Friend or Foe to Female Metabolism?* *Nutrients*, 2014. **6**(3): p. 950-973.
306. von Ahlfen, S., et al., *Determinants of RNA Quality from FFPE Samples*. *PLoS ONE*, 2007. **2**(12): p. e1261.
307. Li, J., et al., *Improved RNA quality and TaqMan Pre-amplification method (PreAmp) to enhance expression analysis from formalin fixed paraffin embedded (FFPE) materials*. *BMC Biotechnol*, 2008. **8**: p. 10.
308. Masuda, N., et al., *Analysis of chemical modification of RNA from formalin-fixed samples and optimization of molecular biology applications for such samples*. *Nucleic Acids Res*, 1999. **27**(22): p. 4436-43.
309. Ribeiro-Silva, A., H. Zhang, and S.S. Jeffrey, *RNA extraction from ten year old formalin-fixed paraffin-embedded breast cancer samples: a comparison of column purification and magnetic bead-based technologies*. *BMC Mol Biol*, 2007. **8**: p. 118.
310. Strand, C., et al., *RNA quality in frozen breast cancer samples and the influence on gene expression analysis--a comparison of three evaluation methods using microcapillary electrophoresis traces*. *BMC Mol Biol*, 2007. **8**: p. 38.
311. Therasse, P., et al., *New guidelines to evaluate the response to treatment in solid tumors*. *European Organization for Research and Treatment of Cancer, National Cancer Institute of the United States, National Cancer Institute of Canada*. *J Natl Cancer Inst*, 2000. **92**(3): p. 205-16.
312. Zhong, S., et al., *MiR-222 and miR-29a contribute to the drug-resistance of breast cancer cells*. *Gene*, 2013. **531**(1): p. 8-14.
313. Lu, J., et al., *Predictive value of miR-9 as a potential biomarker for nasopharyngeal carcinoma metastasis*. *Br J Cancer*, 2014. **110**(2): p. 392-8.
314. Zhou, X., et al., *MicroRNA-9 as Potential Biomarker for Breast Cancer Local Recurrence and Tumor Estrogen Receptor Status*. *PLoS ONE*, 2012. **7**(6): p. e39011.
315. Wang, H., et al., *MiR-224 promotes the chemoresistance of human lung adenocarcinoma cells to cisplatin via regulating G(1)/S transition and apoptosis by targeting p21(WAF1/CIP1)*. *Br J Cancer*, 2014. **111**(2): p. 339-54.
316. Zhao, H., et al., *Expression of miR-224-5p is associated with the original cisplatin resistance of ovarian papillary serous carcinoma*. *Oncol Rep*, 2014. **32**(3): p. 1003-12.
317. Kawaguchi, T., et al., *Clinical impact of circulating miR-221 in plasma of patients with pancreatic cancer*. *Br J Cancer*, 2013. **108**(2): p. 361-369.
318. Li, P., et al., *Circulating miR-221 expression level and prognosis of cutaneous malignant melanoma*. *Med Sci Monit*, 2014. **20**: p. 2472-7.
319. Qi, P., et al., *Serum MicroRNAs as Biomarkers for Hepatocellular Carcinoma in Chinese Patients with Chronic Hepatitis B Virus Infection*. *PLoS ONE*, 2011. **6**(12): p. e28486.

320. Godfrey, A.C., et al., *Serum microRNA expression as an early marker for breast cancer risk in prospectively collected samples from the Sister Study cohort*. *Breast Cancer Res*, 2013. **15**(3): p. R42.
321. Mavridis, K., K. Stravodimos, and A. Scorilas, *Downregulation and prognostic performance of microRNA 224 expression in prostate cancer*. *Clin Chem*, 2013. **59**(1): p. 261-9.
322. Zhuang, L.-p. and Z.-q. Meng, *Serum miR-224 Reflects Stage of Hepatocellular Carcinoma and Predicts Survival*. *BioMed Research International*.
323. Fei, D., et al., *Serum miR-9 as a prognostic biomarker in patients with osteosarcoma*. *J Int Med Res*, 2014. **42**(4): p. 932-937.
324. Lu, J., et al., *Predictive value of miR-9 as a potential biomarker for nasopharyngeal carcinoma metastasis*. *Br J Cancer*, 2014. **110**(2): p. 392-398.
325. Mattick, J.S. and I.V. Makunin, *Small regulatory RNAs in mammals*. *Human Molecular Genetics*, 2005. **14**(suppl 1): p. R121-R132.
326. Xiang, M., et al., *U6 is not a suitable endogenous control for the quantification of circulating microRNAs*. *Biochem Biophys Res Commun*, 2014. **454**(1): p. 210-214.
327. Biosystems, A. *Control miRNA Assays*. Available from: [https://www.lifetechnologies.com/order/genome-database/searchResults?searchMode=keyword&CID=&productTypeSelect=microRNA&alternateProductTypeSelect=&originalCount=&alternateTargetTypeSelect=&targetTypeSelect=mirna\\_controls&species=Homo+sapiens&otherSpecies=&selectedInputType=&keyword=&sequenceInput=&chromosome=&chromStart=&chromStop=&vcfUpload=&batchText=&batchUpload](https://www.lifetechnologies.com/order/genome-database/searchResults?searchMode=keyword&CID=&productTypeSelect=microRNA&alternateProductTypeSelect=&originalCount=&alternateTargetTypeSelect=&targetTypeSelect=mirna_controls&species=Homo+sapiens&otherSpecies=&selectedInputType=&keyword=&sequenceInput=&chromosome=&chromStart=&chromStop=&vcfUpload=&batchText=&batchUpload).
328. Wang, J., et al., *Prognostic significance of microRNA-221/222 expression in cancers: evidence from 1,204 subjects*. *Int J Biol Markers*, 2014. **29**(2): p. e129-41.
329. Leontieva, O.V. and M.V. Blagosklonny, *CDK4/6-inhibiting drug substitutes for p21 and p16 in senescence: duration of cell cycle arrest and MTOR activity determine geroconversion*. *Cell Cycle*, 2013. **12**(18): p. 3063-9.
330. Zhu, D., et al., *Decreased microRNA-224 and its clinical significance in non-small cell lung cancer patients*. *Diagn Pathol*, 2014. **9**(1): p. 198.
331. Xu, S.H., et al., *MicroRNA-9 expression is a prognostic biomarker in patients with osteosarcoma*. *World J Surg Oncol*, 2014. **12**: p. 195.
332. Gwak, J.M., et al., *MicroRNA-9 is associated with epithelial-mesenchymal transition, breast cancer stem cell phenotype, and tumor progression in breast cancer*. *Breast Cancer Res Treat*, 2014. **147**(1): p. 39-49.
333. Liu, D., et al., *Downregulation of Erbin in Her2-overexpressing breast cancer cells promotes cell migration and induces trastuzumab resistance*. *Molecular Immunology*, 2013. **56**(1-2): p. 104-112.
334. Galardi, S., et al., *miR-221 and miR-222 Expression Affects the Proliferation Potential of Human Prostate Carcinoma Cell Lines by Targeting p27Kip1*. *Journal of Biological Chemistry*, 2007. **282**(32): p. 23716-23724.
335. Dutta, S., et al., *Angiogenin interacts with the plasminogen activation system at the cell surface of breast cancer cells to regulate plasmin formation and cell migration*. *Mol Oncol*, 2014. **8**(3): p. 483-507.
336. Li, M., et al., *A role for CCL2 in both tumor progression and immunosurveillance*. *Oncoimmunology*, 2013. **2**(7): p. e25474.
337. Lebrecht, A., et al., *Monocyte chemoattractant protein-1 serum levels in patients with breast cancer*. *Tumour Biol*, 2004. **25**(1-2): p. 14-7.

338. Li, Q., et al., *MicroRNA-224 is upregulated in HepG2 cells and involved in cellular migration and invasion*. J Gastroenterol Hepatol, 2010. **25**(1): p. 164-71.
339. Huang, L., et al., *MicroRNA-224 targets RKIP to control cell invasion and expression of metastasis genes in human breast cancer cells*. Biochemical and Biophysical Research Communications, (0).
340. Zhu, S., et al., *Ubc9 promotes breast cell invasion and metastasis in a sumoylation-independent manner*. Oncogene, 2010. **29**(12): p. 1763-72.
341. Milde-Langosch, K., et al., *FosB is highly expressed in normal mammary epithelia, but down-regulated in poorly differentiated breast carcinomas*. Breast Cancer Res Treat, 2003. **77**(3): p. 265-75.
342. Langer, S., et al., *Jun and Fos family protein expression in human breast cancer: correlation of protein expression and clinicopathological parameters*. Eur J Gynaecol Oncol, 2006. **27**(4): p. 345-52.
343. Dos Santos, G.A., L. Kats, and P.P. Pandolfi, *Synergy against PML-RAR $\alpha$ : targeting transcription, proteolysis, differentiation, and self-renewal in acute promyelocytic leukemia*. J Exp Med, 2013. **210**(13): p. 2793-802.
344. Paroni, G., et al., *Synergistic antitumor activity of lapatinib and retinoids on a novel subtype of breast cancer with coamplification of ERBB2 and RAR $\alpha$* . Oncogene, 2012. **31**(29): p. 3431-43.
345. Alsafadi, S., et al., *Retinoic acid receptor alpha amplifications and retinoic acid sensitivity in breast cancers*. Clin Breast Cancer, 2013. **13**(5): p. 401-8.
346. Ma, L., et al., *miR-9, a MYC/MYC $N$ -activated microRNA, regulates E-cadherin and cancer metastasis*. Nat Cell Biol, 2010. **12**(3): p. 247-56.
347. Zhu, L., et al., *MicroRNA-9 up-regulation is involved in colorectal cancer metastasis via promoting cell motility*. Med Oncol, 2012. **29**(2): p. 1037-43.
348. Guo, L.M., et al., *MicroRNA-9 inhibits ovarian cancer cell growth through regulation of NF-kappaB1*. FEBS J, 2009. **276**(19): p. 5537-46.
349. Wan, H.Y., et al., *Regulation of the transcription factor NF-kappaB1 by microRNA-9 in human gastric adenocarcinoma*. Mol Cancer, 2010. **9**: p. 16.
350. Zhou, X., et al., *MicroRNA-9 as Potential Biomarker for Breast Cancer Local Recurrence and Tumor Estrogen Receptor Status*. PLoS ONE, 2012. **7**(6): p. e39011.
351. Rodriguez-Otero, P., et al., *Deregulation of FGFR1 and CDK6 oncogenic pathways in acute lymphoblastic leukaemia harbouring epigenetic modifications of the MIR9 family*. British Journal of Haematology, 2011. **155**(1): p. 73-83.
352. Liu, D.-Z., et al., *Integrated analysis of mRNA and microRNA expression in mature neurons, neural progenitor cells and neuroblastoma cells*. Gene, 2012. **495**(2): p. 120-127.
353. Sun, R., et al., *Co-delivery of all-trans-retinoic acid and doxorubicin for cancer therapy with synergistic inhibition of cancer stem cells*. Biomaterials, 2015. **37**(0): p. 405-414.
354. Schenk, T., S. Stengel, and A. Zelent, *Unlocking the potential of retinoic acid in anticancer therapy*. Br J Cancer, 2014. **111**(11): p. 2039-45.
355. Sheikh, M.S., et al., *Estrogen receptor-negative breast cancer cells transfected with the estrogen receptor exhibit increased RAR alpha gene expression and sensitivity to growth inhibition by retinoic acid*. J Cell Biochem, 1993. **53**(4): p. 394-404.

356. van der Leede, B.J., et al., *Retinoic acid receptor alpha 1 isoform is induced by estradiol and confers retinoic acid sensitivity in human breast cancer cells*. Mol Cell Endocrinol, 1995. **109**(1): p. 77-86.
357. Rishi, A.K., et al., *Regulation of the human retinoic acid receptor alpha gene in the estrogen receptor negative human breast carcinoma cell lines SKBR-3 and MDA-MB-435*. Cancer Res, 1996. **56**(22): p. 5246-52.
358. Koay, D.C., et al., *Anti-tumor effects of retinoids combined with trastuzumab or tamoxifen in breast cancer cells: induction of apoptosis by retinoid/trastuzumab combinations*. Breast Cancer Res, 2010. **12**(4): p. R62.
359. Nassirpour, R., et al., *miR-221 promotes tumorigenesis in human triple negative breast cancer cells*. PLoS ONE, 2013. **8**(4): p. e62170.
360. Wong, Q.W., et al., *MiR-222 overexpression confers cell migratory advantages in hepatocellular carcinoma through enhancing AKT signaling*. Clin Cancer Res, 2010. **16**(3): p. 867-75.
361. Bozzuto, G., P. Ruggieri, and A. Molinari, *Molecular aspects of tumor cell migration and invasion*. Ann Ist Super Sanita, 2010. **46**(1): p. 66-80.
362. Møller, M.B., *p27 in Cell Cycle Control and Cancer*. Leuk Lymphoma, 2000. **39**(1-2): p. 19-27.
363. Moshiri, F., et al., *Inhibiting the oncogenic mir-221 by microRNA sponge: toward microRNA-based therapeutics for hepatocellular carcinoma*. Gastroenterol Hepatol Bed Bench, 2014. **7**(1): p. 43-54.
364. Newman, L., et al., *Correlation of p27 protein expression with HER-2/neu expression in breast cancer*. Mol Carcinog, 2001. **30**(3): p. 169-75.
365. Yang, H.-Y., et al., *Oncogenic Signals of HER-2/neu in Regulating the Stability of the Cyclin-dependent Kinase Inhibitor p27*. Journal of Biological Chemistry, 2000. **275**(32): p. 24735-24739.
366. Lee-Hoeflich, S.T., et al., *PPM1H is a p27 phosphatase implicated in trastuzumab resistance*. Cancer Discov, 2011. **1**(4): p. 326-37.
367. Liu, S., S.G. Clouthier, and M.S. Wicha, *Role of microRNAs in the regulation of breast cancer stem cells*. J Mammary Gland Biol Neoplasia, 2012. **17**(1): p. 15-21.
368. Ailles, L.E. and I.L. Weissman, *Cancer stem cells in solid tumors*. Curr Opin Biotechnol, 2007. **18**(5): p. 460-6.
369. Xu, J., S. Lamouille, and R. Derynck, *TGF-beta-induced epithelial to mesenchymal transition*. Cell Res, 2009. **19**(2): p. 156-72.
370. Rokavec, M., et al., *IL-6R/STAT3/miR-34a feedback loop promotes EMT-mediated colorectal cancer invasion and metastasis*. J Clin Invest, 2014. **124**(4): p. 1853-1867.